DEPARTMENT OF THE INTERIOR
GEOLOGICAL SURVEY

MINUTES OF THE
NATIONAL EARTHQUAKE PREDICTION EVALUATION COUNCIL
September 8 & 9, 1985
Anchorage, Alaska

by
Clement F. Shearer

Open File Report 86-92

This report is preliminary and has not been edited or reviewed for conformity with U.S. Geological Survey publication standards and stratigraphic nomenclature.

TABLE OF CONTENTS

PREFACE

The National Earthquake Prediction Evaluation Council (NEPEC) was established in 1979 pursuant to the Earthquake Hazards Reduction Act of 1977 to advise the Director of the U.S. Geological Survey (USGS) in issuing any formal predictions or other information pertinent to the potential for the occurrence of a significant earthquake. It is the Director of the USGS who is responsible for the decision whether and when to issue such a prediction or information.

NEPEC, also referred to in this document as the Council, according to its charter, is comprised of a Chairman, Vice Chairman, and from 8 to 12 other members appointed by the Director of the USGS. The Chairman shall not be a USGS employee, and at least one-half of the membership shall be other than USGS employees.

The USGS recently has begun to publish the minutes of NEPEC meetings. This open-file report is the fourth in an anticipated series of routinely published proceedings of the Council.

NATIONAL EARTHQUAKE PREDICTION EVALUATION COUNCIL

Dr. James H. Dieterich   Research Geophysicist
                          Branch of Tectonophysics
                          U.S. Geological Survey
                          345 Middlefield Road, MS 977
                          Menlo Park, California 94025
                             Office: 415/323-8111, ext. 2573
                             Home: 415/856-2025

Dr. William L. Ellsworth Chief, Branch of Seismology
                          U.S. Geological Survey
                          345 Middlefield Road, MS 977
                          Menlo Park, California 94025
                             Office: 415/323-8111, ext. 2782
                             Home: 415/322-9452

Dr. Hiroo Kanamori   Division of Geological & Planetary Science
                          California Institute of Technology
                          Pasadena, California 91125
                             Office: 818/356-6914
                             Home: 818/796-8452

Dr. Thomas V. McEvilly   Department of Geology and Geophysics
                          University of California, Berkeley
                          Berkeley, California 94720
                             Office: 415/642-4494
                             Home: 415/549-0967

Dr. I. Selwyn Sacks   Department of Terrestrial Magnetism
                          Carnegie Institution of Washington
                          5241 Broad Branch Road, N.W.
                          Washington, D.C. 20015
                             Office: 202/966-0863
                             Home: 301/657-3271

Dr. Wayne Thatcher   Chief, Branch of Tectonophysics
                          U.S. Geological Survey
                          345 Middlefield Road, MS 977
                          Menlo Park, California 94025
                             Office: 415/323-8111, ext. 2120
                             Home: 415/326-4680

Dr. Robert E. Wallace   Chief Scientist, Office of Earthquakes,
                             Volcanoes, and Engineering
                          U.S. Geological Survey
                          345 Middlefield Road, MS 977
                          Menlo Park, California 94025
                             Office: 415/323-8111, ext. 2751
                             Home: 415/851-0249

Dr. Robert L. Wesson   Research Geophysicist
                              Branch of Seismology
                              U.S. Geological Survey
                              National Center, MS 922
                              Reston, Virginia 22092
                                Office: 703/860-7431
                                Home: 703/476-8815

Dr. Mark D. Zoback   Professor of Geophysics
                              Department of Geophysics
                              Stanford University
                              Stanford, California 94305
                                Office: 415/497-9438
                                Home: 415/322-9570

National Earthquake Prediction Evaluation Council
Minutes of the Meeting
September 8 & 9, 1985
Anchorage, Alaska

Council Members Present

Dr. Lynn R. Sykes, Chairman, Lamont-Doherty Geological Observatory
Dr. John R. Filson, Vice Chairman, U.S. Geological Survey
Dr. Clement F. Shearer, Executive Secretary, U.S. Geological Survey
Dr. John N. Davies, Alaska Department of Natural Resources
Dr. James F. Davis, California Division of Mines and Geology
Dr. James H. Dieterich, U.S. Geological Survey
Dr. William L. Ellsworth, U.S. Geological Survey
Dr. Hiroo Kanamori, California Institute of Technology
Dr. Wayne Thatcher, U.S. Geological Survey
Dr. Robert E. Wallace, U.S. Geological Survey
Dr. Robert L. Wesson, U.S. Geological Survey

Speakers

Dr. John N. Davies, Alaska Department of Natural Resources
Dr. Klaus Jacob, Lamont-Doherty Geological Observatory
Dr. John Beaven, Lamont-Doherty Geological Observatory
Dr. Jim Savage, U.S. Geological Survey
Dr. Stuart Nishenko, U.S. Geological Survey
Dr. John Lahr, U.S. Geological Survey
Dr. Carl Kisslinger, CIRES/University of Colorado, Boulder
Dr. George Plafker, U.S. Geological Survey
Dr. Robert Page, U.S. Geological Survey

SEPTEMBER 8

EXECUTIVE SESSION

Lynn Sykes opened the Council's Executive Session with a review of the
meeting's agenda. The principal objectives of the session include the
conclusion of unfinished business from the previous meeting (July,
Menlo Park, California); discussion of Alaskan seismicity and updating the
existing hazard letter from the U.S. Geological Survey to the State of
Alaska regarding the Yakataga Seismic Gap. Unfinished business from the
July meeting includes 1) conclusions about the San Andreas fault (from Bear
Valley to the Mid-Peninsula) and the Calaveras fault; 2) reflections on the
Wyss-Burford prediction; and 3) conclusions about U.S. Geological Survey
(USGS) catalogues for central California and Parkfield.

Sykes also updated the Council on a proposed meeting with the USGS Director on the Parkfield decision-matrix discussed at the July meeting of the Council. In essence, Filson and his branch chiefs had met and prepared a document entitled "Parkfield Earthquake Prediction Scenarios." The document will be published as a USGS open-file report and will be discussed later in the meeting.

Discussion of Calaveras Fault
<u>Discussion of Calaveras Fault</u>

Wesson offered that there may be a good speculative argument for a magnitude 6 earthquake north of Morgan Hill but isn't certain that the Council received enough information to present this argument as a prediction. **Davis** expressed concern about the public policy implications of the uncertainties regarding the Calaveras fault. He has already forwarded his own concerns and observations to the California Office of Emergency Services, but did leave room for an official expression from the Council. He moved that the Council summarize the circumstances described by William Bakun and others at the Council's July meeting and that the USGS be requested to communicate its concern regarding the potential for damage in that area.

Wesson was concerned about forwarding to the USGS material that the Council has not fully digested. He wondered whether this action would simply serve to increase attention to the problems in that area. Davis emphasized the need to inform the State of our emerging insights in the subject so that it can consider the timing of future events in mitigating actions in a non-threatening manner or emergency situation. In effect, he argued for the need to begin a dialogue with the State regarding seismic hazards in this area. **Ellsworth** suggested that it is important to flag this area but noted that other areas are perhaps even more critical. Further, he is troubled that the Hayward fault is not being considered in this discussion.

The Council voted to adopt Jim Davis' motion. The Office of Earthquakes, Volcanoes, and Engineering, U.S. Geological Survey, will write the summary. Discussion then moved to consideration of the Council's duties and procedures. **Wesson** argued that the Council needs to determine what its output should be and in what format the Council will deliver its assessment. The Council agreed to discuss this topic further at its next Executive Session. **Ellsworth** suggested that the working groups arranged by Thatcher to investigate sites for future clusters of instrumentation use their impending workshops to help the Council assimilate data. The Council continued discussion of the Southern California Special Studies Areas Workshop and how that meeting might be replicated for the other areas of interest.

Sykes asked for conclusions, based on the last meeting, regarding the Calaveras and San Andreas faults. General sentiment of the Council was that the southernmost portion of the 1906 segment is the one that has the

higher seismic potential, but that the details are unknown, and is of higher concern than the Calaveras in terms of probabilities and expected magnitudes and the societal impact should the earthquake be on the order of a magnitude 7. However, there was still some disagreement and concern regarding the significance of what is known. For example, Wesson was uncomfortable that we don't know how strain buildup is transferred from the San Andreas to the Hayward and Calaveras areas and that the Council did not have enough time to adequately discuss all the available data on the area.

Sykes requested discussion of how the Council should respond to presentations forwarded to them that are or may be construed to be predictions; such as the Wyss-Burford prediction or Carl Kisslinger's presentation regarding Adak (which was given later that afternoon). Wesson offered that there are two levels on which the Council should operate. The first level is to review ongoing research, develop ideas, and make statements, reflecting the consensus of the research community, regarding where the next big earthquake is likely to occur. The other level is to respond to specific predictions. Filson cautioned that the Council not become a super review body for random research coming from the scientific community. He suggested that perhaps a filter or screening process is needed to determine which research should be reviewed. Kanamori and Dieterich agreed but noted that it is unlikely that many researchers would request a Council review of their research. Although a formal vote was not taken, the Council appeared to be in agreement on Wesson's and Filson's points.

OPEN SESSION

Sykes outlined the purposes of this meeting of the Council as review of at least two of the major seismic gaps in Alaska, estimates of repeat times of large earthquakes, information on probability estimates of large or great earthquakes, and discussion of other faults near population centers in Alaska such as Anchorage. The focus is on earthquake prediction and adjacent topics such as earthquake risk or earthquake hazards.

Overview of Historical Seismicity

John Davies sketched the historic seismicity in Alaska. Three of the top 10 earthquakes of the world, in terms of M_W energy, occurred in Alaska (in 1957, 1964, and 1965). Further, from 1904-1984 about 30 percent of the world's seismic energy release took place in the Aleutian Islands. And, the number of M 5.5 or greater earthquakes is greatest in Alaska compared to the rest of the United States. About 75 percent of Alaska's M 7.2 or greater earthquakes occurred along the Aleutian arc from Anchorage and Valdez to Attu in the westernmost U.S. Aleutians; about 15 percent of the events occurred in the transform zone from Yakataga to Juneau; and about 10 percent happened in the interior of Alaska. He discussed tectonic settings in Alaska, focal mechanisms for the interior of the State, and whether Alaska behaves as a single rigid plate or is actually comprised of two plates. In the interior of Alaska the activity trends in a broad band from north of Fairbanks to the Seward peninsula.

Aleutian Seismic Zone Focussing on Shumagin Islands Seismic Gap

Klaus Jacob began his presentation with a brief discussion of the entire
plate boundary from Canada to Kamchatka and conditional probabilities for
the occurrence of great earthquakes. Although these probabilities range
widely from their maximum to minimum at any given arc segment because of
the different data sets and methods used to calculate them, there exists a
pronounced segment of high probabilities in the eastern Aleutian arc.
Jacob focussed on the Shumagin Gap. The teleseismic data from the vicinity
of the Shumagin Gap show a significant reduction in the rate of earthquakes
greater than or equal to M 5.5 since 1979, but the precursory implication
of this quiescence is difficult to determine. Jacob discussed the
seismicity patterns of rate changes and changes in focal mechanisms in
various sub-regions. Some of these changes may have resulted from stress
relaxation in the plate slab associated with a slip event in 1978 to 1980.
He suggests that monitoring of stress patterns may be useful for
identifying future slip events. The Shumagin Gap is centered on the
eastern Aleutian long-term probability high; there are conditional
probabilities for the next 20 years of 30 to 90 percent, some of the
highest known in the United States. There are no compelling data
suggesting that yet another slip event is imminent, and he does not feel
that presently there is sufficient evidence for a short-term precursor to a
great Shumagin earthquake. [Ed. note: See however, new information
submitted December 2, 1985, as per letter and short communication by J.
Taber and K. Jacob; Appendix D. 3. a.]

Crustal Deformation Measurements in Shumagin Islands Seismic Gap

John Beavan described results from crustal deformation measurements taken
since 1972 to analyze regional subduction processes. The two lines with
the longest history in the Inner Shumagins show a tilt downwards towards
the trench, followed by a reversal from 1978 to 1980 and then again
downward tilt toward the trench. The rates for these three trends are -1.0
microradians per year; 2.7 microradians per year; and -0.4 microradians per
year; all with high confidence levels, for the periods 1972-78, 1978-80,
and 1980-85 respectively. A level line in the outer Shumagins also shows a
tilt reversal, but not a high confidence level. The 1978-80 reverse tilt
has been interpreted as a result of an approximately 1 meter aseismic
reverse slip episode between 25 km. and 70 km. on the Benioff zone; and the
1972-78 and 1980-85 data have been assumed to represent normal strain
accumulation in the area. There is also a suggested relationship between
the tilt reversal, the occurrence of deep earthquakes, and the cessation of
activity at Pavlof Volcano. Surface displacements during strain
accumulation are calculated using a dislocation model with virtual slip at
the plate convergence rate on the main thrust zone. None of the models in
which the locked zone extends to the trench fit the observed 1980-1985
data. The best fit occurs with the upper end of the zone at a depth of
25-30 kilometers and the lower end at 50-80 kilometers and implies that the
plate boundary shallower than about 25 km. may be slipping aseismically.
Alternatively, the model may be inadequate; for example, viscoelastic
effects may dominate. If the 1978-80 slip episode is a quasi-regular
feature of subduction, loading of the main thrust zone by a future similar
slip episode might trigger the expected great earthquake; hence monitoring
of the gap for the onset of reverse tilting may help to forecast the
earthquake.

Strain Accumulation in the Shumagin and Yakataga Seismic Gaps

Jim Savage described strain accumulation in the Shumagin and Yakataga seismic gaps as measured by deformation of trilateration networks from 1980 to 1985. The results for the Outer Shumagin Islands may be corrupted by the occurrence of two earthquakes in February 1983. For both the Inner and the Outer Shumagin Islands there is no measured shear strain accumulation. However, the situation is different in the Yakataga region where significant strain has been measured. Data there show significant compression perpendicular to the strike of the subduction zone. He'd expect 0.2 microstrain compression and 0.26 is actually detected; therefore he is satisfied that Yakataga is consistent with a locked main thrust zone. At Cape Yakataga he observed a tilt array. The data there show a good rate of tilt accumulation, about 1/2 microradian per year, that does not appear to have been interrupted by the St. Elias earthquake of 1979. The tilt is essentially perpendicular to the direction of plate convergence, which does not fit the tectonic model. Jim commented that while the rapid glacial retreat at Icy Bay may explain some of the uplift and regional deformation, he is satisfied that the orders of magnitudes he observes in this network will not be changed by the inclusion of that effect.

Probabilistic Estimates of Great Earthquakes, South Alaska and Aleutians

Stuart Nishenko discussed probability modelling for the Queen Charlotte-Alaska-Aleutian seismic zone. He suggests that one can constrain the distribution of repeat times for earthquakes and if there is ample data, and actually attempt to model the distribution of repeat times. For a first approximation, one can assume that the repeat times are normally distributed about the mean repeat time. With more data one can try a Weibull distribution and allow the data to define the distribution function. In terms of conditional probability, this asks the question, "given that we know the distribution function, what is the likelihood of getting an event in some increment of time given that the earthquake has not happened yet and that we know the time of the last large shock at that location?"

Nishenko presented conditional probabilities for large and great earthquakes along specific segments of the Queen Charlotte-Alaska-Aleutian seismic zone for the period of 1985-2005. He showed three different models for analyzing the data. One is using historic data and assuming that they represent periodic occurrences and modelling them as a simple normal distribution. For the Poisson model he took the same repeat time and put it into another probability model. And, next he took the complete suite of historic repeats and possible historic repeats and tried to model them using Weibull functions. From this analysis he discerned areas of high and low seismic hazards for the next 20 years. High hazard areas include the Yakataga gap and a large portion of the Alaska Peninsula; low hazard areas are the entire Queen Charlotte seismic zone, the 1964 Gulf of Alaska rupture zone, and the 1965 Rat Island zone; and portions of the 1957 Central Aleutians are interpreted as zones of intermediate hazard. He pointed out that the segments with the largest uncertainties also have the highest probabilities or hazards reflecting a lack of data about the size and location of previous earthquakes in those areas.

Seismicity of the Castle Mountain Fault

John Lahr reviewed source zones that could affect the Anchorage, Alaska, area. He identified three zones: 1) the Aleutian megathrust, the inclined thrust interface between the North American and Pacific plates; 2) the Benioff zone; and 3) the crustal portion of the overriding North American plate. And, he concluded the following about these source zones. The interface of the North American and Pacific plates is about 30-35 kilometers below Anchorage, dipping about 10 degrees NNW. If the downdip limit of the 1964 rupture zone based on the aftershock and coseismic deformation data is correct, the rupture in 1964 did not extend below Anchorage; if the transition between stick-slip and aseismic slip on the plate interface occurs at or below 35 kilometers on the interface, then the plate directly below Anchorage could pose the most serious hazard to the city. During the past 30 years of monitoring, the Benioff zone has been the most active seismic source. In contrast, there have been relatively few crustal shocks. Within the crustal activity there is a diffuse NNE zone of activity, parallel to the Benioff zone passing just west of Anchorage. The closest large historic earthquake to the Castle Mountain fault system with shallow depth assignment occurred in 1933 at a magnitude of 7.

On August 14, 1984, a magnitude 5.7 m_b earthquake occurred 14 kilometers north of Sutton near the trace of the Talkeetna segment of the Castle Mountain fault. The hypocenters for 49 aftershocks define a 10 kilometer x 5-6 kilometers planar zone parallel to the map trace and dipping steeply to the NNW; the shallowest of these is at 11 kilometers depth.

For the purpose of hazard evaluation for the Castle Mountain fault, the maximum credible length of an earthquake should be assumed to be at least 130 kilometers, from the westernmost location of Holocene offset near the Susitna River through the region where seismicity is seen on the Talkeetna segment. Considering the distribution of magnitude versus rupture length, he concludes that the maximum credible earthquake would be about 7.2 to 7.8 M_s.

Adak Seismic Zone - Seismicity Patterns and Short-Term Outlook

Carl Kisslinger presented research results that, he believes, indicate Adak as the likely site for an earthquake in the near future. The Central Aleutians Network provides data for detailed monitoring of a segment of arc between 175° W and 178.8° W, or about 250 kilometers long. The earthquake catalog extends back to August 1974. Adak Canyon not only marks a division between seismic regions with very different characteristics, but is also the site of a likely imminent earthquake.

Kisslinger's framework for prediction is given by the history of earthquakes of magnitudes greater than 7 since 1900. However, the locations, magnitudes, and fault break lengths are quite uncertain for

events before the 1957 great earthquake. The Adak seismic zone seems to have broken in major events around 1909, 1930, and on March 9, 1957. The zone seems to have been quiet for large shocks between those episodes. A 7.2 M_S event in May 1971 is the only recent earthquake of magnitude equal to or greater than 7 since 1957. The locations of all earthquakes big enough to be listed in the PDE reports from August 1974-June 1984 illustrate a clear deficiency of these modern earthquakes in the Adak Canyon area, with a number of events occurring just outside this area.

The intervals between the large events are 21 years and 27 years, and it's now 28 1/2 years since the 1957 event. Based on this and other evidence, it is not unreasonable to expect another great earthquake in this area in the not too distant future. The issue is what are the other things that indicate an earthquake may happen soon. The seismicity data of the local network, valid since 1976, shows that in September 1982 there began a pronounced period of reduced activity continuing to late 1984. The teleseismic data were then combined with the local network to try to confirm this observation. The nucleation point of the next great earthquake was identified as SWZ - a subregion of the Adak Canyon regional thrust zone. This subregion is characterized by 4 years of increased moderate activity, a low b-value, and higher stress microearthquakes within a broader region of quiescence. If the single observed case of a 3-year precursory quiescence is characteristic, the most likely time of occurrence is before November 1985. Kisslinger noted two other possible outcomes. Either the quiescence will just disappear without a large earthquake suggesting that quiescence, if a precursor, is an unreliable one. Or, the area entered a long period of decreased activity and the recent up-turn in activity is a short-term perturbation. It was noted that, based on the 1957 experience, a M 7 earthquake should not cause extensive damage, although consideration should be given to possible tsunami damage to military installations on Adak.

SEPTEMBER 9

EXECUTIVE SESSION

San Francisco Bay Area

The Council discussed how to conclude its deliberations on two faults within the greater San Francisco Bay area - San Andreas, and Calaveras faults - and whether there are significant other points of view that it needs to hear. **Jim Davis** offered that the subject of mid-Peninsula seismicity needs further discussion. **Jim Dieterich** essentially agreed, in part because the Hayward fault was not discussed and an earthquake on the Hayward fault can have significant impact on the heavily populated region. **Ellsworth** suggested that an efficient manner for discussion of the Hayward by the Council would be for the principal researchers to meet in a workshop, reach some conclusion about the data, and present this more digested information to the Council. **Sykes** commented that this raises the question of how the Council is to operate; whether it is to do more than merely respond to committee reports for which the Council did not have the

advantage of hearing and challenging the presentations. He countered that
the proposed workshop and Council meeting be held on successive days so
that members can attend the workshop, and then have the normal Council
session. There was general agreement that this is a sound idea. **Wesson**
believes that the Bay area should be discussed in its entirety. **Dieterich**
followed that he views the area's faults as interacting and that the area
should be discussed together. The Council agreed that the report of the
workshop held in San Diego in early 1985 would be published in a USGS Open
File Report as a special publication of the Council.

Kisslinger Prediction

The Council discussed and then drafted a position statement on Kisslinger's
presentation of data indicating a period of seismic quiescence in the Adak
Canyon region and Central Aleutians and his conclusion that an earthquake
with surface-wave magnitude 7 or greater will occur there in the near
future. This statement is part of the Council's letter to the Director,
USGS, which is appended to this report. In essence, the Council felt that
the prediction methodology on the basis of seismic quiescence is not
established and requires further investigation.

Parkfield Decision Matrix

Bill Ellsworth and **Wayne Thatcher** presented a draft document that both
updates the Parkfield scenario produced 2 1/2 years ago and refines the
response matrix suggested by Mark Zoback. The document briefly reviews the
Parkfield prediction experiment, describes the observed and inferred
precursors to the 1934 and 1966 earthquakes, summarizes the different
instrumentation systems operating at Parkfield, and describes alarm
thresholds. All of this is combined in a response matrix to indicate what
the USGS response should be for a given scientific observation and level of
concern.

Wallace and **Dieterich** consider the document a great step in the right
direction. **Filson** offered that in addition to an orderly progression up
the emergency scale there ought to be a similarly orderly descent down the
scale. For example, one can't stay at a high level of alert interminaoly
while waiting for a predicted earthquake. **Filson** further suggested that
the draft be taken to the Director of the USGS for his thoughts on the
procedure and to see if he will agree to the concept of predelegation of
warning authority. **Jim Davis** noted that the scenario will identify
circumstances where the time frame is so short that it is unwise to have
anything other than a predelegated arrangement that does not go through
either NEPEC or the Director. Further, he believes that the Council's
contribution is consideration of the procedure rather than actual
involvement in real-time data interpretation and prediction. **Filson** will
get the Director's impression of the concept of the matrix and delegated
emergency authority, and assuming this impression is positive, the steps
for an orderly withdrawal down the scenario's emergency scale will be
drafted as part of a revised document.

Sykes proposed that the Council endorse the decision matrix concept with agreed-upon delegated authority for very short time frames and agreed to discuss it further at the next Council meeting. At this meeting the Council will decide upon endorsement of the document. The motion will be voted upon at the next day's Executive Session.

Intermediate-Term Precursors and Predictions

Sykes asked if there is any interest in having discussions about short-term and intermediate-term precursors. He noted some interest by a few members of the Council in achieving more balance between intermediate- and short-term prediction and precursors, such as changes in creep rate and changes in coda parameters, b-values, and rates of small earthquakes. And, he questioned what, if anything, the Council would recommend on the use of intermediate-term precursors, especially for Parkfield. He also noted that this work would require more uniform earthquake catalogs and asked if there is a role for the Council in providing or asking for better data collection and catalogs. Wallace sees the catalog issue as but one approach to intermediate-term prediction and suggests another as a general encouragement for a statement of the need for techniques suitable for intermediate-term prediction. Kanamori suggested that b-values, coda parameters, etc., represent only one aspect of wave-form and cataloging problems, and he doesn't see how the catalog can be made uniform as there are so many parameters involved. To him the most fundamental thing is to have general seismic instrumentation prototype methodologies and more fundamental data bases. Dieterich offered that he is hard pressed to think of any methods of intermediate-term prediction that are, at this point, anything more than untested ideas, and opined that this Council would have a tough time usefully acting upon any methodology of which he is knowledge-able. One case of useful intermediate-term modelling was noted, however. One year prior to the 1980 Long Valley earthquake Allan Ryall was able to show that the area is much more active than it has been for quite some time. Thatcher offered that the first step in looking for intermediate-term precursors is making sure that there is intermediate-term stability in the measurements which are being taken. The Council's role may be to sponsor workshops, or other mechanisms, to help determine how to achieve more stable and sensitive measurement systems. There was some discussion about whether or not such a workshop is a proper role for the Council. During the discussion Wesson offered that it would be helpful to the Council to have some background discussion of these issues in preparation for its debates about such earthquake predictions. Dieterich stressed that the workshops should be a forum for the presentation of research problems on intermediate prediction rather than individual researchers' latest achievements. Filson suggested using the USGS "Red Book" forum, which leads to an open-file report. The Council approved Sykes motion that the USGS conduct a "Red Book" workshop on research problems in short-term and intermediate-term prediction.

GENERAL SESSION

Earthquake Potential and Recurrence in the Yakataga Seismic Gap

George Plafker discussed the marine terraces at Middleton Island and between Yakataga and Ice Bay. Middleton Island is in the region of the

1964 earthquake and was uplifted 3.5 meters thereby exposing a marine terrace. Before that five older terraces were formed on the island, and they are dated with radiocarbon at roughly 4300, 3800, 3100, 2390, and 1350 years B.P. During the island's history the eustatic sea level was either slowly rising or stable requiring that pre-1964 terraces are primarily tectonic in origin. Also, the average uplift rate was about 1 centimeter per year. However, there appears to be an abrupt decrease in the uplift rate to 0.6 centimeters per year in the interval before the 1964 terrace. So, either there is a change in the rate of uplift or the island is overdue for an additional uplift of about 3-4 meters suggesting that an earthquake is overdue, most likley to the east of the 1964 zone but overlapping at the Middleton area. Data from Middleton Island thus suggests recurrence intervals of 500 to 1350 years for large arc-related events of the 1964 type.

Between Cape Yakataga and Icy Cape four marine terraces have been dated at approximate ages of 5700, 4440, 2700, and 1500 years at average elevations of 63 m, 37 m, 21 m and 13 m. The average uplift rate for the past 5000 years is 9 mm/yr. near Icy Cape and about half this amount at Cape Yakataga. Assuming the entire terrace uplift occurred at discrete major coseismic steps, the recurrence intervals would be from 1550 to 1000 yrs. Since the last step occurred about 1550 years ago, and if the recurrence interval averages about 1400 years, the next uplift event from Cape Yakataga to Icy Cape area may be overdue.

Future uplift of the Middleton Island and Cape Yakataga to Icy Cape areas would probably occur during one or more major earthquakes along the zone from the eastern end of the Aleutian Trench along the Pamplona zone to the Fairweather transform fault. And, those earthquakes could generate tsunamis capable of causing coastal damage.

Seismic Activity in the Yakataga Seismic Gap

Robert Page defined the Yakataga gap as occurring between the aftershock zone of the 1964 Prince William Sound earthquake on the west, the 1979 St. Elias earthquake aftershock zone on the east, the edge of the Continental Shelf and the Pamplona deformational front to the south, and the 40-km isobath of the Wrangell Benioff zone on the north. Another interpretation is that the northern boundary may lie updip at a depth of about 25 km. There is strong evidence that the 1899 earthquake did occur in the Yakataga seismic gap. Since then and up to the 1964 Prince William Sound earthquake, there has been only one known M 6 or larger event in or near the gap--an M 6.3 shock in 1958.

Following the 1964 earthquake, there was activity in the M 5 range in the western part of the gap; however, there is a profound decrease in the rate of seismicity along the western boundary. The last M 5 earthquake that occurred within the gap took place in 1965. Since 1966-1971 there has not been any event within the gap larger than a M 4.5. On the eastern side of the gap there is a broad area in the St. Elias region that has been seismically active. Many earthquakes occurring either individually or in sequence on the perimeter of the gap area are observed in the record.

Since 1974 the USGS has been operating a seismograph network in the region. A critical limitation of the network is the wide spacing of stations, which makes depth determinations difficult. Page noted that a remarkable feature of the microseismicity since 1974 is its stationary character in and around the Yakataga gap. The observed features both before and after the St. Elias earthquake are: 1) much activity in the St. Elias rupture zone with a peak in activity after the 1979 main shock; 2) a persistent, broad concentration of earthquakes near the center of the gap at depths of 10-30 km.; and 3) on the western edge of the gap another persistent area of seismicity at depths of 15-30 km.

Page divided the area into subregions based on observed spatial clustering of seismicity for a first-order estimate of the temporal character of seismicity. In the St. Elias region there is a general decay in the level of seismicity since the 1979 earthquake on which are superposed pronounced secondary or independent aftershock sequences. In the Waxell Ridge area the level of seismicity appears reasonably uniform with the exception of a possible concentration of activity in time preceding the 1979 earthquake. The Copper River delta area also is uniform in activity. In summary, Page finds no first-order seismicity features in the gap that would indicate that a gap-filling earthquake is more likely to occur within a year or 2 than would occur in a similar time interval in the next 1 or 2 decades.

Discussion on Yakataga

The Chairman asked the Council and speakers to consider what, if anything, it should recommend to the USGS about the 1979 USGS hazard notice for the Yakataga gap. Opinions included updating the letter with more recent data, for example, that strain data indicates accumulation of strain but noting that there is no change in the long-term situation. Also, there are two types or sizes of earthquakes to note. One is a M 8 earthquake like the two in 1899 which did not generate a tsunami, and the other is a M 9 earthquake breaking beyond the gap and posing a tsunami threat. The 1979 letter addressed shocks like those of 1899. There was some agreement that the Yakataga area, along with the Shumagin area, is the most likely place to experience an M 8 earthquake, although there was also considerable debate about the details of data interpretation for these areas. (Editor's note: the Council discussed Yakataga further in its next Executive Session.)

EXECUTIVE SESSION

This Executive Session included both discussion on Alaska seismicity and followup to the Council's July 1985 meeting on central California seismicity.

Parkfield Decision Matrix

The Council addressed the draft document on Parkfield earthquake prediction scenarios and a statement describing its position on the document. The

Council voted to accept the general concept of the draft document and a proposed position statement with two provisions; the addition of a mechanism for cancelling an alert and the understanding the Council would review a revised document at its first meeting in 1986. The Council hopes, however, that much movement will take place on the issue before then, especially in the areas of consultation with the Director of the USGS over predelegation of authority to issue predictions. A revised Decision Matrix is included as an appendix. The Council discussed the nature of alarm thresholds to be used in the matrix. **Thatcher** pointed out that the authors based the alarm thresholds on the past record to see how frequently various threshold events have been occurring. Such an analysis has been completed for the Middle Mountain creep meters and this summary is printed as an appendix to this report.

USGS Catalogs - Assessment of Magnitudes, Completeness, and Uniformity

The Council discussed William Bakun's document "Work Plan to Update Magnitudes in USGS Catalogs." The Council's comments included acknowledgement of the importance of improving the assessment of magnitudes. **Sykes** believes the document needs a statement from the USGS that it will begin to produce more uniform magnitudes. He also recommends soliciting written suggestions and comments from other sources, such as University of California at Berkeley and Drs. Habermann and Wyss.

The Council also had lengthy discussions about the nature of the catalog, earthquake detection thresholds, and how one might proceed to improve the catalog and achieve uniformity among the various seismic networks.

Calaveras Fault

The Council discussed a draft position statement regarding the Calaveras fault. The statement notes that historical seismicity suggests a recurrence rate of about 80 years and permits consideration of a M 6 earthquake on the Calaveras fault NW of Morgan Hill as likely in the next decade. The statement concludes with the recommmendation that the USGS so notify the State of California.

San Andreas Fault

The Council continued its discussion of the San Andreas fault from San Juan Bautista to the mid-San Francisco peninsula. The Council's opinion, based on the presentations at its July meeting, is that uncertainties about the amount of slip in 1906 and the rate of strain accumulation preclude a definitive assessment of the likelihood of a large earthquake. It did recognize, though, that one interpretation is that if this section breaks, the resulting earthquake would be M 7 and would have significant public impact in the heavily populated region. Although the Council is very concerned about this possibility, the members are of divergent opinion regarding the interpretation of available data.

Alaska

In its discussion of the Shumagin Gap, the Council notes that spatial and temporal patterns of seismic activity clearly show a seismic gap extending 200-250 km. along the Aleutian arc near the Alaska Peninsula. It also notes that geodetic data indicate negligible strain accumulation in the Shumagin gap while seismic data can be interpreted as signalling a high potential for a great earthquake in the Shumagin gap in the next 20 years. Since the Council can't resolve this conflict, it suggests that the USGS advise the State of Alaska of the data and the prudence of considering tsunami effects on coastal communities on the Alaskan Peninsula.

APPENDIX A. 1.

Overview of Alaskan Historical Seismicity

J. N. Davies

OVERVIEW OF ALASKAN HISTORICAL SEISMICITY

A Presentation to the National Earthquake Prediction Evaluation Council

by

John N. Davies, Alaska State Seismologist

Alaska Division of Geological and Geophysical Surveys

September 8, 1985

OVERVIEW OF ALASKAN HISTORICAL SEISMICITY

Alaska is one of the seismically most active areas in the world. Three of the 10 largest earthquakes in the world since 1904 have occurred in Alaska: vis: (1) the 1957 Andreanof-Fox Islands, (2) the 1964 Prince William Sound, and (3) the 1965 Rat Islands earthquakes (Table 1). A comparision with California (Figure 1) shows about 6 times as many events of $M_b > 5.5$ in Alaska during the 5 year period 1976-1980. Of the major earthquakes ($M_s > 7.0$) in Alaska (Figure 2 and Table 2) about 75% occur in the Alaska-Aleutian subduction zone, 15% in the S.E. Alaska transform zone, and the remaining 10% occur in the Central Alaska seismic zone (a broad area of mainland Alaska north of Anchorage to Fairbanks and west of Fairbanks toward the Seward Peninsula). The instrumental record for Alaska appears to be complete for $M_s > 7.0$ events back to the turn of the century (Figure 3); although it should be noted that there are some 4,000 Alaskan events listed in the NEIS data file for which no magnitudes have been assigned, so there may be a few large events missing from Table 2. Using the number of events of $M_s > 7.0$ (Table 2) and assuming a "b" value of 0.9 one can calculate the expected frequency of occurence of potentially damaging earthquakes ($M_s > 6.5$) for each of the three major seismic zones of Alaska. This computed frequency and the observed frequency for events of $M_s > 7.0$, and 7.8 are given in Table 3. For most regions of Alaska and most magnitude categories the elapsed time since the last event exceeds the mean interevent time by at least a factor of two and for several cases it exceeds the interevent time of 95% of previous cases (mean plus 1.645 times one standard deviation). More detailed discussions of the Alaska-Aleutian subduction zone and the S.E. Alaska transform zone will be
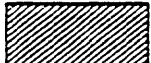
given in other presentations, so only the central Alaska seismic zone will be discussed any further here. The central Alaska seismic zone is loosely defined as the region of mainland Alaska, north of Anchorage where most of the shallow (crustal) M > 6.0 earthquakes occur. Figure 4 shows the location of these earthquakes (north of 63.5 N latitude) plotted on a representation of a stress trajectory map for Alaska as propsed by Nakamura et al (1980). Focal mechanisms (Figures 5, 6, and 7) for the central Alaska seismic zone are generally consistent with the stress trajectories shown in Figure 3, showing roughly NW-SE trending axes of maximum horizontal compression. If the basic tenet of the stress trajectory model is correct, then the earthquakes in interior, northern and western Alaska are the consequence of a far-reaching regional deformation in response to the interaction of the Pacific and North American plates in South-central Alaska. The seismicity patterns shown in Figures 8, 9 and 10 also are consistent with this model of a regional deformation: (1) the overall pattern is one of the greatest activity being concentrated just north of the NE corner of the Pacific plate; (2) the larger events are sub-parallel to the principal slip line which would emanate from this corner if it were taken as a rigid indentor; and (3) there is a suggestion that some of the lineations of epicenters correspond with the major faults (Figure 11), in particular, the Kaltag and Tintina systems. The idea that most of the Alaskan crust is deforming is response to a large-scale right-lateral shear between the Pacific and North American plates has some implications for earthquake prediction research in mainland Alaska. First and foremost it underscores the need for a uniform long term seismic and geodetic monitoring program in all of Alaska including northern and western Alaska, areas which are now very inadequately instrumented. Secondly it points out

the need for paleoseismic work on the major fault systems. These are large

structures and might be capable of rare, great earthquakes, if we are to judge

on the basis of their length alone. Lastly it suggests some interesting basic

research questions which have to do with the seismotectonic framework. The

major implication of the consistent pattern of stress trajectories extending

clear across Alaska is that the crust must be decoupled from the upper

mantle.

References

Abe, K., Magnitudes of large shallow earthquakes from 1904 to 1980, Physics of the Earth and Planetary Interiors, 27, 72-92, 1981.

Abe, K. and Noguchi, S., Determinations of magnitude for large shallow earthquakes, 1898-1917, Physics of the Earth and Planetary Interiors, 32, 45-59, 1983.

Abe, K. and Noguchi, S., Magnitudes of large shallow earthquakes from 1904 to 1980, Physics of the Earth and Planetary Interiors, 27, 72-92, 1981.

Biswas, N. N., J. Pujol, G. Ttgat and K. Dean, Synthesis of seismicity studies for western Alaska, Final Report, National Oceanic and Atmospheric Administration Contract No. NA 81-RAC00112, pp. 69, 1983.

Davies J. N., Seismicity of the Interior of Alaska -- a direct result of Pacific-North American plate convergence?, EOS, Transactions, Am. Geophys. Un. 64, 9, 90, 1983.

Estabrook, Charles H., Seismotectonics of Northern Alaska, M.S. Thesis, University of Alaska, Fairbanks, Alaska, 1985.

Gedney, L. and S. A. Estes, A recent earthquake on the Denali fault in the southeast Alaska Range, Short Notes on Alaskan Geology -- 1981, Ak. Div. Geol. and Geophys. Survs. Geologic Report 73, 1982.

Kamamori, H., The Energy Release in Great Earthquakes, Journal of Geophysical Research, Vol. 82, No. 20, pp. 2981-2988, July 10, 1977.

King, P. B., Tectonic Maps of North America, U.S. Geol. Surv. Publ., 1969.

Minster B, T. Jordan, P. Molner, and E. Haines, Numerical Modeling of Instantaneous Plate Tectonics, Geophys. Jour. of the RAS, Vol. 36, pp. 541-576, 1974.

Nakamura, K., G. Plafker, K. H. Jacob and J. N. Davies, A tectonic stress trajectory map of Alaska using information from volcanoes and faults, Bull. Earthquake Res. Inst., 55, 89-100, 1980.

Stephens, C. D., K. A. Fogleman, J. C. Lahr and R. A. Page, Wrangell Benioff zone, Southern Alaska, Geology, 12, pp. 373-376, 1984.

Stone, D. B., Present day plate boundaries in Alaska and the Arctic, Jour. Alaska Geol. Soc., 1983.

Table 1. The World's Ten Largest Earthquakes
1904 - 1984

No.	Location	Year	M_w	Energy*	
1.	CHILE	1960	9.5	2000	RUPTURE SURFACE AREA
2.	ALASKA	1964	9.2	820	
3.	ALASKA	1957	9.1	585	
4.	KAMCHATKA	1952	9.0	350	
5.	ECUADOR	1906	8.8	204	
6.	ALASKA	1965	8.7	125	
7.	ASSAM	1950	8.6	100	
8.	BANDA SEA	1938	8.5	70	
9.	CHILE	1922	8.5	69	
10.	KURILES	1963	8.5	67	

*Energy in dyne-cm x 10^{27}

Source: Based on data from Kanamori[1] (1977)

Table 2

MAJOR SHALLOW ALASKAN EARTHQUAKES: 1897 -1980

(After Abe and Noguchi, 1981 and 1983)[*]

#	YEAR	MO	DY	TIME	LAT.	LONG.	M_s	LOCATION	ZONE*
1	1898	6	29	1836	52.	+172.	7.6	Near Is.	S+
2	1898	10	11	1637	50.	180.	6.9	Rat/Andreanof Is.	S-
3	1899	4	16	1342	58.	-138.	6.9	S.E. Alaska	T-
4	1899	7	14	1332	(60.)*	(-150.)*	7.2	(Kenai Penin.)*	S+
5	1899	9	4	0022	60.	-142.	7.9	Gulf of Alaska	T+
6	1899	9	4	0440	60.	-142.	6.9	Gulf of Alaska	T-
7	1899	9	10	1704	60.	-140.	7.4	S.E. Alaska	T+
8	1899	9	10	2141	60.	-140.	8.0	S.E. Alaska	T+
9	1899	9	17	1250	59.	-136.	6.9	S.E. Alaska	T-
10	1899	9	23	1104	60.	-143.	6.9	Gulf of Alaska	T-
11	1899	9	23	1250	60.	-143.	7.0	Gulf of Alaska	T+
12	1900	10	9	1228	(60.)*	(-142.)*	7.7	(Kodiak)*	S+*
13	1901	1	18	0439	60.	-135.	7.1	S.E. Alaska	T+
14	1901	12	31	0902	52.	-177.	7.1	Andreanof Is.	S+
15	1902	1	1	0520	55.	-165.	7.0	Unimak Is.	S+
16	1903	1	17	1605	50.	-170.	7.0	(Fox Is.)	S+
17	1903	2	5	1826	52.	+175.	6.8	Near/Rat Is.	S-
18	1903	6	2	1317	57.	-156.	6.9	Alaska Penin.	S-
19	1904	8	27	2156	64.	-151.	7.3	Central Alaska	M+
20	1905	2	14	0846	53.	-178.	7.3	Andreanof Is.	S+
21	1905	3	22	0338	50.	180.	7.0	Rat/Andreanof Is.	S+
22	1905	9	15	0602	55.	+165.	7.4	Komandorsky	O+
23	1905	12	10	1236	50.	180.	6.9	Rat/Andreanof Is.	S-
24	1906	8	17	0010	51.	+179.	7.8	Rat Is.	S+
25	1906	12	23	1722	53.	-165.	7.3	(Unimak Is.)	S+
26	1907	9	2	1601	52.	+173.	7.4	Near Is.	S+
27	1908	5	15	0831	59.	-141.	7.0	S.E. Alaska	T+
28	1909	4	10	1936	52.	+175.	7.0	Near/Rat Is.	S+
29	1910	9	9	0113	51.5	-176..	7.0	Andreanof Is.	S+
30	1910	11	6	2029	53.	-135.	6.8	Queen Charlotte Is.	O-
31	1911	9	17	0326	51.	180.	7.1	Rat/Andreanof Is.	S+
32	1911	11	13	1613	52.	+173.	6.9	Near Is.	S-
33	1912	6	10	1606	59.	-153.	6.9	Kodiak Is.	S-
34	1912	7	7	0757	64.	-147.	7.2	Central Alaska	M+
35	1915	7	31	0131	54.	+162.	7.6	Kamchatka	O+
36	1917	1	30	0245	56.5	+163.	7.8	Kamchatka	O+
37	1917	5	31	0847	54.5	-160.	7.9	Alaska Penin.	S+
38	1923	5	4	1626	55.5	-156.5	7.1	Alaska Penin.	S+
39	1925	8	19	1207	55.25	+168.	7.0	Unimak Is.	S+
40	1926	10	13	1908	52.	-176.	7.0	Andreanof Is.	S+

#	YEAR	MO	DY	TIME	LAT.	LONG.	M_s	LOCATION	ZONE*
41	1927	10	24	1559	57.5	-137.	7.1	S.E. Alaska	T+
42	1928	6	21	1627	60.	-146.5	6.8	Gulf of Alaska	S-
43	1929	3	7	0134	51.	-170.	7.5	Fox Is.	S+
44	1929	7	5	1419	51.	-178.	7.0	Andreanof Is.	S+
45	1929	7	7	2123	52.	-178.	7.3	Andreanof Is.	S+
46	1929	12	17	1058	52.5	+171.5	7.8	Near Is.	S+
47	1933	4	27	0236	61.25	-150.75	6.9	S. Central Alaska	M-
48	1935	2	22	1705	52.25	+175.	7.1	Near/Rat Is.	S+
49	1936	11	13	1231	55.5	+163.	7.1	Kamchatka	O+
50	1937	7	22	1709	64.75	-146.75	7.3	Central Alaska	M+
51	1938	11	10	2018	55.5	-158.	8.3	Alaska Penin.	S+
52	1938	11	17	0354	55.5	-158.5	7.3	Alaska Penin.	S+
53	1940	4	16	0607	52.	+173.5	6.8	Near Is.	S-
54	1940	4	16	0643	52.	+173.5	7.1	Near Is.	S+
55	1940	8	22	0327	53.	-165.5	7.0	Unimak Is.	S+
56	1943	11	3	1432	61.75	-151.	7.4	S. Central Alaska	M+
57	1944	12	12	0417	51.5	+179.5	6.9	Rat Is.	S-
58	1945	4	15	0235	57.	+164.	7.2	Komandorsky	O+
59	1946	1	12	2025	59.25	-147.25	6.7	Gulf of Alaska	S-
60	1946	4	1	1228	52.75	-163.5	7.3	Unimak Is.	S+
61	1946	11	1	1114	51.5	-174.5	7.0	Andreanof Is.	S+
62	1947	10	16	0209	64.5	-147.5	7.2	Central Alaska	M+
63	1948	5	14	2231	54.5	-161.	7.5	Alaska Penin.	S+
64	1949	8	22	0401	53.75	-133.25	8.1	Queen Charlotte Is.	O+
65	1949	9	27	1530	59.75	-149.	6.7	Kenai Penin.	S-
66	1951	2	13	2212	56.	-156.	7.1	Alaska Penin.	S+
67	1953	1	5	0748	54.	+170.5	7.1	Near Is.	S+
68	1957	3	9	1422	51.3	-175.8	(8.1)	Andreanof Is.	S+
69	1957	3	9	2039	52.25	-169.5	7.1	Fox Is.	S+
70	1957	3	11	0958	52.25	-169.25	7.0	Fox Is.	S+
71	1957	3	11	1455	51.5	-178.5	6.9	Andreanof Is.	S-
72	1957	3	12	1144	51.5	-177.	7.0	Andreanof Is.	S+
73	1957	3	14	1447	51.	-177.	7.1	Andreanof Is.	S+
74	1957	3	16	0234	51.5	-178.75	7.0	Andreanof Is.	S+
75	1957	3	22	1421	53.75	-165.75	7.0	Unimak Is.	S+
76	1957	4	10	1129	56.	-154.	6.9	Kodiak Is.	S-
77	1957	4	19	2219	52.25	-166.	6.5	Unimak Is.	S-
78	1958	4	7	1530	65.5	-155.5	7.3	Central Alaska	M+
79	1958	7	10	0615	58.3	-136.5	7.9	S.E. Alaska	T+
80	1960	11	13	0920	51.4	-168.9	6.7	Fox Is.	S-
81	1964	2	6	1307	55.7	-155.9	7.0	Alaska Penin.	S+
82	1964	3	28	0336	61.1	-147.5	(8.4)*	Gulf of Alaska	S+
83	1965	2	4	0501	51.3	+178.6	(8.2)*	Rat Is.	S+
84	1965	2	4	0840	51.4	+179.6	7.0	Rat Is.	S+
85	1965	3	30	0227	50.3	+177.9	7.4	Rat Is.	S+
86	1965	7	2	2058	53.0	-167.6	6.5	Fox/Unimak Is.	S-
87	1965	7	29	0829	51.1	-171.3	6.7	Fox Is.	S-
88	1965	9	4	1432	58.3	-152.5	6.8	Kodiak Is.	S-

#	YEAR	MO	DY	TIME	.LAT.	LONG.	M_s	LOCATION	ZONE*
89	1966	7	4	1833	52.0	+179.9	6.8	Rat Is.	S-
90	1966	8	7	0213	50.6	-171.2	6.4	Fox Is.	S-
91	1969	11	22	2309	57.7	+163.6	7.1	Kamchatka	O+
92	1971	12	15	0829	56.0	+163.2	7.5	Kamchatka	O
93	1972	7	30	2145	56.8	-135.9	7.4	S.E. Alaska	T+
94	1975	2	2	0843	53.1	+173.6	7.4	Near Is.	S+
95	1979	2	28	2127	60.6	-141.6	7.0	S.E. Alaska	T+

*Explanation:

(1)   Data for 1897-1912 from Abe, K. and S. Noguchi, "Review of magnitudes of
       large shallow earthquakes, 1897-1912", Physics of the Earth and Planetary
       Interiors, 33, 1-11, 1983.

(2)   Data for 1913-1917 from Abe, K. and S. Noguchi, "Determinations of magnitude
       for large shallow earthquakes, 1898-1917", Physics of the Earth and Planetary
       Interios, 32, 45-59, 1983.

(3)   Data for 1918-1980 from Abe, K., "Magnitudes of large shallow earthquakes
       from 1904 to 1980", Physics of the Earth and Planetary Interiors, 27, 72-92,
       1981.

(4)   The following notes apply to the respective earthquake number:
       4 - location very uncertain, felt reports suggest a more westerly epicenter,
            perhaps near the Shumagin Islands
       12 - location very uncertain, felt reports suggest a more westerly epicenter,
            perhaps near Kodiak Island
       68 - moment magnitude 8.7
       82 - moment magnitude 9.2
       83 - moment magnitude 8.7

(5)   Earthquake zones were defined as follows:

       S = Alaska-Aleutian subduction zone
       T = S.E. Alaska transform zone
       M = Mainland Alaska
       O = Outside of Alaska (Kamchatka, Komandorsky, Queen Charlotte)
       + = M_s greater than or equal to 7.0
       - = M_s less than 7.0

Table 3
Alaskan Earthquake Statistics
January 1897 - August 1985

Region	Damaging ($M_s > 6.5$)	Major ($M_s > 7.0$)	Great ($M_s > 7.8$)
Alaska-Aleutian Subduction Zone			
Number in 88.7 years	130	46	7
Mean repeat time (years)	0.7	1.9	11.3
Time since last event (years)	2.5	4.6	20.6
Time for 95% of cases (years)	1.9	5.7	22.3
Date of the last event	2-14-83	1-30-81	2-4-65
S.E. Alaska Transform Zone			
Number in 88.7 years	28	10	3
Mean repeat time (years)	3.4	8.5	28.7
Time since last event (years)	6.6	6.6	27.1
Time for 95% of cases (years)	9.0	25.3	77.1
Date of the last event	2-28-79	2-?3-79	7-10-58
Central Alaska Seismic Zone			
Number in 88.7 years	17	6	0
Mean repeat time (years)	5.2	13.5	>100
Time since last event (years)	16.8	27.4	>100
Time for 95% of cases (years)	13.8	30.1	>265
Date of last event	10-28-68	4-7-58	?
All of Alaska			
Number in 88.7 years	175	62	10
Mean repeat time (years)	0.5	1.4	8.6
Time since last event (years)	2.5	4.6	20.6
Time for 95% of cases (years)	1.3	4.2	20.3
Date of last event	2-14-83	1-30-81	2-4-65

NOTES

1) The data base for these calculations is the catalog of $M_s > 7.0$ events based on the papers of Abe and Noguchi given in Table 2 augmented by data for the period Jan. 1981 - Aug. 1985 from the National Earthquake Information Service (NEIS).

2) The statistics for M_s 6.5 are calculated from the Gutenberg and Richter relation: log N = a - b M, assuming a "b" value of 0.9 and using the data for $M_s > 7.0$ events from Table 2 for the period 1897 - 1980.

3) The mean repeat time for $M_s > 6.5$ is 88.7 years divided by the number of events during that period; for $M_s > 7.0$ and $M_s > 7.8$ it is the average of the observed interevent times, including the time since the last event as one of the interevent times.

4) The "time for 95% of cases" is the mean interevent time plus 1.645 times one standard deviation of the interevent times about the mean.

Figure Captions

Figure 1. International Seismological Center reports for earthquakes greater than or equal to magnitude 5.5 during the 5-year period from 1976 to 1980.
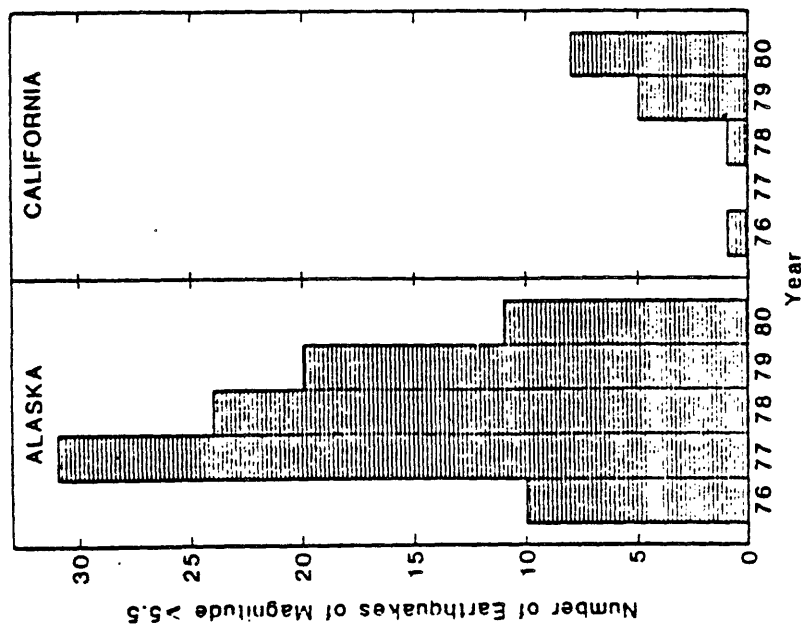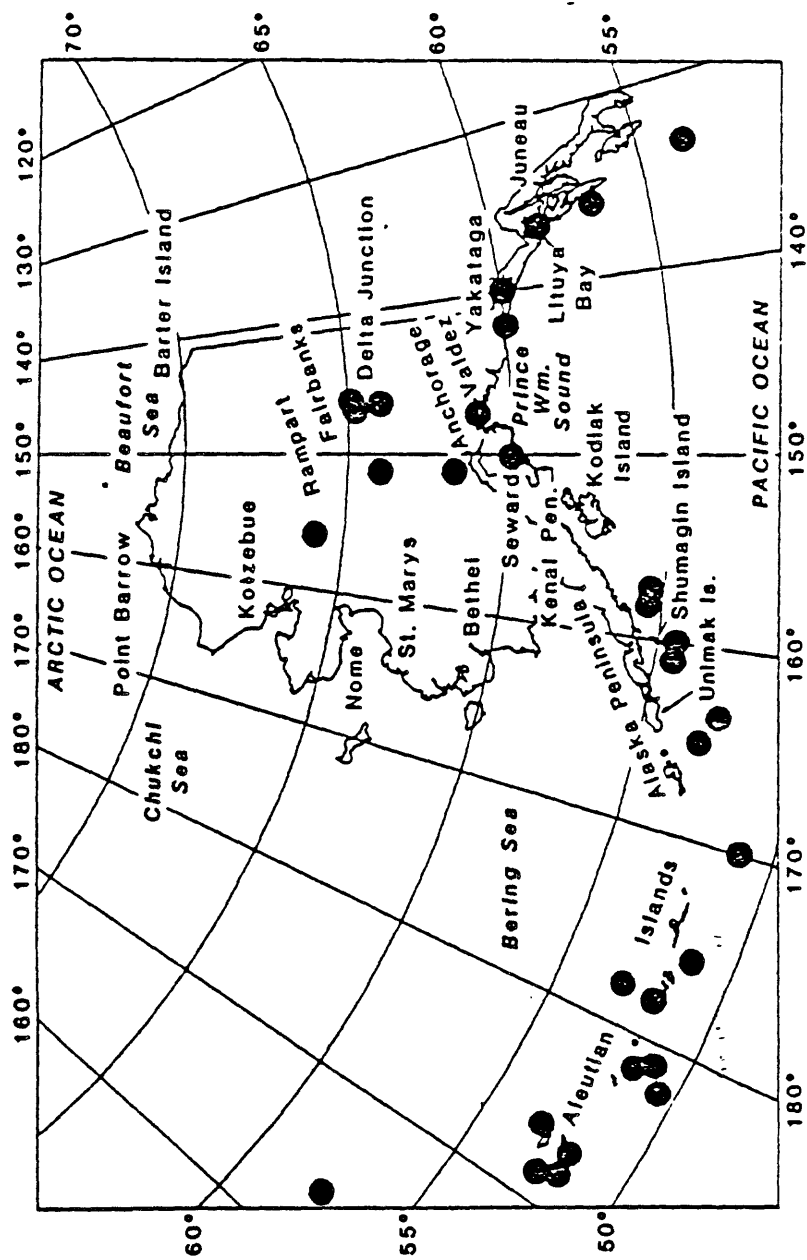
Figure 2. The dots show the epicenter locations of all shallow (depth less than 70 km) earthquakes in Alaska of magnitude 7.2 or more from 1897 through 1980. The map shows 31 events, but two dots in the Yakutat-Yakaaga area actually represent two events each, and two in the westernmost Aleutians are off the map. The 83-year record thus indicates that Alaska had 35 earthquakes of at least magnitude 7.2, or one every 2.3 years.

Figure 3. Histogram of the number of large, shallow earthquakes in Alaska, 1897-1980. In the top graph six events are plotted with $M_s \geq 8.0$; in the bottom graph 66 events with $M_s \geq 7.0$ are plotted. The ratio of about 10:1 for the number of events with $M_s \geq 7.0$ vs. those with $M_s \geq 8.0$ implies the record of $M_s \geq 7.0$ is probably complete. This assumes that all events of $M_s \geq 8.0$ have been detected and that the "b" value for all of Alaska is close to 1; both reasonable assumptions. Note, also that the distribution in time of the $M_s \geq 7.0$ events is reasonably uniform. The data for this histogram are from Abe and Noguchi; see Table 2 for references.

Figure 4. Stress trajectory map from Estabrook, (1985). Stress trajectories, heavy broken lines, after Nakamura et al (1980). Earthquake epicenters for $M \geq 6.0$ events, solid dots, from National Earthquake Information Service (NEIS). The 50 km depth contour of the Wadati-benioff zone, medium heavy lines, from Stone (1983) and Stephens et al (1984). The RM-1 line and the plate convergence rate are after Minster et al (1974). The rigid indentor, shown by stippled area between the trench and the 50 km depth contour, is after Davies (1983).

Figure 5. Focal mechanisms in Interior Alaska, from Gedney (1982). Mechanisms are shown by lower hemisphere, stereographic plots of first-motion directions where the shaded quadrants represent compressions and the unshaded represent rarefactions.

Figure 6. Focal mechanisms in Northern Alaska from Estabrook (1985). Mechanisms are as shown in Figure 4. Also shown are $M \geq 4.0$ earthquakes, open circles (NEIS); and faults after King (1969). Mechanisms are plotted with north up, not parallel to the map grid.

Figure 7. Focal mechanisms in Western Alaska, from Biswas (1985). Mechanisms are upper hemisphere, sterographic plots of first-motion where the shaded quadrant represent rarefactions and the unshaded ones represent compressions.

Figure 8. Epicenter map for northern Alaska from Estabrook (1985). The open circles represent epicenters for all $M \geq 5.0$ events in the NEIS files for this region through 1983.

Figure 9. Epicenter map for northern Alaska from Estabrook (1985). The open circles represent epicenters for all $M \geq 3.0$ events for the years 1976-1979, a time period of relatively good station coverage.

Figure 10. Epicenter map for northern Alaska from Estabrook (1985). The
open circles represent the relocated epicenters of all earthquakes
located by the Geophysical Institute for the period 1967-1983. Note NW-
SE trending lineation of epicenters at about 65.5 N and 145 W which is
coparallel with the trace of the Tintina Fault.

Figure 11. Map of major fault systems in Alaska from Estabrook (1985) after
Stone (pers. comm., 1985).

Figure 2. The dots show the epicenter locations of all shallow (depth less than 70 km) earthquakes in Alaska of magnitude 7.2 or more from 1897 through 1980. The map shows 31 events, but two dots in the Yakutat - Yakataga area actually represent two events each, and two in the westernmost Aleutians are off the map. The 83-year record thus indicates that Alaska had 35 earthquakes of at least magnitude 7.2, or one every 2.3 years.

Figure 1. International Seismological Center reports for earthquakes of magnitude ≥ 5.5 during the 5-year period from 1976 to 1980.

LARGE SHALLOW EARTHQUAKES IN ALASKA 1897-1980
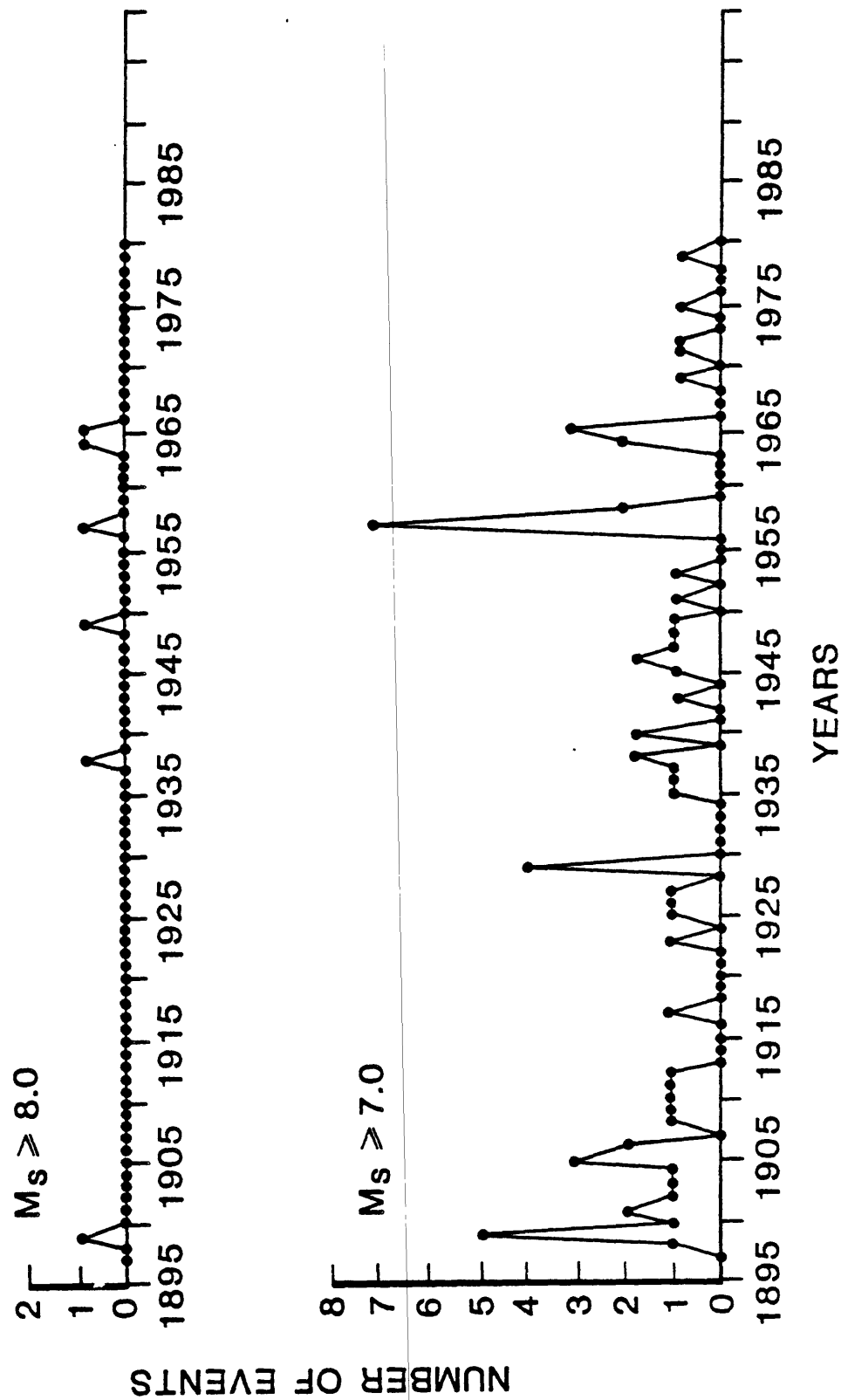
Figure 3
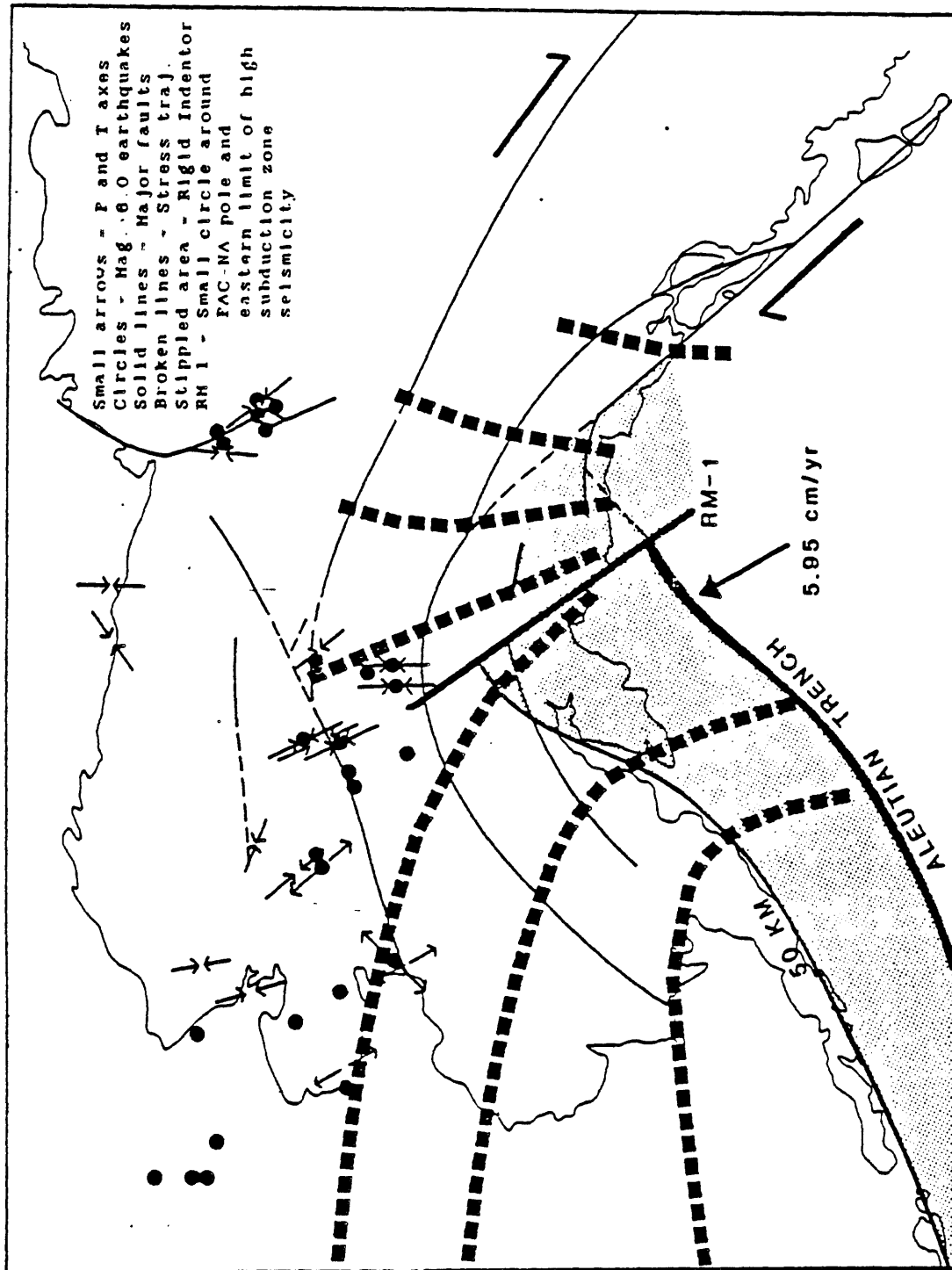
Figure 4. Model proposed for deformation of continental Alaska and northwest Canada. The exact boundaries of the "Rigid Indentor" are speculative. The 50 km Wadati-Benioff Zone contour of Stephens et al. (1984) and Stone (1983). Pacific-North America pole of rotation (RM-1) is from Minster et al. (1974). The convergence rate is from Stone (1983). Stress trajectories are from Nakamura et al (1980). earthquakes are from NEIS. faults are from Stone (pers.comm. 1985). Large arrows represent shear zone discussed in the text.

Small arrows - P and T axes
Circles - Mag. .6.0 earthquakes
Solid lines - Major faults
Broken lines - Stress traj.
Stippled area - Rigid Indentor
RM 1 - Small circle around
FAC-NA pole and
eastern limit of high
subduction zone
seismicity

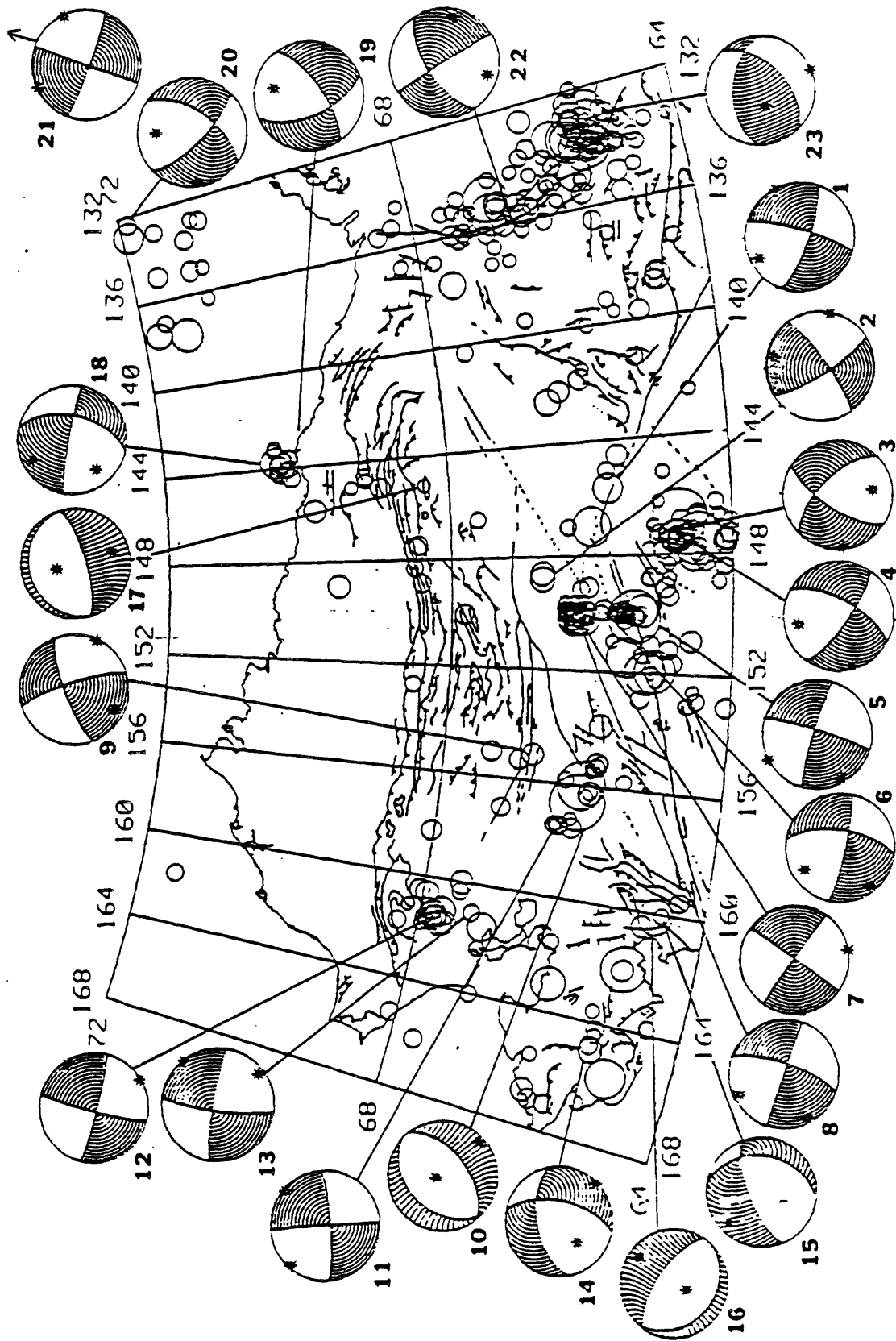ALEUTIAN TRENCH

RM-1

5.95 cm/yr

50 KM

Figure 5

31
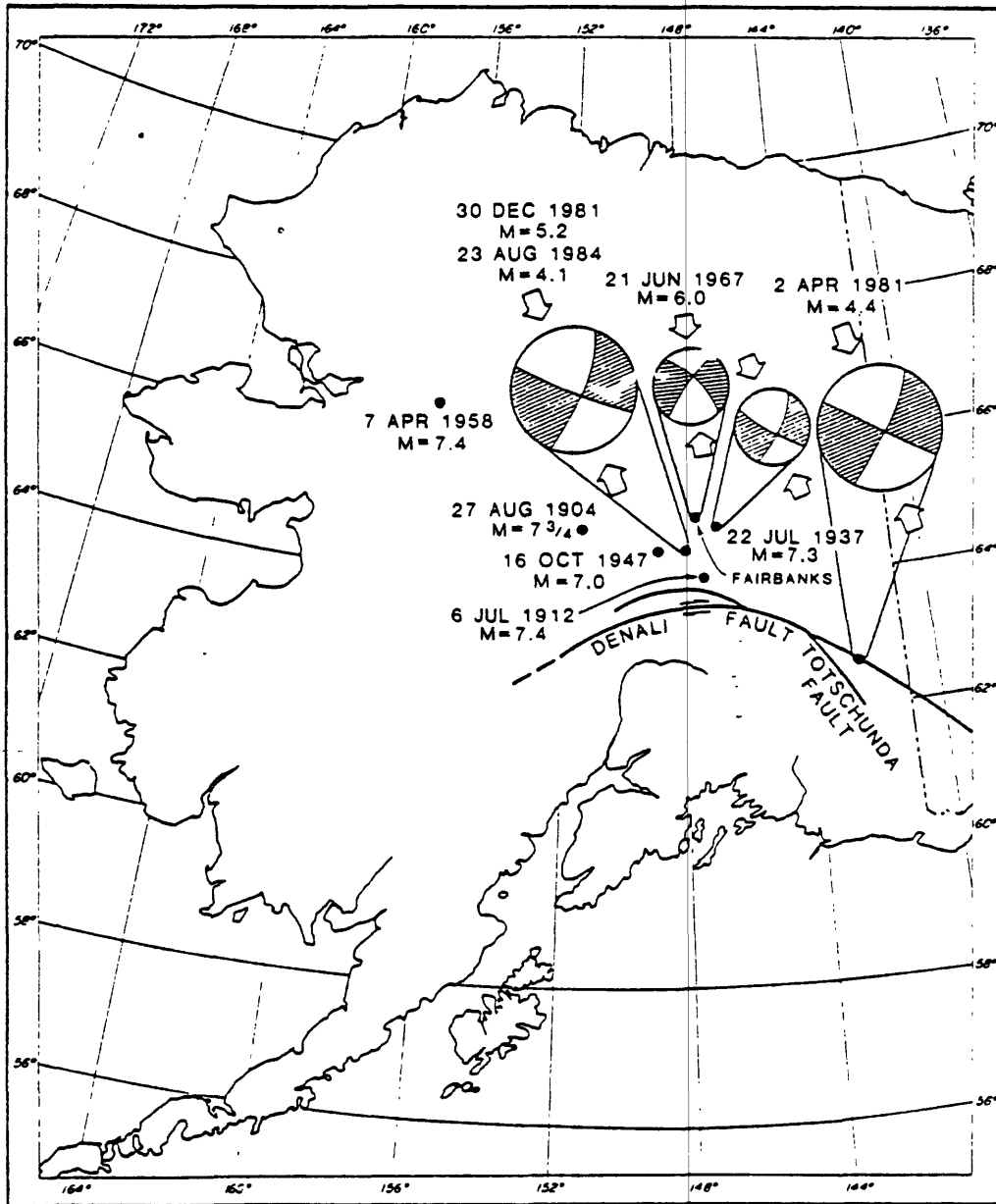
Figure 6 Map showing fault plane solutions, mag. 4 and larger earthquakes (source NEIS) and geologic faults (after King, 1969). Fault plane solutions are equal-area lower hemisphere projections showing quadrants of compressional (shaded) and tensional first motion, containing the T and P axes respectively Mechanisms are oriented with north parallel to the right edge of the paper, not parallel to map north
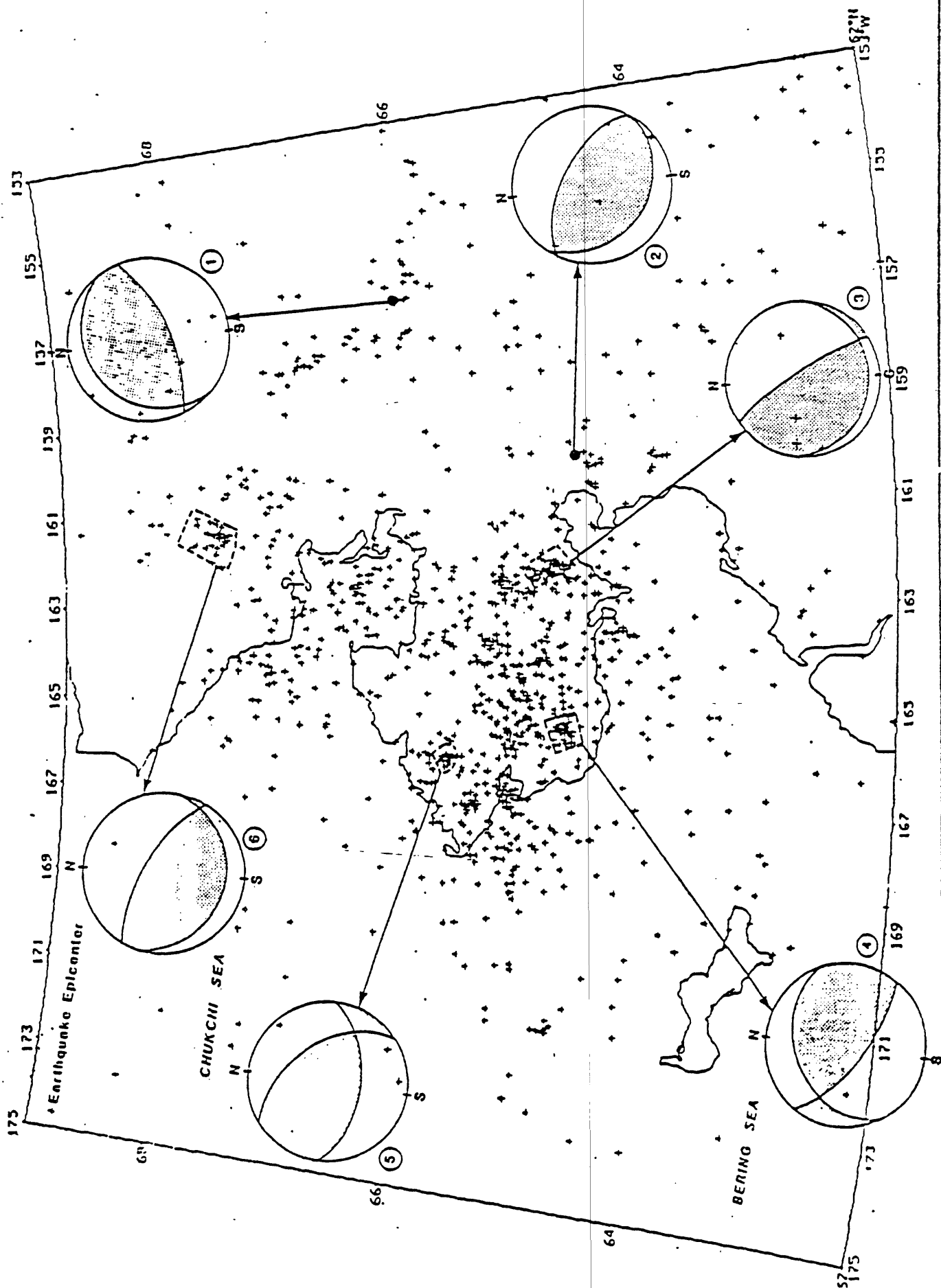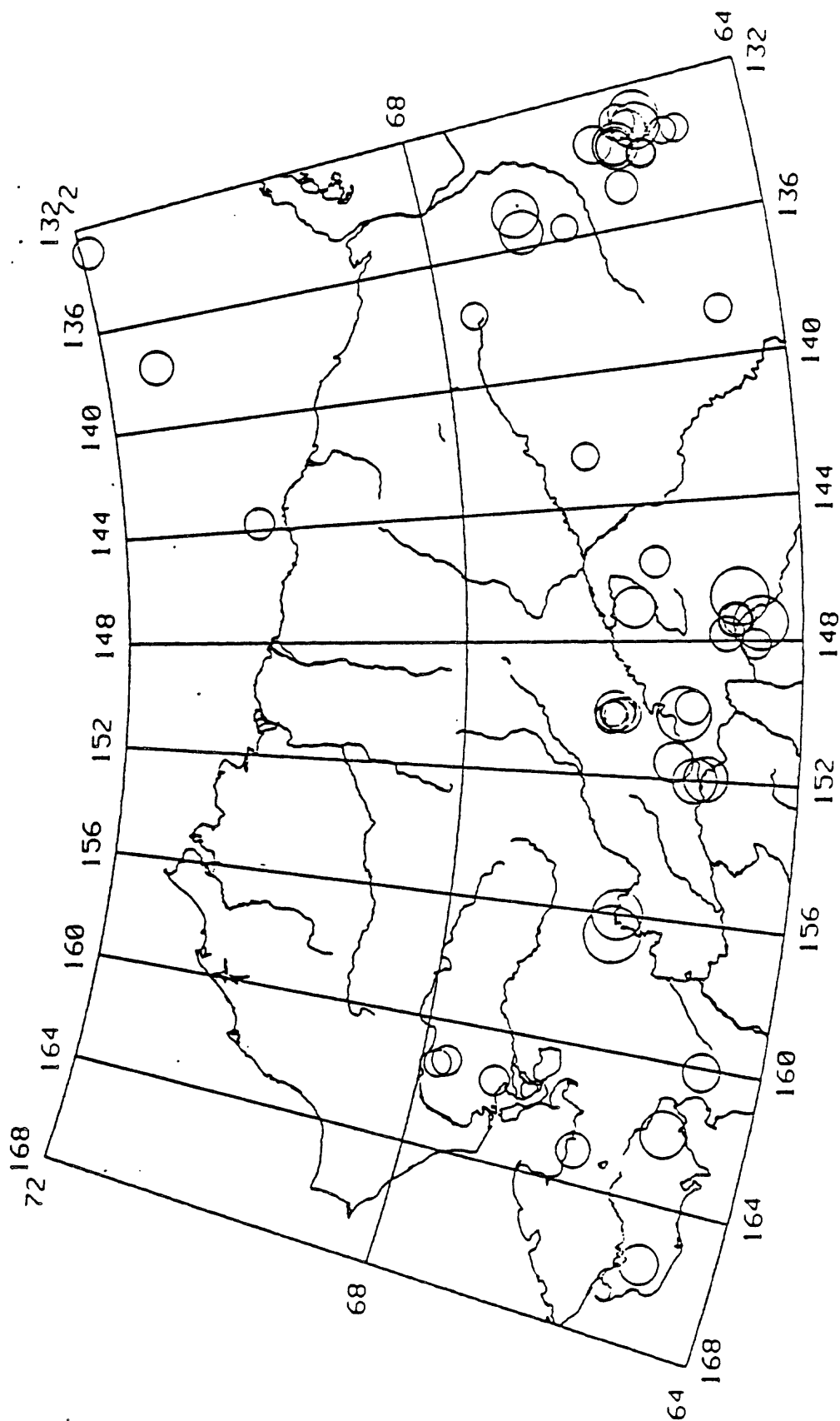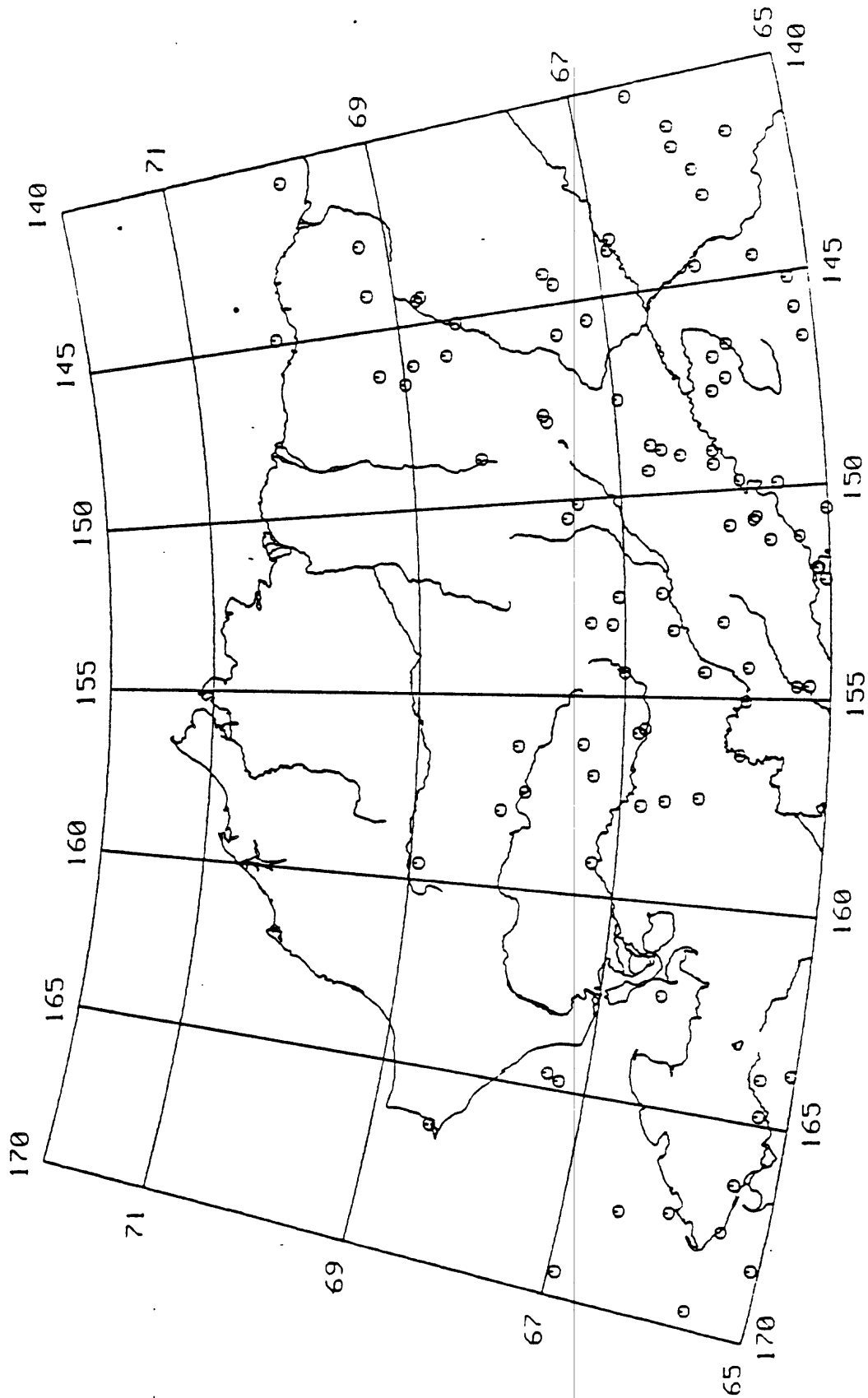
Figure 7

Figure 8

Figure 9   Earthquakes with magnitudes greater than 3 for
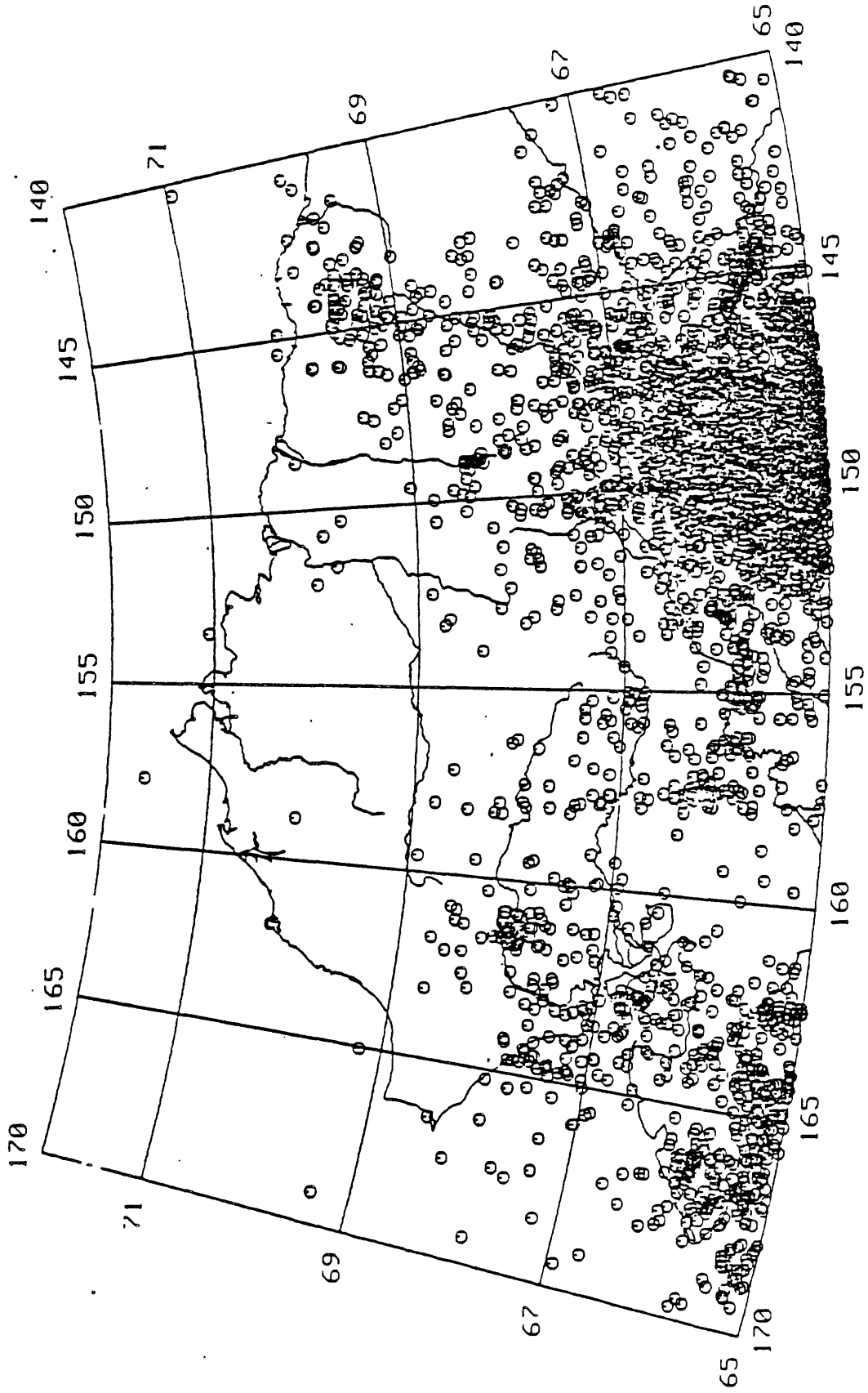the years 1976 to 1979.   Source this study.

Figure 10

Arctic Ocean

Bering

Sea

Pacific Ocean

BROOKS RANGE

SEWARD PENINSULA

RICHARDSON MTS

ALASKA RANGE

ALEUTIAN TRENCH

EL
P
KT
K
CH
INF
FW
CM
HC
S
D
BR
C
TC
YB
F
CS
Q
T
D

BR Border Ranges Fault
C   Contact Fault
CB Chitina Bay Fault
CM Castle Mountain Fault
CS Chilkat Straits Fault
D   Denali Fault
EL Eskimo Lake Fault
F   Fairweather Fault
FW Farewell Fault
HC Hines Creek Fault
INF Iditarod-Nixon Fork Fault
K   Kaltag Fault
KT Kobuk Trench
P   Porcupine Lineament
Q   Queen Charlotte Fault
T   Tintina Thrust
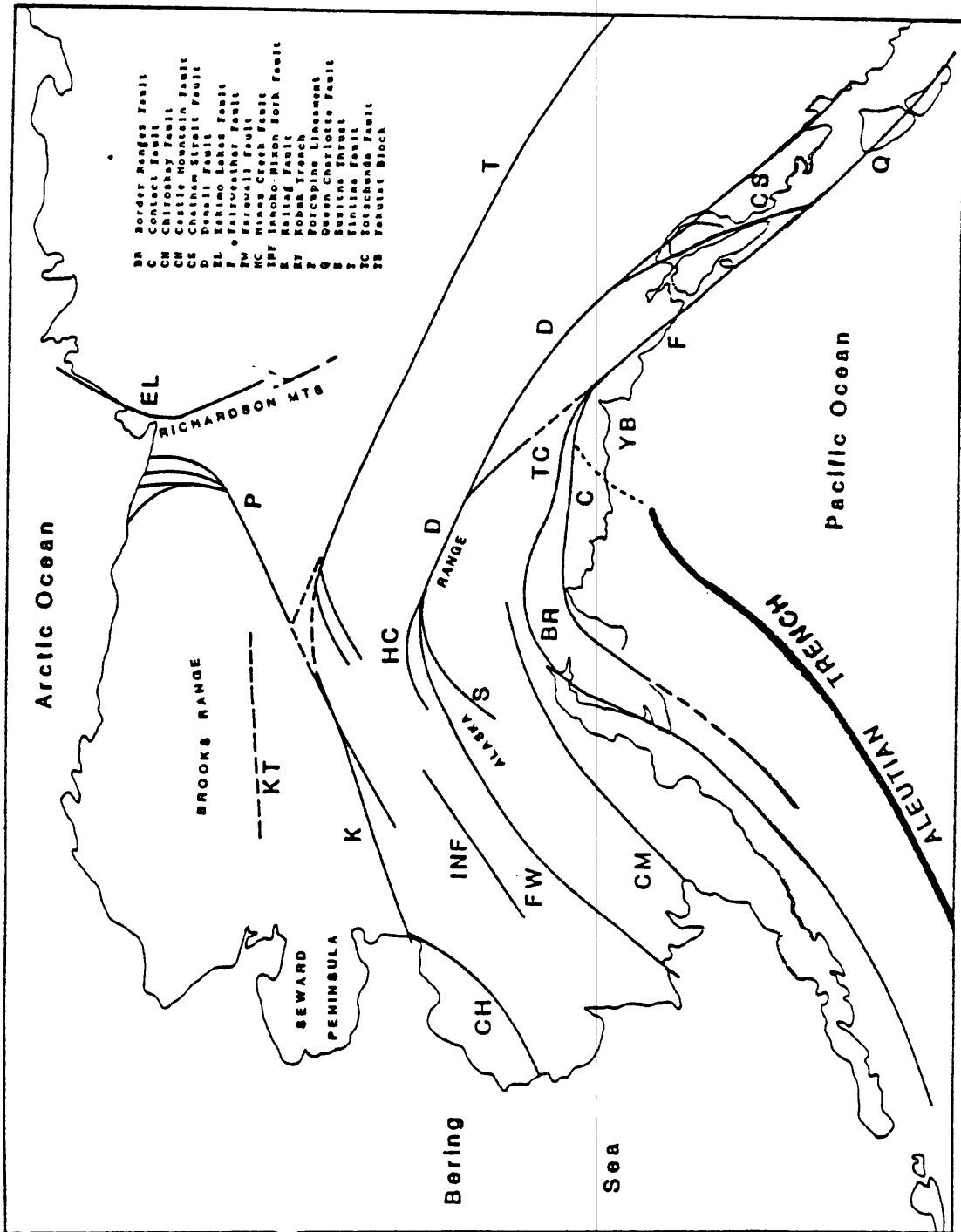TC Tintina Fault
TL Totschunda Fault
YB Yakutat Block

Figure 1; Map of major faults in Alaska. After Stone (pers. comm., 1985).

APPENDIX A. 2.

Results from Earthquake Research on the Alaska Aleutian Seismic Gap

K. Jacob, J. Taber, and T. Boyd

RESULTS FROM EARTHQUAKE RESEARCH ON THE ALASKA ALEUTIAN SEISMIC ZONE WITH SPECIAL FOCUS ON THE SHUMAGIN ISLANDS SEISMIC GAP

Klaus Jacob, John Taber, and Tom Boyd
Lamont-Doherty Geological Observatory of Columbia University
Palisades NY 10964

Extended Abstract

High probabilities in the Eastern Aleutians

Various estimates of the long-term probabilities for the occurrence of great earthquakes (Mw ≥ 7.8) in the Alaska-Aleutian seismic zone reveal a broad region in the Eastern Aleutian with moderate to high probabilities for great earthquakes during the next two decades (Figure 1). The probabilities range from less than 30% to more than 90% for the 20 year period from 1985 to 2005 (Jacob, 1984). These values are among the highest probabilities presently observed in the entire U.S. for great earthquakes. They are distinctly higher than the 5 to 30% probability range obtained for the adjacent zones that ruptured in 1964 and 1957 by Mw = 9.2 and Mw ≤ 9 earthquakes, respectively. The high-probability region in the Eastern Aleutians is centered on the Shumagin Islands Seismic Gap and covers the zones of the 1938 (Mw=8.2) rupture, the Shumagin Seismic Gap, the 1946 (Ms=7.4, Mt=9.3) highly tsunamigenic event, and possibly the Unalaska Seismic Gap, a 200 km long segment that may or may not have broken in the 1957 (Mw =9) rupture.

Local studies in the Shumagin Seismic Gap

The broad region of the Eastern Aleutian probability high is about 1000 km long, of which only the central 300-350 km long segment within the Shumagin Islands Seismic Gap is being currently monitored. Monitoring in this section of the arc includes a high-gain seismic network, strong motion stations, precision level lines, a tiltmeter and sea level gauges. Net strain is also calculated using laser distance measurements collected every two years by the USGS. The Shumagin seismic network consists of 18 telemetered stations with a variety of instrumentation (Figure 2) so that earthquakes can be recorded onscale over a wide range of magnitudes. There are also 12 strong-motion accelerographs (Kinemetrics SMA-1, 1g), 10 of which are co-located with seismic stations.

Figure 3 shows a map view and cross section of well located earthquakes recorded by the Shumagin network since 1979. There is relatively little activity along the shallow part of the main thrust zone but there is a cluster of events at the lower end of this probably locked zone. Below 40 km there is a clear double Benioff zone, with most of the events occurring in the upper plane. The apparent bend in the slab at ~130 km is due mainly to mislocations arising from the relatively high velocity of the descending slab (Hauksson, 1985).

The upper crustal seismicity is also concentrated above the downdip edge of the main thrust zone. This forms a band of seismicity parallel to the mainland and about 100 km offshore. There is very little shallow seismicity on the mainland itself. Further west, in the area of the 1946 Ms=7.4 event, the rate of seismicity increases and the events are spread over a larger portion of the distance between the volcanic arc and the offshore trench.

Quiescence. In the Shumagin Seismic Gap a reduction in the rate of moderate-magnitude seismicity (M ≥ 5.5) has been observed since 1979 (Hauksson et al, 1984). This reduction has now become significant at the 98-99%

confidence level according to the Z test as used by Habermann (1981). The level of significance depends on the choice of endpoints for the gap. Figure 4 shows the location of both 5.5+ events (solid circles) and all other events ≥ 5.0. The cumulative rate is shown in Figure 5 while a time vs distance plot is shown in Figure 6. The latter plot shows that while the decrease is statistically significant, there are other periods of quiescence for only slightly shorter time periods and arc segments that did not end in a major earthquake. A more statistically significant rate change is shown in Figure 7 for a smaller section of arc and a smaller minimum magnitude. This arc length corresponds in part to the aftershock zone of the 1946 Ms=7.4 earthquake. In both cases the sampling period is too short to allow us to make a prediction based merely on the time since the rate change.

Effects of a deep slip event. Changes in focal mechanisms, rates of seismicity and volcanicity were observed in the Shumagin segment of the arc since 1978 and correlated in time approximately with a tilt reversal observed between 1978 and 1980 (Figure 8)(Beavan et al. 1983). These events were interpreted as being jointly related to a deep-seated (at 30-80 km depth) slip event in which the descending slab slipped down-dip by about 80 cm beneath the overriding plate, but remained locked to the upper plate at the shallow thrust interface. If this interpretation is correct, then the shallow locked portion of the thrust zone may have been further stressed by the deep-seated slip event. The 80-cm slip amplitude corresponds to about 10 years of accumulated plate motion. Recent refinements show that the seismicity rate changes from this event may have been restricted to the 150 km long central portion of the gap (Figure 9), and thus the slip event may have been also limited to this portion of the gap.

During the slip event (1978-80) the state of stress in the descending slab (at depths 50-120 km) was inferred from composite focal mechanisms. Downdip-tension dominated in the upper zone and downdip-compression in the lower zone of a double-planed seismic zone (Reyners and Coles, 1982). This stress pattern is opposite what is usually observed globally in double-planed Benioff zones, including the Aleutians (Figure 10)(House and Jacob, 1983). Normally the upper zone shows downdip compression and the lower one downdip tension, which is in accordance with both unbending and thermal stress calculations (House and Jacob, 1982). The anomalous stress pattern was originally interpreted as an anomaly or a possible precursor to an impending rupture and was thought to be related to the dominance of slab pull over unbending, while the shallow thrust zone remains locked. Composite focal mechanisms for 1981 (after the termination of the slip event) showed that the stress pattern almost reversed to what is globally typical (Hauksson, et al. 1984). Events consistent with down-dip tensional focal mechanisms were not as frequent in the upper seismic zone as they were during the slip event (Figure 11). The change in focal mechanisms may have been due to the relaxation of stresses in the slab after the slip event. Focal mechanisms from 1982-1984 are similar to the results from 1978-79, i.e. primarily downdip tension in the upper plane, though as in the 1981 data set, the composite results are not as consistent as the results from events that occurred during the slip event. If the pattern repeats itself, a lining up of down-dip tension axes would be expected before or during the next slip event. The monitoring of these stress patterns continues and may be used for comparison with tilt (leveling) data to identify future slip events, one of which may trigger, or accelerate into, a larger rupture at the locked shallow thrust zone.

Stress Drops. Two moderate sized (M~6) high stress drop events (600-900 bars) were observed at the 40 km downdip end of the main thrust zone in 1974 (House and Boatwright, 1980). In 1983 two moderate stress drop events (70-80 bars, Ms =5.9 and 6.2) were observed at 26 km depth at the eastern edge of the

Shumagin Seismic Gap. Obviously neither sequence triggered a larger rupture. The earlier sequence of events occurred before the proposed 1978-79 slip event. If the slip event brought the shallow portion of the thrust zone closer to failure, one might have expected the later sequence of events to produce even higher stress drops. The later events occurred, however, at a much shallower depth (Figure 12) and thus it appears that high stresses are limited to the base of the thrust zone.

Short-term vs. Long-term Potential of the Shumagin seismic gap. At present we consider that the computed conditional probabilities for great earthquakes in the Shumagin Gap constitute a long-term moderate to high level of earthquake potential for great events. The mentioned onset of "quiescence" for M > 5.5 earthquakes in 1979/80 could be a candidate for a medium-term precursor, but not knowing what false alarm probability should be assigned to quiescence, we do not know how much, if at all, this quiescence constitutes a temporary probability gain. If another tilt or slip event should occur in the future, we may assign a possible false to true alarm rate of 8:1, based on the assumption that slip events release 10 years worth of plate motion at depth, and that the average recurrence times for great earthquakes is 80 years. Thus on average every 8th event should trigger a great earthquake. Other than a 1 year quiescence of Pavlof volcano, we do not have any data suggesting that another slip event is about to begin. Thus we do not think that at present we have any evidence of short-term or even of intermediate-term precursors for an impending great Shumagin earthquake. Since the other regions in the Eastern Aleutian probability high are presently unmonitored, except for teleseismic activity, we do not know whether any intermediate to short term precursors have taken place there. But if they do occur there and only there, and if they precede a rupture that extends then into the Shumagin Gap, we may not be able to predict such a Shumagin-Gap-rupturing event.

Maximum Sizes of Future Events. Various scenarios must be considered for future great events in the Shumagin Gap proper, and for the entire Eastern Aleutian probability high. Depending on whether and how much the Unalaska Gap broke in 1957, 1902, 1878, or earlier (prior to 1776), the Unalaska segment may at present sustain at most a Mw=8.0 to 8.6 event, unless it is a permanent seismic gap with aseismic release of plate motion, a most unlikely possibility (Boyd and Jacob, 1986).

The 1946 event off Unimak Island had an apparently low seismic moment release (Ms=7.4), but may have triggered a large underwater landslide leading to a gigantic tsunami (Mt=9.3)(e.g. Davies et al.,1981). If this assumption is correct the <150 km long section off Unimak may at present be able to sustain a Mw=8-8.5 event.

The 300-350 km long Shumagin segment ruptured in great earthquakes, either entirely or partly, during the July and August 1788 events, in 1847, perhaps (but not likely) in 1903 (M=8.3?, depth=100km?, uncertain location probably farther east), in 1917 (Ms<7.8?), and had its last large (7.5) earthquake in 1948 (Figure 13)(Davies et al, 1981). Given the low moments of the two most recent events, and assuming that the 1903 event did not rupture the shallow thrust zone, the maximum event that the entire gap may sustain is probably near Mw=8.6 to 8.8.

The ~300 km long segment of the 1938-rupture (Mw=8.2) should be able to sustain a Mw<8.5 event.

Several of the adjacent high-probability regions may rupture together and thus their moments could be combined to give higher magnitudes than the ones quoted. For instance, the July 1788 event may have broken the Kodiak section

of the 1964 event, the 1938 segment, and the eastern half of the Shumagin Gap, probably representing a Mw=8.7-8.8 earthquake. In an extreme scenario one may consider the unlikely case that the entire Eastern Aleutian high-probability zone from west of Kodiak to Unalaska will break in a single giant event; we estimate its magnitude could measure Mw≑8.9 to 9.0.

Miscellaneous arc-wide observations

Moment Release. The 3800 km long plate boundary between Yakutat Bay and Kamchatka had a moderate cumulative seismic moment release ($\sim$25x10^{28} dyn-cm) during the period 1898-1907, low seismic release (<15x10^{28} dyn-cm) from 1908 to 1956, very high moment release ($\sim$100x10^{28} dyn-cm) from 1957 through 1965, and practically none (<1x10^{28} dyn-cm) during the last 20 years (1966-1985). Except perhaps for a 22-year period from 1907 to 1929, that may or may not have been shortened by a possible 7.8 event in 1917 near the Shumagin Islands, never since the beginning of the instrumental record in 1898 has the Aleutian arc been quiescent for great earthquakes for as long as in the last 20 years (Figure 14). Thus an increase in major activity is likely in the future somewhere in the arc. Besides the Eastern Aleutians, the Yakataga and Kommandorski seismic gaps are estimated to be the most likely future sites of great earthquakes. A possible $\sim$150 km long seismic gap in the Queen Charlotte Sound segment, south of the 1949 rupture zone, has been suggested by Canadian researchers.

Repeat times. The combined historic and instrumental seismicity record of large and great earthquakes for the entire Alaska-Aleutian arc, when analyzed as a single data population irregardless of systematic regional differences, suggests that on average one Mw=7.8 event should occur every 60±20 years per 300-km arc segment, or one Mw=9.2 event every 360±100 years per 800-km arc segment. Average repeat times for any great earthquake (Mw≥7.8) are expected to recur (at the same arc segment) about every 80 years, but one standard deviation from the mean allows a range of $\sim$45 to 135 years. The data also suggest that only a 5% probability that great earthquakes repeat earlier than 30 years and longer than 200 years. This result needs to be reconciled with geologic observations of ages of uplifted marine terraces (e.g. on Middleton Island) and interseismic subsidence rates from sediments that have been interpreted to indicate that repeat times of several hundred years, and coseismic slip of a few tens of meters are not uncommon there.

Interseismic moment rates and extrapolations to great earthquakes. Figure 15 shows the moment-release rate of shallow (<50 km deep) seismicity along the entire northern Pacific plate boundary over the past 16 years. During this time interval there have occurred no great earthquakes along the Alaska-Aleutian arc. These moment-release rates, therefore, are due to interseismic background activity. Except locally, the moment-release rate due to interseismic processes is from 1 to 2.5 orders of magnitude lower than the rates estimated from plate-kinematic parameters. The latter usually measure several 10^{24} dyn-cm/yr/km arc length, while the former measure between a few 10^{22} to 10^{23} dyn-cm/yr/km.

Since the interseismic activity is accommodating very little moment-release along the main plate boundary, b-values estimated from individual arc segments for this short-term data set cannot be extrapolated to obtain the correct recurrence rates of the great events which relieve most of the moment accumulation along the arc. If one did, the estimated repeat times for the great events would be too long. Similar observations were initially made by Wesnousky et al. (1983) for Japanese intraplate earthquakes and have been extended to the Alaska-Aleutian arc by Davison and Scholz (1985).

Characteristic Length of Seismotectonic Blocks. Strong spatial fluctuations in the interseismic seismicity during the last 16 years are observed not only between but also within the rupture zones of the most recent series of great earthquakes. A typical wavelength of these seismicity fluctuations measured along the arc is about 150 km. This wavelength does not appear to be an artifact of the moving average window length (90 km), although we can not rule out the possibility that it is due to poor spatial sampling of the release rate along the arc. If, however, this periodicity is inherent in the data, it may be delineating the characteristic length of the seismotectonic building blocks along the northern Pacific plate boundary.

If the latter is the case, great earthquakes rupturing along this plate boundary break several seismotectonic blocks. For example, the 1964 and 1957 rupture zones are much longer than 150 km and are characterized by large amounts of interseismic moment-release near their western extremes and small amounts in their central portions. This observation may relate to differential slip occurring between these blocks during the respective great earthquake. If this is the case, one would expect different times to elapse before the next great earthquake not only for different rupture zones, but also for different sections within any one previous rupture zone. As a consequence of this, the next series of great earthquakes to affect the northern Pacific plate boundary may define different rupture zones from those observed during the previous series.

REFERENCES

Beavan, J., E. Hauksson, S.R. McNutt, R. Bilham, and K.H. Jacob, Tilt and seismicity changes in the Shumagin seismic gap, Science, 222, 322-325, 1983.

Boyd, T.M., and K. Jacob, Seismicity of the Unalaska Region, Alaska, submitted to Bull. Seismol. Soc. Am., 1986.

Davies, J., L. Sykes, L. House, and K. Jacob, Shumagin seismic gap, Alaska Peninsula; History of great earthquakes, tectonic setting and evidence for high seismic potential, J. Geophys. Res., 86, 3821-3856, 1981.

Davison, F.C., and C.H. Scholz, Frequency-moment distribution of earthquakes in the Aleutian Arc: A test of the characteristic earthquake model, in press, Bull. Seismol. Soc. Am., 1985.

Geller, R.J., Scaling relations for earthquake source parameters and magnitudes, Bull. Seismol. Soc. Am., 66, 1501-1523.

Habermann, R.E., Precursory seismicity patterns: Stalking the mature seismic gap, in Earthquake Prediction, An International Review, Maurice Ewing Series, 4, edited by D.W. Simpson and P.G. Richards, pp. 29-42, AGU, Washington, D.C., 1981.

Hauksson, E., Structure of the Benioff zone beneath the Shumagin Islands, Alaska: Relocation of local earthquakes using 3-D ray tracing, J. Geophys. Res., 90, 635-649, 1985.

Hauksson, E., J. Armbruster, and S. Dobbs, Seismicity patterns (1963-1982) as stress indicators in the Shumagin seismic gap, Bull. Seismol. Soc. Am., 74, 2541-2558, 1984.

House, L., and J. Boatwright, Investigation of two high stress-drop earthquakes in the Shumagin seismic gap, Alaska, J. Geophys. Res., 85, 7151-7165, 1980.

House, L., and K.H. Jacob, Earthquakes, plate subduction and stress reversals in the eastern Aleutian arc, J. Geophys. Res., 88, 9347-9373, 1983.

Jacob, K.H., Estimates of long-term probabilities for future great earthquakes in the Aleutians, Geophys. Res. Lett., 11, 295-298, 1984.

Purcaru, G. and H. Berckhemer, A magnitude scale for very large earthquakes, Tectonophysics, 49, 189-198, 1978.

Reyners, M. and K. Coles, Fine structure of the dipping seismic zone and subduction mechanics in the Shumagin Islands, Alaska, J. Geophys. Res., 87, 356-366, 1982.

Wesnousky, S.G., C.H. Scholz, H. Shimazuhi, and T. Matsuda, Earthquake frequency distribution and mechnics of faulting, J. Geophys. Res., 88, 9331-9340, 1983.

Figure Captions

Figure 1. Top: Aftershock areas of earthquakes of magnitude M ≥ 7.4 in the Aleu-
tians, southern Alaska and offshore British Columbia from 1938 to 1979. Heavy
arrows denote motion of Pacific plate with respect to North American plate. Two
thousand fathom contour is shown for Aleutian trench. (from Davies et al., 1981)
Bottom: Conditional probabilities for great earthquakes (Mw ≥ 7.8) in all major
segments in the Aleutian arc in the next 20 years. Open blocks and diagonal
hatching are the minimum and maximum values, respectively, calculated from
recurrence times and the slip of the last event. Solid bar is the value calcu-
lated for a Poisson distribution.

Figure 2. The Shumagin seismic network, Alaska. Filled circles are short period,
single (vertical) component stations. The hexagons are short period, three com-
ponent stations. An inverted triangle indicates a low-gain site with a three com-
ponent force-balance accelerometer (FBA). Strong motion accelerographs
(SMA's) are also located at the seismic stations SNK, DRR, DLG, SGB, SAN, NGI,
BKJ, IVF, and CNB. Upward triangles denote SMA's only. At SAN we also operate
a digitally recording PDR-1 strong motion recorder with FBA sensors.

Figure 3. Map view and cross section of well located events recorded by the
Shumagin seismic network from 1979-1984. Note concentration of seismicity at
the base of the main thrust zone and the double Benioff zone beneath it.

Figure 4. All events with Mb ≥ 5.0 and shallower than 70 km as recorded in PDE
catalogue from 1963-84. Solid circles are events ≥ 5.5. The sections of arc from
B to B' and B to B'' correspond to the areas of quiescence shown in Figure 5.
Also shown is the area that displays a reduced rate for events with Mb ≥ 5.2.

Figure 5. Cumulative number of PDE epicenters in the Shumagin region for
earthquakes of Mb ≥ 5.5. Beginning in late 1979 the rate of occurrence of events
is significantly lower at the 99% confidence level.

Figure 6. Time-distance plot of events with Mb ≥ 5.5 that were plotted in the pre-
vious figure. Statistical significance of a reduced rate is 99% for part of the
Shumagin region and 98% for the entire region.

Figure 7. Time-distance plot of events with Mb ≥ 5.2. Statistical significance of a
reduced rate is still 99% but the arc length is much smaller than in the previous
figure.

Figure 8. Tilt, seismicity rates, Pavlof eruptive activity, and deep earthquakes in
the Shumagin region for the time period 1972-1985. At the time of the tilt rever-
sal in 1977-80, the seismicity rate for microearthquakes was higher, Pavlof vol-
cano was not erupting, and most of the teleseismically recorded deep earth-
quakes occurred in a cluster behind Pavlof. Deep earthquakes are from PDE
catalogue with x's being events with no calculated magnitude.

Figure 9. Top: Subdivision of the Shumagin gap into 3 subregions. Bottom: The
cumulative number of events in each of the boxes in the top figure is plotted
against time for the period 1979-1984. The rate decrease in 1979 in region B at
the end of the tilt reversal is not evident in regions A and C.

Figure 10. Side view of well-located intermediate-depth earthquakes and focal mechanisms for the Aleutian arc from 155-176° W. Focal mechanisms are plotted in back hemispheres. Larger symbols denote earthquakes with recalculated depths. Depths of remaining earthquakes are from the ISC, based on reported pP arrivals. Symbol types distinguish events within the western (triangles, 172-176°), central (squares, 162-172°), and eastern (circles, 155-162°) segments of the Aleutian arc. Magnitudes range from 5.5 to 6.5. Earthquakes are plotted with reference to the volcanic line. The dotted line indicates the approximate location of the inferred main thrust zone. Dashed line connects earthquakes inferred to be within the lower zone of seismicity. (Figure from House and Jacob, 1983.)

Figure 11. Composite focal mechanisms for intermediate depth events that are part of the double Benioff zone in the Shumagins. Left: Upper and lower zone mechanisms calculated by Reyners and Coles (1982). The upper zone exhibits downdip tension while the P axis lies within the plane of the lower zone. Dotted lines show the trace of the dipping plane. Right: Mechanisms calculated by Hauksson et al.,(1984) after the proposed slip event. P and T axes appear to be reversed from the 1979 results but note that the upper and lower planes are not clearly separated (x's are events defined to be in the lower plane for the purpose of the focal mechanisms) and the number of inconsistent polarities is much higher.

Figure 12. Cartoon showing relative locations of high and average stress drop events. The high stress drop events occurred at the base of the locked main thrust zone while the average stress drop events were located at a much shallower depth.

Figure 13. Space-time plot of instrumental (1898 to 1982) and historical (1788 to 1897) seismicity of the Aleutian arc for great (Mw≥7.8) earthquakes. We have omitted a Mw=7.9 event in 1929 that occurred presumably as normal faulting in the trench near the eastern end of the 1957 rupture zone. Each event is labeled by year, Mw, and where applicable for historic events, tsunamis reported (T). Magnitudes computed for historic events from 'time-predictable', plate kinematic models are indicated in parenthesis. Uncertain rupture zones are indicated by broken lines.

Figure 14. Seismicity (Mw ≥ 7) of the Aleutian arc (140°W to 169°E versus time for the instrumental period 1898 to 1985. Top: The number of events per year is differentiated for great (Mw ≥ 7.8) and large (Mw < 7.8) events by solid and hatched symbols, respectively. Bottom: Histogram for the periods (years) between subsequent great earthquakes (Mw ≥ 7.8 along the arc. Note the long recent quiescence of 20 years.

Figure 15. Bottom: Map indicates the epicentral locations of the shallow (depth ≤ 50.0 km) thrust-zone earthquakes with mb ≥ 5.0 occurring along the Alaska-Aleutian arc from 1968 through 1984. Numbers indicate the distance along the arc in thousands of kilometers and are for reference to the top figure. Top: Plot of the interseismic moment-release rate along the arc as determined from the events plotted in the lower figure. Moments were determined from Ms using the relationship between Mo and Ms of Purcara and Berckhemer (1978). If no Ms was reported, mb was converted to Ms using the relationships derived by Geller (1976). The moment rate was smoothed with a 90 km long, trapezoidal moving average window. Solid horizontal lines are the predicted moment-release rates from plate kinematics, while dashed horizontal lines are the average rates determined from the interseismic activity.
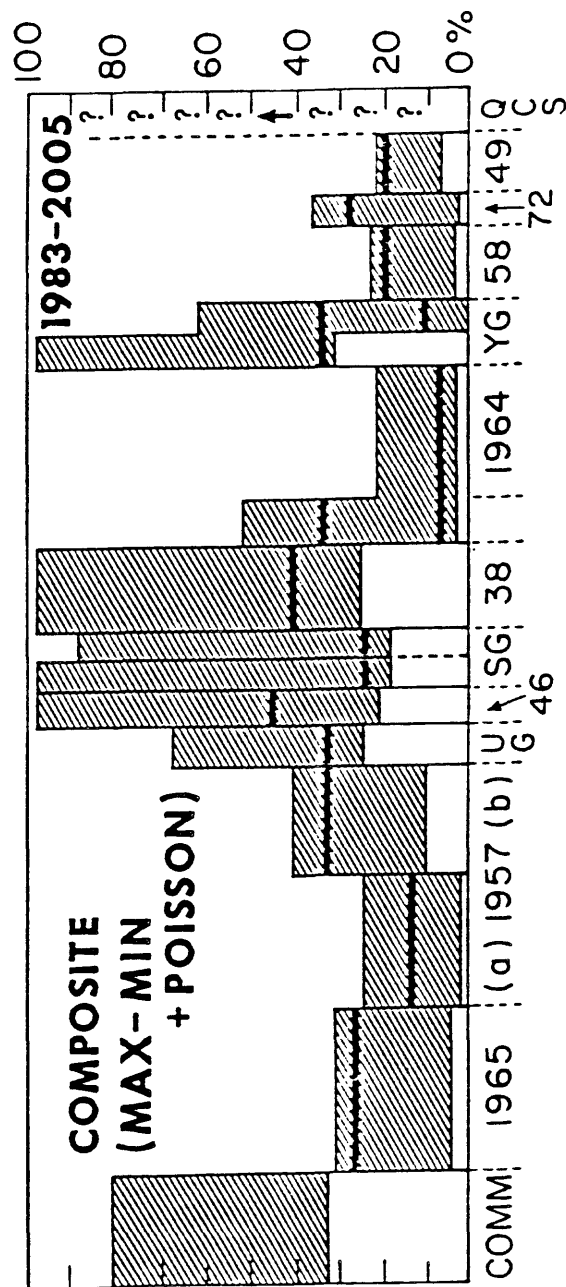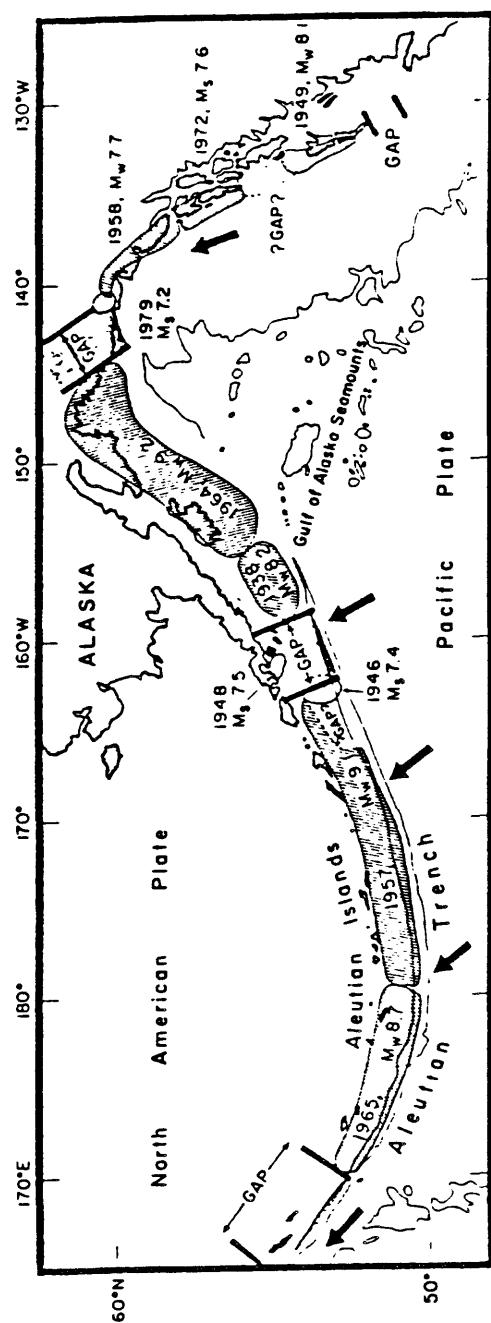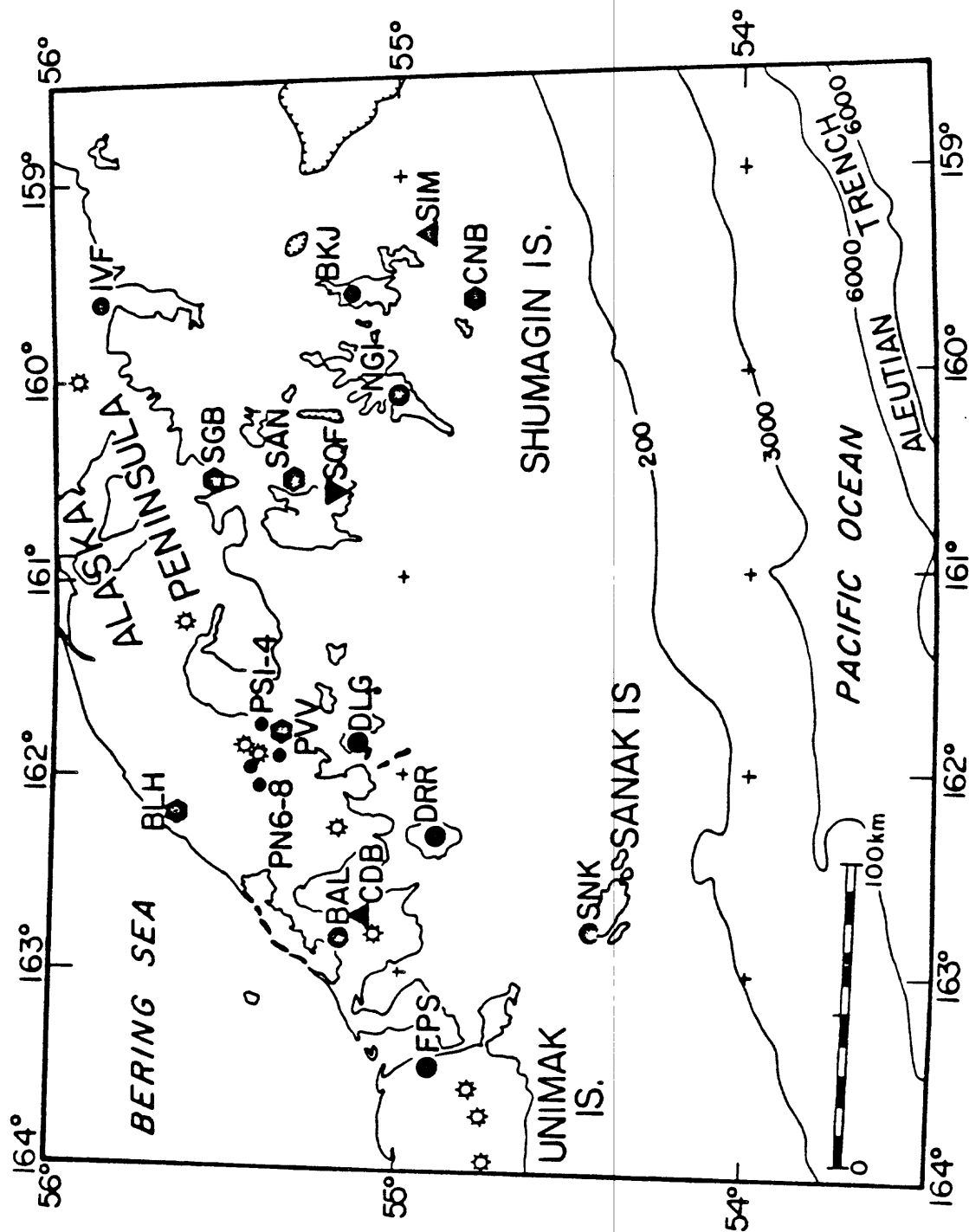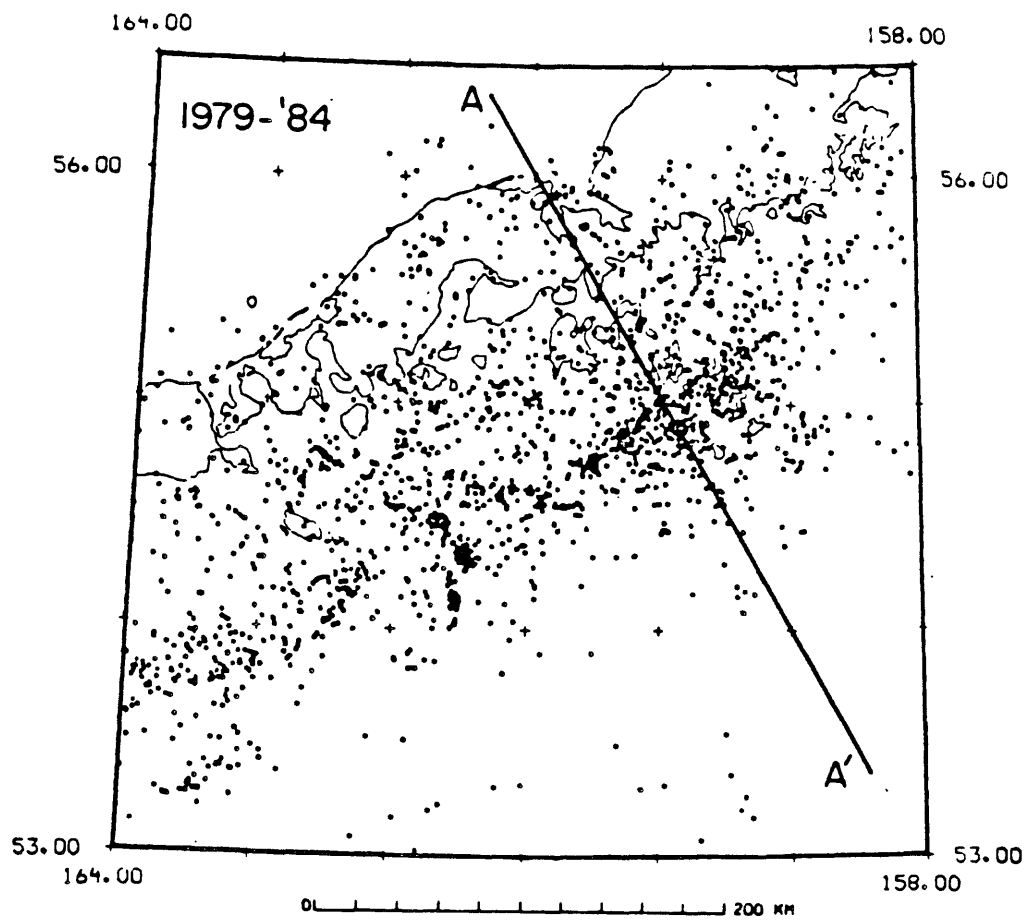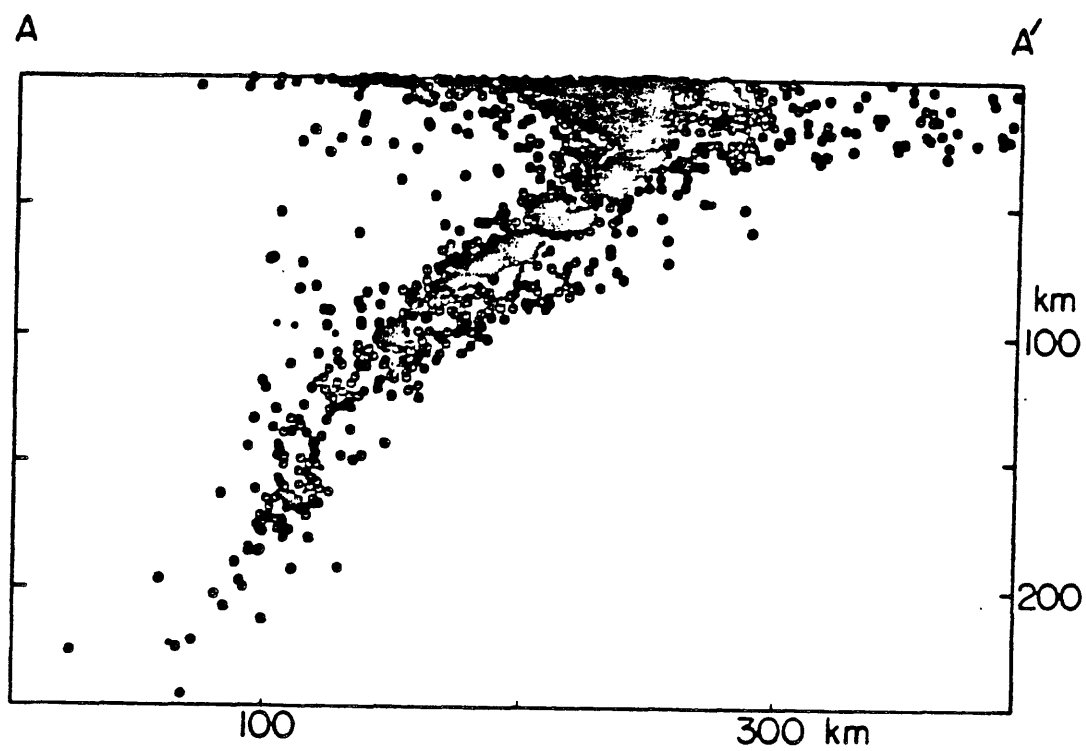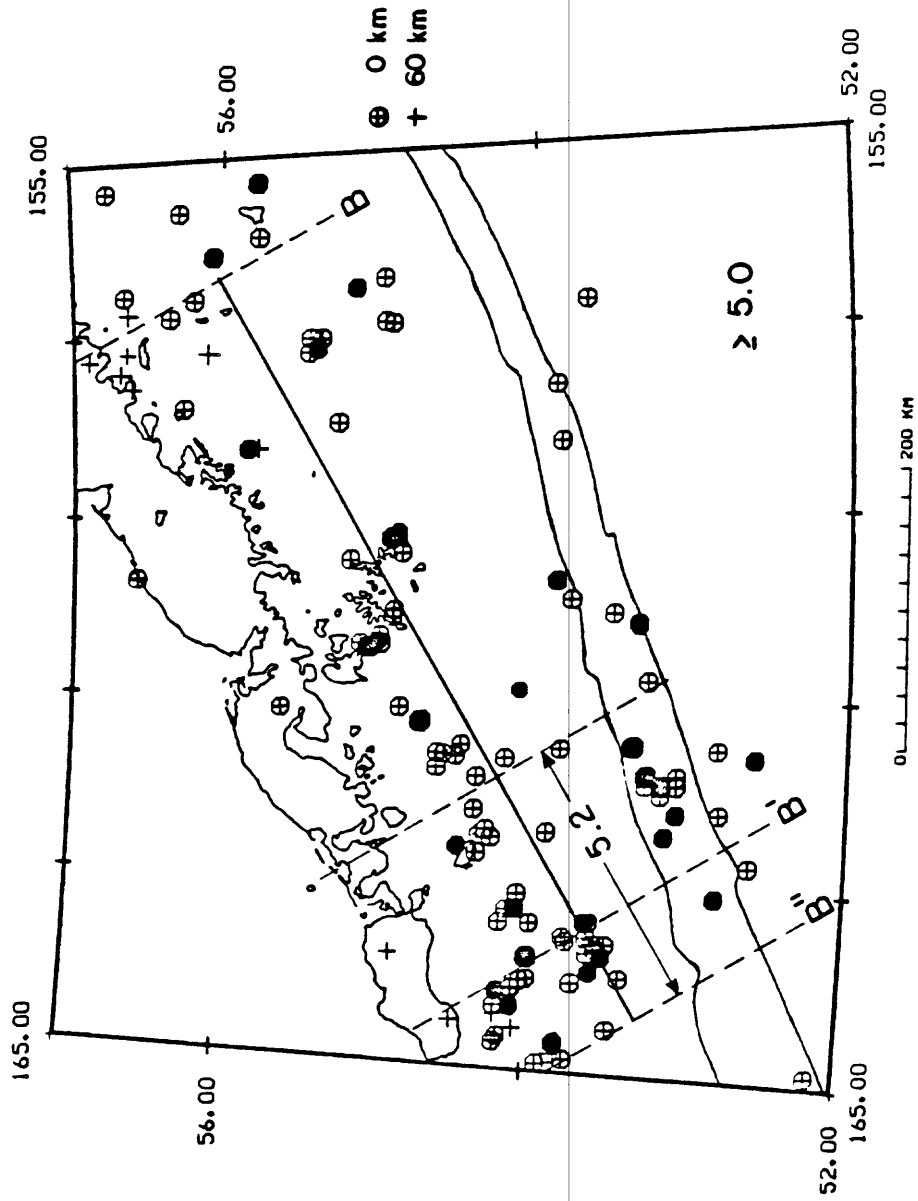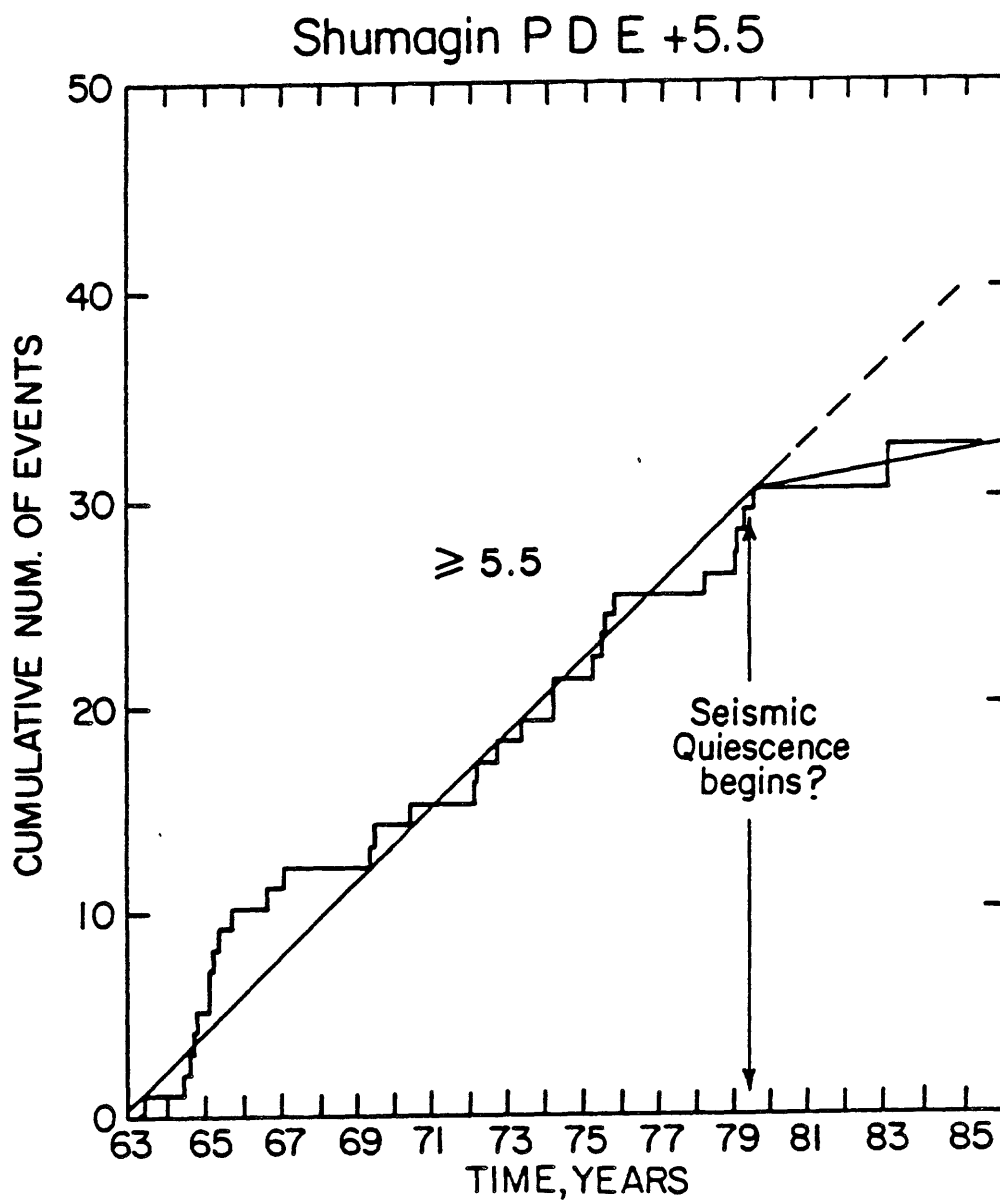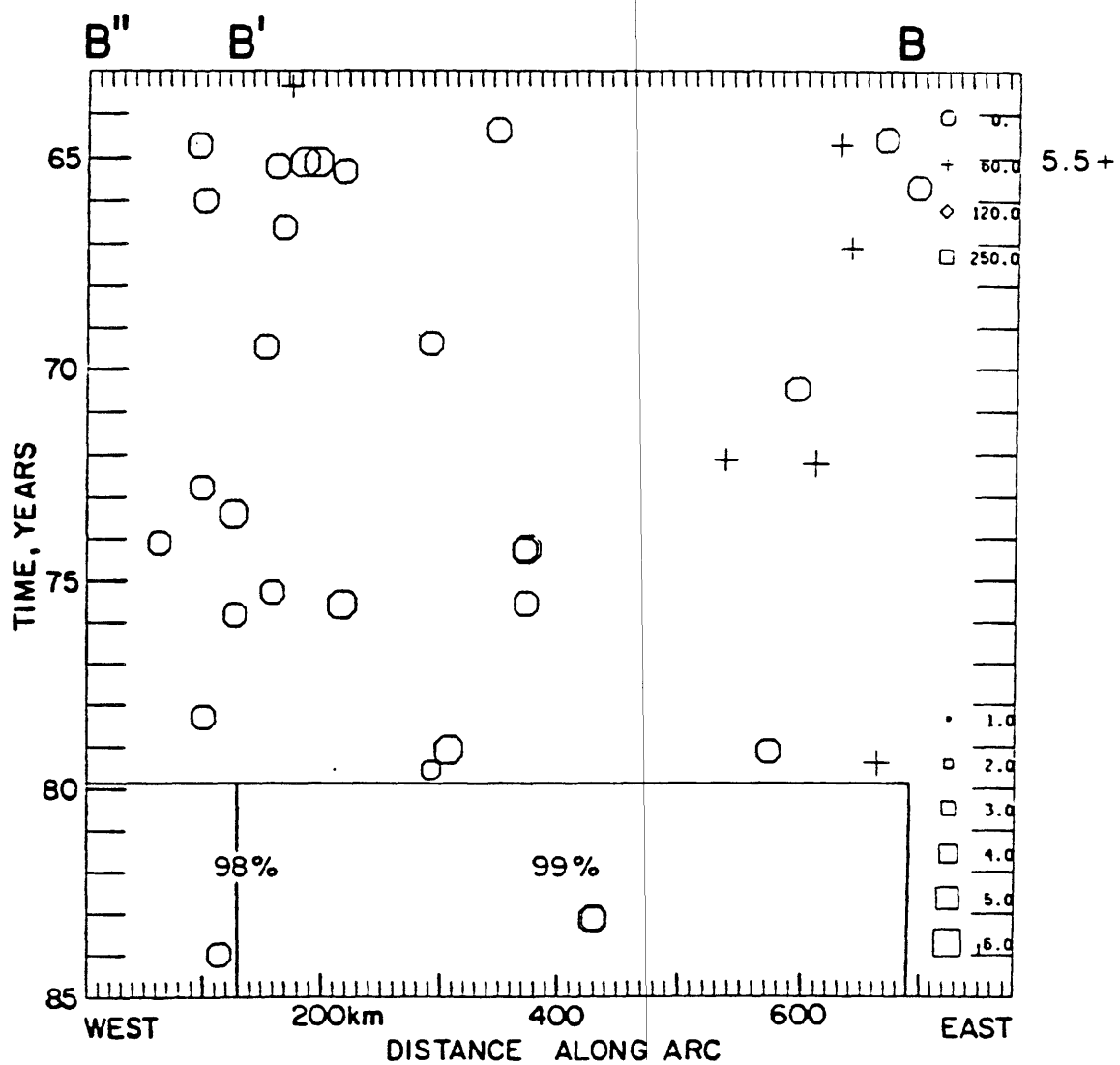
Figure 1.

Figure 2.

Figure 3.

Figure 4.

Shumagin P D E +5.5

Figure 5.

Figure 6.

Figure 7.

TILT IN THE INNER SHUMAGINS

- ● SQH
- □ SDP

DOWN TOWARDS NW (FOR SQH)
N (FOR SDP)

2μrad

72 73 74 75 76 77 78 79 80 81 82 83 84 85

SEISMICITY RATES

CUMULATIVE NUMBER OF EARTHQUAKES

ALEUTIAN ARC
140°-180°W
$M_B \geq 4.0$

SHUMAGINS
156°-165°W
$M_B \geq 4.0$

SHUMAGIN NETWORK
156°-165°W
$M_B \geq 2.5$

500

0

50

0

250

0

72 73 74 75 76 77 78 79 80 81 82 83 84 85

PAVLOF ERUPTIVE ACTIVITY

MAGMATIC
EXPLOSIVE   MAGMATIC
MAGMATIC   EXPLOSIVE   EXPLOSIVE   EXPLOSIVE
MAGMATIC   MAGMATIC   MAGMATIC

72 73 74 75 76 77 78 79 80 81 82 83 84 85
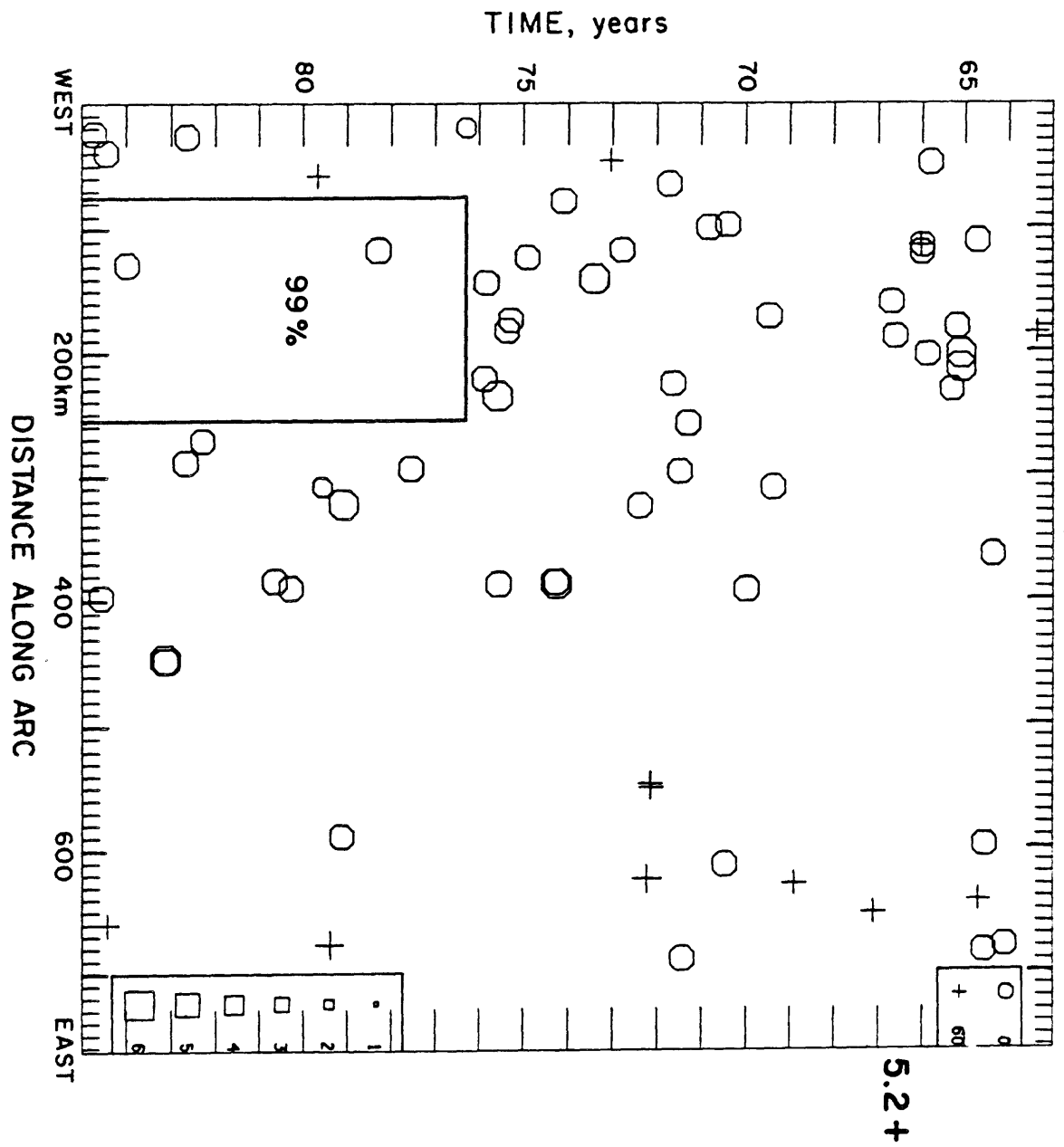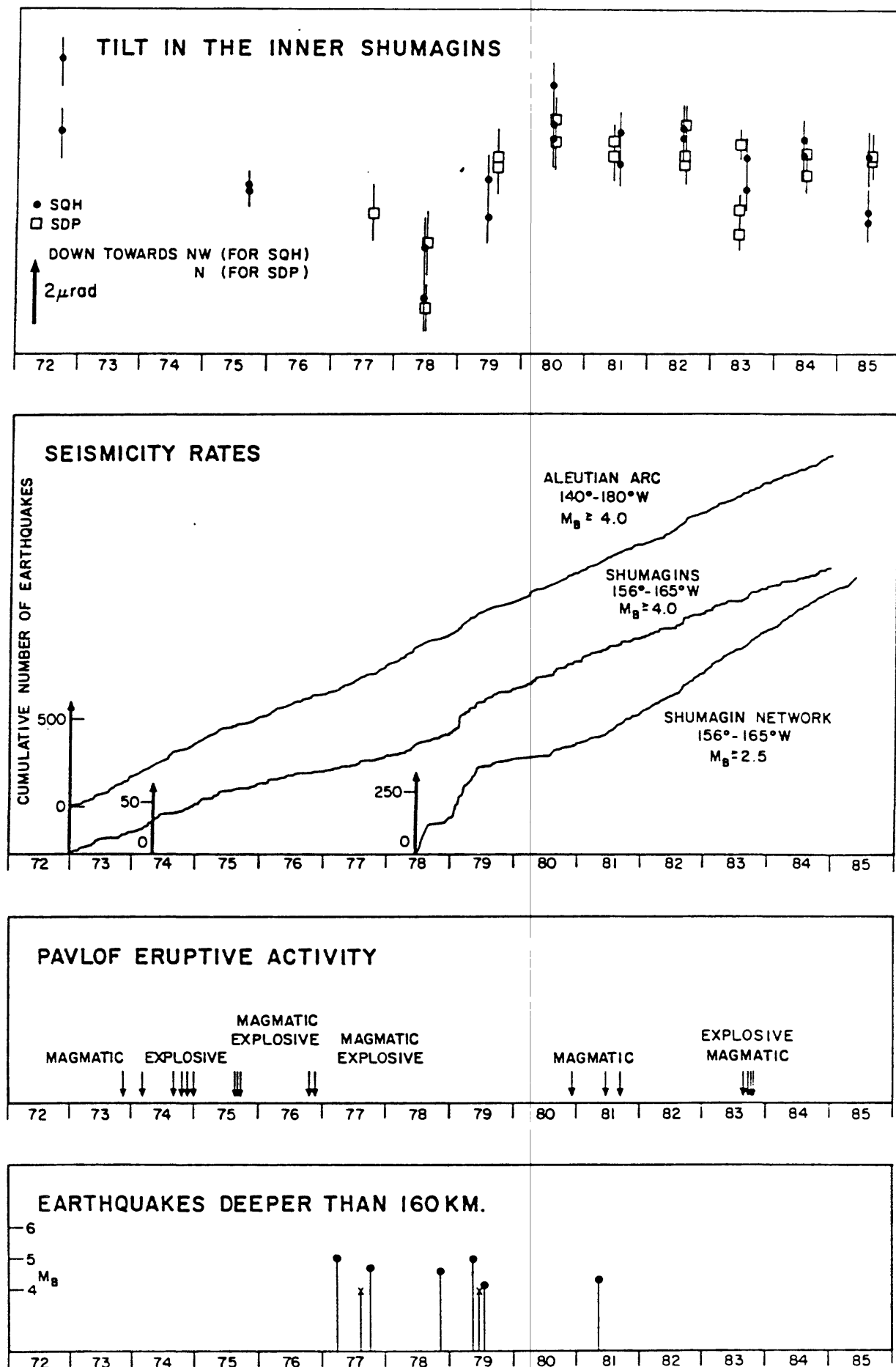
EARTHQUAKES DEEPER THAN 160 KM.

6
5
M_B
4

72 73 74 75 76 77 78 79 80 81 82 83 84 85

Figure 8.

Figure 9.

Figure 10.
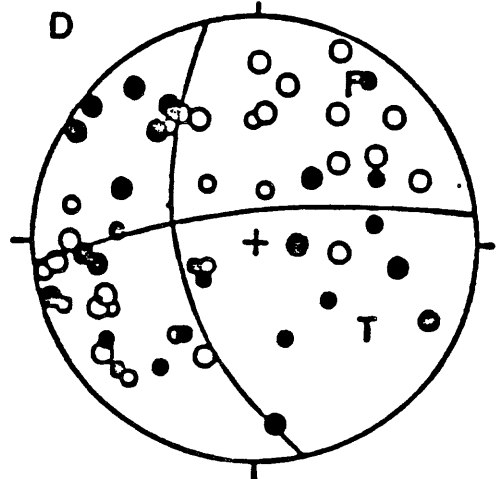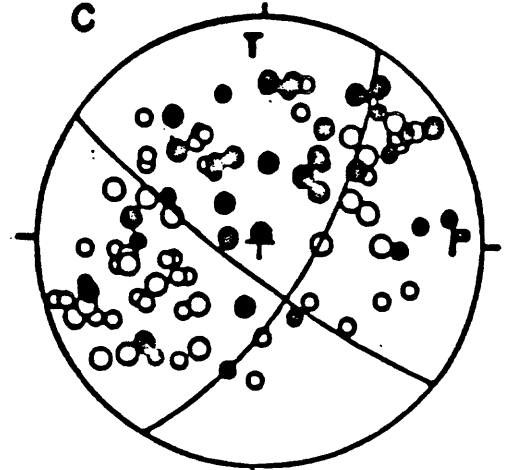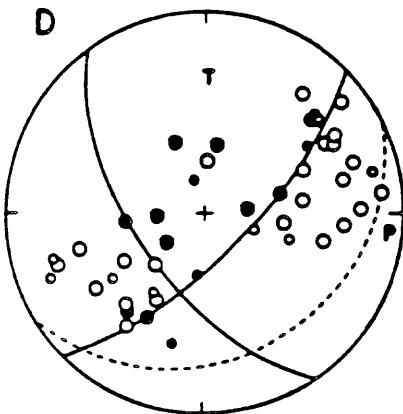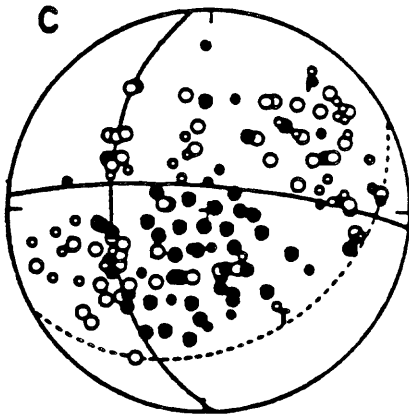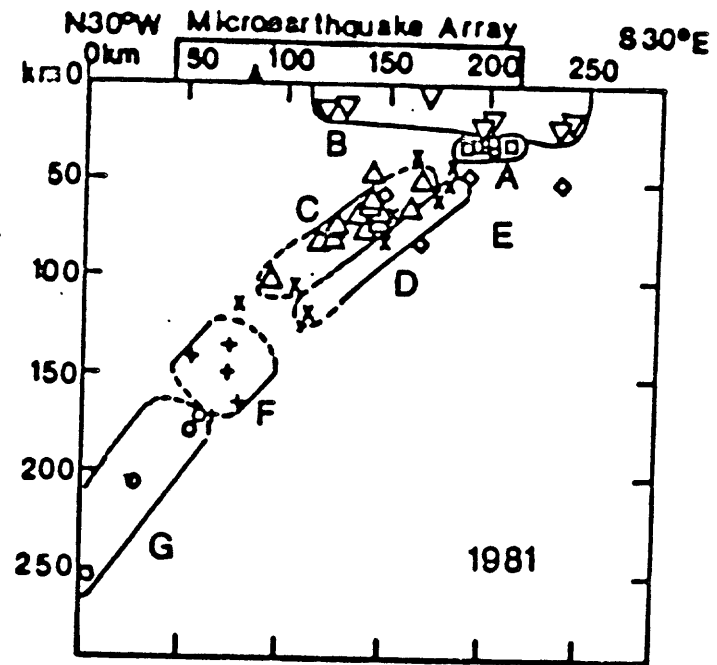
Figure 11.

Figure 12.

Figure 14.

Figure 15.

APPENDIX A. 3.

Results from 13 Years Crustal Deformation Measurements
in the Shumagin Islands Seismic Gap

J. Beavan, K. Hurst, and R. Bilham

RESULTS FROM 13 YEARS CRUSTAL DEFORMATION MEASUREMENTS IN THE SHUMAGIN ISLANDS SEISMIC GAP

John Beavan, Ken Hurst and Roger Bilham

Lamont-Doherty Geological Observatory of Columbia University
Palisades NY 10964

Extended Abstract

Measurements

The Shumagin Islands (Figure 1) have been identified as a mature seismic gap based on studies of historical seismicity and on estimates of great earthquake recurrence rate for the Aleutian arc as a whole (Kelleher 1970; Sykes 1971; Sykes et al 1980, 1981; Davies et al 1981; Jacob 1983). We have been making crustal deformation measurements since 1972 in order to learn more about the subduction process in the region. One short (~1km) level line has been measured since 1972, two additional ones since 1978 and six more since 1980 (Figure 2). Sea level has been measured since 1972 at one site (SDP) by the National Ocea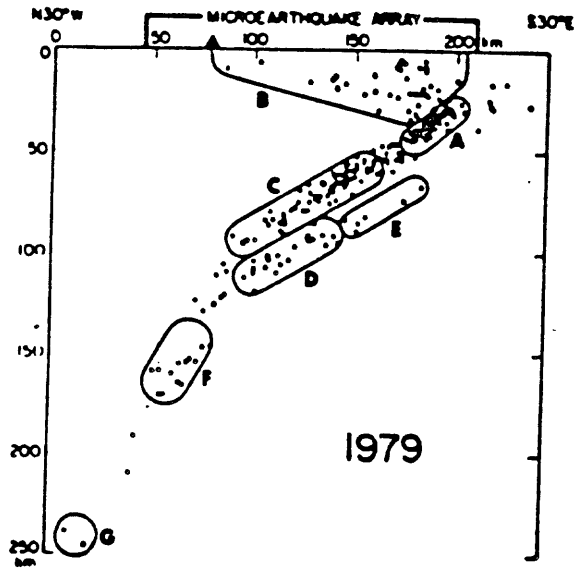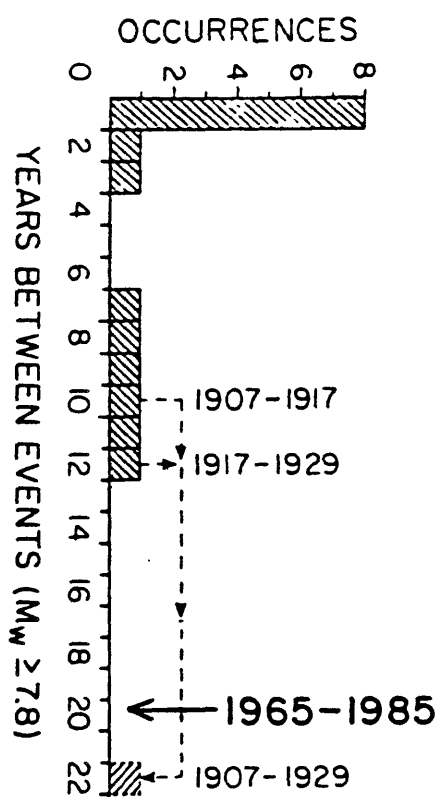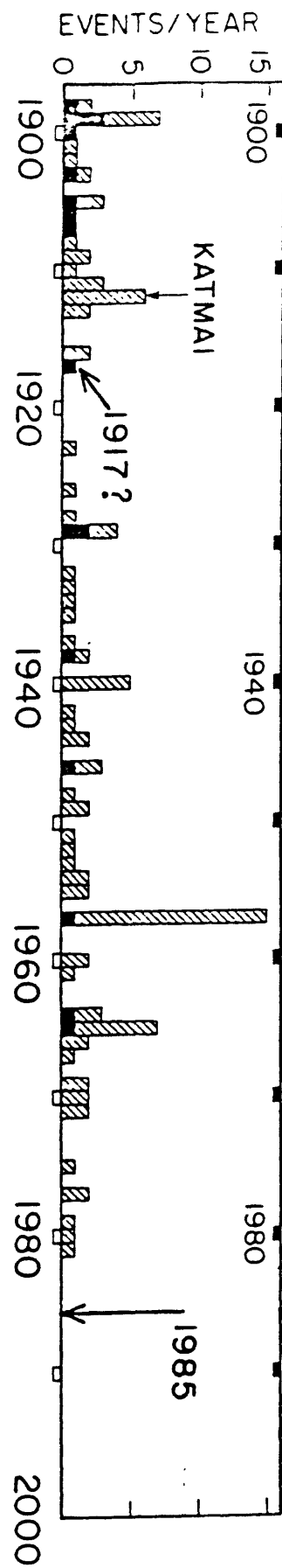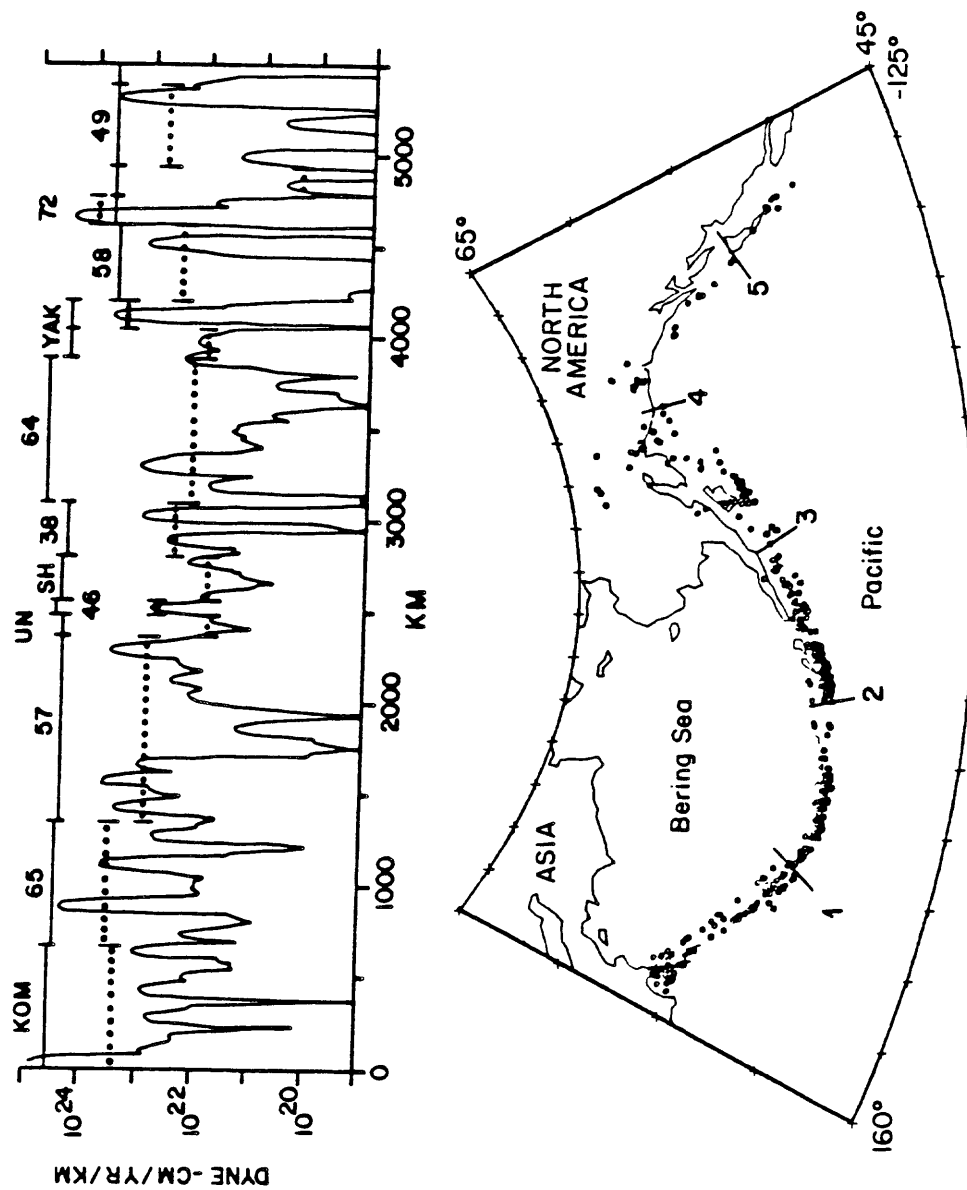n Survey. We installed three additional sea level sites in 1981, increasing to four by 1985 (Figure 3). A continuously recording two-component short-baseline mercury-level tiltmeter has been running at one site (SCT) since 1984 (Figure 3). Related work is being done by the USGS (Savage et al. 1985) who have measured a trilateration network several times since 1980, and by NASA who began annual very-long-baseline-interferometry measurements at one site (SDP) in 1984.

Leveling Data

Data from the level line measurements are shown in Figures 4 and 5. The two lines with the longest history in the Inner Shumagins (SQH and SDP) show a pronounced tilt reversal between 1978 and 1980. Prior to 1978 the tilt was down towards the trench at 1.0 ± 0.3 μrad/yr; since 1980 it has been down towards the trench at 0.4 ± 0.2 μrad/yr. Between 1978 and 1980 the tilt was down away from the trench at 2.7 ± 0.5 μrad/yr. All these rates are significantly different from zero at high confidence levels (Table 1). It is not possible to fit a single straight line through either the SQH or the SDP data set; a statistical test (Crow et al 1960, pp 166-167) shows the data to differ from linearity with 99.5% and 99% confidence, respectively. A line in the Outer Shumagins (SIM) also shows a tilt reversal in 1980, though not at a high confidence level. Between 1978 and 1980 the tilt was down away from the trench at 0.7 ± 0.6 μrad/yr; since then it has been down towards the trench at 0.3 ± 0.2 μrad/yr. Other lines oriented in a NW-SE direction generally show slow tilt down towards the trench since 1980, though there are one or two anomalous data points.

The 1978-1980 reverse tilt has been interpreted as resulting from an ~1m aseismic reverse slip episode on the Benioff zone at depths between ~25km and ~80km (Beavan et al 1983, 1984). The 1972-1978 and 1980-85 data have been assumed to represent the normal strain accumulation in the area. We discuss each of these interpretations below.

1978-80 reverse slip

Figure 6 re-plots the SQH and SDP leveling data along with seismicity rates, activity of Pavlof Volcano and occurrence of deep (>160km) earthquakes. The spatial extent of the tilt reversal (both inner and outer islands), and the temporal coincidence between the tilt reversal and changes in seismicity rates and volcanic activity imply that all may be related to a single deep-seated process. We have assumed that this process is aseismic slip occurring on the plate interface over a zone ~100km along strike centered on the Shumagin Islands. The 100km length is suggested by the along-strike extent of deep earthquakes (Figure 7), and by along-strike changes in seismicity patterns (Taber and McNutt 1984). We have modeled the slip as a dislocation in an elastic half space; the duration of the tilt reversal is < 2 years implying that viscoelastic effects are unimportant. The plate interface is taken from Reyners and Coles (1982). It dips 11° between the trench and 30km depth, then approximately beneath SIM it steepens to 30° (Figure 8), passing through a zone of high stress-drop inter-plate earthquakes at about 45km depth. Below this it follows the top of the zone of seismicity, which is assumed to be mostly internal to the subducting slab. Figure 8 shows surface uplift, tilt and linear strain in the direction of plate motion for various dislocation models. The model results are compared with observations in Table 2; the uplift observation in the Inner Shumagins is taken from the sea level data at SDP which shows < 100mm change between 1978 and 1980. The only models that fit the observations require about 1m of slip on a plane between ~25km and ~80km depth. Davies et al (1981) and House and Jacob (1983) suggest that the main thrust zone (the zone that will fail in a major earthquake) extends from the trench to ~45km depth. Hence the slip episode appears to have broken into, and therefore relieved stress on, part of the main thrust zone.

The postulated slip episode provides a possible explanation for the cessation of activity at Pavlof Volcano (McNutt and Beavan 1985). Figure 9 plots the volume strain changes due to the slip. In the region of mantle beneath Pavlof that may be supposed to be the "feeder" volume for the volcano, the average volume extension is 0.6 μstrain. This may tend to relieve the stresses that force magma out of the volcano, or may provide greater volume for storage of magma within the mantle; either mechanism could provide a temporary lull in eruptive activity. Any physical connection between the slip episode and the deep earthquakes remains enigmatic.

Strain accumulation

Savage (1983) proposed a simple elastic rebound model for strain accumulation in subduction zones. The main thrust zone is assumed to remain locked while the remainder of the plate interface slips steadily and aseismically. Strain therefore accumulates in precisely the reverse of the pattern in which it is released in the eventual earthquake. The surface displacements during the strain accumulation phase can be calculated by applying a dislocation model with virtual slip at the plate convergence rate on the main thrust zone. Thus our Figure 8 can be used to model strain accumulation by changing the sign and multiplying the vertical scales by 0.075 (to match the Minster and Jordan (1978) 75mm/yr plate convergence rate). Table 3 summarizes our observations, Savage et al's (1985) strain observations and various model predictions. The uplift observations are taken from our sea level measurements, and are based on < 100mm change in sea level over the 1981-1985 period. None of the models in which the main thrust zone extends to the trench fit the observed data. The best fit is obtained with the upper end of the zone at 25-30km and the lower end

at 50-80km. This is not inconsistent with the available seismic evidence and implies that much of the shallow dipping part of the plate boundary is slipping aseismically. It is generally accepted that aseismic slip plays a role near the Earth's surface for many faults; however, whether such a mechanism could operate to 25km depth in a subduction zone remains an open question. An alternative explanation of the discrepancy between model and observation may be that the model is inadequate and that viscoelastic effects (e.g. Thatcher and Rundle 1985) are of dominant importance.

Implications for a future major earthquake

If the 1978-80 slip episode is a rare event then it is of scientific interest, but may not have any direct bearing on Shumagin earthquake risk. However, if it is a quasi-regular feature of subduction in this region, it may be very important. We speculated previously (Beavan et al 1983, 1984) that loading of the main thrust zone by a future similar slip episode might trigger the expected great earthquake, and that such an episode may occur around 1990 based on the 75mm/yr convergence rate and the ~1m size of the previous slip event. If the plate interface is locked shallower than 25km then this remains a valid hypothesis.

However, the post-1980 data collected by Savage et al (1985) and ourselves suggest that the upper part (shallower than 25km) of the plate interface may not be storing elastic strain energy for release in a future earthquake. Furthermore, the fairly close coincidence between the fault plane that best fits the 1978-80 reverse tilt data and the locked zone that best fits the 1980-85 strain accumulation data suggest that the entire plate motion in this region may be accommodated aseismically.

Since structural and seismic evidence (Taber and McNutt 1984) suggest that a region 100km along strike centered on the Shumagin Islands may be anomalous, it is possible that aseismic slip may be confined to the Shumagins themselves. The remainder of the Shumagin seismic gap could be storing strain in a manner that would eventually lead to a major earthquake, as is suggested by the historic record.

Future Instrumentation

Our recent aim has been to install continuously recording instrumentation for monitoring future crustal deformation activity within the gap. The sea level data are continuous but to date have been rather noisy; with improved instrumentation installed in 1985 we hope to obtain ~20mm accuracy in relative sea level between sites. Data from the continuously recording tiltmeter are shown in Figure 10. The tilt records show typical initial settling curves and both components presently show long-term rates < 3 μrad/yr. This is still substantially above the rate that would enable us to detect anything but a very rapid reverse slip event in real time. We believe that the only continuously recording instrumentation available that will adequately monitor tilt in this seismic gap are a deep borehole pendulum-type instrument or a long-baseline water-tube tiltmeter (Wyatt et al 1985).

REFERENCES

Beavan, J., E. Hauksson, S. R. McNutt, K. Jacob, and R. Bilham, Tilt and seismicity changes in the Shumagin seismic gap, Science, 222, 322-325, 1983.

Beavan, J., R. Bilham, and K. Hurst, Coherent tilt signals observed in the Shumagin seismic gap; detection of time-dependent subduction at depth?, J. Geophys. Res., 89, 4478-4492, 1984.

Crow, E. L., F. A. Davis, and M. W. Maxfield, Statistics Manual, Dover, New York, 1960.

Davies, J. N., L. Sykes, L. House, and K. Jacob, Shumagin seismic gap, Alaska peninsula: History of great earthquakes, tectonic setting, and evidence for high seismic potential, J. Geophys. Res., 86, 3821-3955, 1981.

House, L. S., and K. H. Jacob, Earthquakes, plate subduction, and stress reversals in the eastern Aleutian arc, J. Geophys. Res., 88, B11, 9347-9373, 1983.

Jacob, K. H., Estimates of long-term probabilities for future great earthquakes in the Aleutians, Geophys. Res. Lett., 11, 295-298, 1984.

Kelleher, J., Space-time seismicity of the Alaska-Aleutian seismic zone, J. Geophys. Res., 75, 5745-5756, 1970.

McNutt, S. R., and R. J. Beavan, Periodic eruptions at Pavlof Volcano, Alaska: The effects of sea level and an aseismic slip event, submitted to J. Geophys. Res., 1985.

Minster, J. B., and T. H. Jordan, Present-day plate motions, J. Geophys. Res., 83, 5331-5354, 1978.

Reyners, M., and K. S. Coles, Fine structure of the dipping seismic zone and subduction mechanics in the Shumagin Islands, Alaska, J. Geophys. Res., 87, 356-366, 1982.

Savage, J. C., A dislocation model of strain accumulation and release at a subduction zone, J. Geophys. Res., 88, 4984-4996, 1983.

Savage, J. C., M. Lisowski, and W. H. Prescott, Strain accumulation in the Shumagin and Yakataga seismic gaps, Alaska, submitted to Science, 1985.

Sykes, L. R., Aftershock zones of great earthquakes, seismicity gaps, and earthquake prediction for Alaska and the Aleutians, J. Geophys. Res., 76, 802-8041, 1971.

Sykes, L. R., J. B. Kisslinger, L. House, J. N. Davies, and K. Jacob, Rupture zones of great earthquakes in the Alaska-Aleutian arc, 1784 to 1980, Science, 210, 1343-1345, 1980.

Sykes, L. R., J. B. Kisslinger, L. House, J. N. Davies, and K. H. Jacob, Rupture zones and repeat times of great earhquakes along the Alaska-Aleutian arc, 1784-1980, in Earthquake Prediction - An International Review, Maurice Ewing Series 4, edited by D. W. Simpson and P. G. Richards, American Geophysical Union, 1981.

Taber, J. J., and S. R. McNutt, Temporal and spatial changes in seismicity associated with subduction near the Shumagin Islands, Alaska (Abst.), EOS Trans. AGU, 65, 987, 1984.

Thatcher, W., and J. B. Rundle, A viscoelastic coupling model for the cyclic deformation due to periodically repeated earthquakes at subduction zones, J. Geophys. Res., 89, 7631-7640, 1984.

Wyatt, F., R. Bilham, J. Beavan, A. G. Sylvester, T. Owen, A. Harvey, C. MacDonald, D. D. Jackson, and D. C. Agnew, Comparing tiltmeters for crustal deformation measurement - a preliminary report, Geophys. Res. Lett., 11, 963-966, 1984.

TABLE 1

SHUMAGIN TILT RATES

	TIME PERIOD	RATE* μrad a^{-1}	AZIMUTH* degrees	CONFIDENCE LEVEL
INNER SHUMAGINS	1972-78	-1.0±0.3	NW[†]	95%
	1978-80	2.7±0.5	-27±21	99%
	1980-85	-0.4±0.2	-58±38	90%
OUTER SHUMAGINS	1978-80	0.7±0.6	NW[†]	---
	1980-85	-0.3±0.2	-65±37	---

* Positive rates indicate that the tilt is downwards towards the given azimuth.

[†] Level line only measured in one azimuth, so tilt azimuth is indeterminate.

TABLE 2

1978-80 1 m SLIP EPISODE IN SHUMAGINS

	OBSERVED	DISLOCATION MODEL for fault depth:			
		a 30-50 km	b 25-50 km	c 30-80 km	d 25-80 km
INNER SHUMAGINS					
TILT μrad	+5.4±1.0	-0.6	-1.0	+4.3	+3.8
UPLIFT mm	-100<u<100	-35	-45	+46	+36
OUTER SHUMAGINS					
TILT μrad	+1.4±1.2	+0.6	+5.1	-7.4	+1.4
UPLIFT mm	---	+249	+150	+370	+272

TABLE 3

STRAIN ACCUMULATION IN SHUMAGINS

	OBSERVED 1980-85	ELASTIC REBOUND MODEL for locked zone in depth range:				
		a 30-50 km	b 25-50 km	c 30-80 km	d 25-80 km	e 0-30 km
INNER SHUMAGINS						
TILT μrad/yr	-0.4±0.2	+0.05	+0.07	-0.32	-0.29	+0.04
STRAIN μstrain/yr	+0.01±0.03*	+0.02	-0.05	+0.03	-0.04	-0.15
UPLIFT mm/yr	-25<u<25	+2.6	+3.4	-3.5	-2.7	+1.0
OUTER SHUMAGINS						
TILT μrad/yr	-0.3±0.2	-0.04	-0.38	+0.56	-0.11	-0.05
STRAIN μstrain/yr	-0.03±0.05*	-0.04	-0.01	-0.13	-0.10	-0.23
UPLIFT mm/yr	-25<u<25	-18.7	-11.2	-27.7	-20.4	+13.6

* from Savage et al. [1985], assuming zero strain along strike of arc.
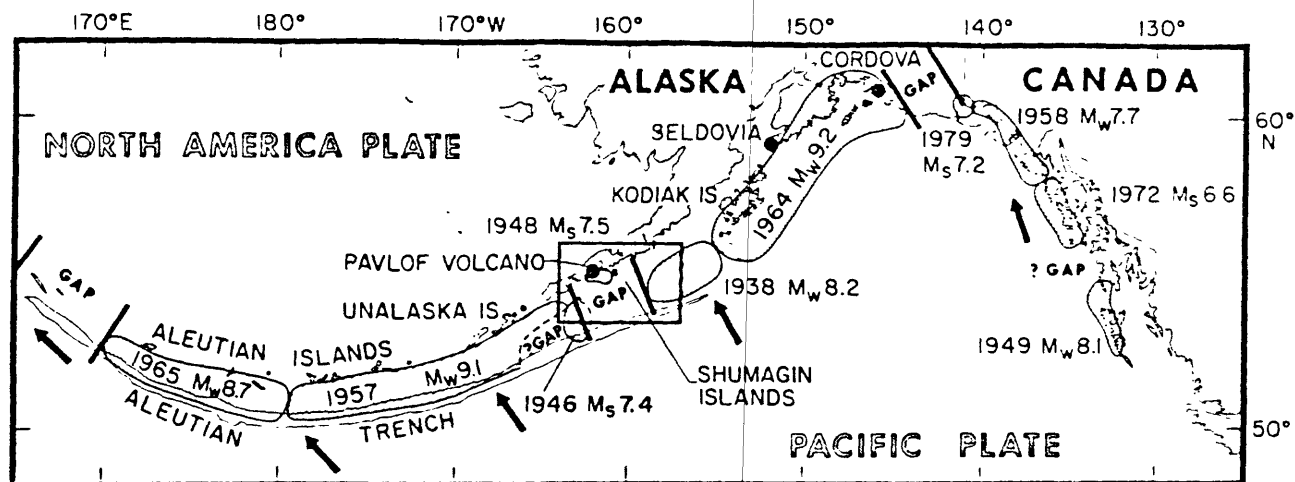
Figure 1. Recent earthquakes (shaded) and seismic gaps in the Aleutian arc (adapted from Davies et al (1981)). The heavy arrows show the relative plate motion direction. The rectangle shows the area of Figure 3.
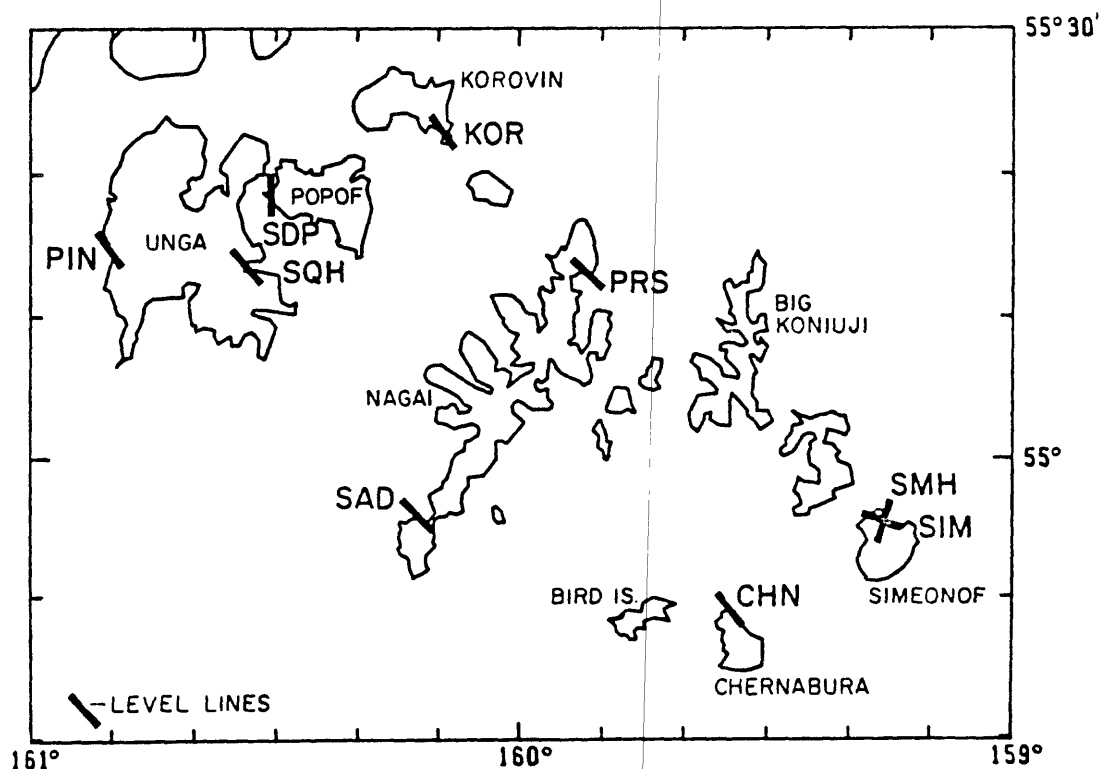
Figure 2. The Shumagin Islands, showing the locations and directions of first-order level lines, whose lengths vary between 600m and 1200m. The resultant of the data from lines SDP and SQH is used to estimate the tilt direction in the Inner Shumagins. The resultant of SIM and SMH is used for the Outer Shumagins.
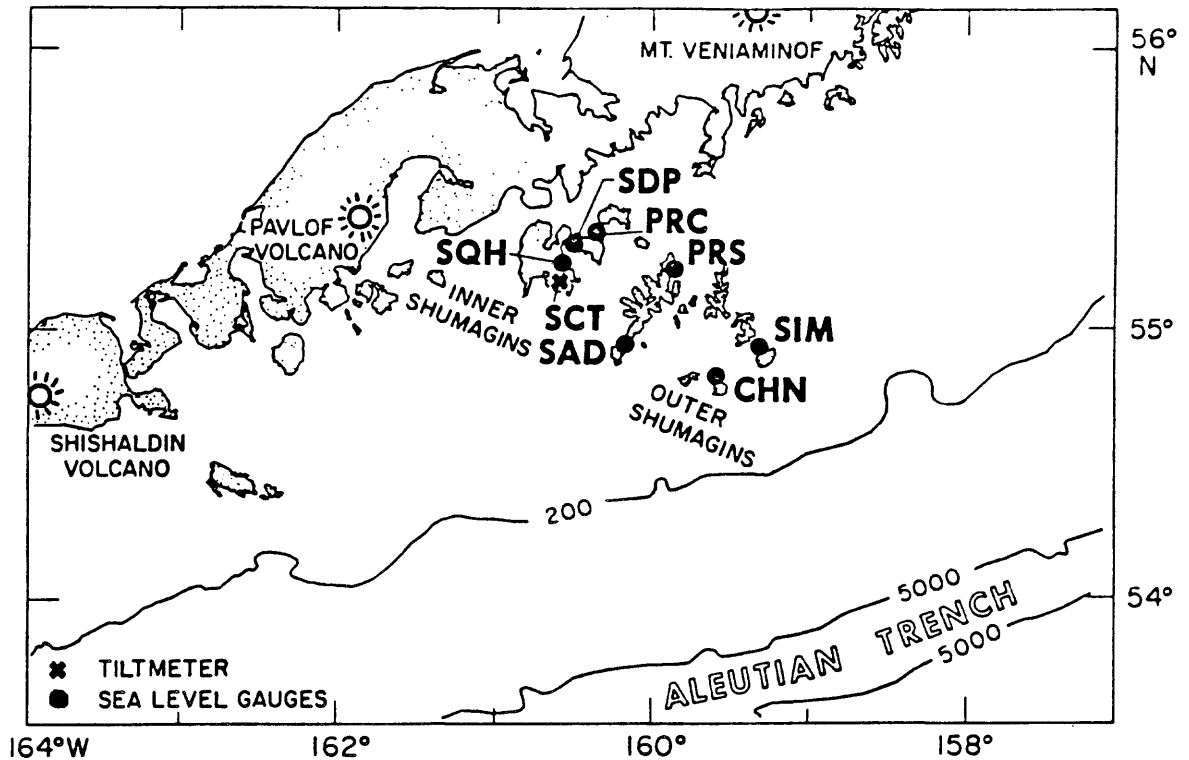
Figure 3. Location of the Shumagin Islands with respect to the trench and the volcanic arc. Depth contours are in metres. Note the locations of Pavlof Volcano and the Inner and Outer Shumagins. Also shown are the sites of sea-level gauges operated by Lamont-Doherty and by the National Ocean Survey (SDP), and the site of a short-baseline tiltmeter (SCT). Station SAD is no longer operative because of storm damage. Station CHN is not operating this year.
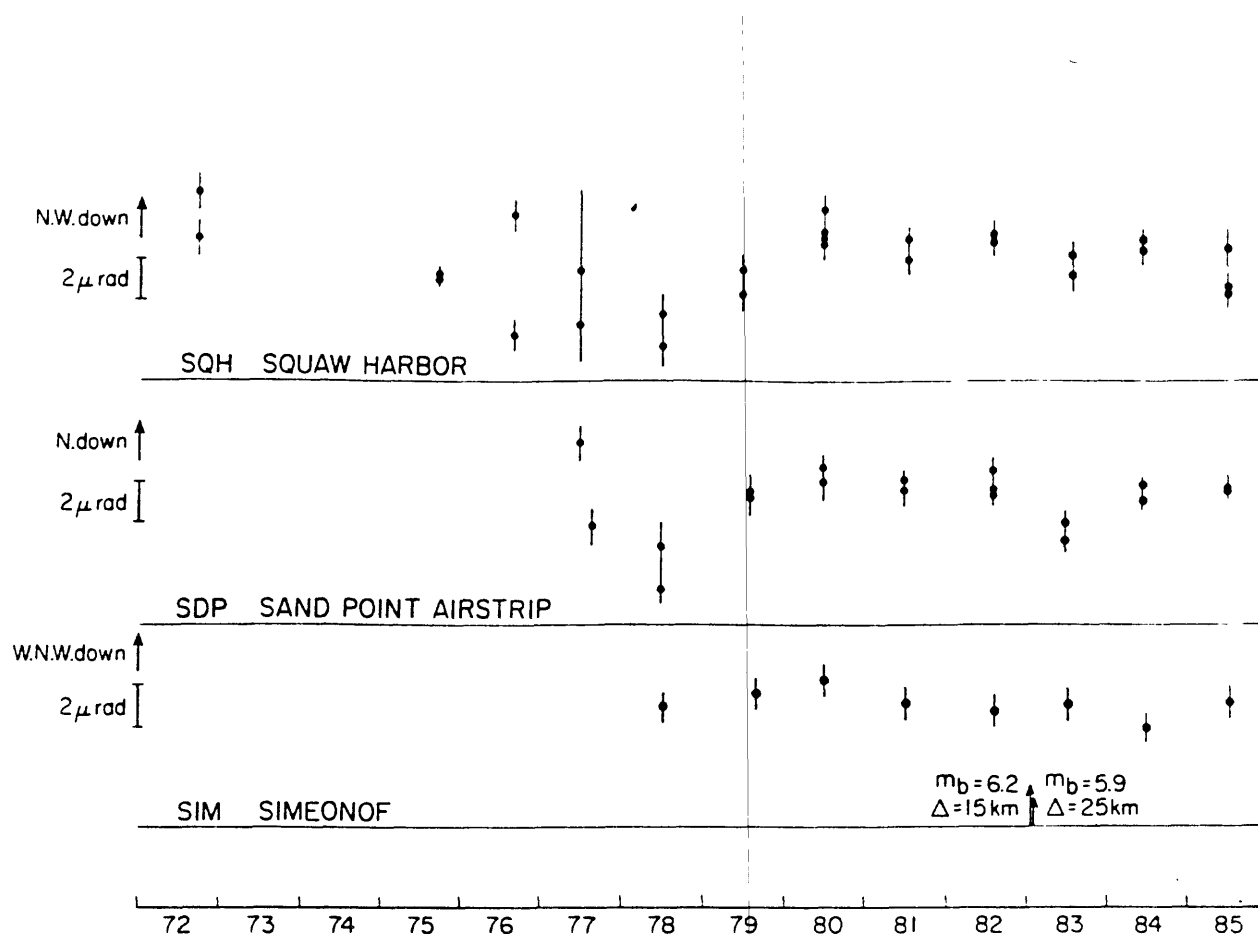
Figure 4. See also Figure 5. All data (1972-1985) from level lines in the Shumagin Islands. All lines except SMH are oriented approximately in the direction of relative plate motion. The two data points each year represent the forward and backward runs of leveling. The error bars are $\pm 1\sigma$, based on variations in multiple readings of each stadia rod from each tripod position. The height differences between the ends of the lines have been converted to slope by dividing by the line length; changes in slope from year to year are due to ground tilt. Several benchmarks are set at each end of each line to guard against benchmark instability. Lines SIM and SAD have only one data point plotted for each year; this is because they have benchmarks between almost every tripod position and the overall tilt is estimated by averaging tilts between adjacent benchmarks.

Note particularly the 1.0 ± 0.3 μrad/yr tilt down toward the trench between 1972 and 1978 on line SQH. The resultant of lines SQH and SDP shows a reversal of tilt (2.7 ± 0.5 μrad/yr down away from the trench) between 1978 and 1980, and a return to tilt down towards the trench (0.4 ± 0.2 μrad/yr) between 1980 and 1985. The line at SIM in the Outer Shumagins may also show a tilt reversal in 1980, though not at high confidence level.
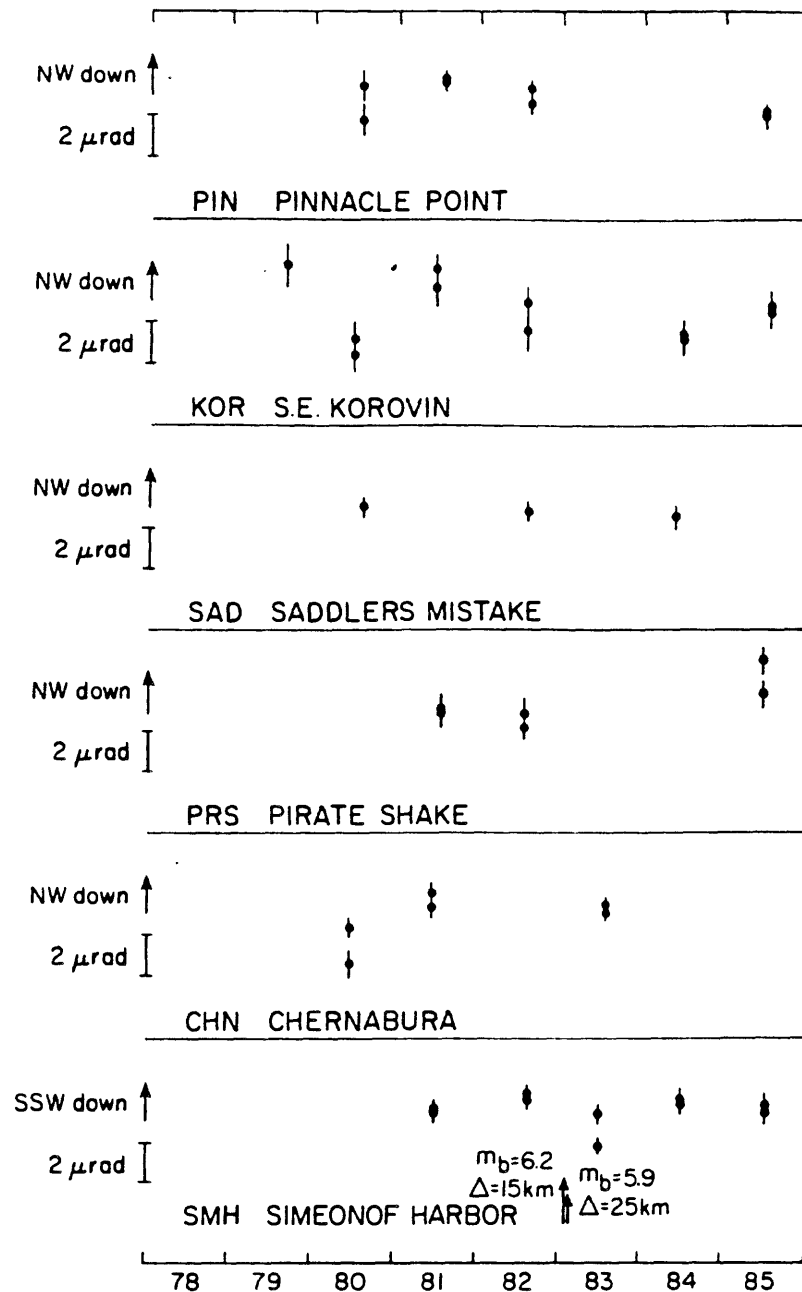
Figure 5. See Figure 4. Most of the NW-SE oriented lines show coherent behavior since 1980, with slow tilting down towards the trench. Clusters of microseismicity at shallow depths below KOR in 1978 through 1980 may contribute to its noisy behavior. The 1980 measurement on CHN was made immediately after setting the benchmarks, so there may be some settling error due to hardening of the concrete.
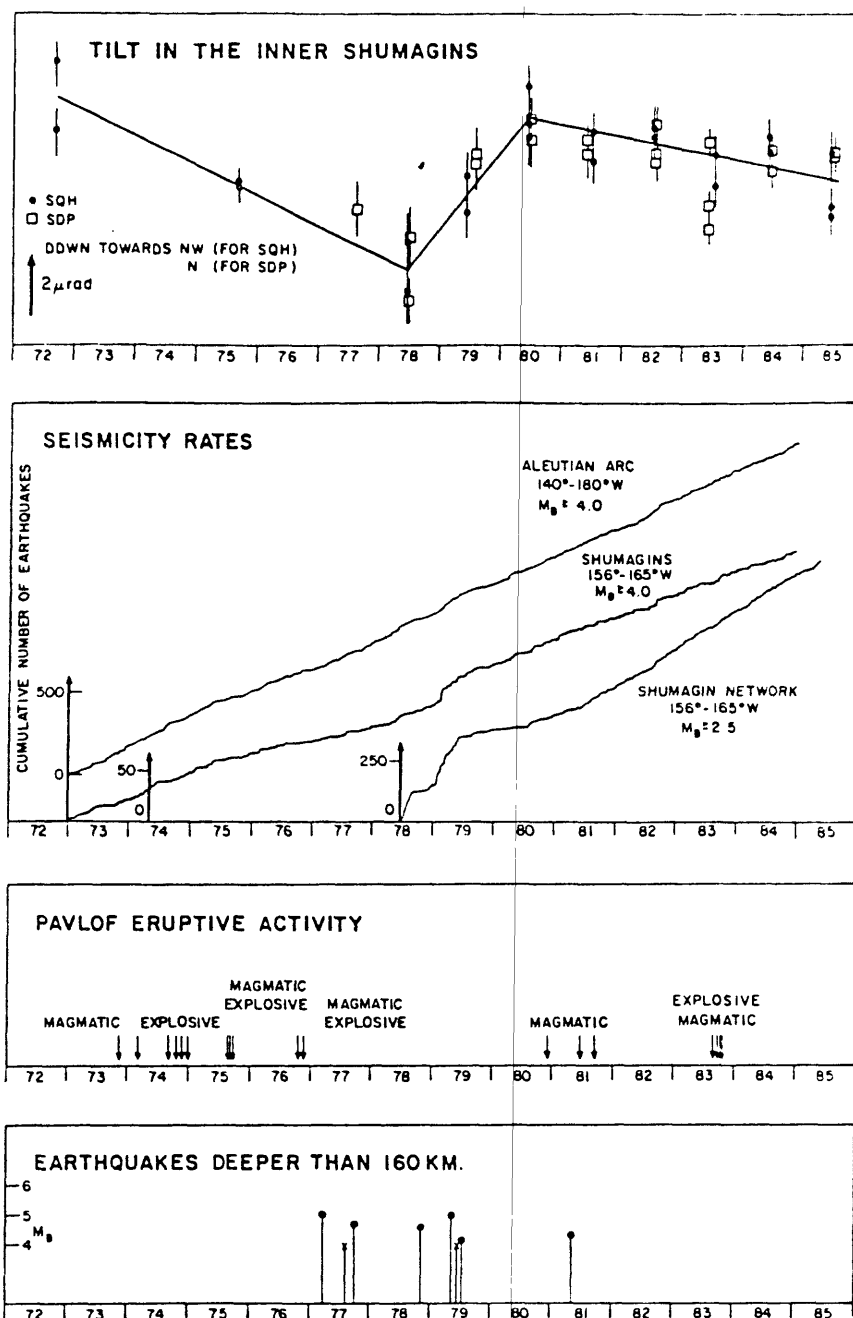
Figure 6. (a) Superposition of data from SQH and SDP level lines. The line drawn through the data is a schematic interpretation of Inner Shumagins tilt. (b) Seismicity rates in the Shumagins and the Aleutian arc as a whole. The local seismicity is significantly higher during 1978 and 1979 than it has been since. The small plateau during late 1978 is probably caused by low reporting due to station failures. (c) Activity of Pavlof Volcano, showing a marked cessation of activity during 1977-80, the approximate duration of the tilt reversal. (d) Earthquakes deeper than 160km in the Shumagin region, as reported in the PDE catalog. The approximate level for full reporting is M_b 4.5. Events marked with an x were not assigned a magnitude in the catalog. The earthquakes all fall behind the volcanic arc in a band centered on the Shumagin Islands (see Figure 7).
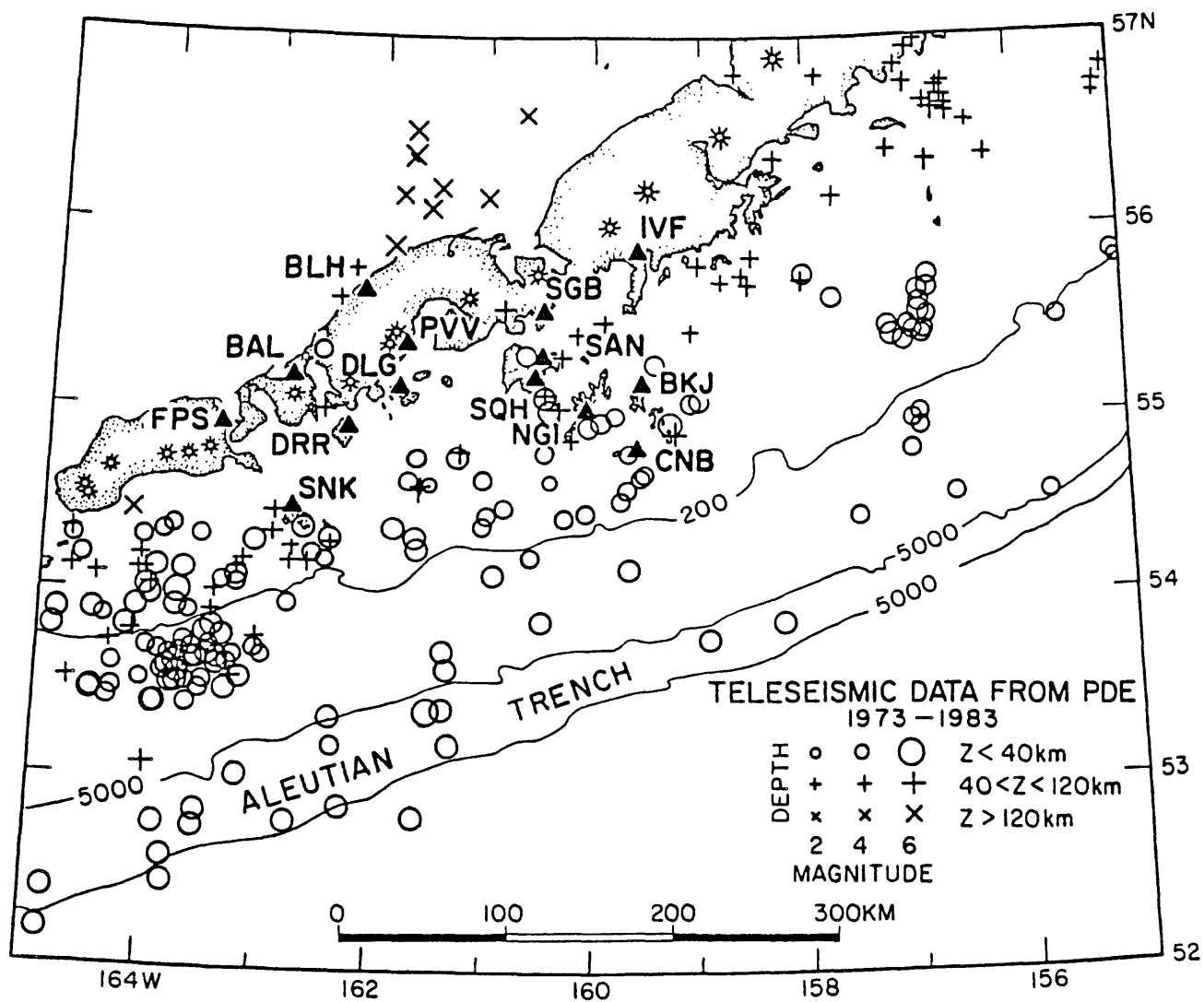
Figure 7. Teleseismic data from the PDE catalog. Note the locations of the deep earthquakes in a band ~100km along strike of the arc, centered on the Shumagin Islands.
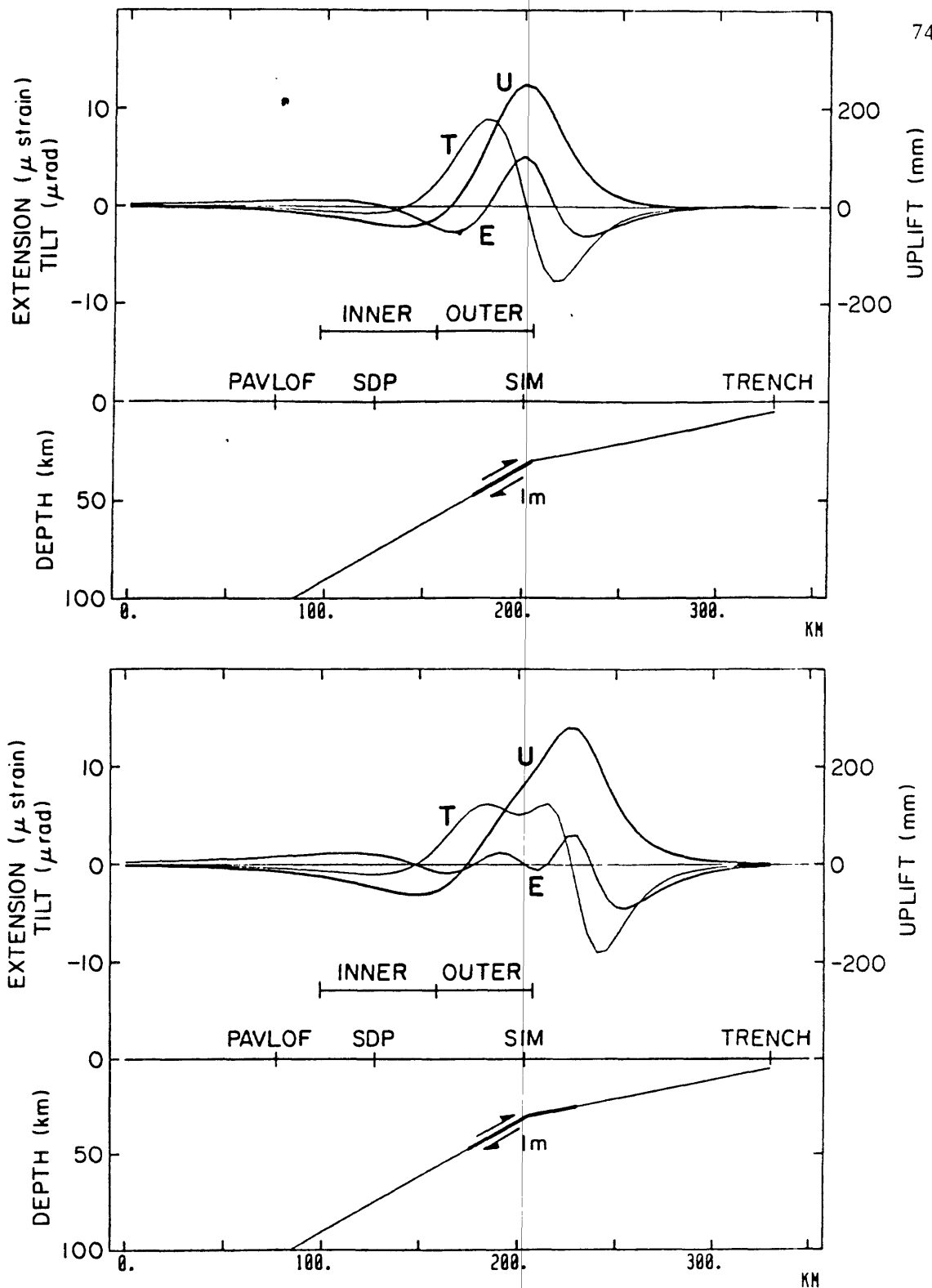
Figure 8 (a,b). Dislocation models showing surface uplift (U), tilt in the plate convergence direction (T), and horizontal linear strain in the plate convergence direction (E), for 1m reverse slip on the fault plane shown. Table 2 gives uplift and tilt at the positions of SDP and SIM, and average strain over the intervals marked as the "inner" and "outer" islands. These are compared with our tilt and uplift observations, and with Savage et al's (1985) strain observations in Table 2.

The figures can also be used to show strain accumulation using Savage's (1983) model. The polarity of uplift, tilt and strain should be changed, and the vertical scales multiplied by 0.075 to give annual deformation rates assuming a 75 mm/yr plate convergence rate. This comparison is made in Table 3.
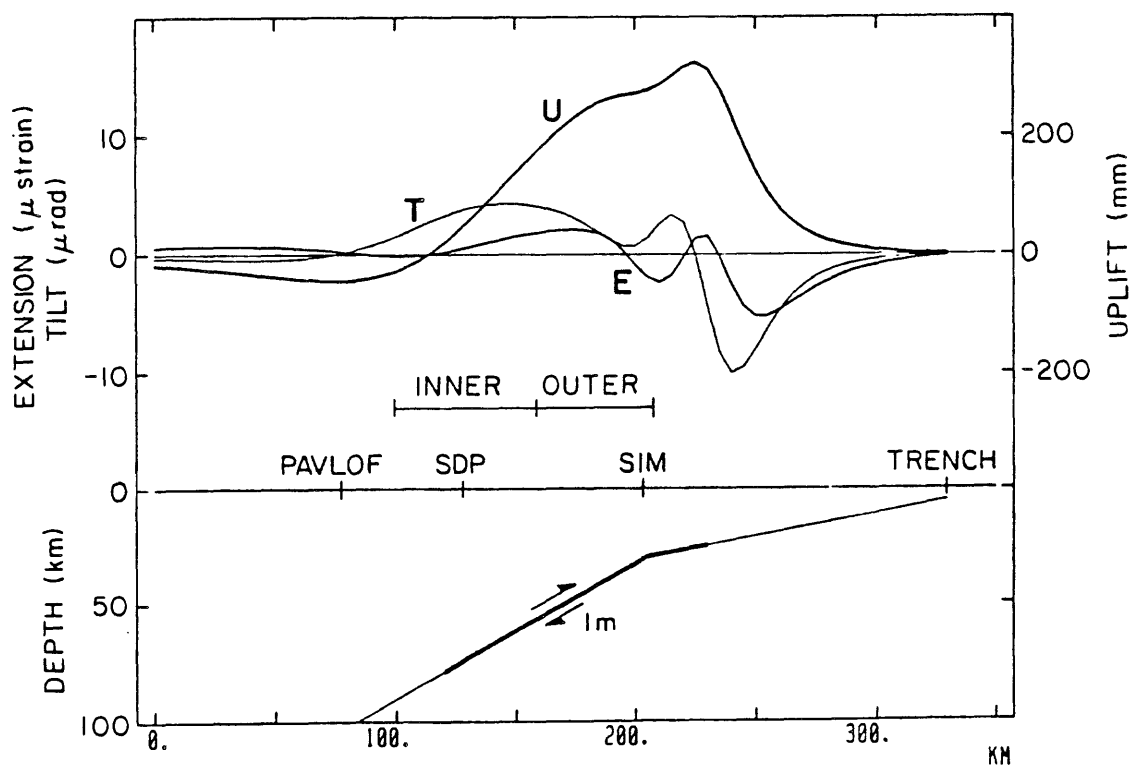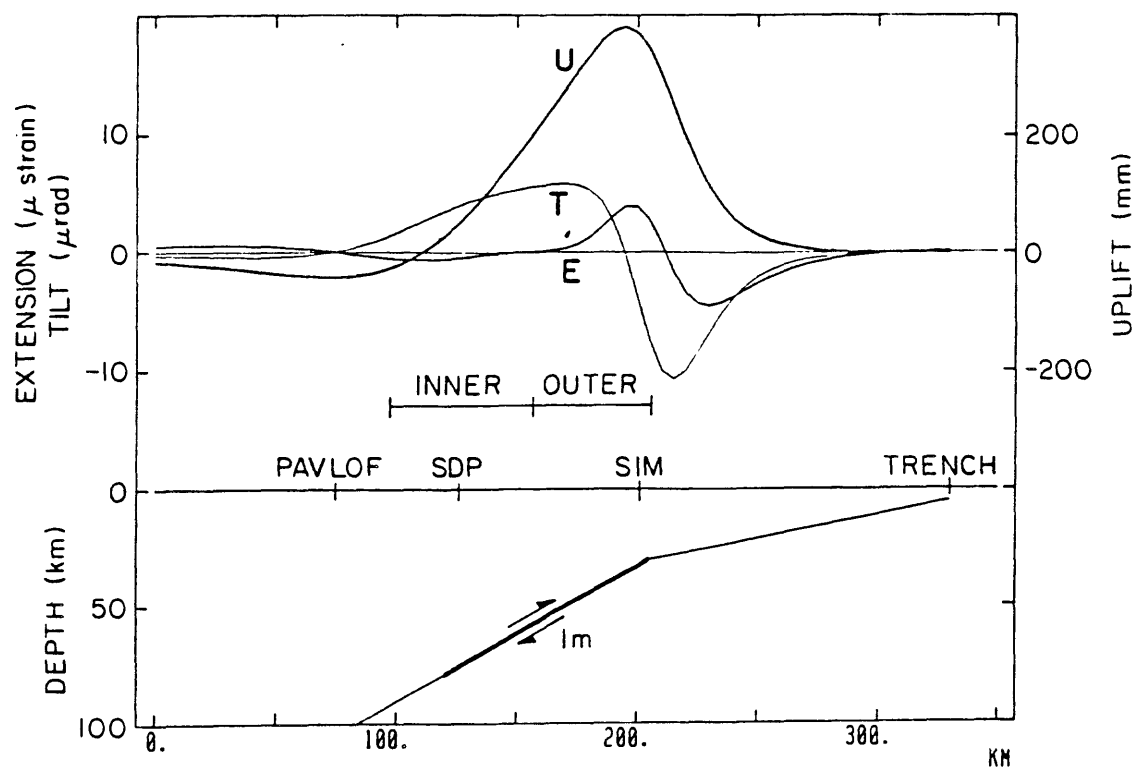
Figure 8 (c,d). See Figure 8a.
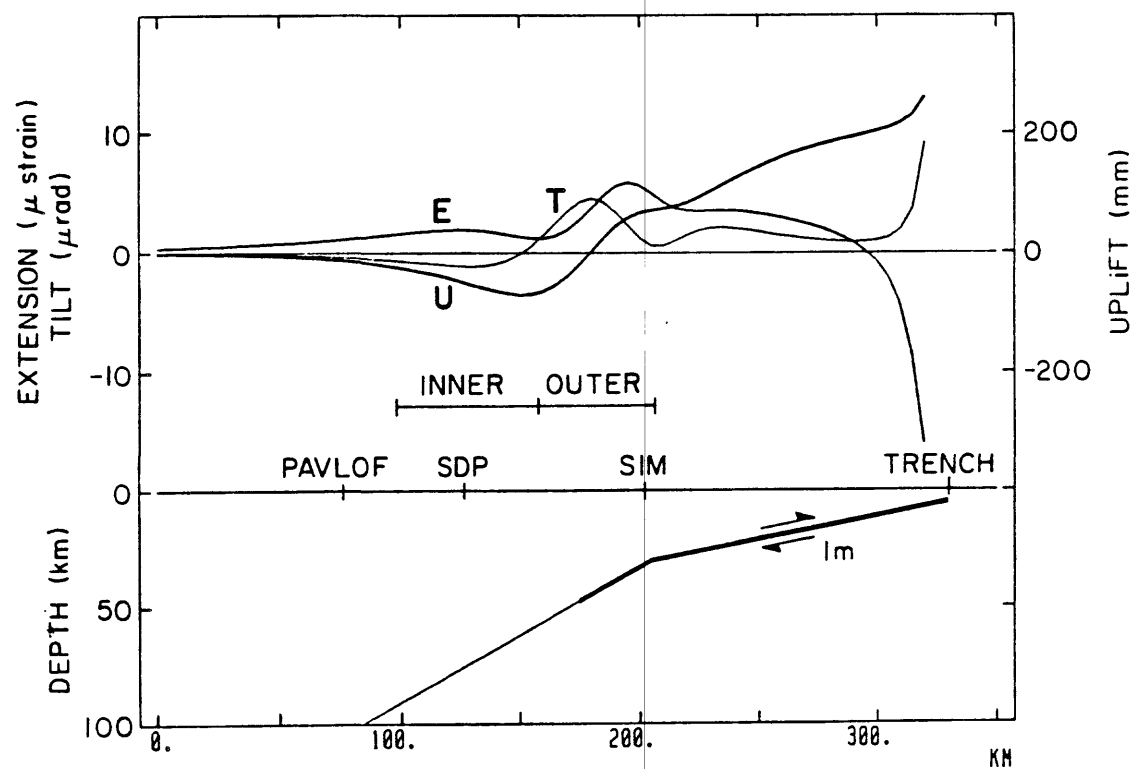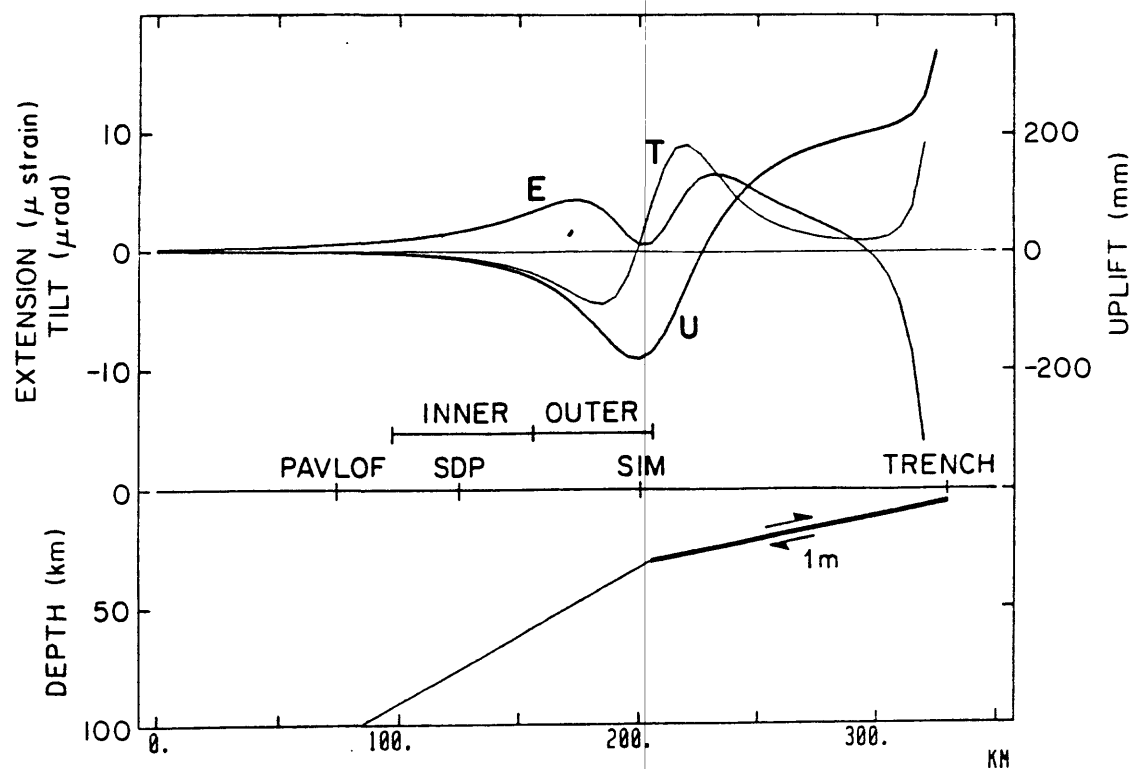
Figure 8 (e,f). See Figure 8a.
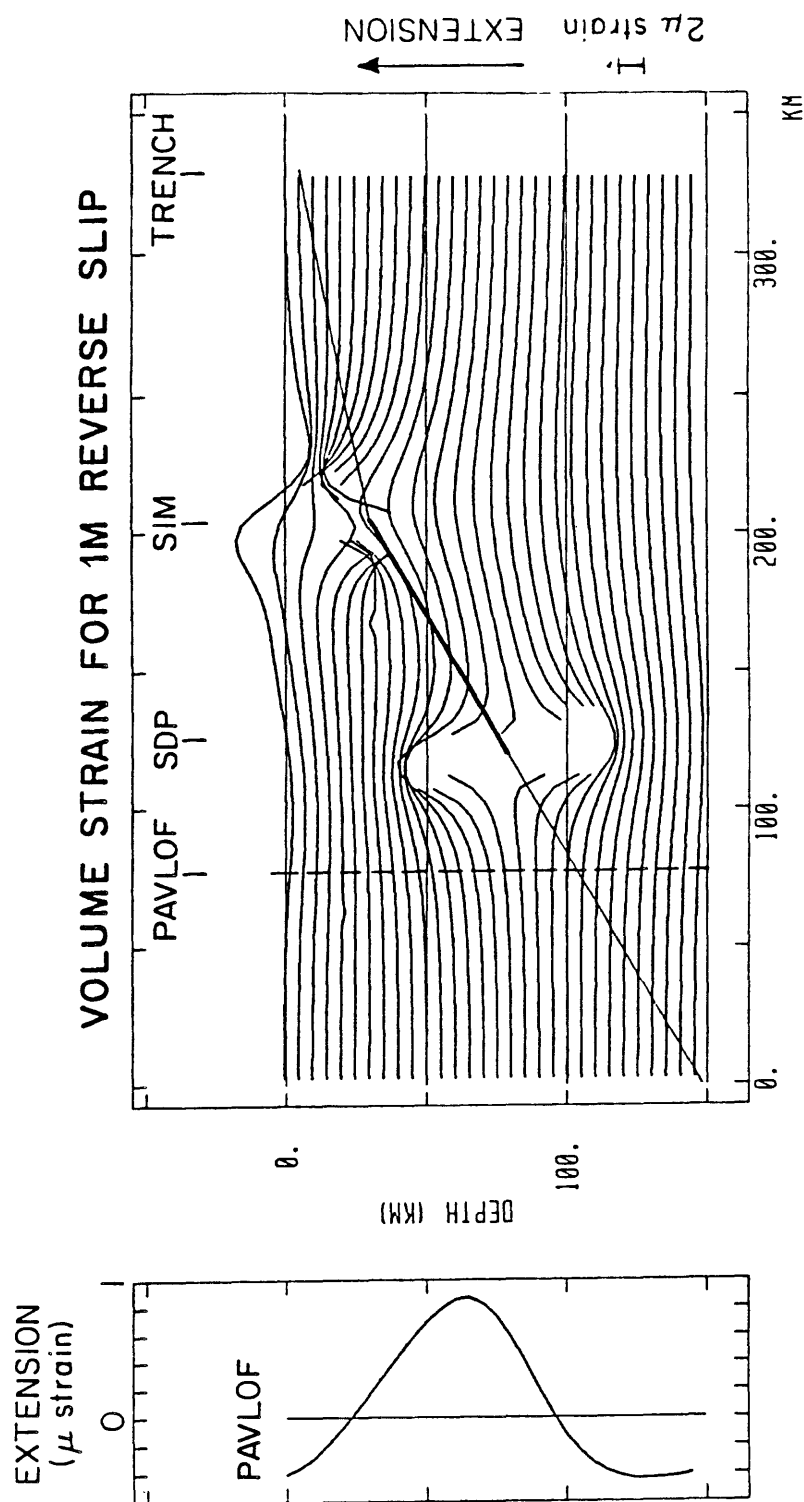
Figure 9. Volume strain at depth due to 1m reverse slip on the 30° dipping fault plane shown. The profiles show volume strain as a function of distance at 5km depth intervals. The profiles are truncated near the ends of the model fault for clarity and because they are not physically realistic in these regions. Note an increase in volume strain in the region below Pavlof Volcano. The panel on the left shows a vertical profile beneath Pavlof on an expanded scale. The average volume extension in the mantle above the sinking slab is about 0.6 μstrain.
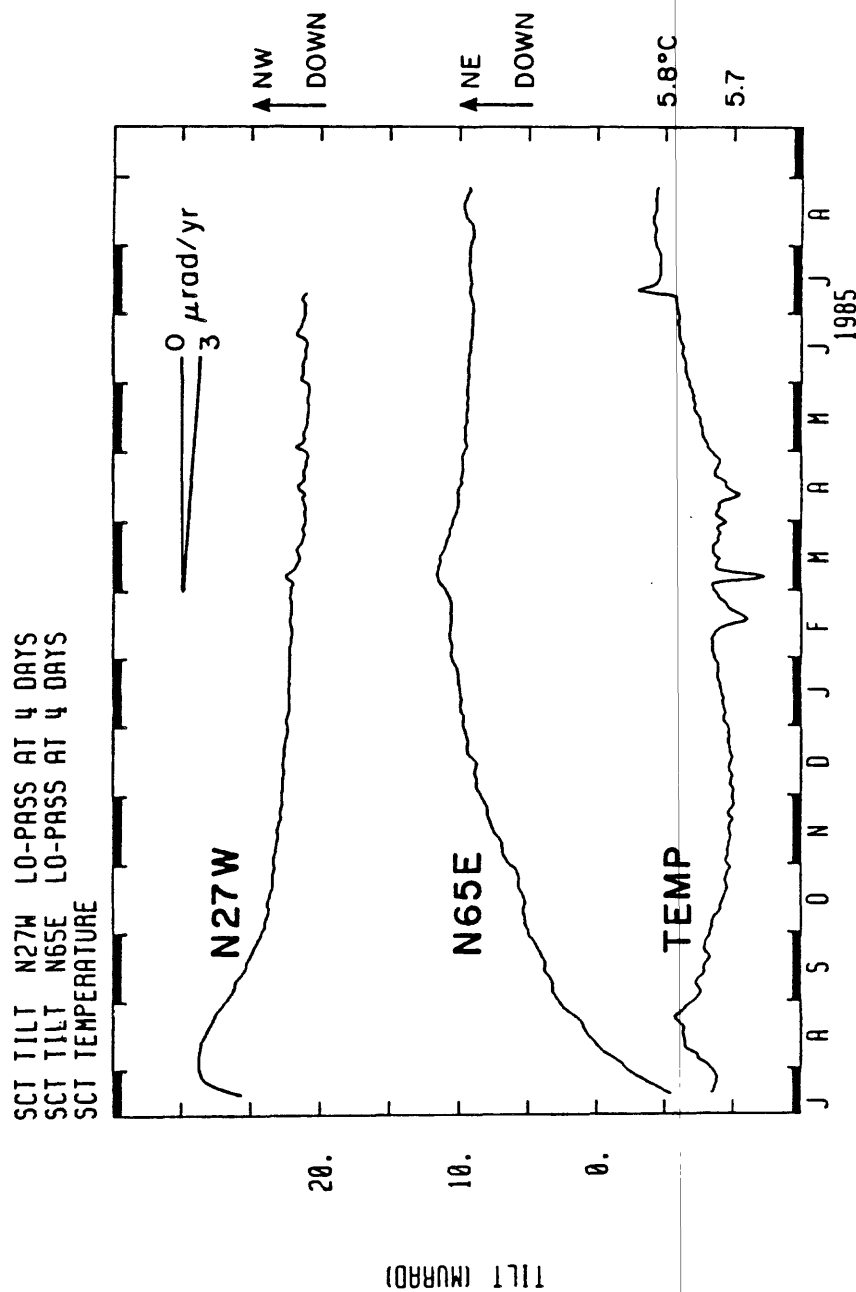
Figure 10. Low-pass filtered tilt and temperature records from the tiltmeter installation. The tiltmeters use mercury to define an equipotential, and capacitance transducers to measure tilt. They have a base-length of 600mm and are mounted on steel girders concreted to bedrock in a disused mine approximately 40m below ground level.

APPENDIX A. 4.

Strain Accumulation in the Shumagin and Yakataga Seismic Gaps

J. C. Savage

STRAIN ACCUMULATION IN THE SHUMAGIN AND YAKATAGA SEISMIC GAPS

J. C. Savage

Strain accumulation in the Shumagin and Yakataga seismic gaps has been measured from the deformation of trilateration networks during the 1980-1985 interval. The measured rates are shown in Table 1. No significant deformation was detected in the Shumagin gap although the detection threshold was well below the expected strain accumulation rate. The presumption is that strain accumulation in the Shumagin gap is either aseismic or episodic. The strain rate in the Yakataga gap is consistent with that expected for the 60 mm/a plate convergence rate, although the observed transverse component of shear may suggest a somewhat more westerly direction of convergence than expected. Surveys of a 1-km-aperture tilt array at Cape Yakataga indicate a relatively uniform tilting at the rate of 0.7 μrad/a down in the direction of N53°E, roughly perpendicular to the rate of plate convergence.

FIGURE CAPTIONS

Fig. 1. Trilateration network in the Shumagin Islands. Nagai Island has been taken as the boundary between the inner and outer Shumagin Islands.

Fig. 2. Line length L less a nominal length L_0 plotted as a function of time for the lines in the Shumagin trilateration network.

Fig. 3. Accumulation of shear strain (γ_1 and γ_2) and dilatation in the inner and outer Shumagin Islands as a function of time.

Fig. 4. Trilateration network near Cape Yakataga (Station Furr is on the cape).

Fig. 5. Line length L less a constant nominal length L_0 as a function of time for 18 of the lines in the Yakataga network.

Fig. 6. Accumulation of tensor strain as a function of time as indicated by the 18 lines in the Yakataga network shown in Figure 5.

Fig. 7. Velocity vectors for stations in the Yakataga network 1979-1984.

Fig. 8. Tilt measured at Cape Yakataga 1974-1983. The tilt arrays (solid triangles) used to determine tilt in the two intervals (1974-1979 and 1979-1983) are shown in the bottom sketch.

Table 1. Surface strain rates measured in the Shumagin and Yakataga seismic gaps. The 2-axis is oriented parallel to the direction of plate convergence (N30°W in the Shumagin gap and N20°W in the Yakataga gap) and the 1-axis directed into the NE quadrant. Extension is reckoned positive. The quoted uncertainties are standard errors.

Network	Interval	$\dot{\gamma}_1 = \dot{e}_{11} - \dot{e}_{22}$	$\dot{\gamma}_2 = 2\dot{e}_{12}$	$\dot{\Delta} = \dot{e}_{11} + \dot{e}_{22}$
Shumagin Islands				
All	1980-85	-0.01 ± 0.03	-0.03 ± 0.03	-0.12 ± 0.07
Inner	1913-80	0.06 ± 0.06	-0.01 ± 0.05	-
	1980-85	-0.01 ± 0.03	-0.02 ± 0.03	-0.12 ± 0.07
Outer	1981-85	0.03 ± 0.05	-0.05 ± 0.06	-0.20 ± 0.10
Yakataga	1979-84	0.26 ± 0.05	0.19 ± 0.04	-0.11 ± 0.08

83

2

ϵ'_{11} $0.07 \pm 0.04\, \mu\epsilon/a$

ϵ'_{12} $0.09 \pm 0.02\, \mu\epsilon/a$

ϵ'_{22} $-0.19 \pm 0.04\, \mu\epsilon/a$

YAKATAGA

Isle
Jun
Carol
Anchor Ecc
Anchor
Rob
Ice
Mac
Hanna
Allison
Kul
Gull
Ocean
Pacific

20
10
mm/a
km
0

7

N70°E
0.66±0.12 μrad/a

N20°W
0.20±0.15 μrad/a

EQ

ST ELIAS

TILT, μrad

300 m

N

LEVEL ARRAY
BEFORE JUL 1979

LEVEL ARRAY
AFTER JUL 1979

8
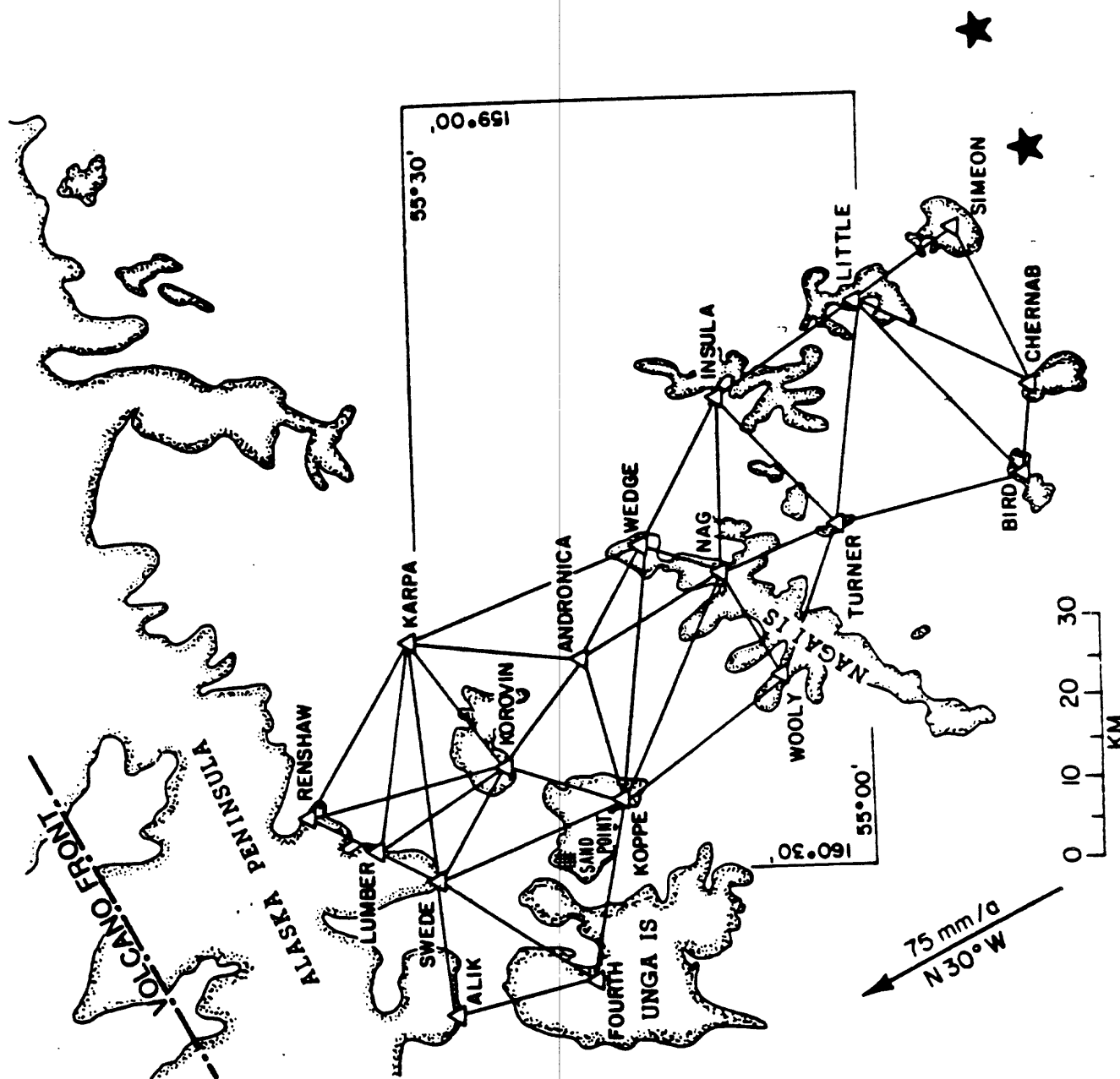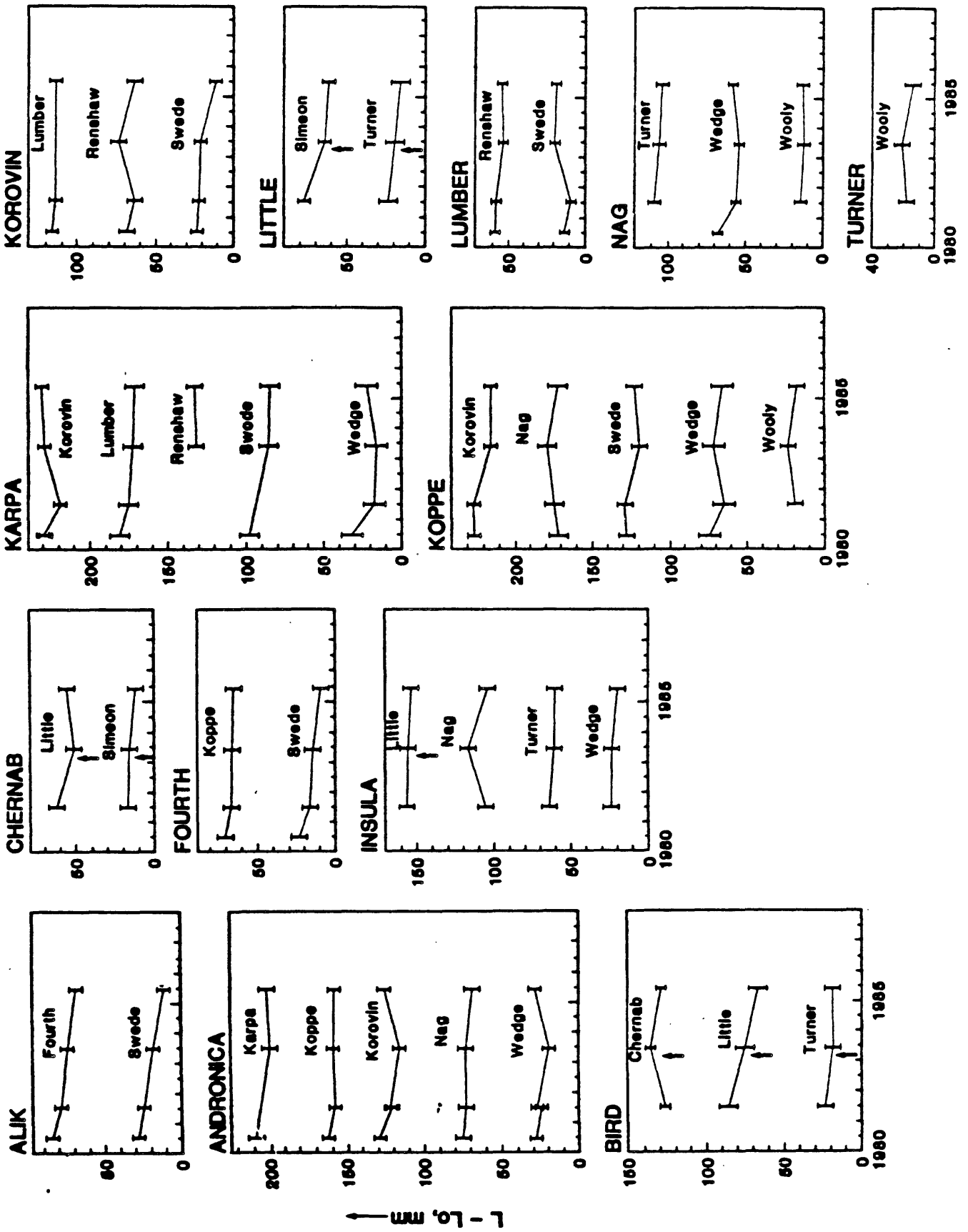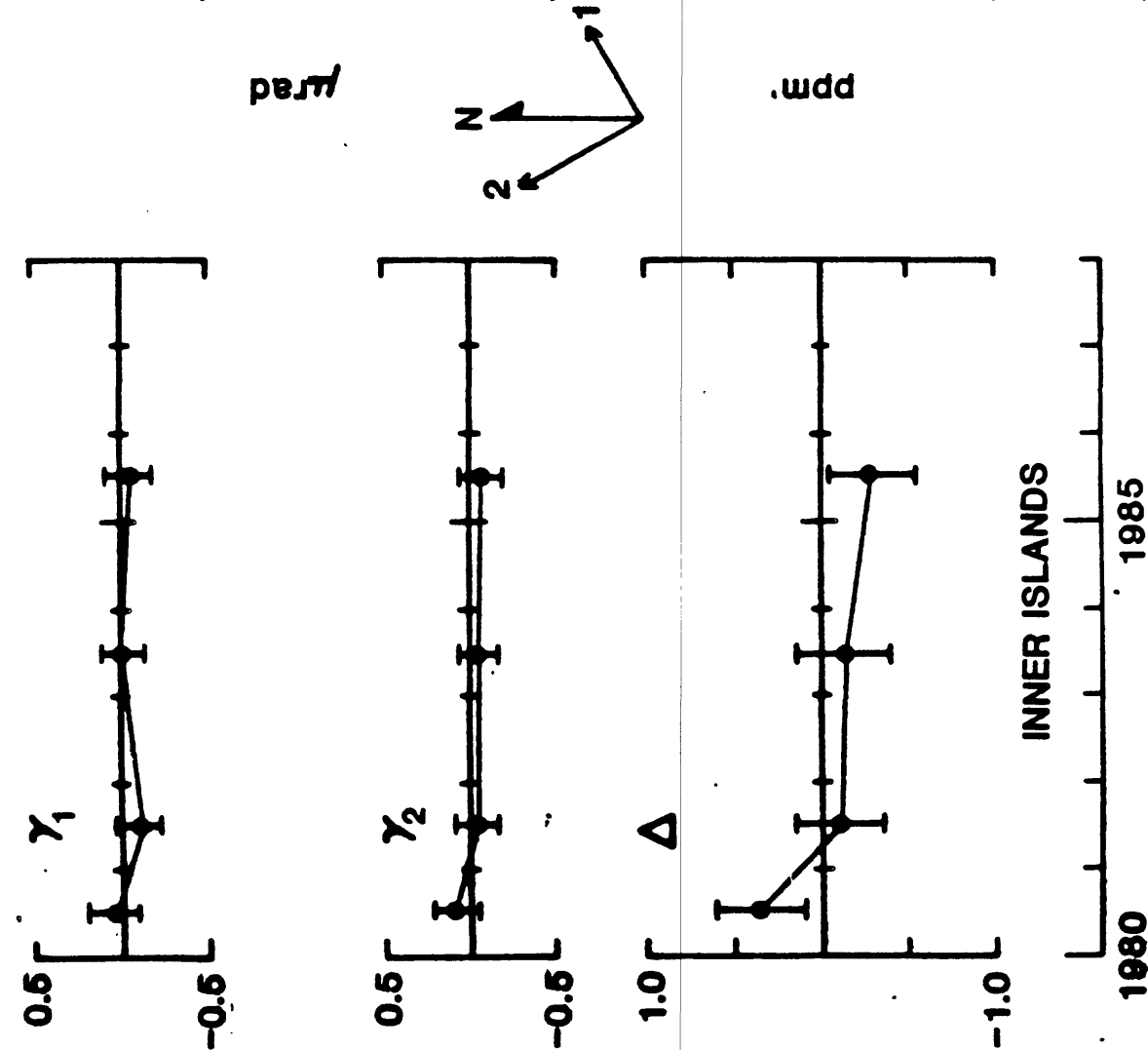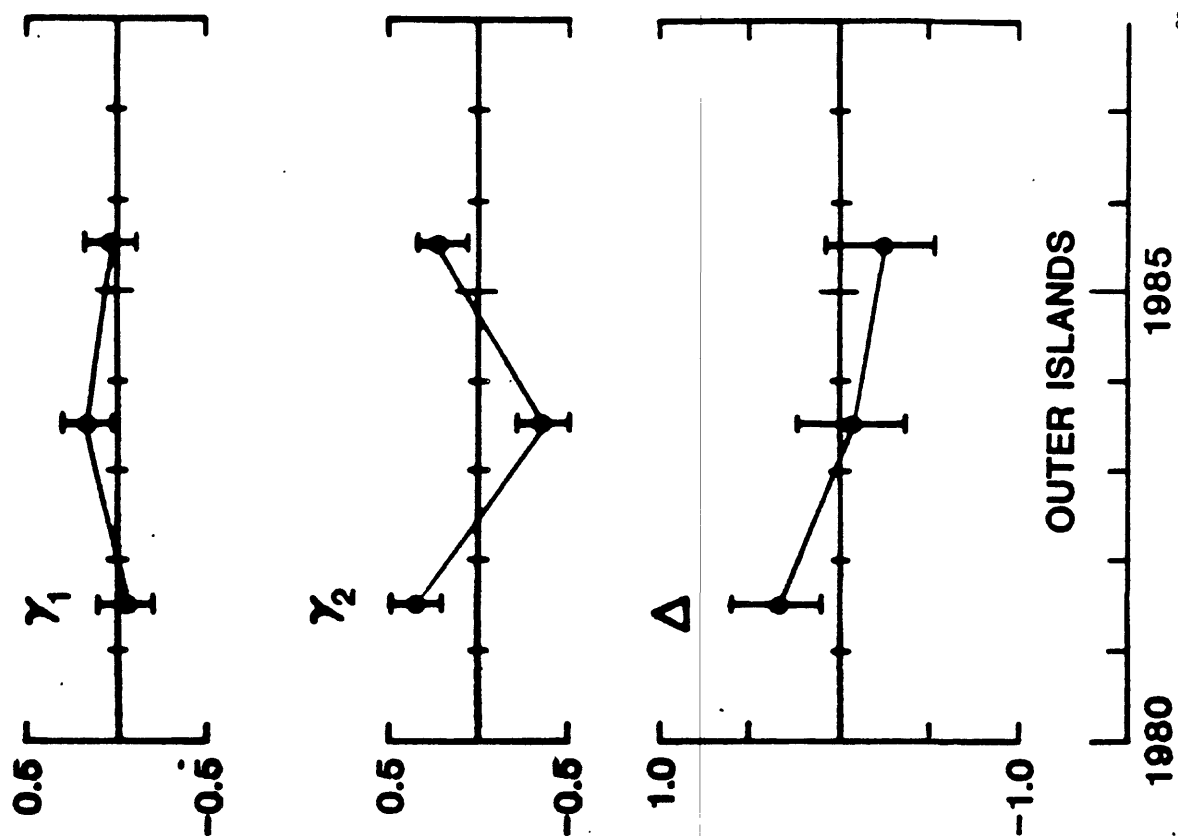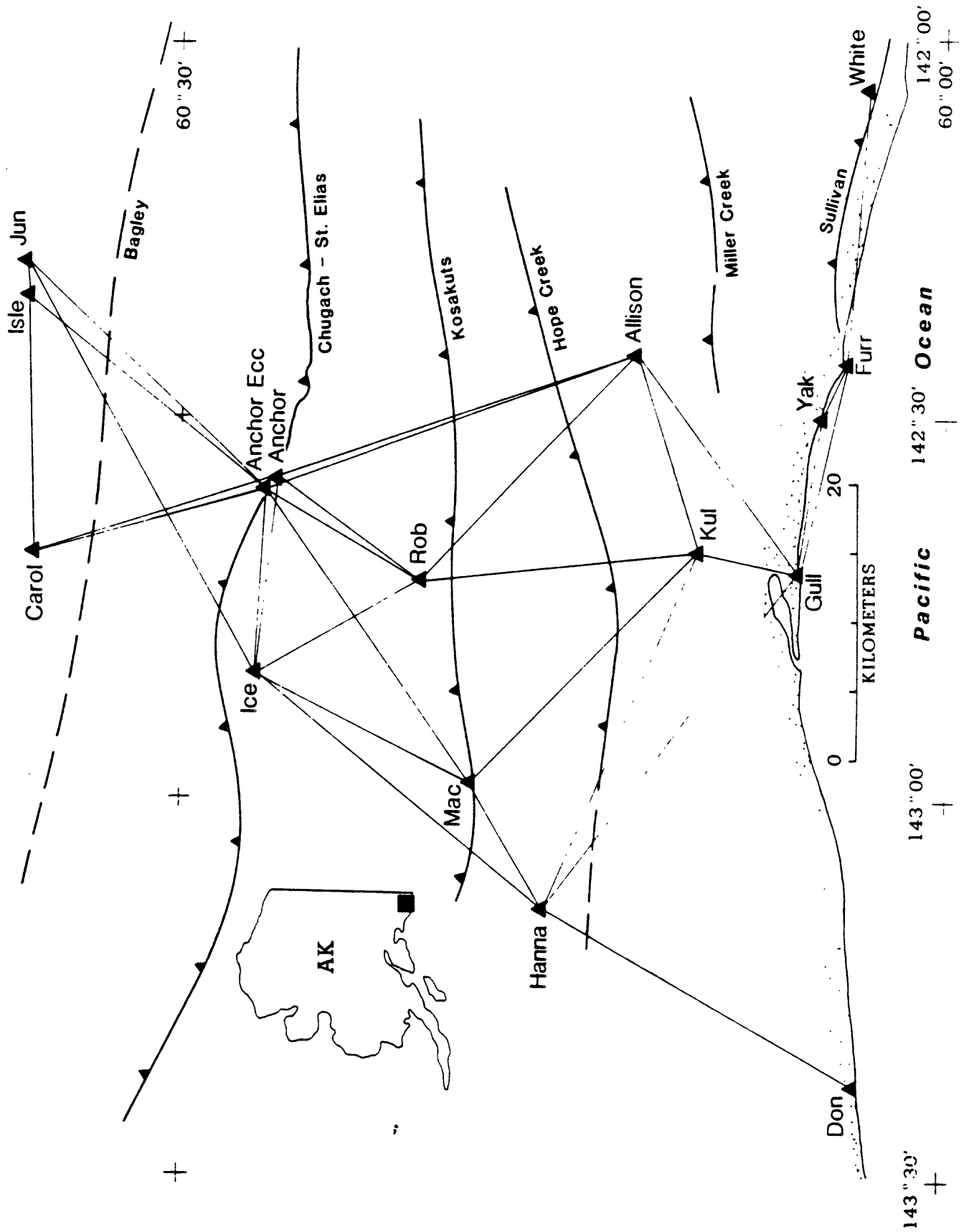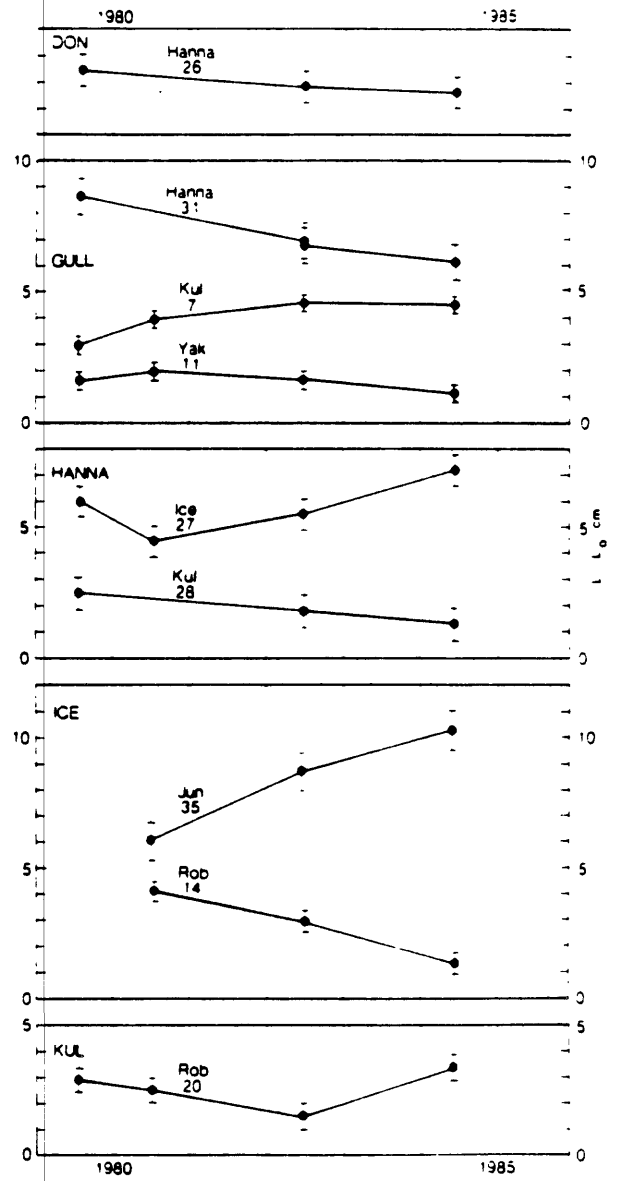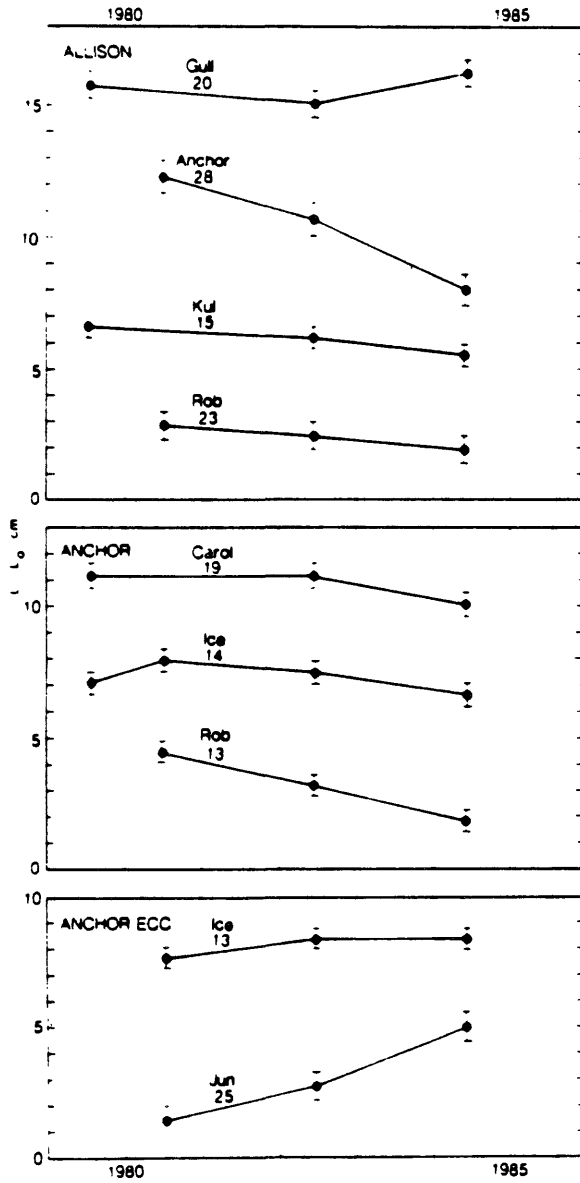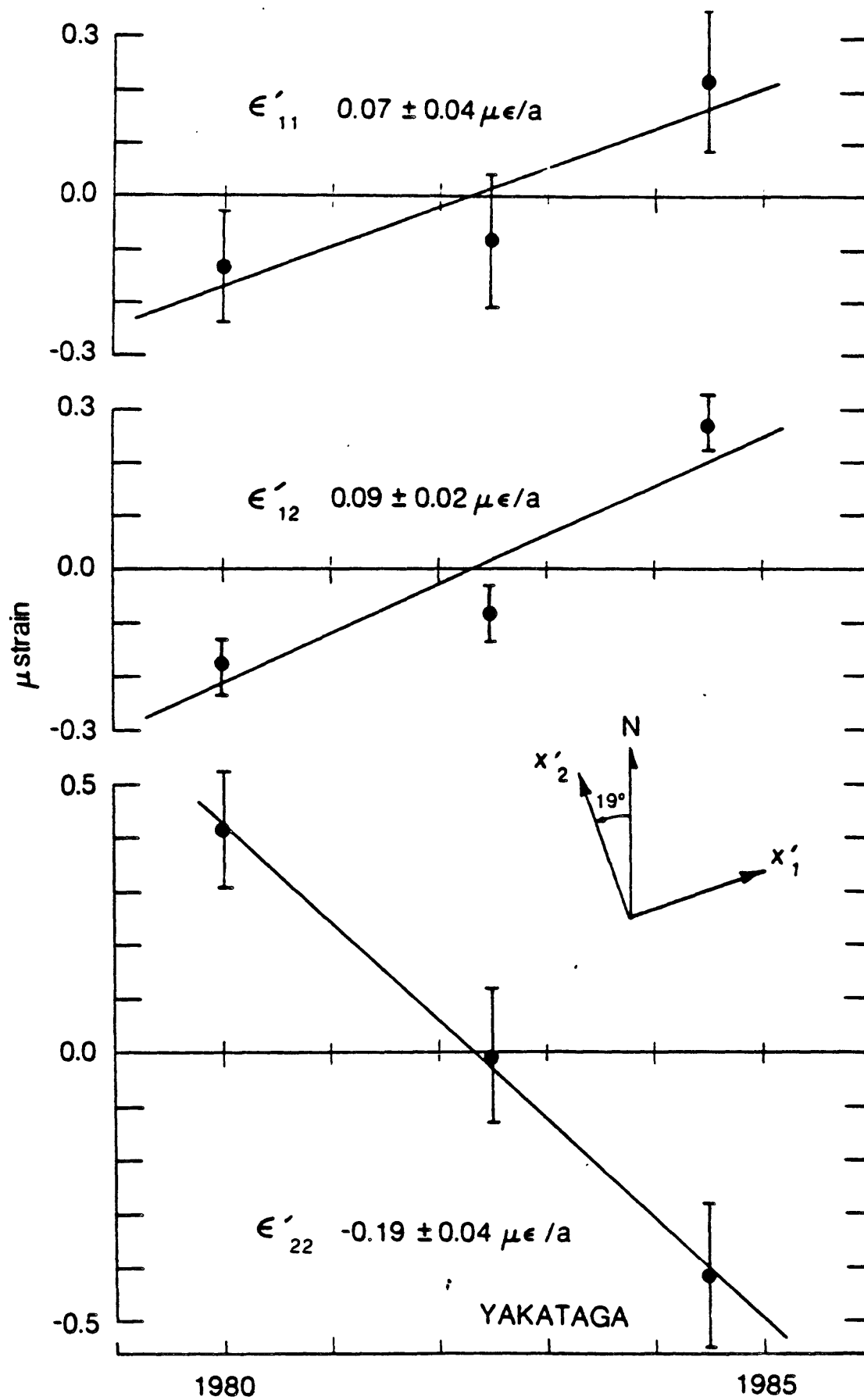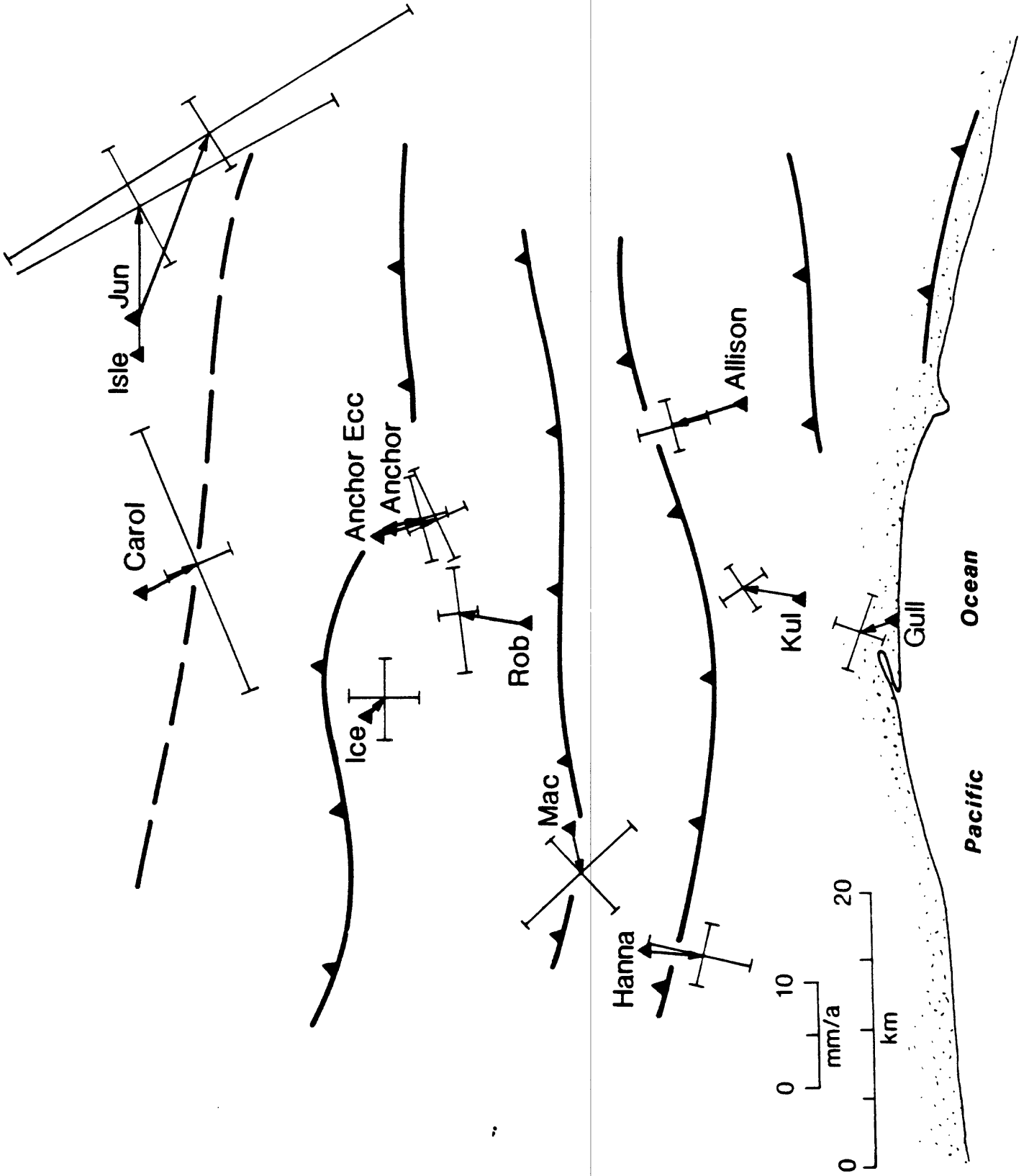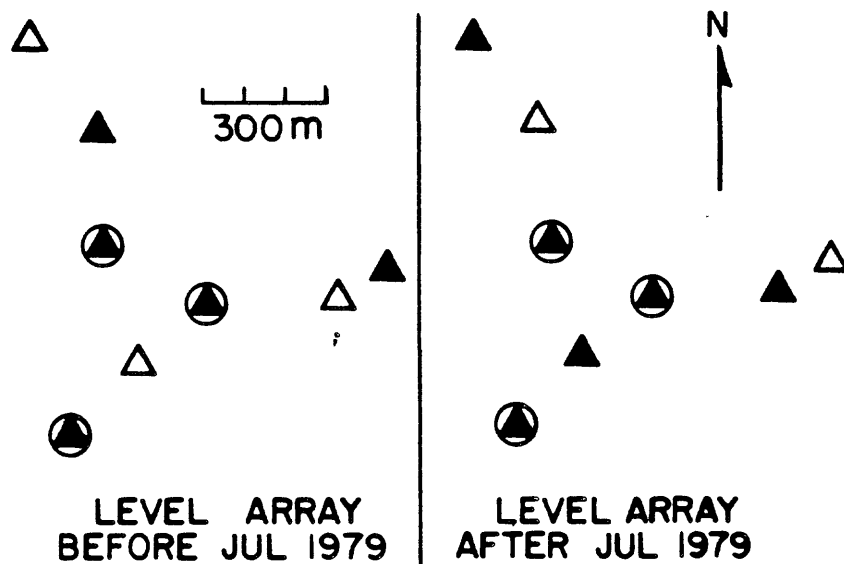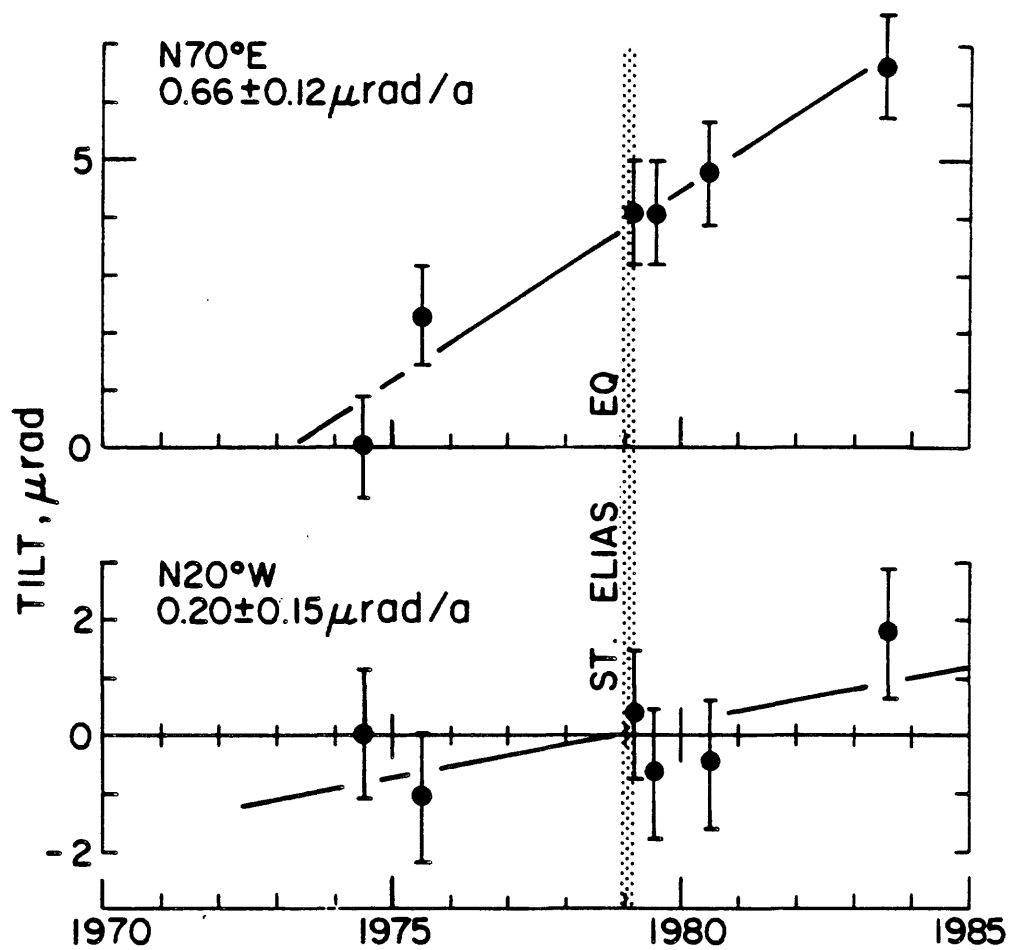
APPENDIX A. 5.

Hazards Evaluation for Large and Great Earthquakes along the
Queen Charlotte - Alaska-Aleutian Seismic Zone: 1985-2005

S. P. Nishenko and K. Jacob

HAZARDS EVALUATION FOR LARGE AND GREAT EARTHQUAKES ALONG THE
QUEEN CHARLOTTE - ALASKA - ALEUTIAN SEISMIC ZONE: 1985-2005

by

Stuart P. Nishenko

National Earthquake Information Center

U.S. Geological Survey, Denver, CO 80225

Klaus Jacob

Lamont-Doherty Geological Observatory

of Columbia University

Palisades, NY 10964

INTRODUCTION

Conditional probabilities for the ocurrence of large, great (and giant)

earthquakes along specific segments of the Queen Charlotte-Alaska-Aleutian

(QC-A-A) seismic zone are presented for the time interval 1985-2005. Time-

dependent recurrence models are combined with simple Gauss and Weibull

distribution functions to forecast the likelihood of future events in this

region. At present, areas of high seismic hazard include the Yakataga gap as

well as a large portion of the Alaska Peninsula (including the 1938, Shumagin

gap and 1946 segments as well as possibly the Unalaska gap). Areas of low

seismic hazard include the entire Queen Charlotte seismic zone (1949

[excluding the possible Cape St. James gap], 1972 and 1958 rupture zones), the

1964 Gulf of Alaska, portions of the 1957 Central Aleutian and the 1965 Rat

Islands zones.

The QC-A-A seismic zone is divided into 17 segments based on (1) the rupture zones of the most recent large or great earthquakes, as defined by aftershock distributions, and (2) variations in the amount of coseismic displacement within individual rupture zones.

For each individual segment or gap along the QC-A-A seismic zone, input for the time-dependent Gaussian model consists of the date of the last large earthquake, the estimated repeat time and the standard deviation of time intervals between events (the coefficent of variation). For the majority of the QC-A-A seismic zone, the date and size of the last event is known. Estimates of repeat time are calculated by dividing the coseismic displacement in the previous event by the rate of fault motion. Note that these estimates do not account for the effects of aseismic slip on recurrence intervals, and hence, represent minimum repeat time and maximum probability estimates. Where available, repeat time estimates are supplimented by historic and geologic data as well. The coefficient of variation along any segment of the margin is poorly known, and we uniformly assign a standard deviation equal to 33% of the estimated repeat time in our estimates. A standard deviation of 33% is similar to that found in studies along other simple transform and convergent plate boundaries (Sykes and Nishenko, 1984; Nishenko, 1985).

For comparison to the above evaluation, we have also modeled the catalog of historic repeats (and possible repeats) from Jacob (1984) along sections of the A-A seismic zone using a Weibull distribution function.

Both of these time-dependent descriptions of earthquake hazard (or conditional probability) are compared and contrasted to estimates of seismic hazard baed on a Poisson model of recurrence. The Poisson based estimates of conditional probability are termed time-independent or static, as they do not include the amount of time elapsed since the previous shock. In general, conditional probabilities based on the Poisson model cluster around 10-40% for a 20-year time window throughout the entire QC-A-A seismic zone. Estimates of seismic hazard based on all 3 models are presented in Table 1 and Figures 1 and 2.

Overall, as seen in Table 1 and Figures 1 and 2, recurrence time estimates based on both the last shock and historic/geologic data vary by a factor of two, while the range of probability estimates for each model, are within 10-20% of each other. This reflects the fact that 2/3 of the margin has ruptured within the last 20-30 years, and is now within the first 1/3 or less of a new seismic cycle. The segments with the largest uncertainties (and possibly the highest probabilities) are along the Alaskan Peninsula (the 1938 and Shumagin gaps). The poor resolution reflects a fundimental lack of data concerning the sizes and locations of previous earthquakes in this area.

Time-dependent estimates of conditional probability that are lower than the Poisson estimates for any particular segment are suggested to indicate a low level of seismic hazard. Areas of low hazard (i.e. less than 10-20% for the next 20 years) presently include the entire Queen Charlotte seismic zone (1949 [excluding the possible Cape St. James gap], 1972 and 1958 rupture zones), the 1964 Gulf of Alaska, portions of the 1957 Central Aleutians and the 1965 Rat Islands zones. Note that while the hazard for Mw>9 earthquakes along the 1964 Gulf of Alaska zone is presently low, we cannot rule out the possibility for

the ocurrence of smaller (Mw7.5-8) events in this area, as is seen historically for the Kodiak Island region. Time-dependent estimates that are greater than the Poisson estimates are judged to indicate a high level of seismic hazard. Areas of high seismic hazard (i.e. greater than 50% for the next 20 years) presently include the Yakataga gap as well as a large portion of the Alaska Peninsula (including the 1938, Shumagin gap and 1946 segments as well as possibly the Unalaska gap). While the degree of resolutuion is poor for some of these gaps, the spatial proximity of a number of high hazard areas along the Alaskan Peninsula raises the scenario whereby rupture in one segment may trigger activity in adjacent segments and produce a larger event than any one single segment. Historically, this section of the margin, Kodiak Island to the Shumagins, was ruptured by a great (M>8) earthquake in 1788 with an estimated rupture length of at least 600 km. The Commander Islands gap, in the westernmost Aleutians, presently has a high probability for recurrence based on the extrapolation of the Weibull data. Few other data, however, exist to independently constrain the hazard level in the Commander Islands area.

REFERENCES

Jacob, K., Estimates of long-term probabilities for future great earthquakes in the Aleutians, Geophys. Res. Lett., 11, 295-298, 1984.

Nishenko, S. P., Seismic potential for large and great interplate earthquakes along the Chilean and southern Peruvian margins of South America, Jour. Geophys. Res., 90, 3589-3615, 1985.

Sykes, L. R. and S. P. Nishenko, Probabilities of occurrence of large plate

   rupturing earthquakes for the San Andreas, San Jacinto and Imperial

   faults, California: 1983-2003, Jour. Geophys. Res., 89, 5905-5928, 1984.

TABLE 1: CONDITIONAL PROBABILITY ESTIMATES FOR THE QUEEN CHARLOTTE - ALASKA - ALEUTIAN SEISMIC ZONE : 1985 - 2005

LOCATION	LAST SHOCK	DT (yrs)	Mo (x10^27 d-c)	LENGTH (km)	WIDTH (km)	SLIP (cm)	SLIP RATE (cm/yr)	ESTIMATED REPEAT TIME	OTHER DATA	CONDITIONAL PROBABILITY POISSON	GAUSS	WEIBULL
1. Cape St. James	??											
2. Queen Charlotte Is.	1949 Mw 8.1	36	12	490	(15)	550	5.5	100		18.1%	6.6%	
3. Sitka	1972 Ms 7.4	13	4	175	(15)	500	5.2	90	1927, 45 y 1880, 47 y	19.9% 35.3%	2.3% 18.4%	
4. Lituya Bay	1958 Mw 7.7	27	7	350	(15)	450	5.2	86	Max.Disp. 6.5 m, 118 y 1848. 110 y	20.7% 15.6% 16.6%	6.7% 2.4% 3.0%	
5. Yakutat Bay	1899 Mw 8.2	86	20	100-125	75	600	4.8	125	Geodetic 380 y	14.8% 5.1%	18.1% 0.5%	50.6-59.1%
6. Yakataga	1899 Mw 8.1	86	20	125-200	75	250	4.2	52		31.9%	96.5%	50.6-59.1%
7. Prince William Sound	1964 Mw 9.2	21	820	750	180	1215 3000	6.5	187	Geodetic 461 y Geologic 897 y	10.0% 4.2% 2.2%	0.5% 0.1% 0.03%	18.1-19.6%
8. Gulf of Alaska	1964 Mw 9.2	21						187		10.0%	0.5%	18.1-19.6%
9. Kodiak Is.	1964 Mw 9.2	21						187		10.0%	0.5%	18.1-19.6%
9A. Kodiak Is.									Historic Ms 7.4-8 40-60 y	28.3-39.3%	14.8-49.2%	

TABLE 1: CONDITIONAL PROBABILITY ESTIMATES FOR THE QUEEN CHARLOTTE - ALASKA - ALEUTIAN SEISMIC ZONE : 1985 - 2005

LOCATION	LAST SHOCK	DT (yrs)	Mo ($\times 10^{27}$ d-c)	LENGTH (km)	WIDTH (km)	SLIP (cm)	SLIP RATE (cm/yr)	ESTIMATED REPEAT TIME	OTHER DATA	CONDITIONAL PROBABILITY		
										POISSON	GAUSS	WEIBULL
10. Alaska Pen.	1938 Mw 8.2	47	50	300	120	200-300	7.1	28-42	Historic 50-91 y	37.9-51.0% 19.7-32.9%	90.0-99.9% 15.1-73.5%	33.6-36.1%
11. Shumagins	1903 MB.3,Ms6.9 1847	82 138		(250)	(100)				Historic 60-100 y(?)	18.1-28.3%	33.0-87.3% 68.4-99.1%	49.1-57.0% 66.9-79.6%
12. Unimak Is.	1946 Ms 7.4	39	13	100	100	200-300	7.7	24-42		37.9-56.5%	81.2-99.9%	29.6-30.6%
13. Unalaska	1957 Mw 8.8	28		(1200)	70		8.3					23-23.6%
14. Central Aleutians	1957 Mw 8.8	28		(1200)	70	400-600	8.3	48-72		24.2-34.8%	12.8-44.2%	23-23.6%
15. Andreanof Is.	1957 Mw 8.8	28	200	600	70	950-1580	8.3	115-191		9.9-15.9%	0.6-2.8%	23-23.6%
16. Rat Is.	1965 Mw 8.7	20	125	500	70	700 280	8.6 5	81 56	Historic 59 y	21.8% 30% 28.7%	5.2% 17.2% 14.5%	17.4-19%
17. Commander Is.	1849/587	136										66.4-78.9%

References for Table 1

Entire QC-A-A seismic zone:

   Sykes, L.R., J. Geophys. Res., 76, 8021-8041, 1971.

   Sykes, L.R., J.B. Kisslinger, L.House, J.N. Davies and K.H. Jacob,
      Science, 210, 1343-1345, 1980.

Specific segments along the QC-A-A seismic zone:

1 and 2]   Bostwick, T.D., Ph.D. thesis, Univ. British Columbia, 1984.

             Rodgers, G.C., Earthquake Pred. Res., in press, 1985.

      3]   Page, R., Earthquake Info. Bull., 5, 4-9, 1973.

      4]   Plafker, G., T. Hudson and T. Bruns, Can. J. Earth Sci.,
             15, 805-816, 1978.

5 and 6]   McCann, W.R., O.J. Perez and L.R. Sykes, Science, 207,
             1309-1314, 1980.

             Plafker, G., T. Hudson and M. Rubin, EOS, Trans. AGU,
             61, 1110, 1980.

             Thatcher, W. and G. Plafker, Geol. Soc. America abs. with
             Programs, 9, 515, 1977.

7, 8, 9]   Plafker, G., U.S. Geol Survey Prof. Paper 543-I, 1967.

             Plafker, G. and M. Rubin, U.S. Geol. Survey Open File Rpt.
             78-943, 687-722, 1978.

             Ruff, L. and H. Kanamori, Phys. Earth Planet. Int., 31,
             202-230, 1983.

10, 11, 12] Davies, J., L. Sykes, L. House and K. Jacob, J. Geophys.
             Res., 86, 3821-3855, 1981.

13, 14, 15] Wahr, J. and M. Wyss, J. Geophys. Res., 85, 6471-6477,
             1980.

             Ruff, L., H. Kanamori and L. Sykes, EOS, Trans. AGU,
             66, 298, 1985.

      16]   Ruff, L. and H. Kanamori, Phys. Earth Planet. Int., 31,
             202-230, 1983.

FIGURE 1:   Conditional probability estimates for large
and great interplate earthquakes along the Queen Charlotte-Alaska-
Aleutian seismic zone: 1985-2005. Encircled numbers refer to fault
zones or segments listed in Table 1. Foe each segment, the percentages
and the height of box represent represent the range of calculated
probabilities based on Gaussian, Poisson and Weibull models (see bottom
of figure for appropriate symbol). Dates and vertical bars at the top
of the histogram refer to the time and lateral extent of the last large
or great earthquake in each segment. For zone 9 (Kodiak Island),
probabilities are presented for rerupture as a part of the 1964 zone
and as an independent unit. Note that the zones with the highest
overall probabilities also have the largest uncertainties.
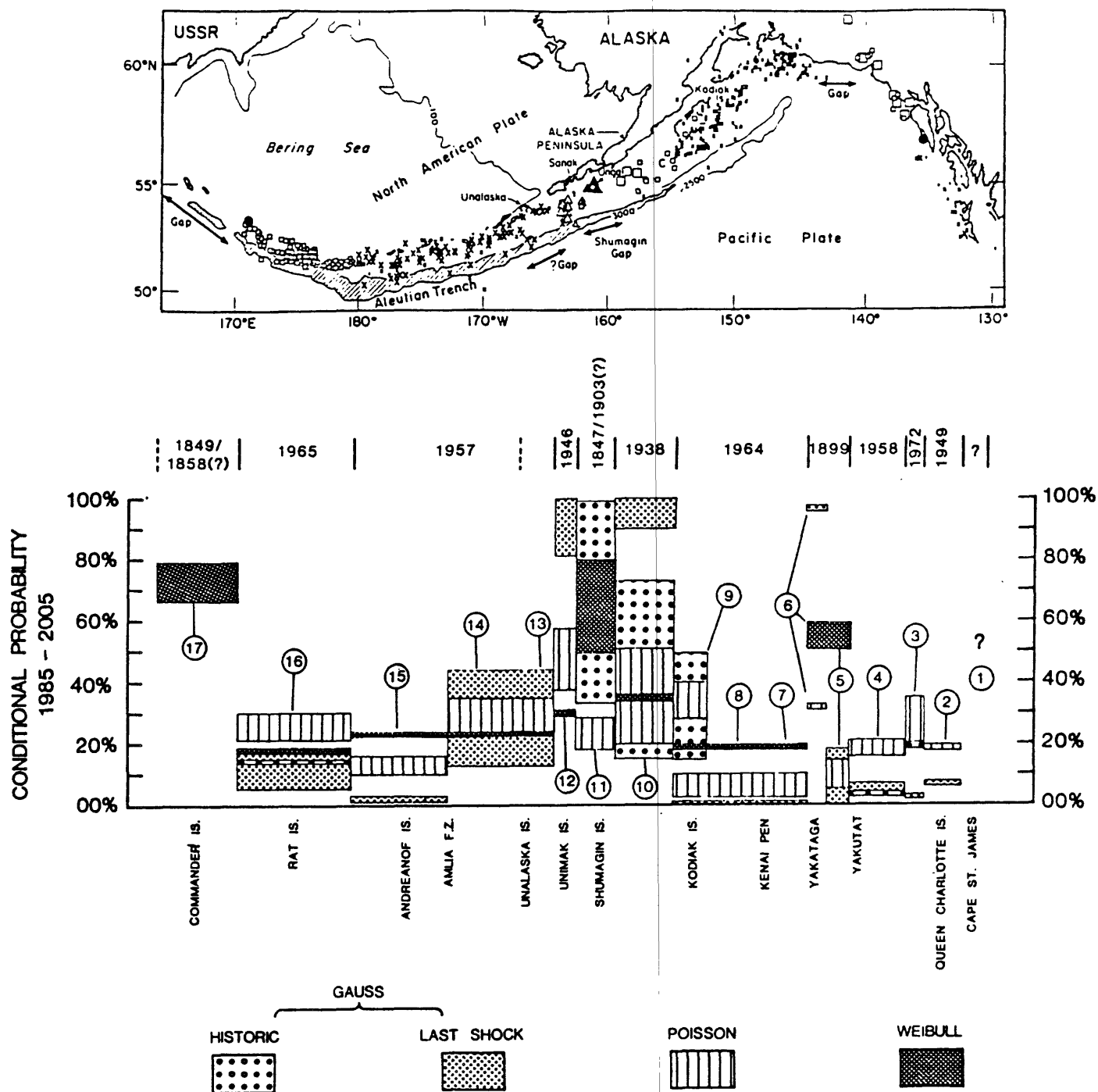
FIGURE 1.

FIGURE 2:   Comparison of conditional probability estimates
for large and great interplate earthquakes along the Queen Charlotte-
Alaska-Aleutian seismic zone: 1985-2005. Encircled numbers refer to
the fault zones or segments listed in Table 1.   The percentages beside
each zone represent the range of calculated probabilities from Gaussian
(top), Poisson (middle) and Weibull (bottom) models.   The shading of
each fault segment corresponds to the mean probability estimate (see
bottom of figure for key).   Blank areas denote segments with lack of
sufficent data for a particular recurrence model.

CONDITIONAL PROBABILITY
QUEEN CHARLOTTE – ALASKA – ALEUTIAN
SEISMIC ZONE
1985 – 2005

GAUSS

- ⑯ 5–17%
- 81–99% ⑫
- ⑨ 15–49%
- ⑥ 96%
- ⑤ 1–18%
- ④ 3–7%
- ③ 2–18%
- ② 6%
- ⑦–⑨ ⟨1%
- (13,14) 13–44%
- ⑮ 1–3%
- ⑩ 15–99%
- ⑪ 33–99%

ALASKA

POISSON

- ⑯ 22–30%
- 38–56% ⑫
- ⑨ 28–39%
- ⑥ 32%
- ⑤ 5–15%
- ④ 16–21%
- ③ 20–35%
- ② 18%
- ⑦–⑨ 2–10%
- (13,14) 24–35%
- ⑮ 10–16%
- ⑩ 20–51%
- ⑪ 18–28%

ALASKA

WEIBULL

- ⑰ 66–79%
- ⑯ 17–19%
- 30% ⑫
- ⑥ 50–59%
- ⑤ 50–59%
- (13–15) 23%
- ⑦–⑨ 18–20%
- ⑩ 33–36%
- ⑪ 49–80%

ALASKA

0 – 20% 20 – 50% 50 – 100%
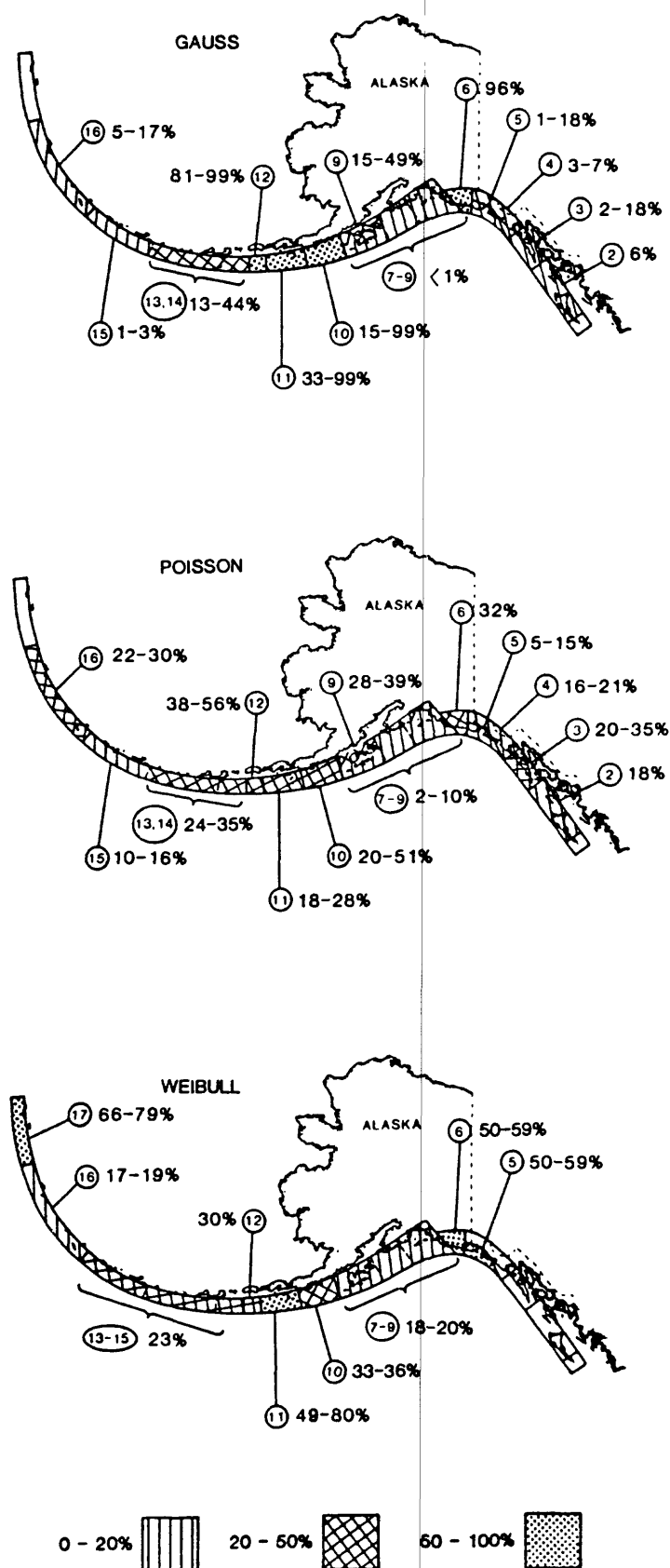
FIGURE   2.

APPENDIX A. 6.

Evidence for Activity of the Castle Mountain Fault System:
A Review for the 1985 NEPEC Workshop

J. C. Lahr and R. A. Page

EVIDENCE FOR ACTIVITY OF THE

CASTLE MOUNTAIN FAULT SYSTEM: REVIEW FOR 1985 NEPEC WORKSHOP

J. C. Lahr and R. A. Page

According to one tectonic model for southern Alaska (Lahr and Plafker, 1980), the part of the North American plate bordering on the Gulf of Alaska is divided into three subblocks. The Castle Mountain fault lies within the Wrangell block of this model and is shown along with the principal regional tectonic features of southern Alaska in Figure 1. A schematic cross section of the Aleutian arc from Mount Spurr volcano to the Aleutian trench, with selected routinely located earthquakes superimposed, appears in Figure 2. The three source zones for potentially damaging earthquakes in this region are: 1) Aleutian megathrust – earthquakes on the inclined thrust interface between the North American plate and the Pacific plate, such as the 1964 Prince William Sound earthquake; 2) Benioff zone – earthquakes which occur within the subducted Pacific plate; and 3) crustal – shallow events related to faulting and volcanic processes in the overriding North American plate. During the past thirteen years of regional monitoring, the Benioff zone has been the principal seismic source near Anchorage; 141 earthquakes larger than magnitude 4, including 5 larger than magnitude 5, have occurred below 30 km depth within 100 km of Anchorage. In contrast, there have been relatively few crustal (depth less than 30 km) shocks, including only 11 larger than magnitude 4. The largest of these was the 1984 Sutton earthquake whose epicenter is located just north of the trace of the Castle Mountain fault.

The Castle Mountain fault system extends about 200 km from the Susitna River ENE across the Susitna Lowland and along the southern margin of the

Talkeetna Mountains to the edge of the Copper River Basin (Figure 3). The

fault system passes 40 km from Anchorage, 15 km from Palmer, and 10 km from

Wasilla. Because of its proximity to the principal population center of

Alaska, the seismic potential of the fault system is an important issue.

Although future earthquakes as large as magnitude 7.25 to 8.5 (M_s) have

been postulated for the this fault system in various seismic hazard studies

(Patwardhan and others, 1980; Thenhaus and others, 1985), this is the first

study in which specific earthquakes have been unequovically associated with

the fault system.

The Castle Mountain fault system is divided into two segments (Detterman

and others, 1974): the western, or Susitna segment, and the eastern, or

Talkeetna segment. Although the Susitna segment of the fault system has long

been recognized as active on the basis of Holocene scarps (Detterman and

others, 1974), definitive geologic or seismic evidence concerning the

activity of the Talkeetna segment has been lacking (Detterman and others,

1976).

On August 14, 1984, a magnitude 5.7 m_b (5.2 M_s) earthquake occurred

14 km north of Sutton in the vicinity of the mapped trace of the Talkeetna

segment. No surface breakage was discovered in an aerial reconnaissance and

ground inspection of the fault conducted two weeks after the earthquake

(T. P. Miller, U.S. Geol. Survey, oral comm., August 29, 1984). Well-located

hypocenters for 49 aftershocks (Figure 4) occurring between August 14 and

December 18 define a buried planar zone striking parallel to the mapped trace

and dipping steeply to the NNW, with dimensions of 10 km along strike and 5

or 6 km down dip. The shallowest of these events is located at 11 km depth;

the absence of shallower events is consistent with the lack of observed

surface breakage. The main shock is located at 19 km depth, near the depth

of the deepest aftershocks. Within the uncertainty of the data, the main

shock and aftershocks can be associated with a single, steeply

north-dipping fault, consistent with the mapped trace of the Talkeetna
segment.

The focal mechanism of the main shock was determined from 65 P-wave first
motions, primarily at regional distances (Figure 5). The slip plane is
inferred from the close correspondence between the ENE-striking nodal plane
and the attitude of the aftershock zone. Thus, the earthquake involved
dextral slip on the ENE nodal plane, consistent with the sense of lateral
Holocene offsets on the Susitna segment (Detterman and others, 1976). Based
on the orientation of convergence between the Pacific and North American
plates with respect to the Castle Mountain fault, thrust rather than lateral
displacement would have been expected. The dextral slip requires a
compressive stress direction rotated counterclockwise from the plate-
convergence direction. This rotation may be due to variation in the level of
convergent stresses along the Gulf of Alaska. Convergent stresses along the
eastern Gulf of Alaska, within the zone of collision between the Yakutat and
Wrangell blocks, may be higher than those to the west, where a normal
subduction process occurs. This may be particularly true now, due to the
recent release of compressive stress by the 1964 Prince William Sound
earthquake.

The closest large historic earthquake (Figure 6) to the Castle Mountain
fault system is a magnitude 7.0 in 1933 with an epicenter 16 km south of the
Susitna trace, which was followed by a prominent aftershock sequence. Within
the uncertainty in the epicenter location, this event may have occurred on
the fault. Another large event (magnitude 7.3) occurred 40 km north of the
Susitna trace in 1943. There are few aftershocks reported for this event, an
observation which could indicate a Benioff zone source.

The Sutton earthquake sequence supports the conjecture of previous
authors (for example, Woodward-Clyde Consultants, 1980; Thenhaus and others,
1985) that the Talkeetna segment of the fault system is active. In addition,

a re-examination of the locations of small earthquakes recorded since 1971 by the southern Alaska regional seismograph network suggests the association of a few scattered earthquakes with that part of the Talkeetna segment west of the bifurcation of the Castle Mountain and Caribou faults (see Figures 7 and 8). For the purpose of hazard evaluation, therefore, at least 130 km of the Castle Mountain fault system should be considered active, from the westernmost location of Holocene offset near the Susitna River, to the bifurcation of the Caribou fault at about 148.5°W. Considering the distribution of magnitude versus rupture length for previously studied earthquakes (Slemmons, 1977; Bonilla and others, 1984), we conclude that if this length of the fault were to rupture in one strike-slip event, the magnitude would be within the range 7.2 to 7.8 M_s.
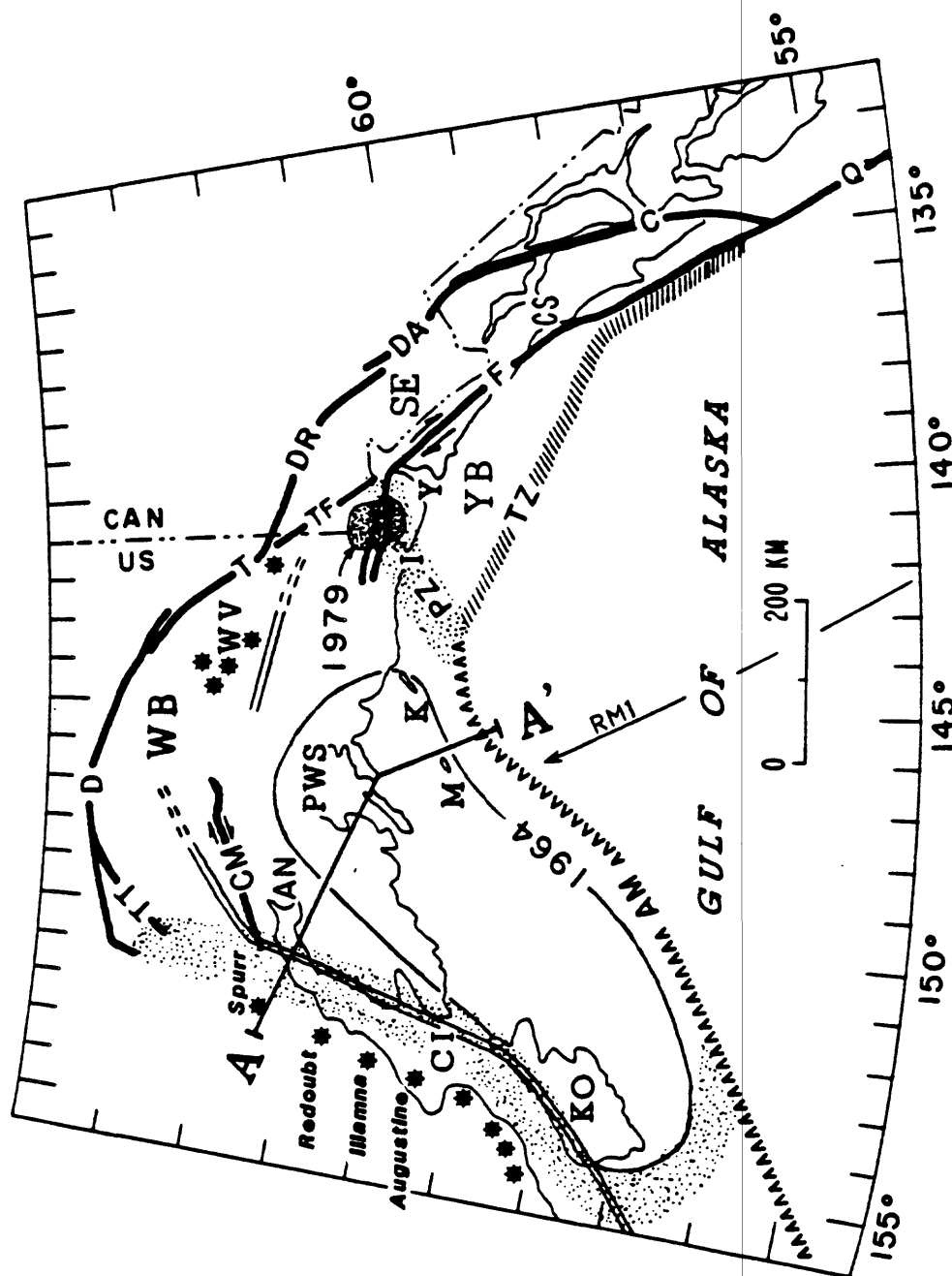
Figure 1. Map of southern Alaska and western Canada emphasizing principal regional tectonic features (Lahr and Plafker, 1980; Stephens and others, 1984). Location of cross section A–A' of Figure 2 is shown. KO, Kodiak Island; M, Middleton Island; K, Kayak Island; CI, Cook Inlet; AN, Anchorage; PWS, Prince William Sound (Valdez is near S of PWS); I, Icy Bay; Y, Yakutat Bay; CS, Cross Sound; WV, Wrangell volcanoes; 1964, rupture zone of 1964 Prince William Sound earthquake; 1979, rupture zone of 1979 St. Elias earthquake; AM, Aleutian megathrust; TZ, Transition zone; Q, Queen Charlotte Islands fault; C, Chatham Strait fault; DA, Dalton fault; DR, Duke River fault; TF, Totschunda–Fairweather fault; T, Totschunda fault; D, Denali fault; TT, unnamed faults; CM, Castle Mountain fault; F, Fairweather fault; PZ, Pamplona zone; double line, 50 km isobath of Benioff zone, dashed where inferred; YB, Yakutat block; SE, St. Elias block; WB, Wrangell block; shaded zone from TT through CI to AM is speculative northwestern boundary of WB; RM1, Pacific–North American plate relative motion direction.
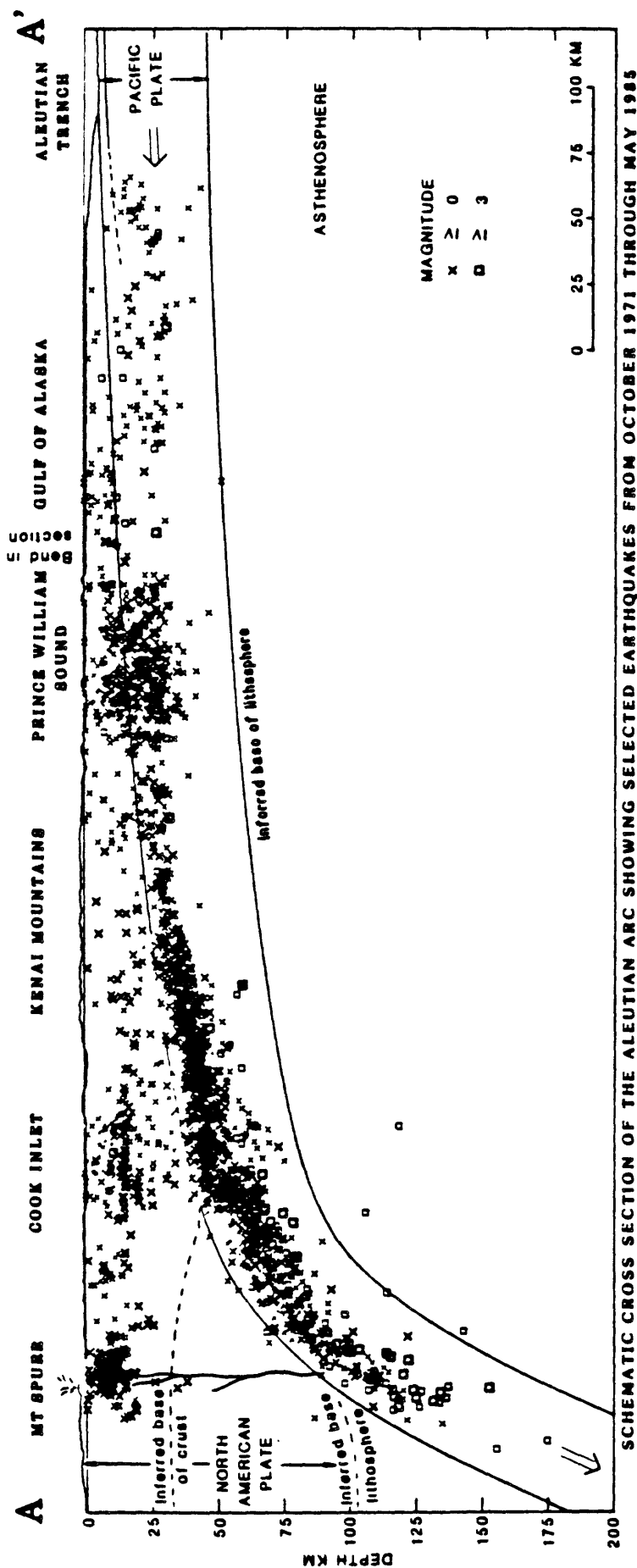
Figure 2. Cross section showing hypocenters of earthquakes with 4 or more P-phase readings, 1 or more S-phase readings and root-mean-square residual less than or equal to 0.6 s. View is northeast. 2604 events within 50 km of line A-A', shown in Figure 1, are included. Structures modified from Plafker and others, 1982. The offsets within the Benioff zone below Cook Inlet and the tendency for crustal events to concentrate near certain depths are thought to be artifacts of the location proceedure.
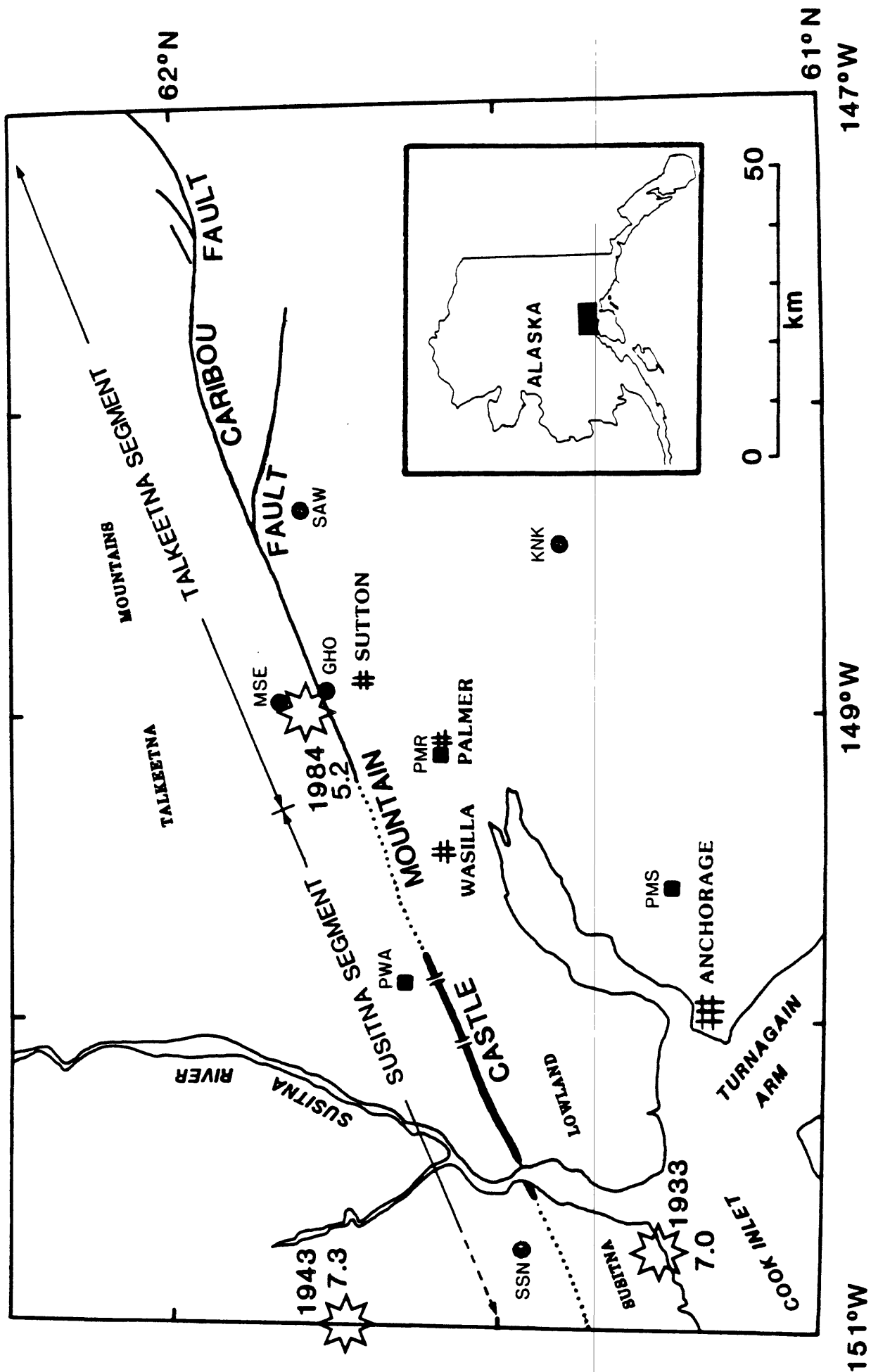
Figure 3. Map of Castle Mountain fault system after Detterman et al. (1974, 1976) and Magoon et al. (1976), showing section with Holocene scarps (heavy line) and locations of trenches. Solid circles and squares, USGS and ATWC seismograph stations. Stars, epicenters of 1933, 1943, and 1984 earthquakes.
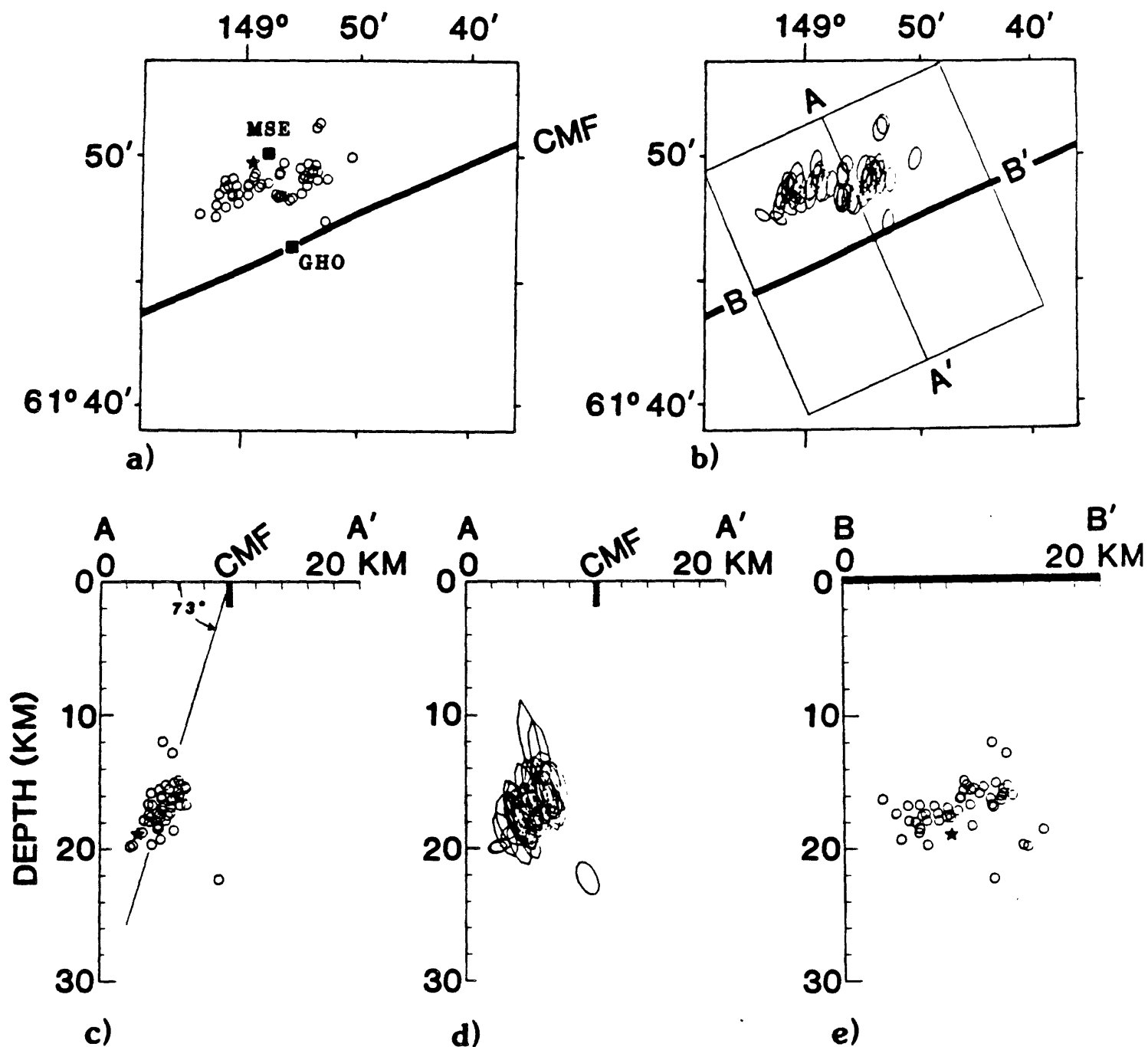
Figure 4. Hypocenters of 1984 Sutton mainshock (star) and 49 aftershocks (circles) located with a nearly homogeneous set of P and S phases and with a local velocity model and associated station corrections. a) Map of epicenters in relation to trace of Castle Mountain fault (CMF). Solid squares, temporary stations GHO and MSE. b) Map of 68 % confidence ellipses for epicenters in (a). Letters indicate end points of cross sections in (c), (d) and (e). c) Vertical section of hypocenters in plane A - A' perpendicular to fault strike. d) Vertical section of 68% confidence ellipses in plane A - A'. e) Vertical section of hypocenters in plane B - B' parallel to fault strike.
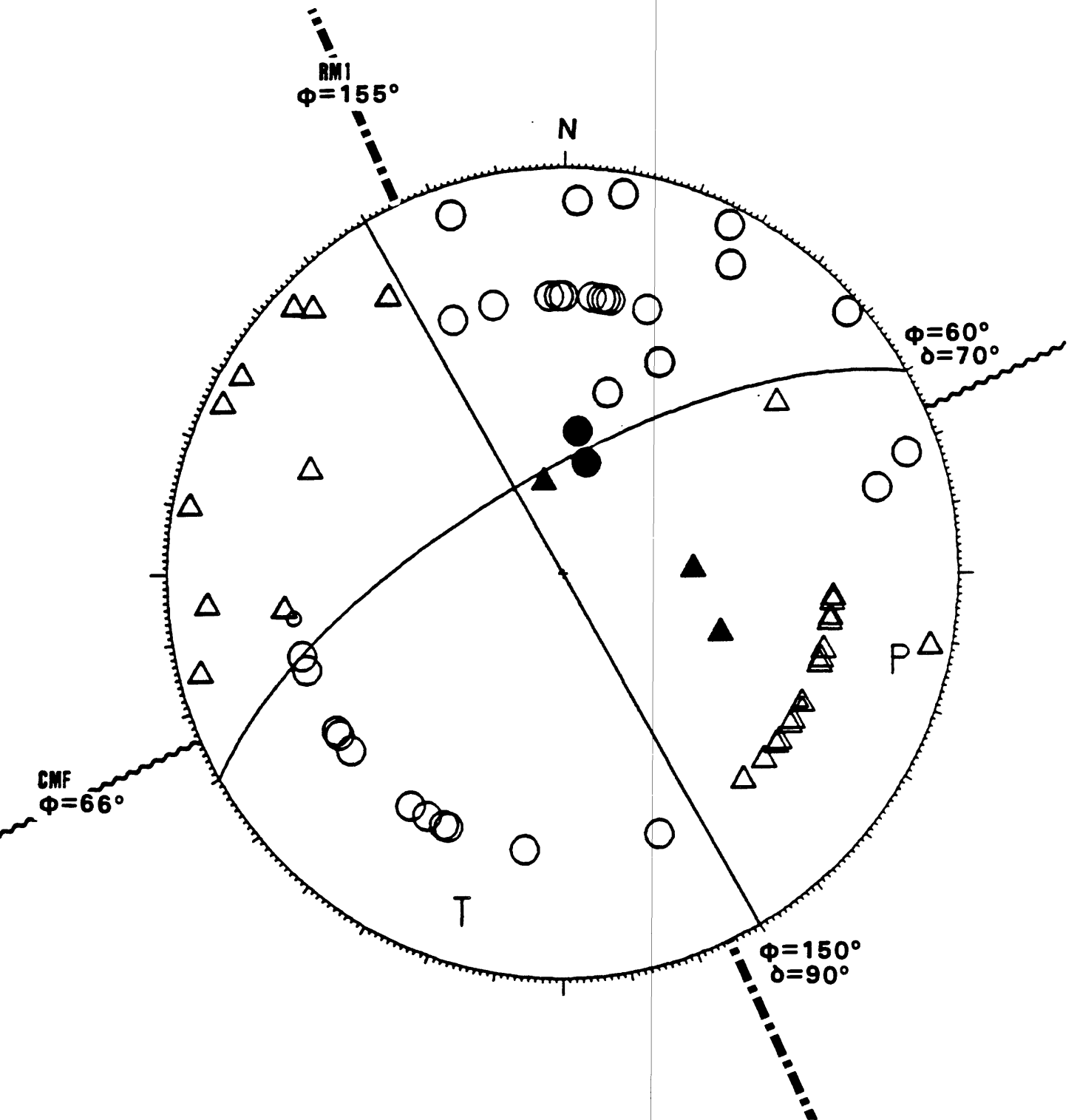
Figure 5. First-motion focal-mechanism solution (equal-area lower-hemisphere projection) for 1984 Sutton earthquake. Triangles, dilatations; circles, compressions; solid symbols, data from long-period teleseismic records; open, from short-period regional records; smaller symbols, nodal first motion. Symbols "P" and "T" indicate P and T axes. Strike (φ) and dip (∂) of nodal planes are given, as well as strike of Castle Mountain fault (CMF) and strike of relative motion vector between Pacific and North American plates (RM1).
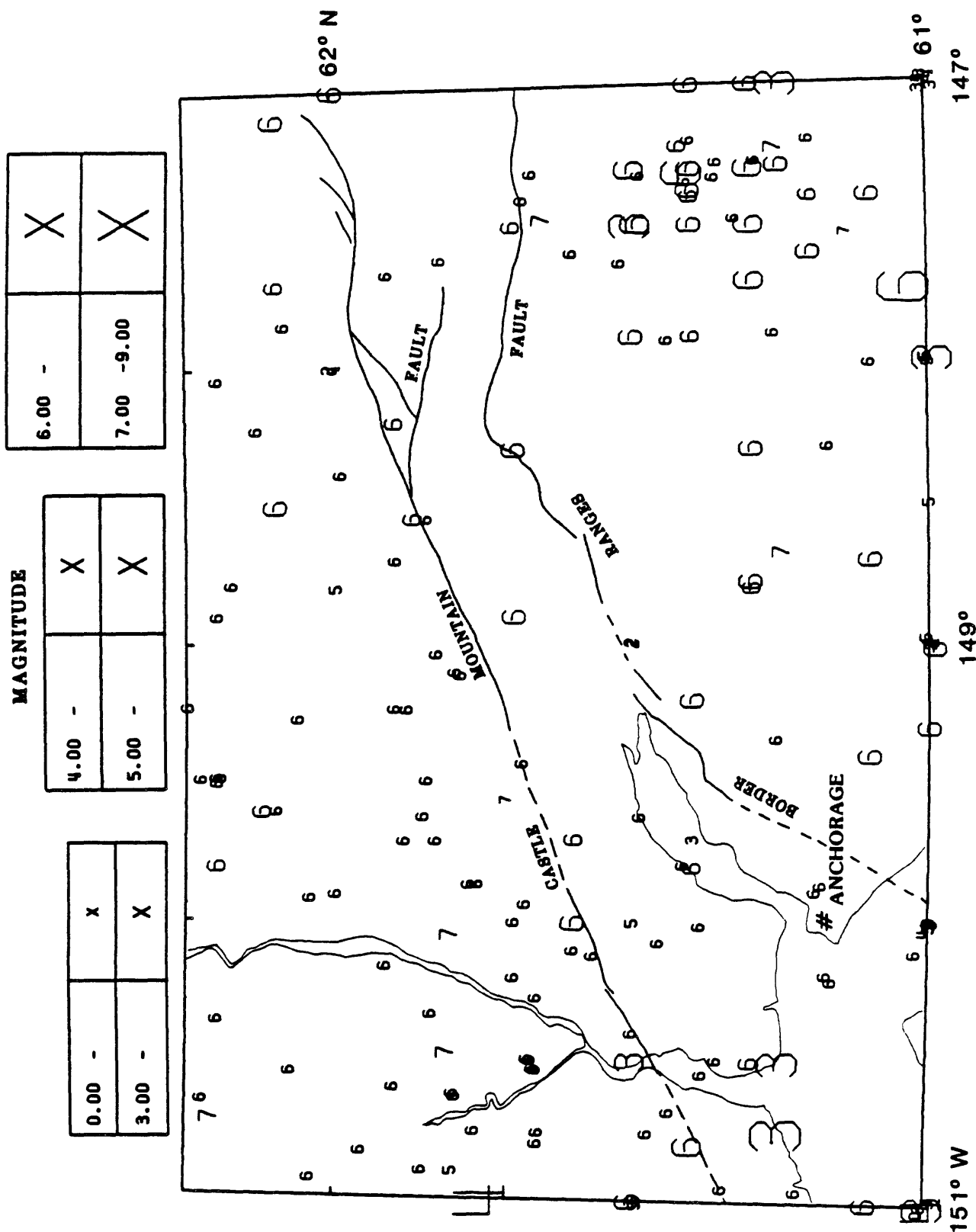
Figure 6. Epicenters from NOAA Earthquake Data File (EDF) for earthquakes with depth less than or equal 35 km occurring through September 1971 . Earliest event shown occurred in 1898. Number, decade in which event occurred; size proportional to magnitude, as in key. Epicenters that would plot at exactly the same point, due to location to nearest degree or .1 degree, are randomly shifted by a small amount. In addition to the Castle Mountain fault system, the Border Ranges fault is shown after Belkman (1974).
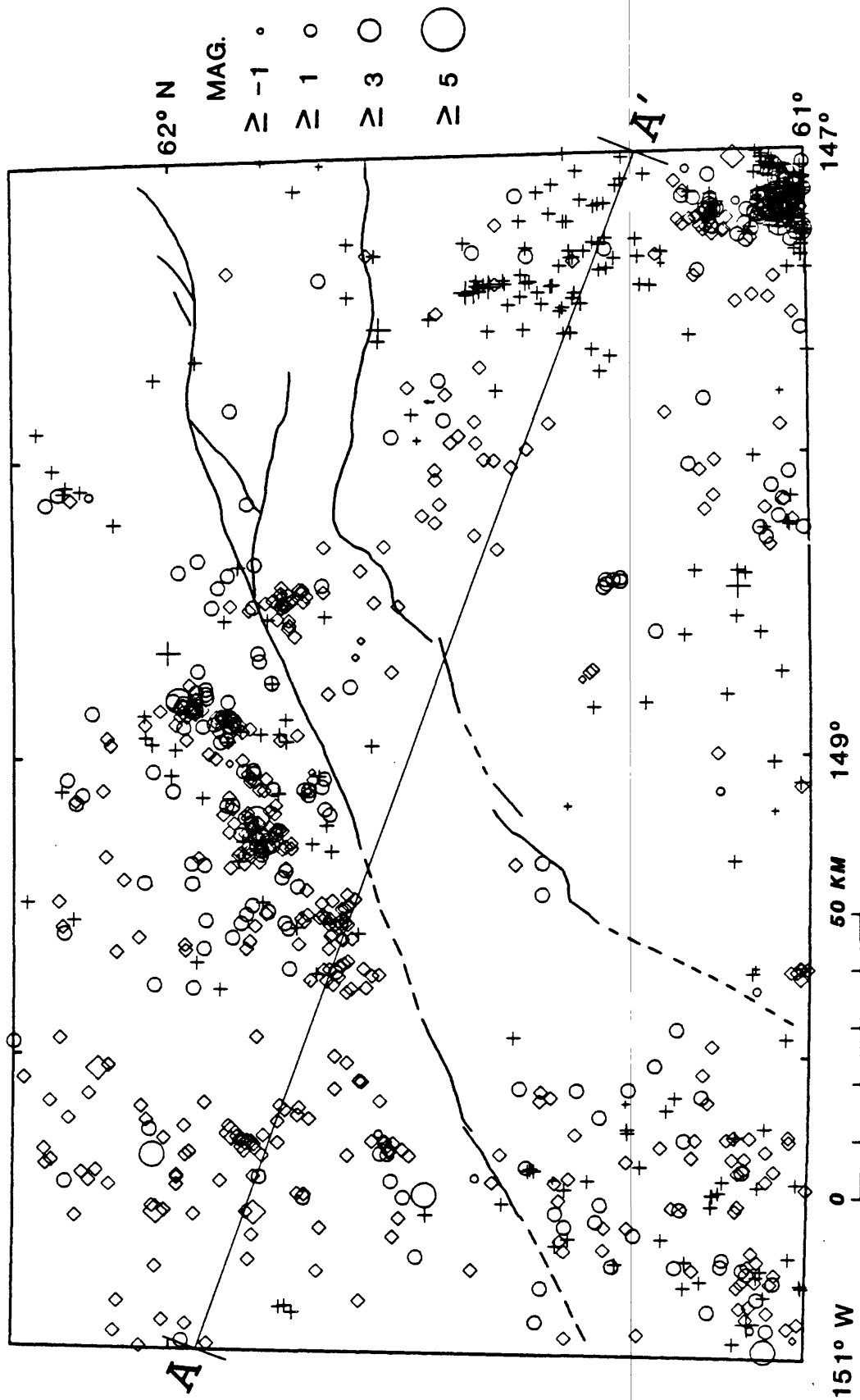
Figure 7. Map of relocated epicenters for 1,022 regionally recorded earthquakes with depths less than or equal 30 km that occurred between October 1971 and the Sutton earthquake (August 14, 1984). Symbol correspondence with depth: diamond, 0 – 10 km; circle, 10 – 20 km; plus, 20 – 30 km. AA', location of section in Figure 10.
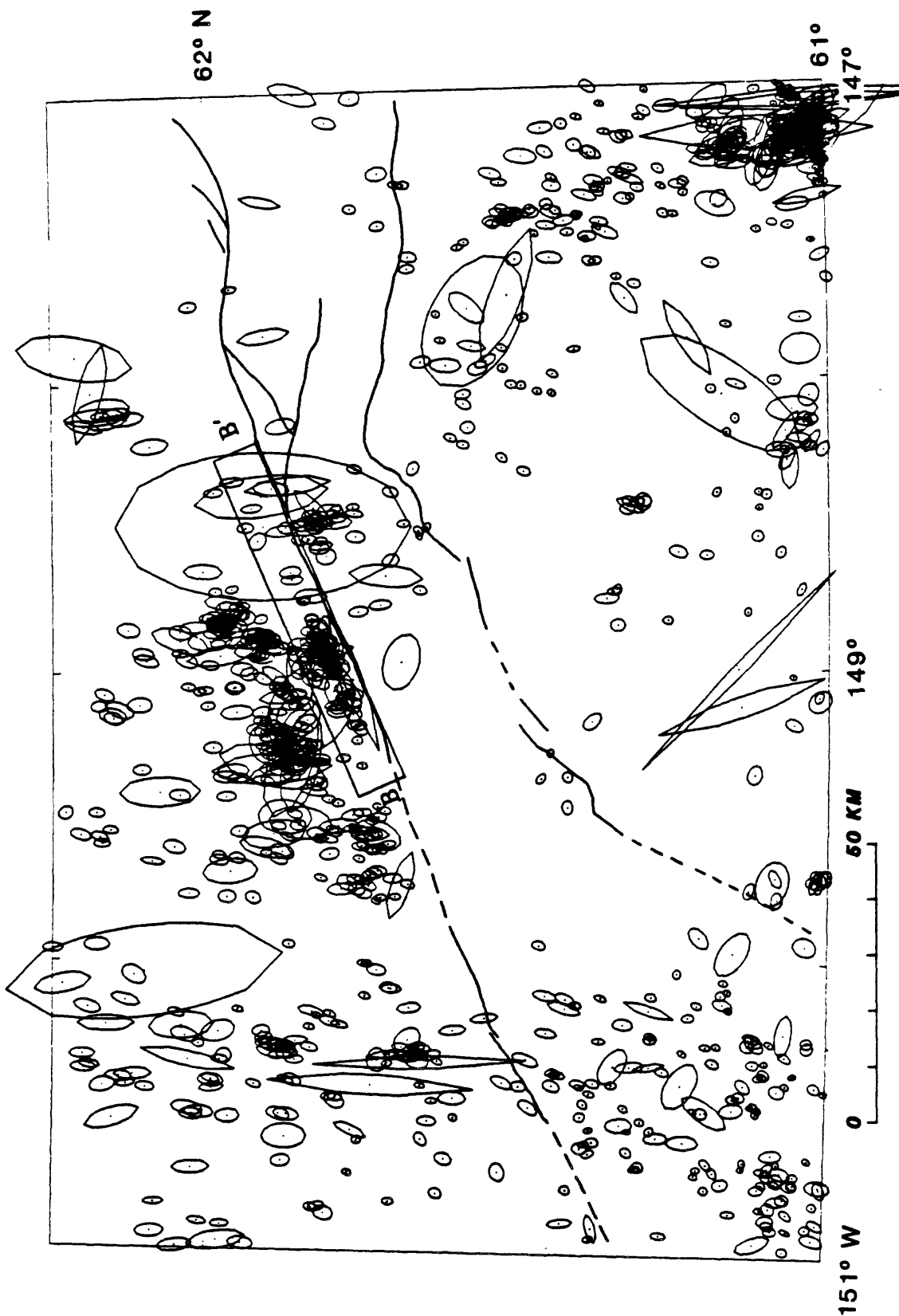
Figure 8. Map of 68% epicentral error confidence ellipses for the 1,184 relocated earthquakes with epths less than 30 km that occurred from October 1971 through December 1984 (includes all events shown in Figure 7 plus time period that includes Sutton sequence). Large ellipse axes are truncated to 25 km.
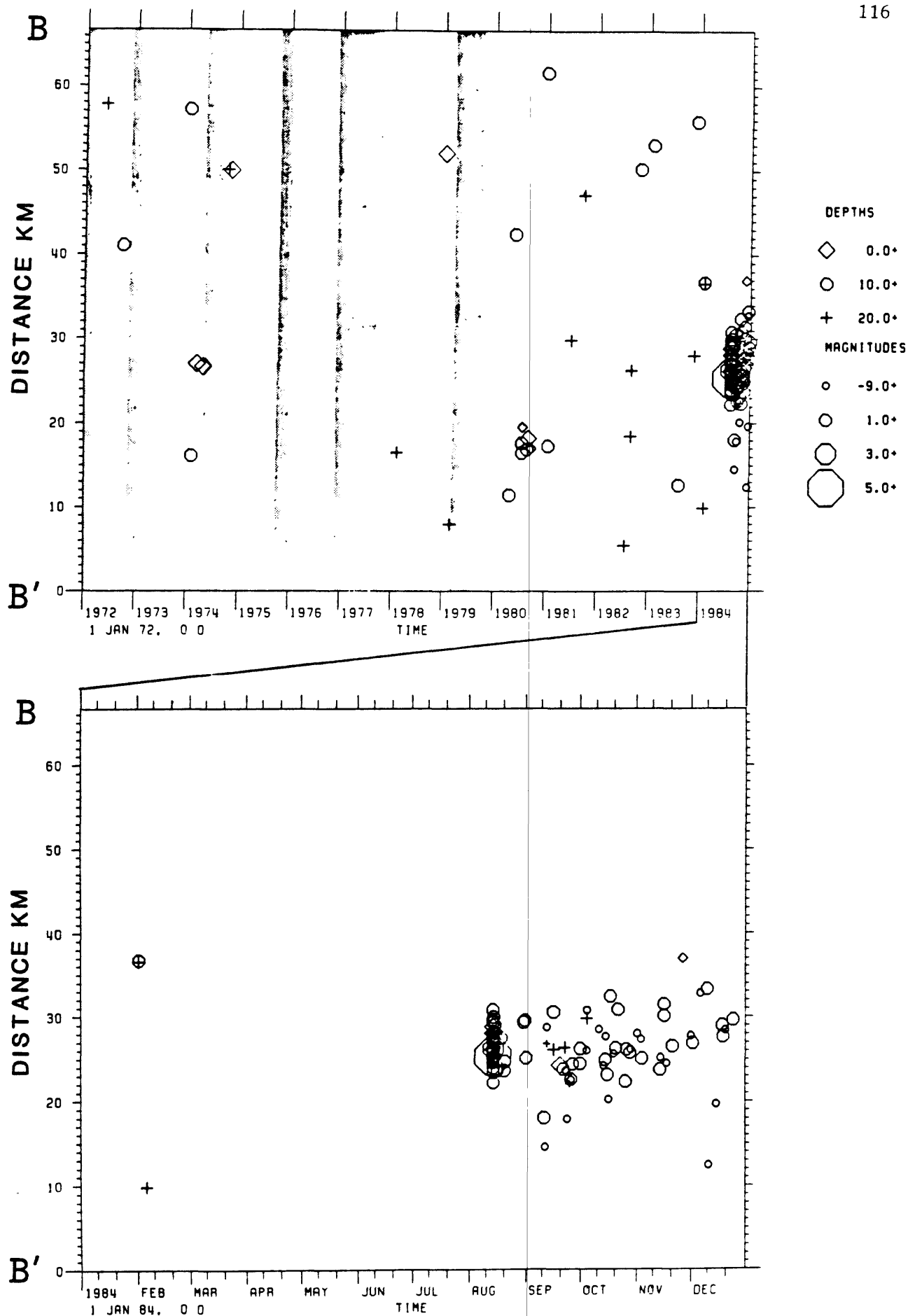
Figure 9. Space-time plot of the 137 events within box BB' shown in Figure 8. Upper – January 1, 1972 through December 31, 1984; lower – January 1 through December 31, 1984. Shaded bands indicate the major gaps in data processing.
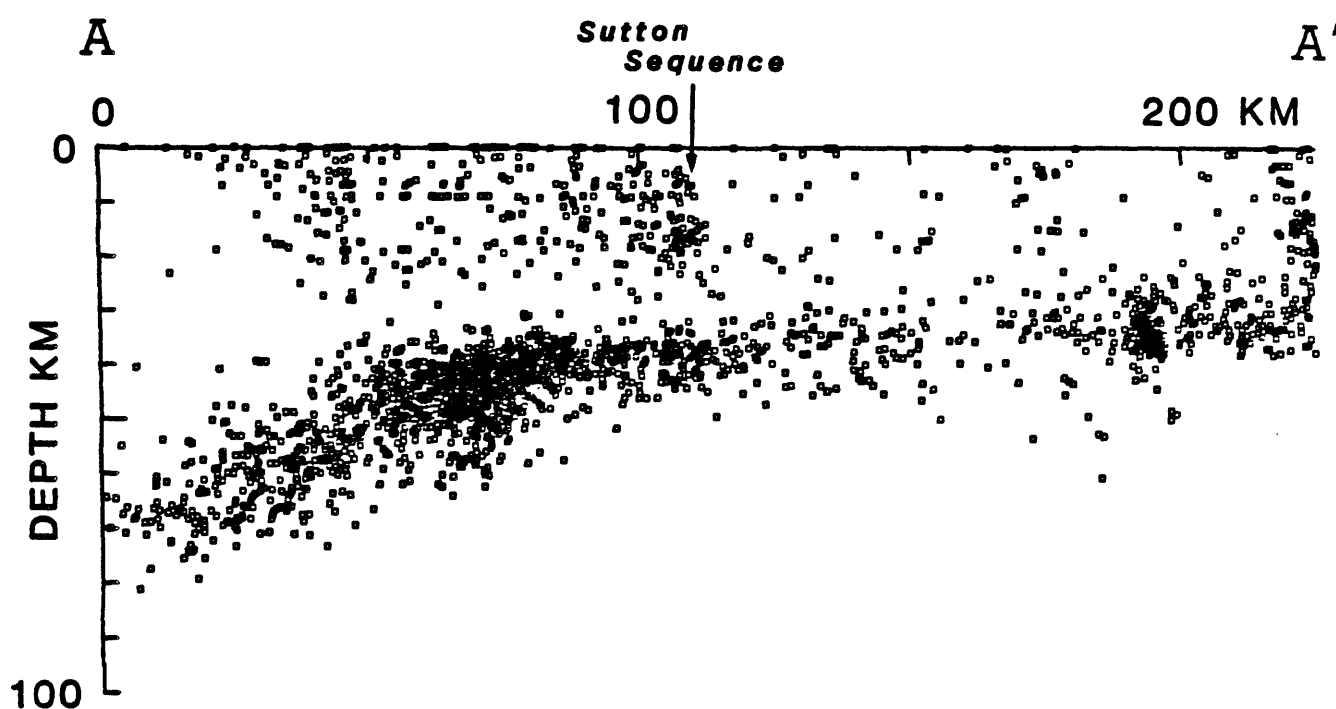
Figure 10. Vertical hypocentral section of 2,447 relocated earthquakes for October 1971 through December 1984. Location of section is given in Figure 7. Section is parallel to local dip direction of Benioff zone.
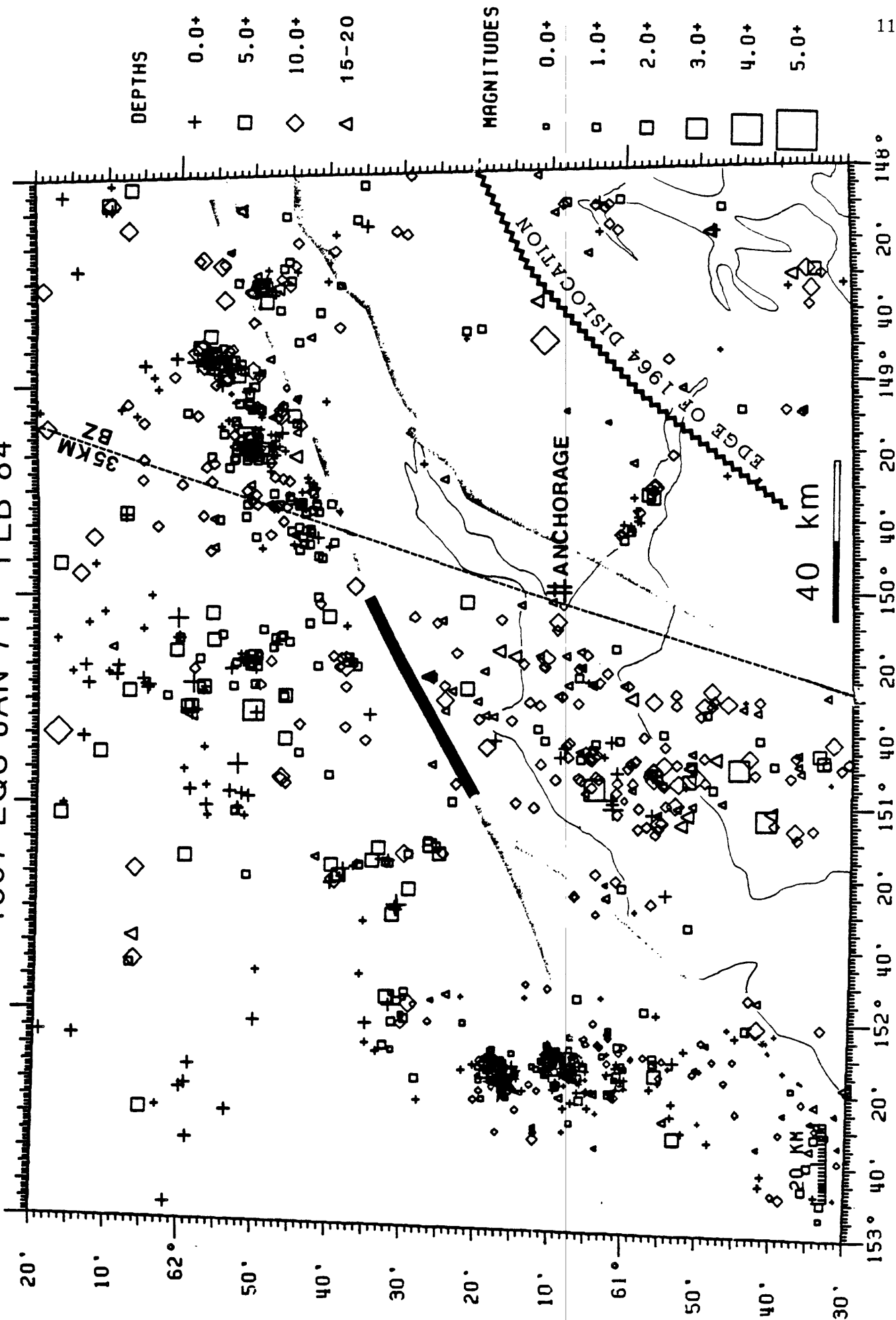
Figure 11. Epicenters of shallow (depths less than 20 km) routinely located earthquakes that occurred from January 1971 through February 1984. 35-km-depth contour on upper surface of Benioff zone is shown. Edge of 1964 dislocation based on aftershock distribution.

118

APPENDIX A. 7.

Seismicity Patterns in the Adak Seismic Zone and
Short-term Outlook for a Major Earthquake

C. Kisslinger

Abstract of presentation to NEPEC, Anchorage, Alaska, September 8, 1985

Seismicity Patterns in the Adak Seismic Zone
and the Short-term Outlook for a Major Earthquake

Carl Kisslinger
CIRES/Department of Geological Sciences
University of Colorado, Boulder

The prediction of earthquakes in an island arc subduction zone must be based primarily on the information provided by the patterns of occurrence and physical characteristics of the earthquakes themselves. Because the epicenters of the earthquakes in which we are most interested occur under several kilometers of water, other approaches to prediction, found promising in continental environments, cannot be applied to the subduction zone associated with a typical island arc with present technology and limited resources.

The Adak Seismic Zone and the Central Aleutians Network are shown in Fig. 1. The network provides data for monitoring in fair detail a segment of the arc about 250 km long, between about 175°W and 178.8°W. The catalogue assembled since August, 1974 is homogeneous down to about M_D 2.3.

Some seismotectonically significant features of the seafloor are also shown in Fig. 1. Adak Canyon is a prominent and tectonically important feature. It is the easternmost of the transverse canyons that cut the arc from here out to 170°E, and has been revealed by our studies to separate regions with quite different characterisitics along the main seismic zone.

The framework for our attempts at prediction is provided by the history of major earthquakes within the main thrust zone since 1900, shown for $M \geq 7$ in the lower part of Fig. 2, and moderate activity since 1974, shown in the upper part. The locations, magnitudes and fault break lengths shown are very uncertain for events prior to the 1957 great earthquake, with the 1901 event carrying a location uncertainty of 5°. This is the best record we have been able to assemble from available catalogues. It shows three episodes during which the whole length of the Adak seismic zone seems to have broken in major events, around 1909, around 1930, and in the great event of March 9, 1957. The intervals are 21 years and 27 years. Since it is now 28 1/2 years since the 1957 event, it is not unreasonable to anticipate a series of 7 or greater events beginning in the near future, if there is other evidence that the region may be in the late stages of preparation for renewed major activity. The upper part of the figure shows the marked deficiency of moderate magnitude events in the past 11 years.

We noted a pronounced decrease in the number of events being located with the local network, starting in September, 1982, a decrease that lasted until late in 1984, when the rate of activity began to recover slowly. Because the drop in occurrence rate of earthquakes in all magnitude bands was so pronounced, we have examined the phenomenon in detail. Because of lingering doubts that the quiescence was due to some unknown change in our detection capability, we have compared the Adak catalogue with the PDE reports of earthquakes for the same interval, a completely independent data set. This study also provides a test

of the utility of teleseismic catalogues for detailed monitoring in small regions.

Because of the well-known bias in PDE locations of earthquakes in this region, due to the effect of the subducting Pacific plate, as well as the location errors typical of teleseismic hypocenter work, there are difficulties in using the PDE data directly for high-resolution seismicity pattern studies. We have relocations using local network data for PDE-reported events since August, 1974. For earlier events, back to 1963, we applied a mean shift in longitude, 0.18° to the east, to all PDE epicenters. The latitude and depth errors are larger and more erratic, so we have considered activity within narrow strips extending north-south across the arc, rather than trying to assign specific locations to these events, and assumed that all events with PDE depths given as less than 100 km were in the main thrust zone. We then compared the PDE-reported activity with the local catalogue for the whole region and for various sub-regions. The regionalization used is shown in Fig. 3. The West region lies mostly in the Delarof Islands block, and was examined, but is not included in the rest of this discussion. "All-Adak" here means sub-regions East, Central, SW2 and Canyon. The catalogues were purged of swarms and aftershocks, and only events stronger than m_b 4.5 were retained in the PDE set and duration magnitudes 2.3 and greater for the local catalogue.

The results are shown in the form of cumulative number plots against time in Figures 4-10. The All-Adak PDE events since 1963 show the strong quiescence discovered by Habermann as a precursor to the February/May strong earthquakes in SW2 and Adak Canyon (6.7/7.2). There is a suggestion of a rate decrease prior to the 1977 event in the east part of the Central region, but this decrease is not highly significant statistically. There is no sign of quiescence beginning in the fall of 1982. When the data for sub-region SW2 are removed, a clear decrease in the remaining data set is seen at the same time as the beginning of the local data quiescence. SW2 became more active since July, 1980, with a steady production of moderate events since, so that the quiescence in the rest of the zone is masked. On the basis of this activation, we correctly forecast the location of a m_b 5.8 event within SW2 that occurred on May 6, 1984. We conclude that SW2 marks an asperity on the thrust zone that has continued to be active.

The comparison of local and PDE data is valid only since May, 1976. As shown, although the numbers of events in the PDE set in these small regions is too small to permit robust conclusions about rate changes, the data do permit interesting comparisons. The data for the East region, in which the number of events is very small, track well, including the recent increase. A significant decrease in the local data began in late 1981. The two data sets for the central region are in very good agreement, and the highly significant drop in the local network rate is confirmed. The rate decreases in SW2, though not as strongly as in the other regions; the activation seen in the PDE data does not appear in the local data. This means that the b-value in this subregion, known for a long time to be the lowest within the study region, has dropped even lower.

The data for Adak Canyon confirm our previous qualitative estimate, that this sub-region has had a deficiency of teleseims since 1974 (top of Fig.1), but the rate of microearthquakes has been steady during this

time. A 5.7 event occurred in the eastern part of Adak Canyon in June,
1982, and there have been several more moderate earthquakes here since.
This activity may be part of the activation seen in nearby SW2.

The clustering of teleseisms and higher stress microearthquakes
around the epicenter of the May 6, 1984 event are shown in the last
figure, taken from published papers.

Conclusions.

1. The quiescence detected in the local network data,
beginning in September, 1982, is a real geological occurrence. It
began at different times in different sub-regions. The activity
began to return to the previous rate in parts of the zone in late
1984. The question remains as to whether the recent behavior
signals the end of a pronounced quiescence with no major event,
or is an increase just prior to a big earthquake.

2. Three intervals of reduced rate of occurrence are seen in
the teleseismic data since 1963. One (1968-71) is very
pronounced and ended with the 1971 strong earthquake in Adak
Canyon. The second (1974-77) is weaker, and ended with the 1977
M. 6.7. The third is recent and its significance is still to be
determined.

3. SW2 is a small region characterized by four years
of increased moderate activity, a low b-value and higher stress
microearthquakes. It is a likely nucleation point for a strong
earthquake.

4. Given: the history of strong earthquakes since 1900 as a
basis; the quiescence lasting three years before the 1971 Adak
Canyon earthquake of May, 1971, which was preceded by a 6.7 in
SW2; the deficiency of moderate earthquakes within Adak Canyon in
the past 11 years; the activation of SW2 since 1980 and the more
recent activation of the eastern part of Adak Canyon; and the
pronounced quiescence over the zone that began in 1982, we
present the following hypothesis:

An earthquake with surface-wave magnitude 7 or greater will occur in
the Adak seismic zone in the near future. If the single observed case
of a three-year precursory quiescence is characteristic, the most likely
time is before the end of October, 1985. A likely place for the
initiation of rupture is at the asperity in sub-region SW2, with the
main break occuring either immediately or soon after under Adak Canyon.

Figure Captions.

1. The Adak Seismic Zone, showing the 14 stations of the local network and the bathymetry.
2. *Top:* Local network locations of events in the PDE catalogue, August, 1974 - June 1984. The epicenters of the May 2, 1971 and November 4, 1977 events (M. 7.2 and 6.7) are marked by stars. The deficiency of teleseismically located events in Adak Canyon is apparent.
Bottom: Time-space plot of major earthquakes (M7 and greater), since 1900. Lengths of fault breaks are estimates, locations of events before 1957 are highly uncertain.
3. Regionalization used for the seismicity analysis. The small rectangles are the sub-regions adopted for local analysis, the broad north-south strips are those used for comparison of PDE and local data. The West region is thought to be outside of the region of current special interest.
4. Independent PDE events 1963-May, 1985, cumulative number vs. time. The arrowheads mark: the 1971 events in SW2 and Adak Canyon, the November,1977 event, the 1980 start of activation in SW2, the 1982 start of quiescence across the zone, and the 1984 5.8 event in SW2. The All Adak data show no quiescence beginnng in 1982, the data with SW2 removed show it clearly, and the SW2 data show the activation of this site since July, 1980.
5-10. Comparison of local and PDE data since 1976 for the whole zone and for the subregions. The local data figures include a running estimate of the significance of the difference of the mean number of earthquakes during the 52 weeks before and after the point plotted; peaks correspond to rate decreases, troughs to rate increases. The 99.7% significance levels for the differences in means are marked by the horizontal lines at 2.57. The arrowheads mark the same times as those in the later part of Fig. 4.
11. Seismicity in SW2, showing (top) the clustering of moderate earthquakes (squares) around the epicenter of the May 6, 1984 event (Bowman and Kisslinger, *BSSA*, February, 1985) and (bottom) the concentration of higher stress microearthquakes with a similar distribution (Scherbaum and Kisslinger, *BSSA*, December, 1984).

Figure 1.

Figure 2.

Figure 3.

PDE, h<100km, m≥4.5

Figure 5.

LOCAL, h <= 75 w/o SW1,2,4
independent events, Md>=2.3
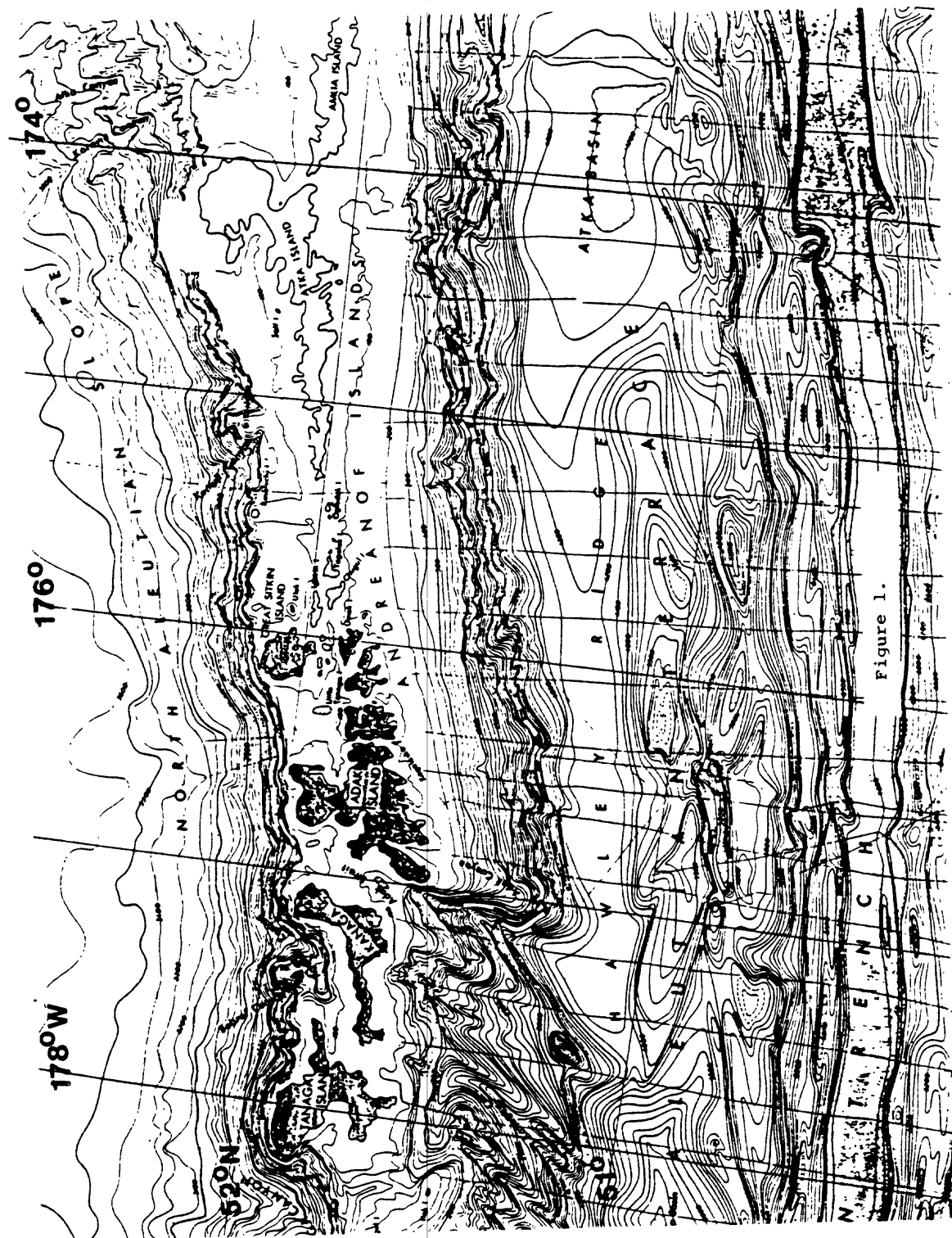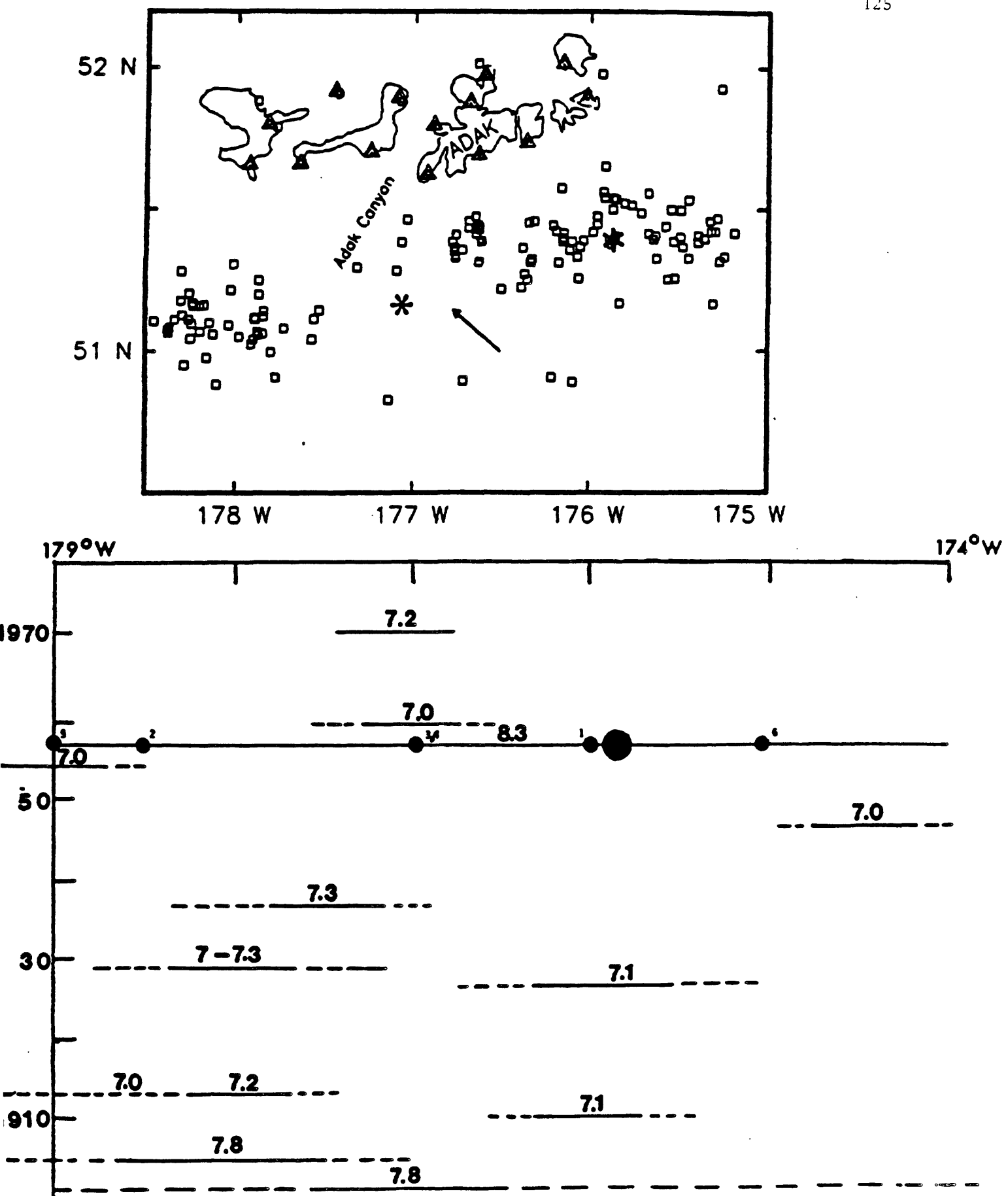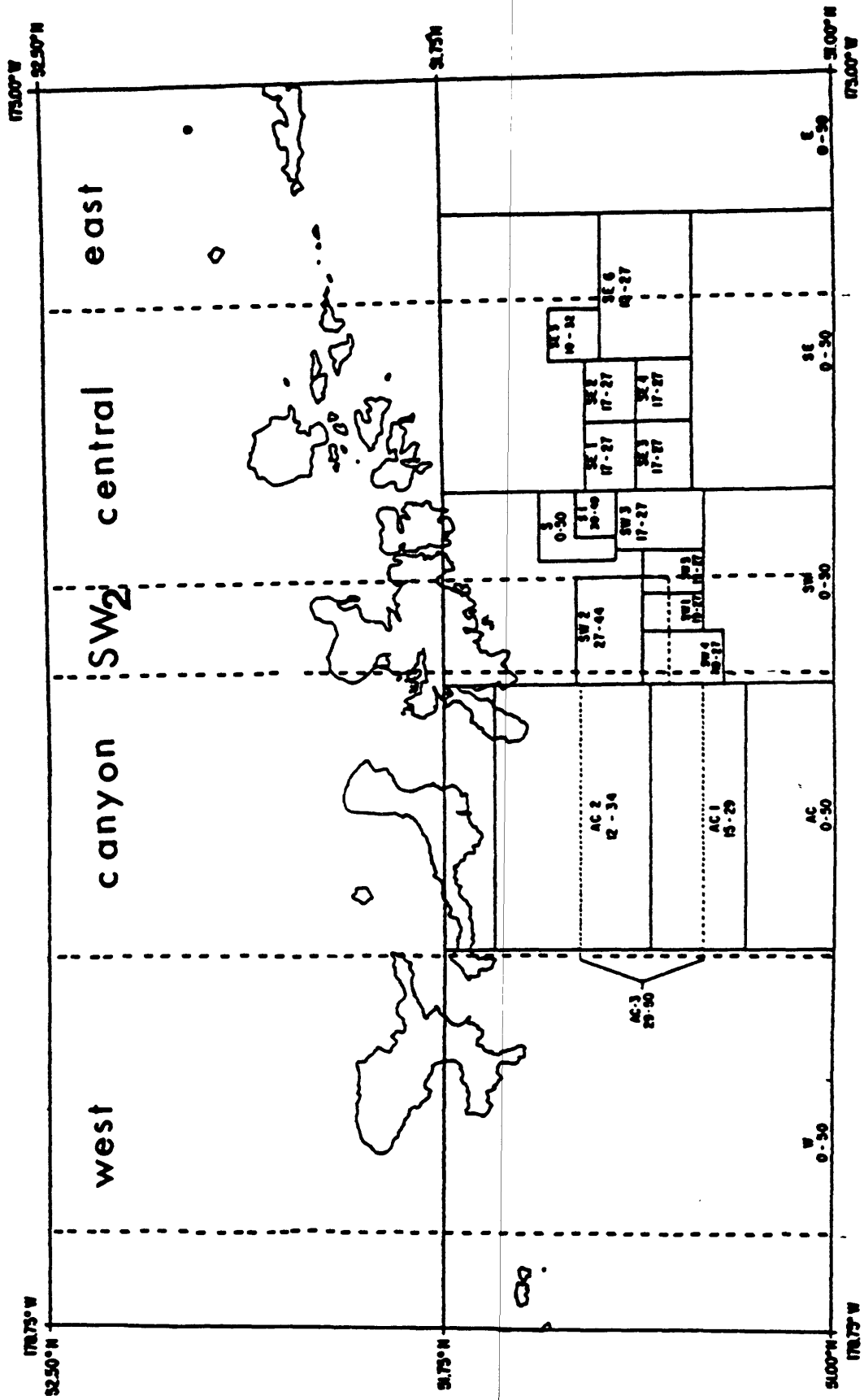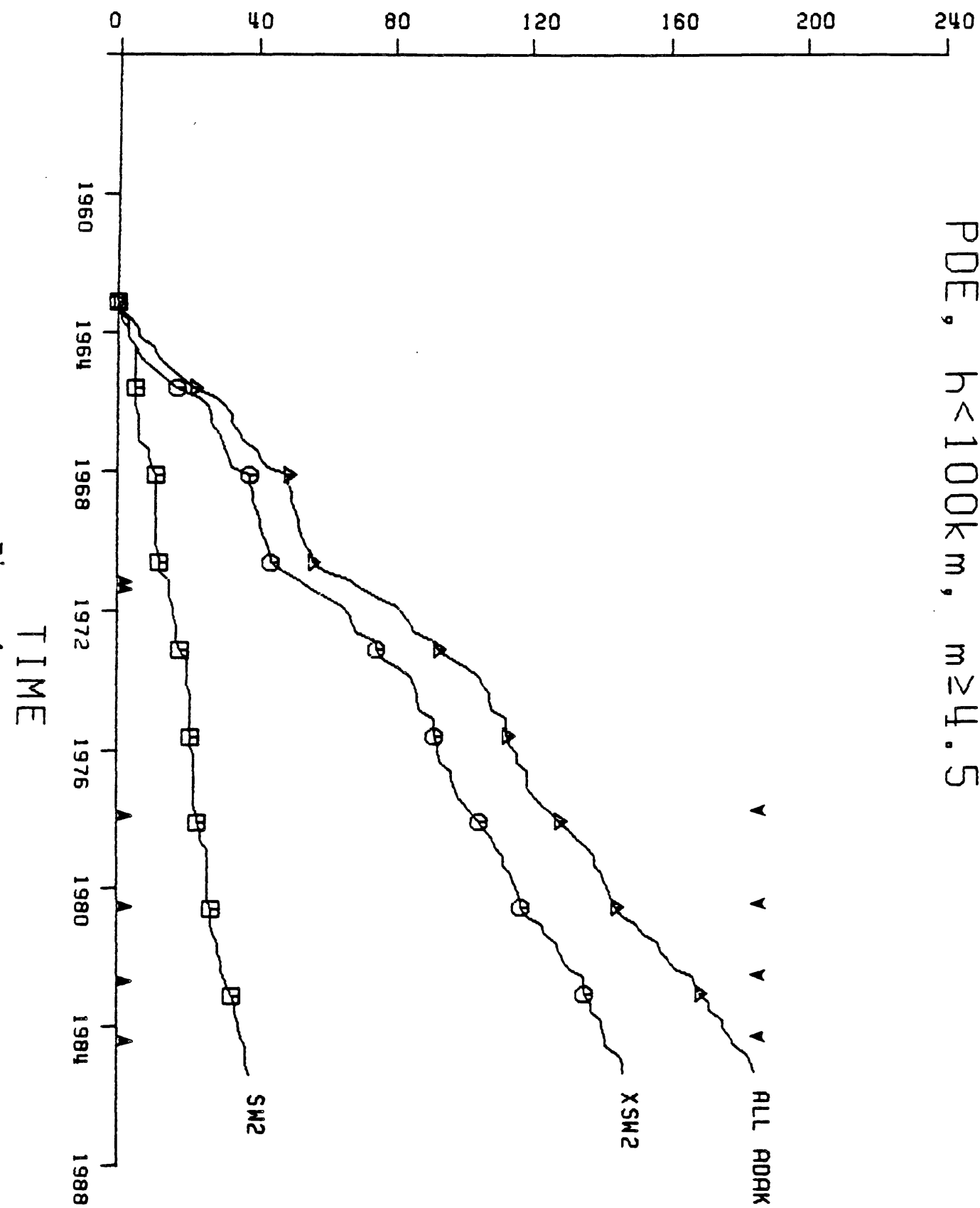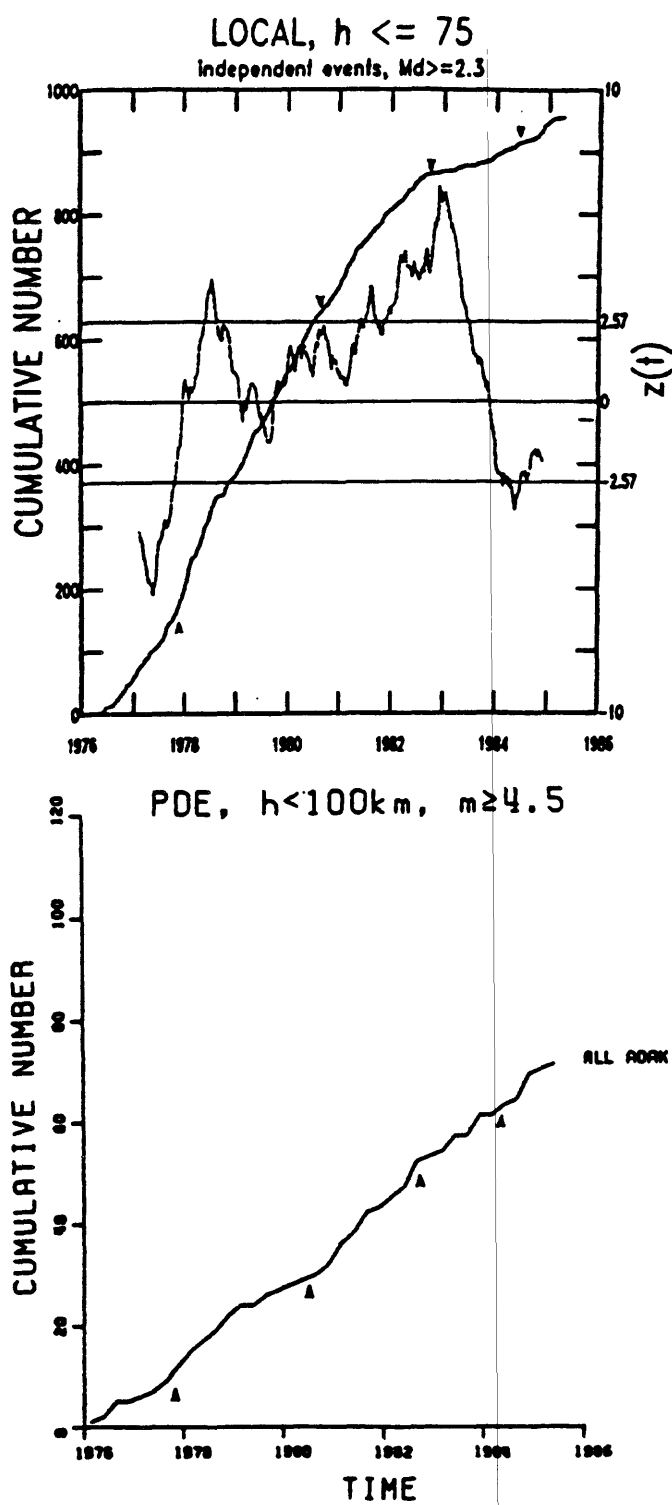
PDE, h<100km, m≥4.5
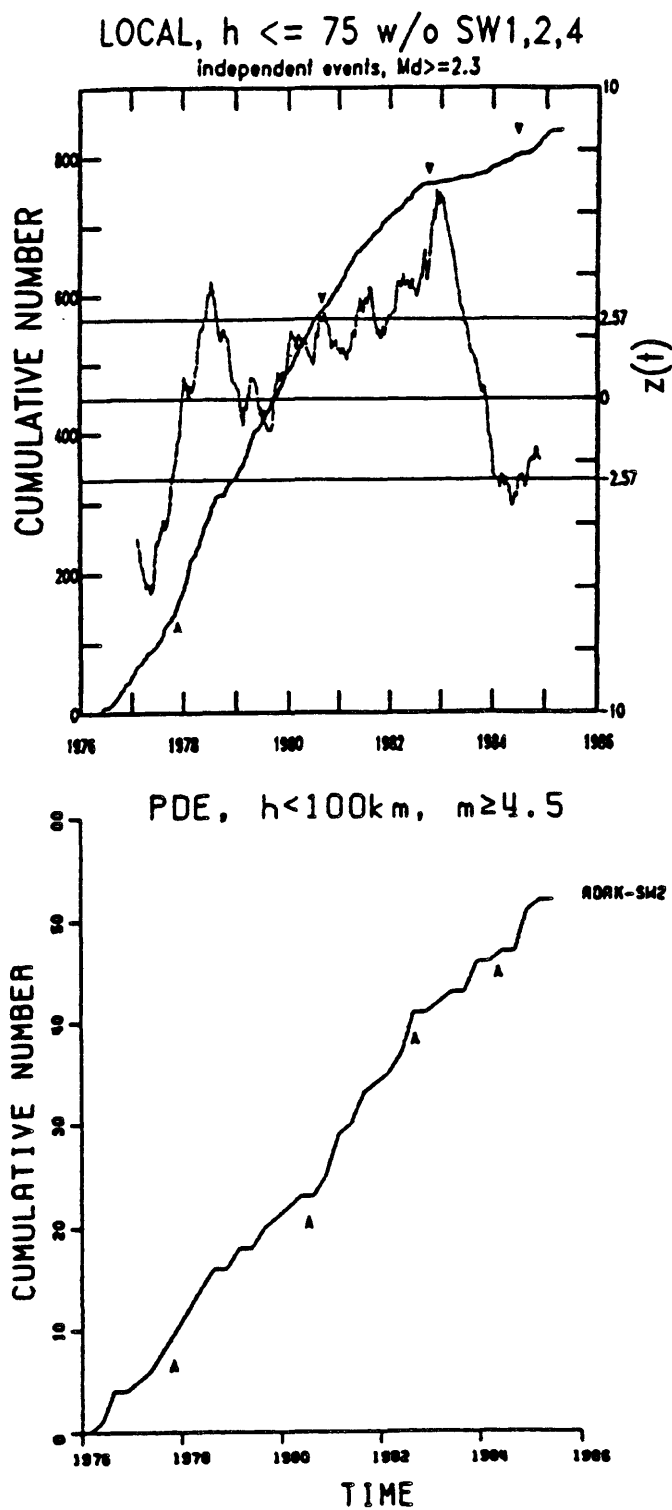
Figure 6.

Figure 8.

Figure 7.

LOCAL, SW1,2 and 4
independent events, Md>=2.3

PDE, h<100km, m≥4.5

TIME

Figure 9.

Figure 10.

APPARENT STRESS
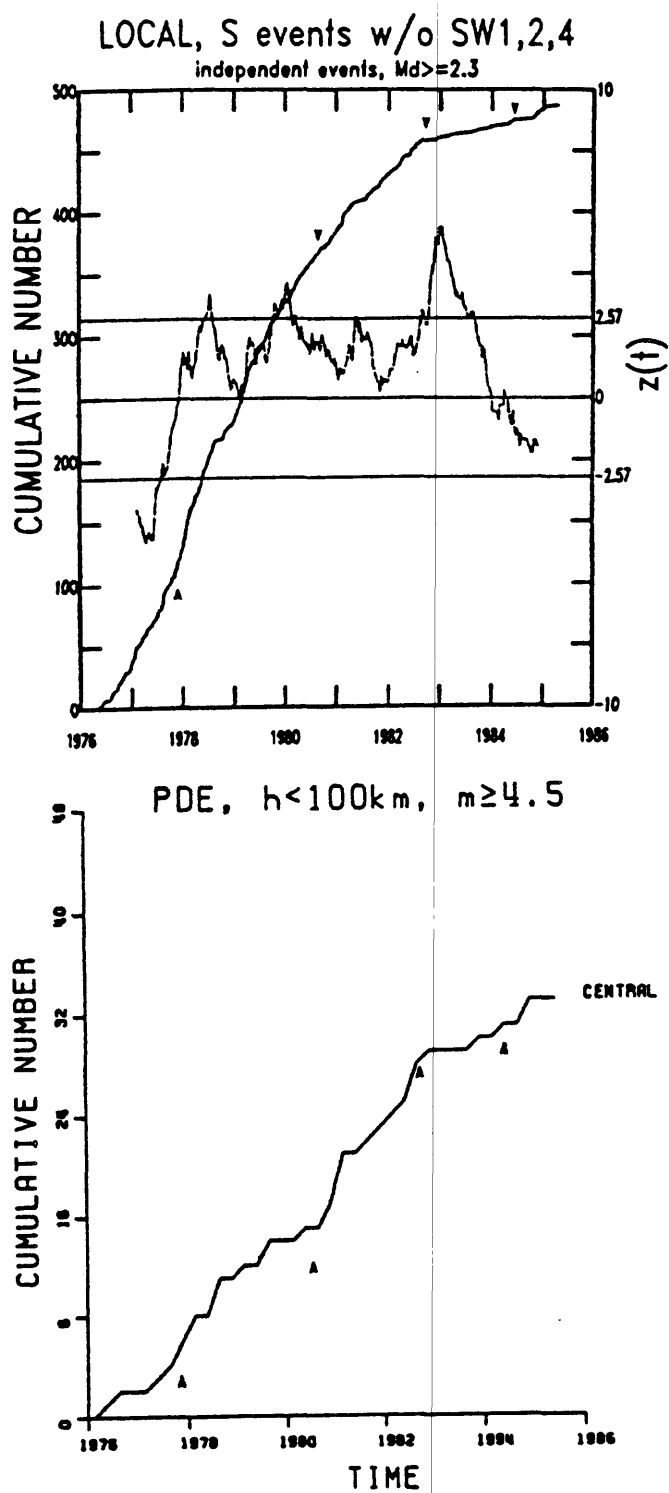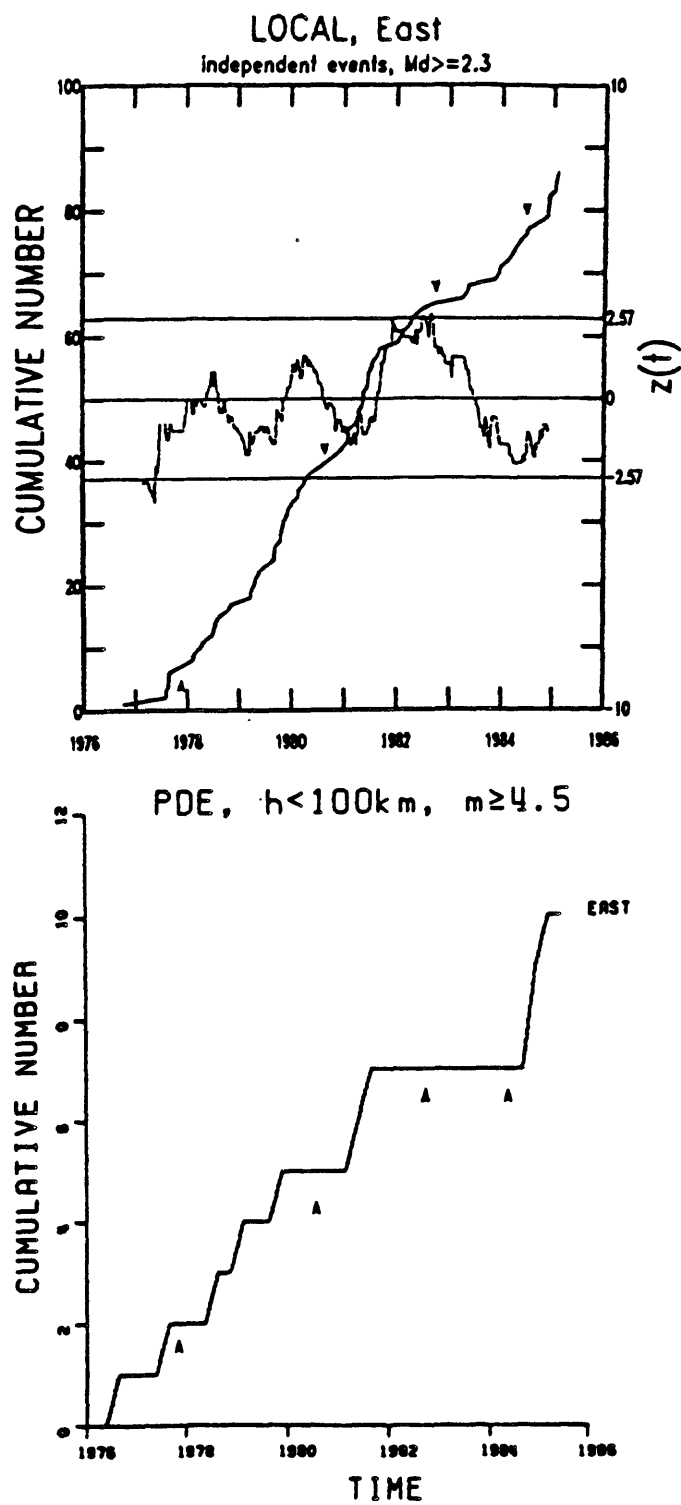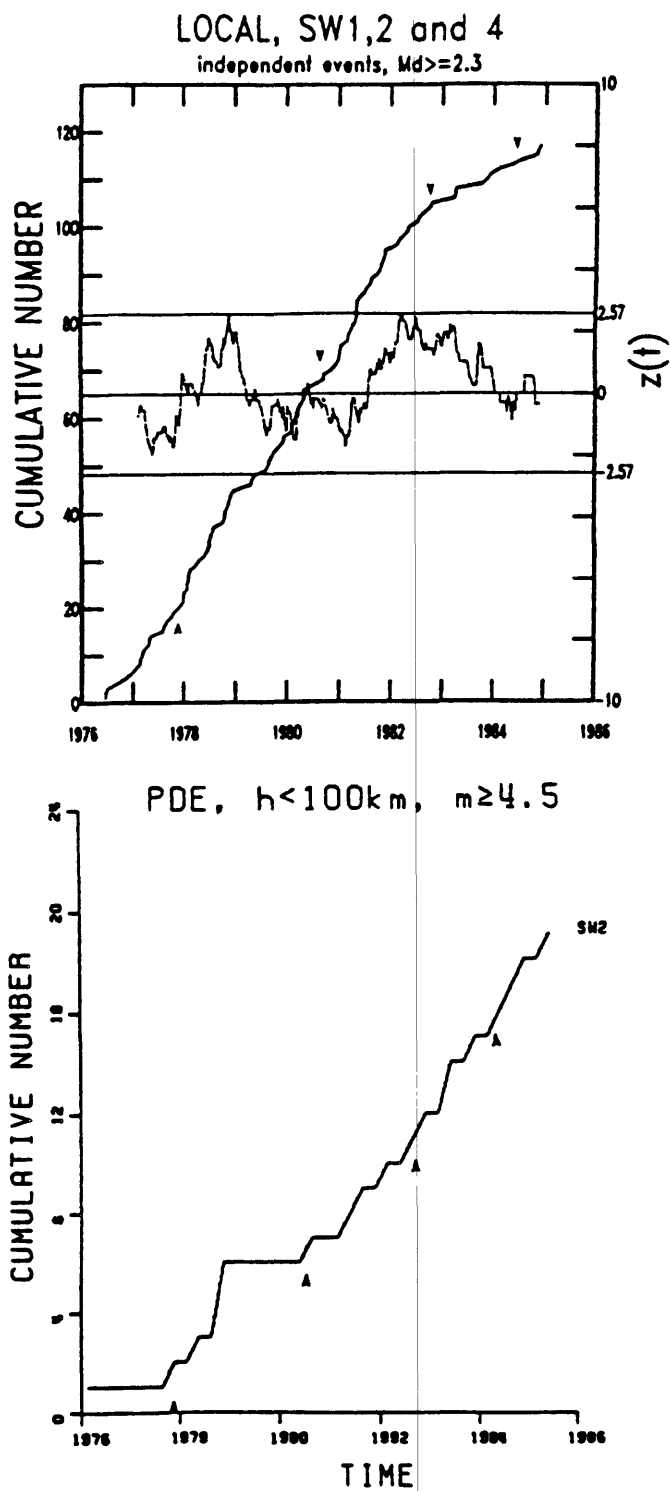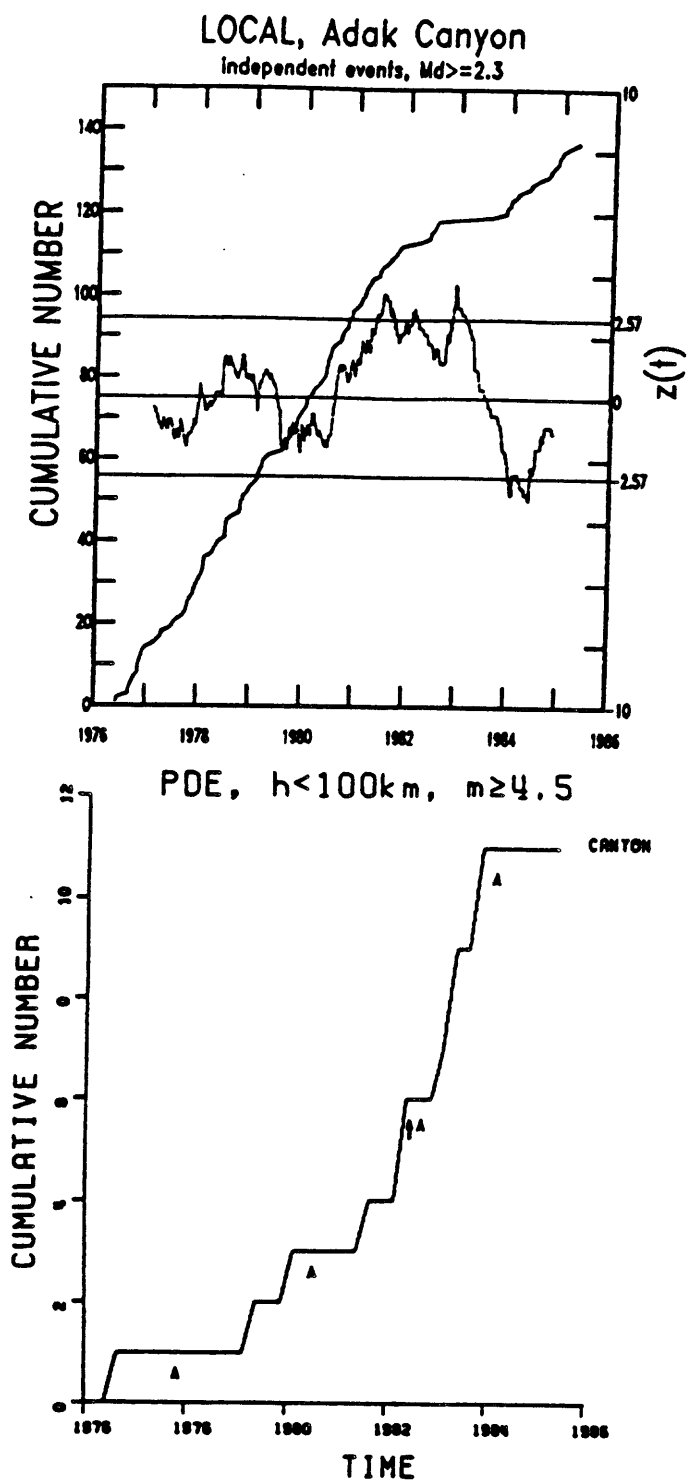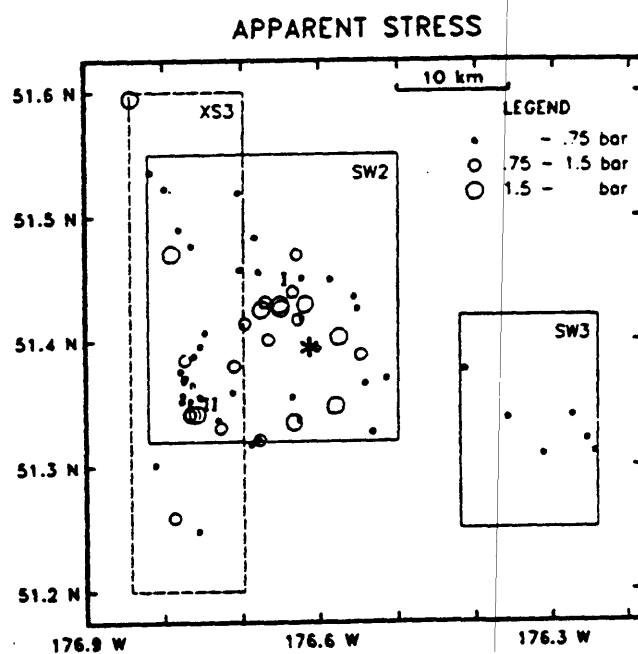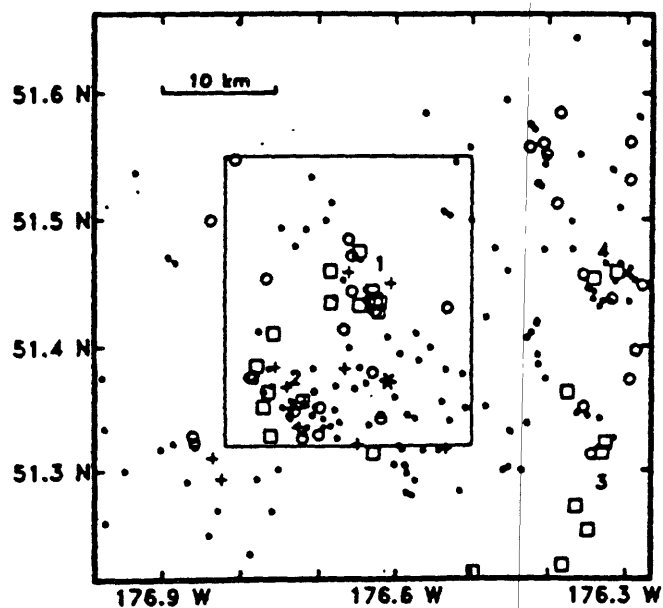
Figure 11.

APPENDIX A. 8.

Geologic Studies Related to Earthquake Potential and
Recurrence in the "Yakataga Seismic Gap"

G. Plafker

Geologic Studies Related to Earthquake Potential and

Recurrence in the "Yakataga Seismic Gap"

George Plafker
U.S. Geological Survey
345 Middlefield Road
Menlo Park, CA 94025

Geologic data relevant to earthquake recurrence times in the "Yakataga seismic gap" are primarily the ages of coseismic marine terraces at Middleton Island in the Gulf of Alaska and along the mainland coast between Yakataga and Icy Bay (Plafker and Rubin, 1967, 1978; Plafker, 1969; Plafker and others, 1981). These terraces are believed to record one or more abrupt coseismic uplifts of the shoreline relative to sea level following long periods of interseismic strain accumulation and relative stability with respect to sea level.

Middleton Island, near the margin of the continental shelf in the northern Gulf of Alaska, has emerged from the sea during six major episodes of coseismic uplift from oldest to youngest of about 7 m, 8 m, 6 m, 9 m, 7.5 m, and 3.5 m which are recorded by exceptionally well-exposed and preserved marine terraces (fig. 1). All but the youngest uplift have been dated by radiocarbon methods at roughly 5,090, 3,890, 3,500, 2,420, and 1,290 (all $\pm$ 250) calendar years before present, respectively, and the most recent uplift occurred during the great March 27, 1964 Alaska earthquake. The radiocarbon-dated material is either driftwood or the oldest peat on the terrace surface. Recurrence time for these movements is on the order of 400 to 1,300 years. During this period, the eustatic level of the sea was either slowly rising or stable; thus the episodic nature of the emerging terraces requires that the pre-1964 terraces are also primarily tectonic in origin. Average

uplift rate is approximately 10 mm/yr since the island first emerged from the sea 5,090 years ago and there appears to be an abrupt decrease in the rate of uplift to 6 mm/yr in the interval preceding uplift of the 1964 terrace. Independent evidence for the long strain accumulation period that preceded the 1964 event comes from radiocarbon dating of shorelines that were tectonically submerged in the eastern part of the earthquake focal region (throughout Prince William Sound, the Copper River Delta, and Cape Suckling). These data indicate that submergence occurred throughout this region and that at Montague Island it was continuous for at least 1,180+70 calendar years prior to the earthquake at an average rate of 6 mm/yr. (fig. 2). These data preclude the possibility that a 1964-type event involving significant uplift affected the Montague Island area for at least 1,180 years prior to 1964.

The accumulated Middleton Island terrace data suggest recurrence intervals of 400 to 1,300 years for large arc-related events of the 1964 type. The data from terrace uplift steps and rates at Middleton Island, together with the results of triangulation resurveys in the earthquake-affected region, suggest that at least half of the strain accumulated during the 1,300 years that preceded the 1964 earthquake has yet to be released, assuming no significant aseismic prequake creep. The accumulated strain could be released either by aseismic creep or in one or more large earthquakes over a time interval that is short, relative to the interval between successive terrace uplifts. Because the tide gage data indicate recovery rather than continued gradual strain release since the 1964 earthquake, it appears more likely that any residual accumulated strain at Middleton Island will be released during future earthquakes.

Along a heavily forested segment of the mainland between Cape Yakataga in the west and Icy Cape, four marine terraces have been dated by their included peat, wood and organic sediment layers. Radiocarbon dates obtained on organic

material from these raised shorelines provide approximate terrace ages of 6,520, 4,990, 2,820 and 1,400 (all ± 250) calendar years for corresponding average uplift of about 63 m, 37 m, 21 m and 13 m (fig. 3). The terraces have similar depositional sequences, with thin deposits of beach and lagoon facies overlying surfaces cut into both unconsolidated sediments and bedrock. The terrace sequences are commonly overlain and concealed by thick fluvial and fluvioglacial deposits; dated material comes from the lagoonal facies on each terrace.

The average uplift rate (corrected for eustatic sea level rise but not isostatic uplift) for the past 6,500 years is about 10 mm/yr near Icy Cape and approximately half this amount at Cape Yakataga. The upward slope in elevation of the terraces eastward towards Icy Cape may be due to an isostatic component related to deglaciation at Icy Bay. Assuming the entire terrace uplift occurred as discrete major coseismic steps, the recurrence intervals from oldest to youngest would be 1,530, 2,170, 1,420, and 1,400 calendar years, with steps of about 15.5, 17, 7.5, and 13.5 meters. However, because of the dense vegetation cover and poor exposure on the terraces, it is probable that not all terrace steps above the stage III terrace have been identified. The plate-convergence rates along this part of the Pacific margin are 50-60 mm/yr so that the terraces record only part of the tectonic deformation in this structurally complex and tectonically active region.

The last uplift step of about 13 m that formed the stage IV terrace occurred about 1,420 years ago. Thus, if the average recurrence interval for major terrace-forming earthquakes in this area is about 1,400 years, as suggested by the interval between the stage III and IV terraces, the data suggest that the next uplift event in the Cape Yakataga-Icy Cape area may be imminent.

In summary, terrace data suggest that tectonic uplift rates in both the

Cape Yakataga-Icy Cape and Middleton areas near both ends of the "Yakataga seismic gap" lag behind the long-term average rates. Future uplift of these areas most probably would occur during one or more major earthquakes along the convergent boundary between the Yakutat and Wrangell blocks which extends northeastward from the eastern end of the Aleutian Trench along the Pamplona zone to the Fairweather transform fault. Because major earthquakes along this boundary are also likely to be accompanied by large vertical displacements on the continental shelf, they could generate seismic sea waves capable of causing coastal damage far from the earthquake focal region.

References Cited

Plafker, George, and Rubin, Meyer, 1967, Vertical tectonic displacements in south-central Alaska during and prior to the great 1964 earthquake: Jour. Geosciences (Osaka City Univ.), v. 10, art. 1-7, p. 1-14.

Plafker, George, 1969, Tectonics of the March 27, 1964 Alaska earthquake: U.S. Geol. Survey Prof. Paper 543-I, 74 p.

Plafker, George, and Rubin, Meyer, 1978, Uplift history and earthquake recurrence as deduced from marine terraces on Middleton Island, Alaska, in Proceedings of Conference VI, Methodology for identifying seismic gaps and soon-to-break gaps: U.S. Geological Survey Open-File Report 78-943, p. 687-721.

Plafker, George, Hudson, Travis, Rubin, Meyer, and Dixon, K. L., 1981, Holocene marine terraces and uplift history in the Yakataga seismic gap near Icy Cape, Alaska, in Coonrad, W. L., ed., The United States Geological Survey in Alaska: Accomplishments during 1980: U.S. Geological Survey Circular 844, p. 111-115.
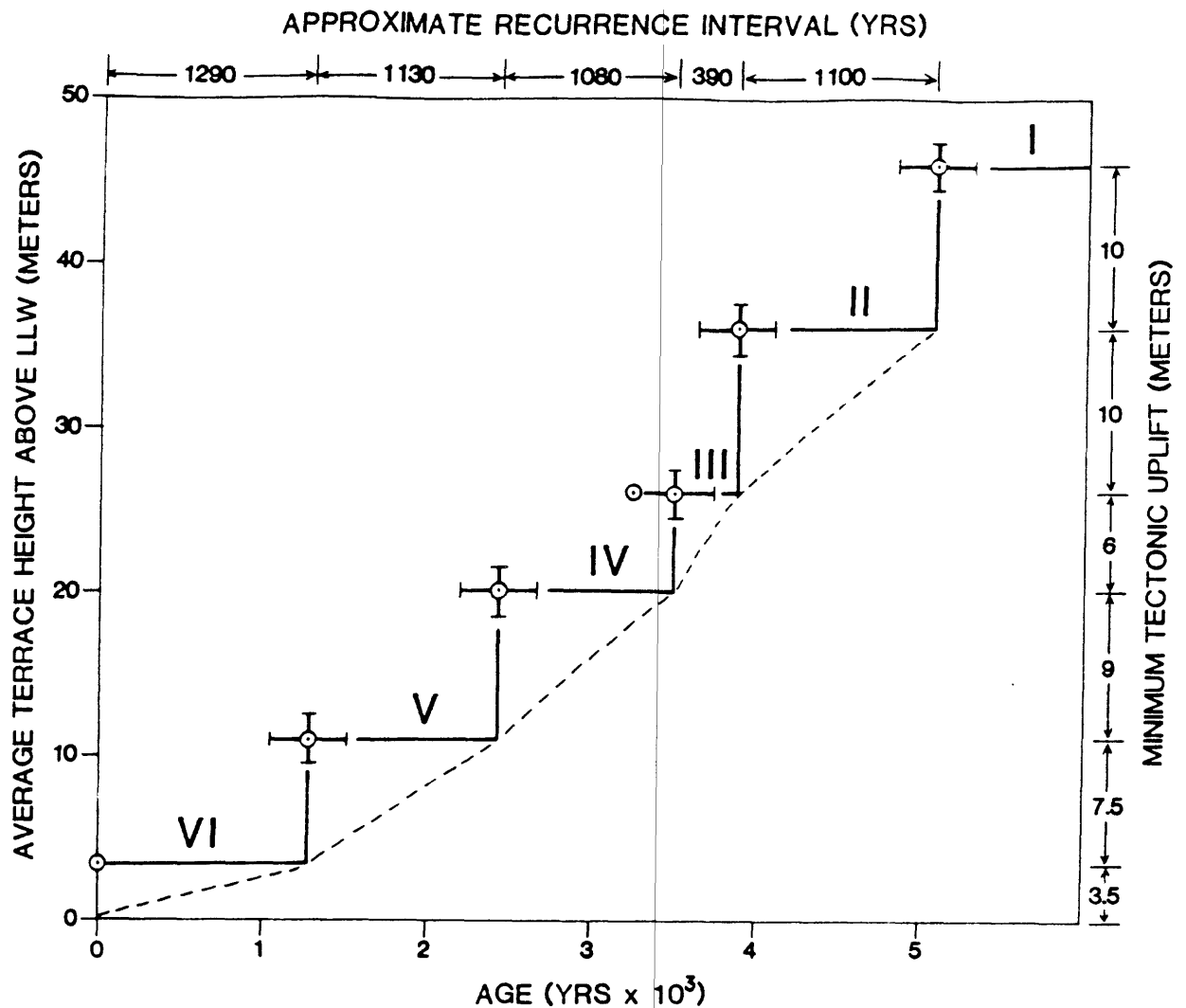
Figure 1. Generalized diagram showing average terrace height at Middleton Island (Roman numerals) and minimum tectonic uplift per event(s), versus terrace age and indicated recurrence interval. Terrace heights corrected forHolocene sea level rise; radiocarbon ages corrected to calendar years. The solid curve shows an inferred uplift sequence assuming no interseismic vertical movement. The dotted line indicates the average uplift rate between terraces. After Plafker and Rubin (1978).

Beaufort Sea

NORTH AMERICA PLATE

ard Peninsula

WB

SE

YB

Gulf of Alaska

PACIFIC PLATE

0 100 300 Miles

0 100 500 Kilometers
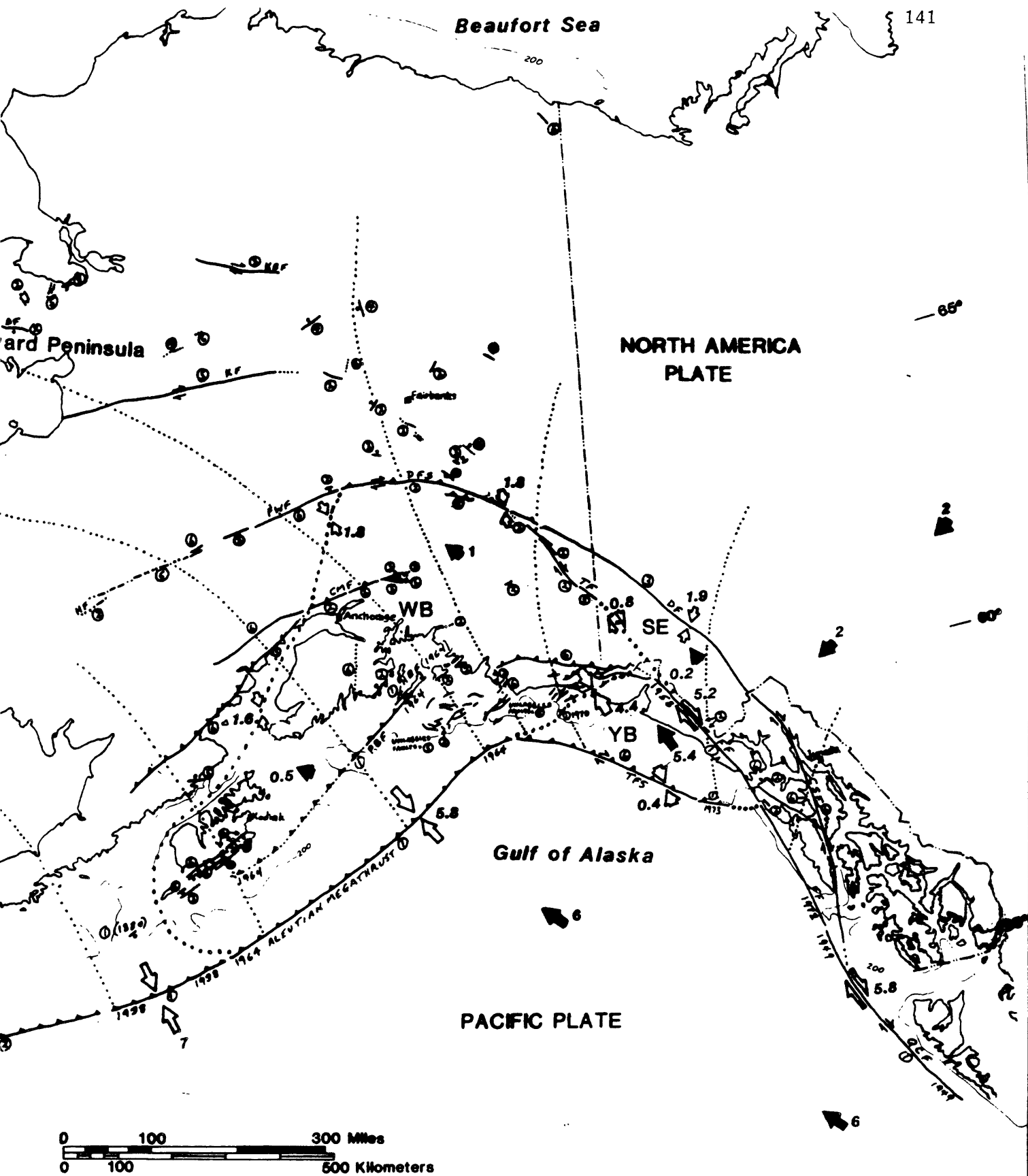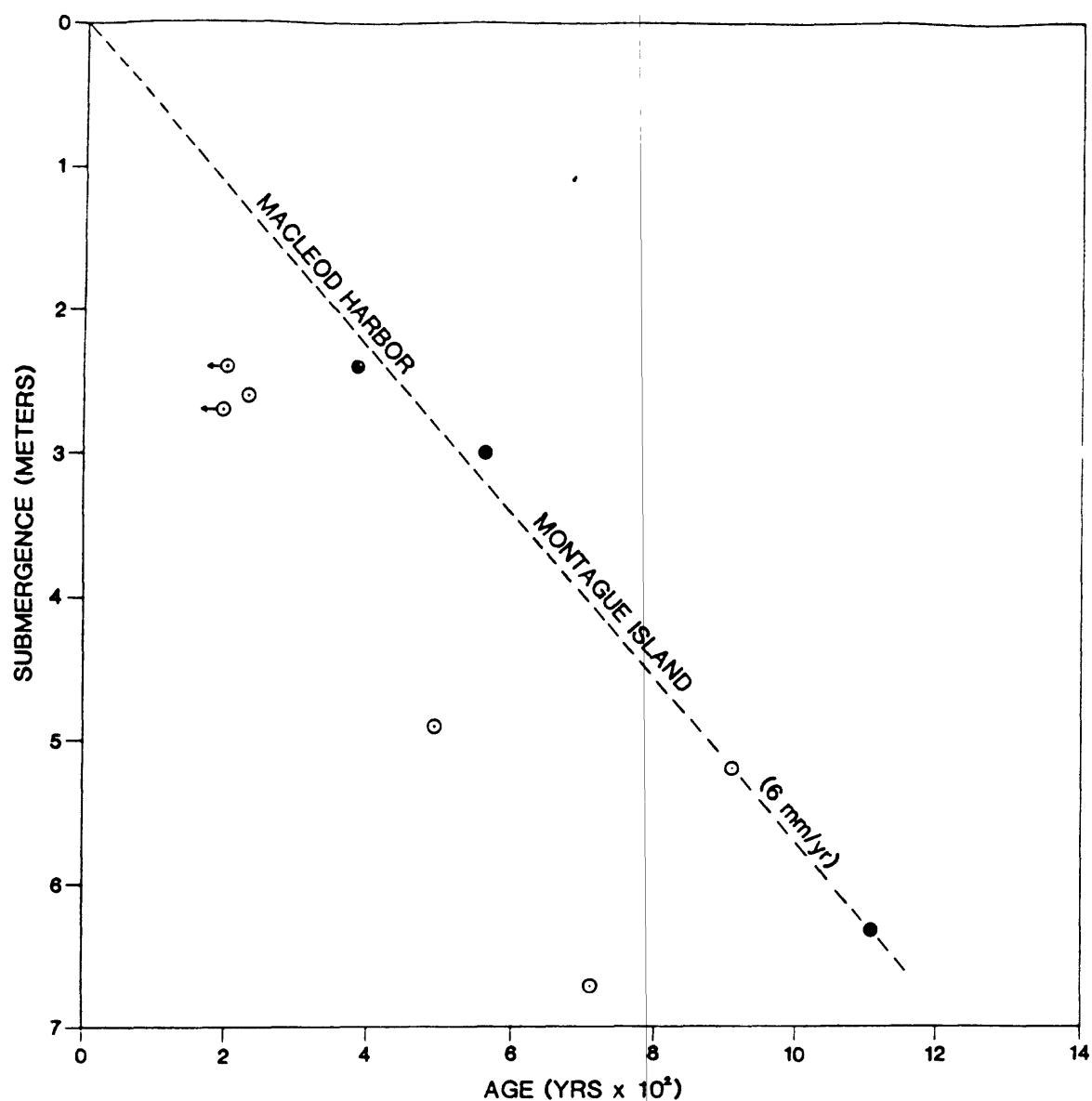
Figure 2. Pre-1964 positions of submerged radiocarbon-dated shoreline samples
(dots) from the eastern end of the 27 March 1964 earthquake focal
region. All sample localities are in the region of coseismic uplift
during the 1964 earthquake; the Montague Island localities (solid dots)
were uplifed about 9 m. Widespread interseismic submergence of
shorelines at average rates ranging from 5 to 11 mm/yr for 1,180 calendar
years indicates an absence of 1964-type tectonic uplift for at least this
period. After Plafker and Rubin (1967), Plafker (1969), and unpublished
data.
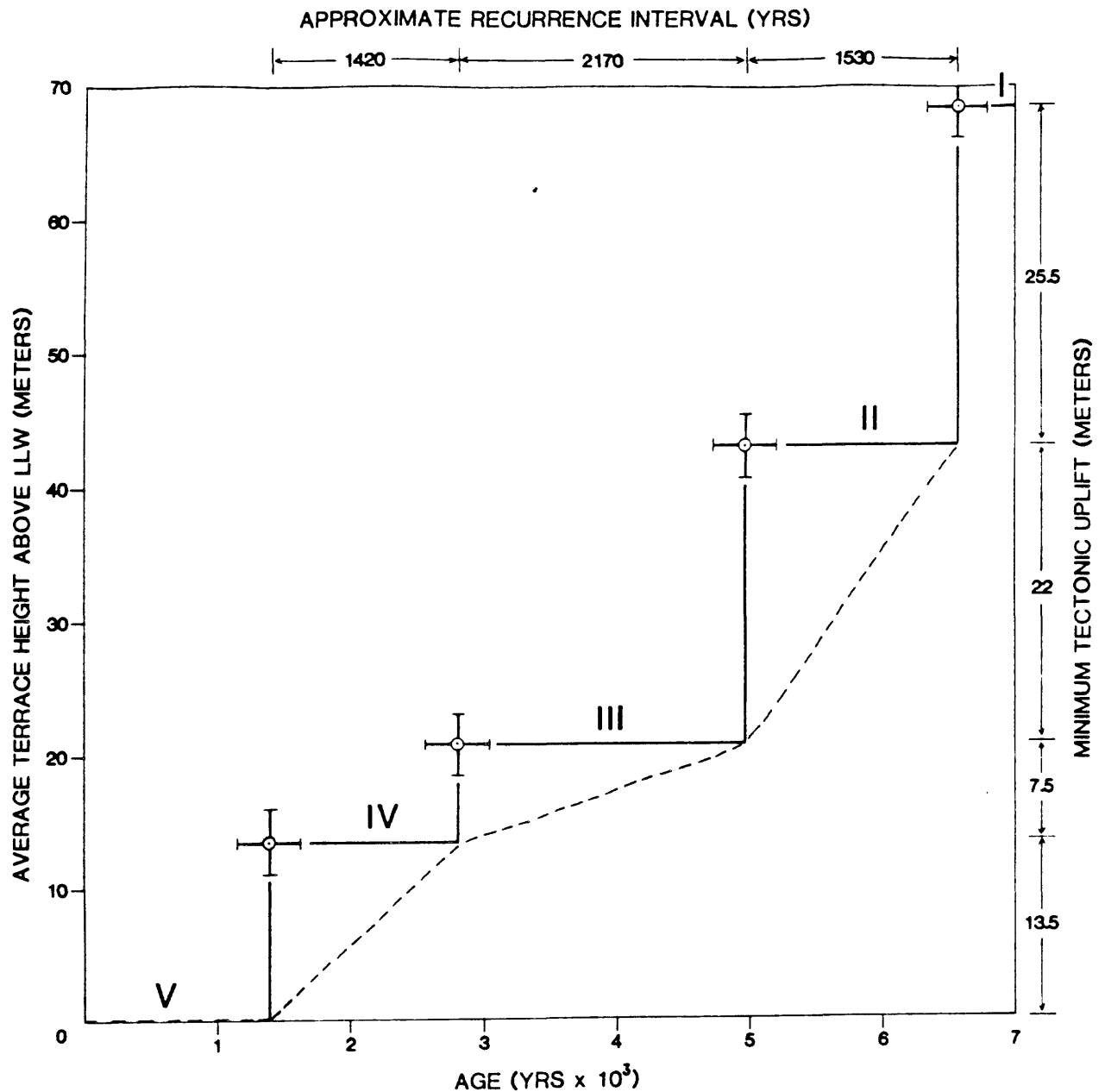
Figure 3. Generalized diagram showing average terrace height in the Icy Cape

area (Roman numerals) and minimum tectonic uplift per event(s), versus

terrace age and indicated recurrence interval. Terrace heights corrected

for holocene sea level rise; radiocarbon ages corrected to calendar

years. The dashed line shows an inferred uplift sequence assuming no

interseismic vertical movement. After Plafker and others (1982) and

Rubin and others (1982).

APPENDIX A. 9.

Review of Seismicity and Microseismicity of the
Yakataga Seismic Gap, Alaska

R. A. Page, J. C. Lahr, and C. D. Stephens

Review of Seismicity and Microseismicity of the Yakataga Seismic Gap, Alaska

by

Robert A. Page, John C. Lahr and Christopher D. Stephens
U.S. Geological Survey, 345 Middlefield Road, Menlo Park, CA 94025

Summary   Review of available seismicity and microseismicity from the vicinity of the Yakataga seismic gap provides no indication that a great, gap-filling earthquake is likely to occur sooner rather than later in the next decade or two. First-order features of microseismicity monitored since 1974 within and adjacent to the gap have been remarkably stable.

The Yakataga seismic gap is bounded on the west by the aftershock zone of the 1964 Prince William Sound earthquake, on the east by the aftershock zone of the 1979 St. Elias earthquake, on the south by the continental shelf edge and the Pamplona zone -- the deformational front within the accreting Tertiary Yakutat block -- and on the north by the 40-km isobath of the NNE-dipping Wrangell Benioff zone (Fig. 1). The seismic gap lies in a region of great tectonic complexity (Fig. 2). North-northwestward motion of the Pacific plate relative to the North American plate results in predominantly dextral slip along the Fairweather fault system in southeastern Alaska and subduction along the Aleutian Islands, the Alaska Peninsula and the Kenai Peninsula. The gap lies in the transitional zone between these two tectonic regimes.

Seismicity (magnitude m_b 4.5 and larger)

The Yakataga gap was ruptured by an M_s 8.5 shock on 4 September 1899 (McCann and others, 1980). A second great (M_s 8.4) earthquake occurred on September 10 on the eastern edge of the gap with the most severe effects reported around Yakutat Bay (McCann and others, 1980). For 1900 to 1958 the known seismic history includes no earthquakes larger than magnitude 6.0 within a distance of about 100 km of the gap, as depicted in Fig. 1. In July 1958, an M_s 7.9 shock broke the northern Fairweather fault; a pronounced group of aftershocks near 60.3°N, 140°W marked the northern end of the inferred rupture (Tobin and Sykes, 1968). A few months later, in September, a magnitude 6.3 event occurred on the southern edge of the gap. No other shocks of magnitude 6.0 or larger occurred in or near the gap prior from 1958 to the time of the 1964 earthquake.

The eastern end of the 1964 rupture zone is commonly identified with the eastern limit of the dense concentration of aftershocks near Kayak Island, at about long. 144.5°W (Fig. 3, upper left), but many shocks occurred in 1964 and 1965 both perpheral to and within the Yakataga gap. McCann and others (1980) interpret these shocks to be a surge of triggered activity rather than evidence of the 1964 rupture extending into the gap. However, observations of coastal uplift (Plafker, 1969) and later geodetic resurveys in an area north and west of Cape Yakataga (Lisowski and Savage, 1980) indicate that significant slip on the megathrust extended about 50 km east of Kayak Island, as far as long. 143°W. Thus, the 1964 shock may have relieved some of the accumulated strain within the western part of the gap.

The seismicity in and around the Yakataga gap since 1960 for magnitudes larger than m_b 4.5 (Figs. 3 and 4) is dominated by the aftershock activity following the 1964 earthquake which decays inversely with time after the main shock (Fig. 4). A second prominent feature in the seismicity is the persistent activity on the eastern edge of the gap in the Icy Bay-St. Elias region, around long. 141°W. This area was active prior to 1964; it was the site of 1979 St. Elias earthquake (M_w 7.6); and it remains active today. Some of the earthquakes that have occurred in the St. Elias-Icy Bay region since 1979 have been followed by pronounced aftershock sequences (for example, a pair of m_b 5.0 shocks on 2 and 3 May 1982; see Fig. 10), while others have been followed by relatively few shocks (for example, an m_b 6.0 shock on 28 June 1983). Elsewhere on the periphery of the gap, several shocks have occurred since 1965, the most noteworthy being the 1970 Pamplona Ridge sequence on the southeastern edge of the gap, including events as large as M_s 6.8 and mb 5.8. In contrast to the activity around the gap, since 1965 only one shock has been located well within the gap -- an m_b 4.8 event in 1967 -- and two shocks (m_b 4.6 and 4.5) near the boundary of the gap.

The pattern of seismicity in the vicinity of the Yakataga gap since 1965 resembles that which has preceded major shocks elsewhere to the extent that prominent earthquake sequences as well as isolated events have occurred on the perimeter of the gap. However, no cluster of seismicity that could be considered as diagnostic of an impending great earthquake has been recognized on the northern edge of the gap -- the downdip edge of the postulated thrust-- where a gap-filling earthquake would likely originate. The only concentration along the downdip boundary is the mainshock and a large aftershock of the 1979 St. Elias sequence, but no sizable shocks have occurred in that area since 1979. Within the gap, no shock larger than m_b 4.5 has occurred since 1970.

Microseismicity since 1974

The USGS regional seismograph network was extended eastward from Prince William Sound through the area of the Yakataga gap in the summer of 1974. The number of stations and the area being monitored (Fig. 5) remained nearly constant from 1974 until the summer of 1985, when 13 stations had to be closed because of budget constraints. Microearthquake activity in and around the seismic gap is shown in Figures 6 through 9 for several consecutive periods, including annual intervals since October 1979. In interpreting these plots, one must allow for three facts. First, the detection threshold is lower for shocks within a 150-km-wide band landward from the coast than for shocks occurring either offshore or farther inland. Second, east of about long. 145°W, all sufficiently well-recorded shocks have been located; whereas, west of that longitude, only those events larger than a threshold magnitude have been located. The threshold increased from a coda magnitude of about 1.5 to about 2.0 in October 1980, or from about m_b 1.7 to mb 2.3. Third, since April 1984, shocks in the St. Elias aftershock zone smaller than about coda magnitude 1.0, or m_b 1.0, have not been located. (Estimates of magnitude based on coda duration are generally low compared to m_b. Based on a preliminary analysis, the empirical relation between m_b and duration magnitude m_D, is m_b = 1.3 m_D - 0.39).

The most striking feature of the microseismicity since 1974 (Figs. 6-9) is the stability of the gross features of the activity from one interval to another. The spatial pattern of shocks in the 4 1/2 years before the 1979

earthquake (Fig. 6, top) is remarkably similar to those in the six 1-year intervals after the earthquake (Figs. 7-9).

Within the Yakataga gap, a diffuse concentration of seismicity has persisted since 1974 in the middle of the gap beneath Waxell Ridge, amidst a 75-km-wide band of scattered activity paralleling the coast. Details of the Waxell Ridge activity have not been resolved because of the lack of seismographs in the area. The largest events range up to about m_b 4.0. Focal depths for the better-quality hypocenters lie in the range 10-30 km; however, depths are not well constrained because of the lack of close stations and uncertainties in the velocity model. Within the limits of the data, these shocks could be associated with a subhorizontal fault -- a patch on the inferred megathrust. Alternatively, they could be related to faulting within either the subducting or overriding plate. Along the eastern margin of the gap, seismicity associated with the Icy Bay-St. Elias zone of activity laps into the gap. Elsewhere within the gap, there are only scattered minor clusters of shocks and isolated events.

Along the northern boundary of the gap, very few shocks have occurred except in the epicentral area of the 1979 St. Elias earthquake. Activity in the epicentral area has been gradually declining since 1979 to the present. Note that a low level of activity was observed in this area before 1979 (Fig. 6, top). On the eastern, southern and western boundaries of the gap, there have been both persistent concentrations of seismicity and isolated events. The most notable concentration is the seismicity in the Icy Bay-St. Elias area, which was active before, as well as after, the 1979 earthquake. The rate of activity in this area has been decreasing slowly since 1979 (Fig. 10, top). The Icy Bay-St. Elias area is characterized by shallow, low-angle thrusting, as observed for the 1979 earthquake. The seismicity is confined to shallow (less than 20 km) depths but is laterally distributed over a broad area. In general, it has been impossible to delineate buried faults in this area by mapping hypocenters, because the spacing between seismograph stations exceeds the depth of the shocks and thus precludes sufficiently precise focal depths. After the 1979 earthquake, however, temporary stations augmented the permanent network and permitted precise location of aftershocks occurring near the center of the rupture zone. The precise hypocenters define a horizontal or very gently dipping failure zone less than about 2 km thick in the depth range 10-15 km, which is inferred to be the principal slip surface in the St. Elias mainshock. No evidence of an upward bend or of surface-directed splays in the southern part of the rupture zone has been found in the microearthquake data, although a few small events have been located above the main thrust zone.

A second persistent concentration of seismicity along the boundary of the gap is near the mouth of the Copper River near 60.5°N, 145°W. This activity is confined to the depth range of about 15-30 km. The pattern of first motions for two of the largest events suggests normal slip on a moderately to steeply inclined fault, but the broad horizontal extent of shocks within a narrow depth range suggests that low-angle faulting (thrusting ?) may also be occurring. Recently obtained microearthquake and seismic refraction data in this region may help to resolve the tectonic details. Elsewhere along the gap boundary, an m_b 5.2 shock in September 1980 near the edge of the continental shelf was neither preceded nor followed by locatable earthquakes.

In the area surrounding the gap, concentrations of persistent seismicity are also observed, notably a northeast-trending zone near 61.5°N, 146.5°W and a more diffuse pattern near the head of Yakutat Bay. North and south of the gap, the seismicity is more diffuse and sporadic. The continental shelf area is characterized by scattered events. The segment southwest of the gap consistently has been more active than that to the southeast, but it has been conspicuously quiet over the last several months (Fig. 9, bottom). North of the gap, a large number of shocks have occurred near the northwestern end of the Duke River segment of the Denali fault system, approximately in the region 61°N - 62°N, 140°W - 142°W. The activity, which includes an m_b 5.3 mainshock and aftershock sequence in 1983, has fluctuated in both space and time.

Histograms of earthquake occurrence within selected regions (Fig. 10) show the general stability in the rates of microseismicity within the Waxell Ridge, Copper River delta and western continental shelf areas and also the overall decay in activity within the St. Elias area since the 1979 earthquake. Outside the St. Elias area, no first-order changes in rates of seismicity are observed. At magnitudes below the completeness threshold, an apparent temporary increase in activity occurred in the Waxell Ridge, Copper River delta and St. Elias areas between about November 1980 and September 1981; however, since 1981, the activity has continued at about its previous, lower level. The patterns of seismicity observed since 1979 do not suggest to us that a gap-filling earthquake is imminent. We find no indication that a gap-filling earthquake is more likely to occur within the next year or two rather than in a comparable interval in the next decade or two.
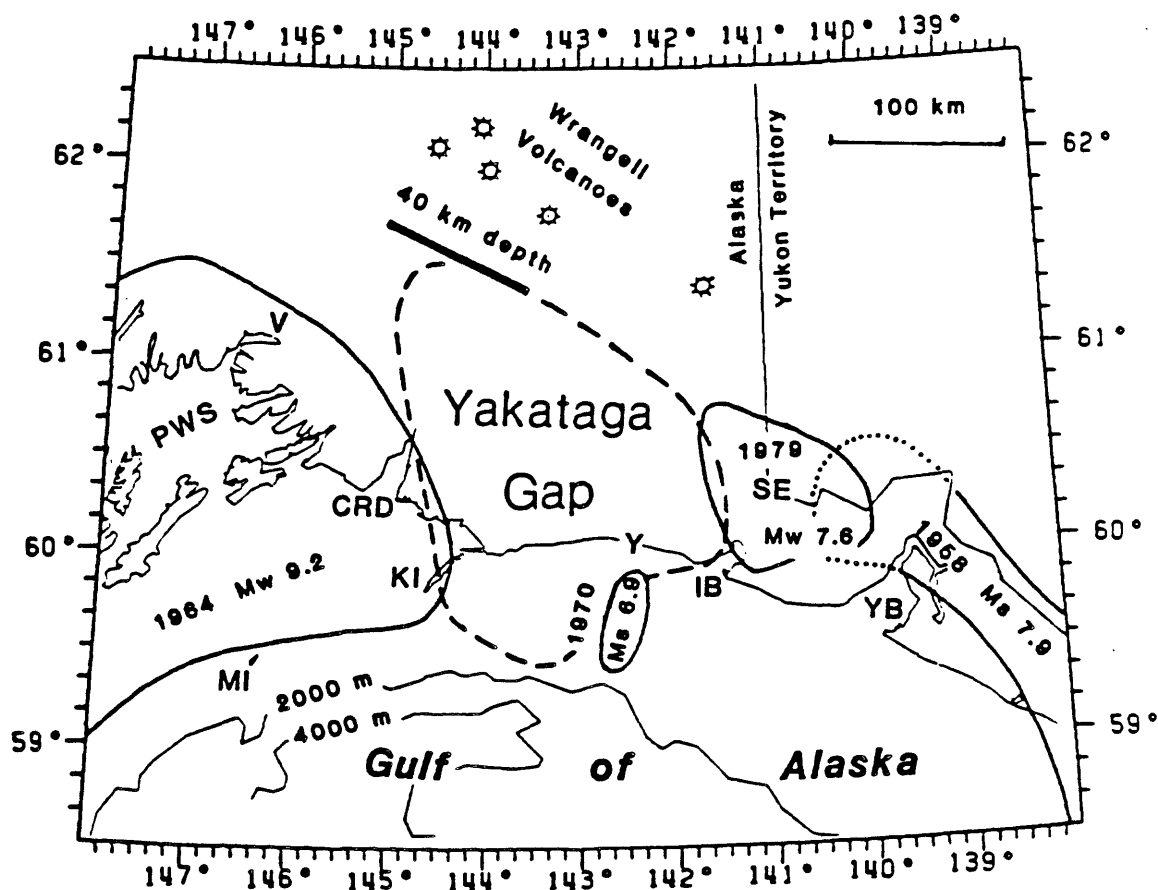
Fig. 1. Yakataga seismic gap (dashed boundary) in relation to aftershock zones of principal earthquakes since 1900 (solid boundaries). Heavy line, 40-km-depth contour on top of Wrangell Benioff zone. CRD=Copper River Delta; IB=Icy Bay; KI=Kayak Island; MI=Middleton Island; PWS=Prince William Sound; SE=Mount St. Elias; V=Valdez; Y=Yakataga; YB=Yakutat Bay.
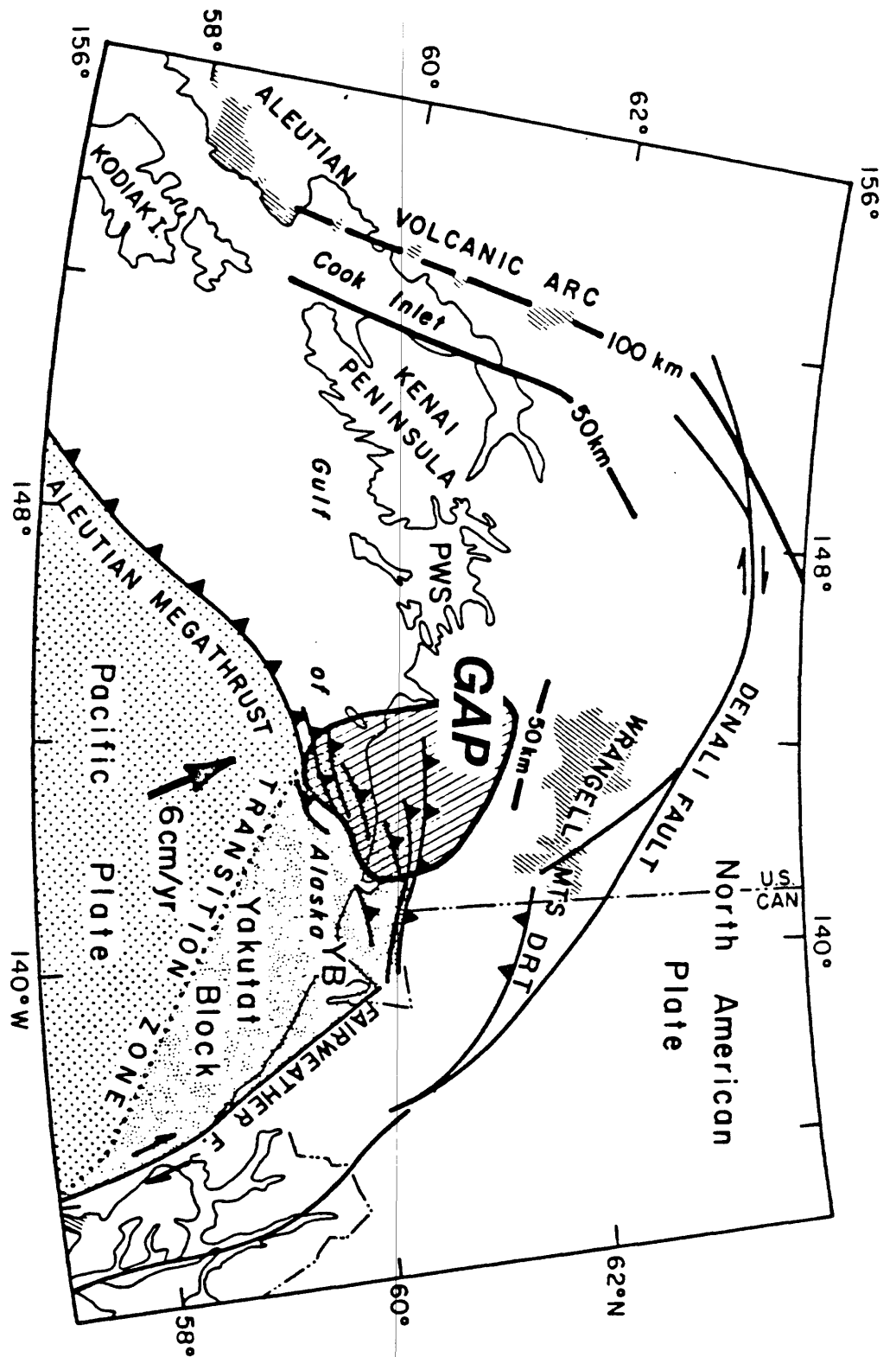
Fig. 2. Seismotectonic setting of Yakataga gap. Pacific plate motion vector relative to North American plate from RM1 pole of Minster and others (1974). Principal faults with known or suspected Cenozoic motion; barbs on upthrown side of reverse faults. Shading within the Aleutian volcanic arc and Wrangell Mountains indicates upper Tertiary and Quaternary volcanic rocks. 50-km and 100-km contours on top of Benioff zones from Lahr (1975) and Stephens and others (1984). Note offset and divergence between 50-km contours of Aleutian and Wrangell Benioff zones. DRT=Duke River thrust; YB=Yakutat Bay.

151
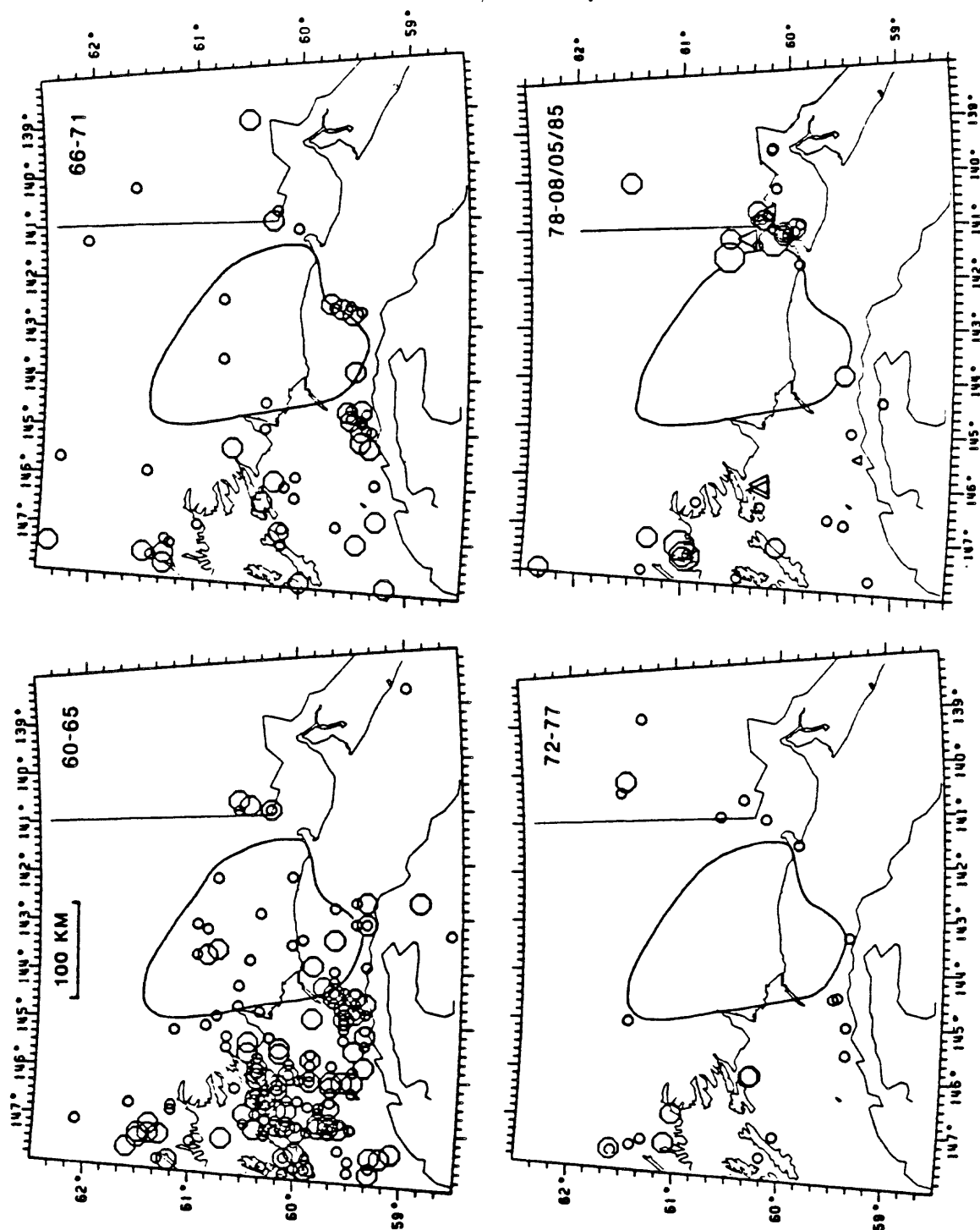
Fig. 3. Epicenter maps of magnitude m_b 4.5 or greater earthquakes in and around Yakataga gap from the PDE file for four consecutive intervals. The intervals are 6 years except for the most recent map to which have been added five events between 1 January 1984 and 5 August 1985 (triangles). Symbol size is proportional to magnitude; small, 4.5-4.9; intermediate, 5.0-5.9; and large, 6.0 or greater. The Yakataga gap is indicated in the center of the maps.
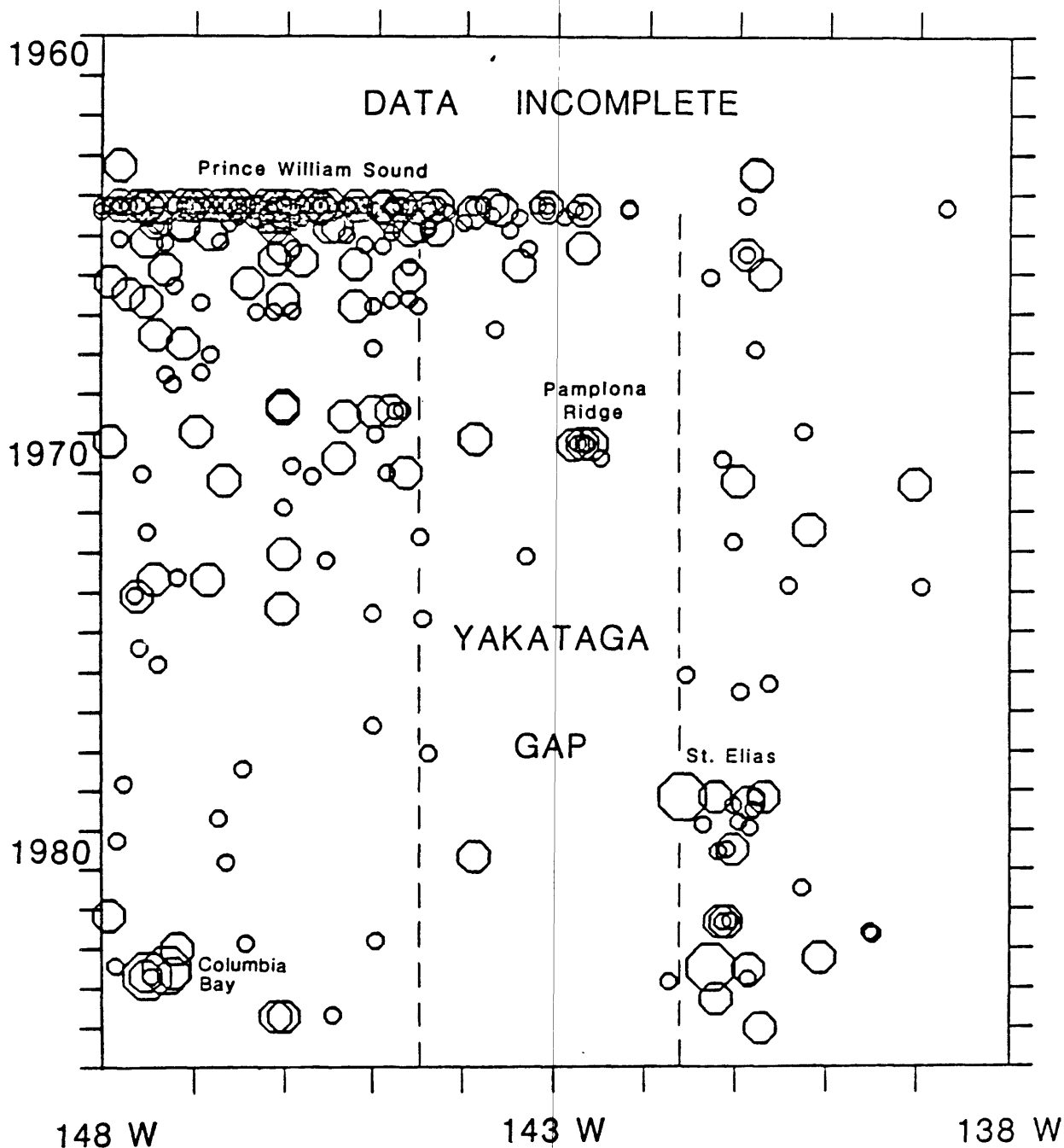
Fig. 4. Longitude-time plot of earthquakes plotted in Figure 3. The data are incomplete before 1964; body-wave magnitudes have been routinely computed by the PDE program only since April 1963. Symbol size as in Figure 3. Four prominent earthquake sequences are observed; 1964 Prince William Sound, 1970 Pamplona Ridge, 1979 St. Elias, and 1983 Columbia Bay. The approximate extent of the Yakataga gap is shown.
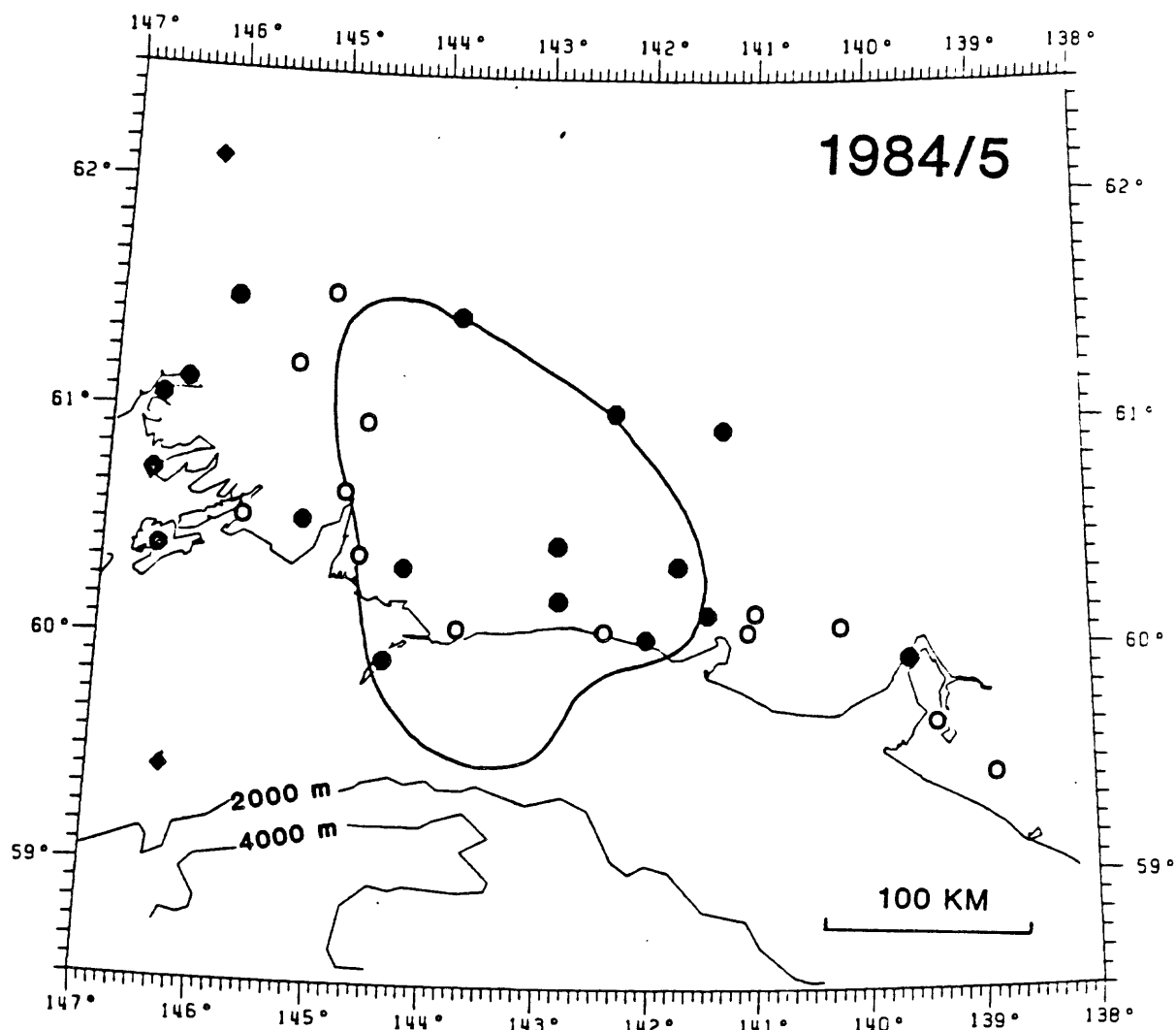
Fig. 5. Seismograph stations operated in and around the Yakataga gap during 1984/5 by the USGS (circles) and the Alaska Tsumani Warning Center (diamonds). Open circles are stations closed in the summer of 1985. The number and locations of stations changed little from 1974 until 1985.
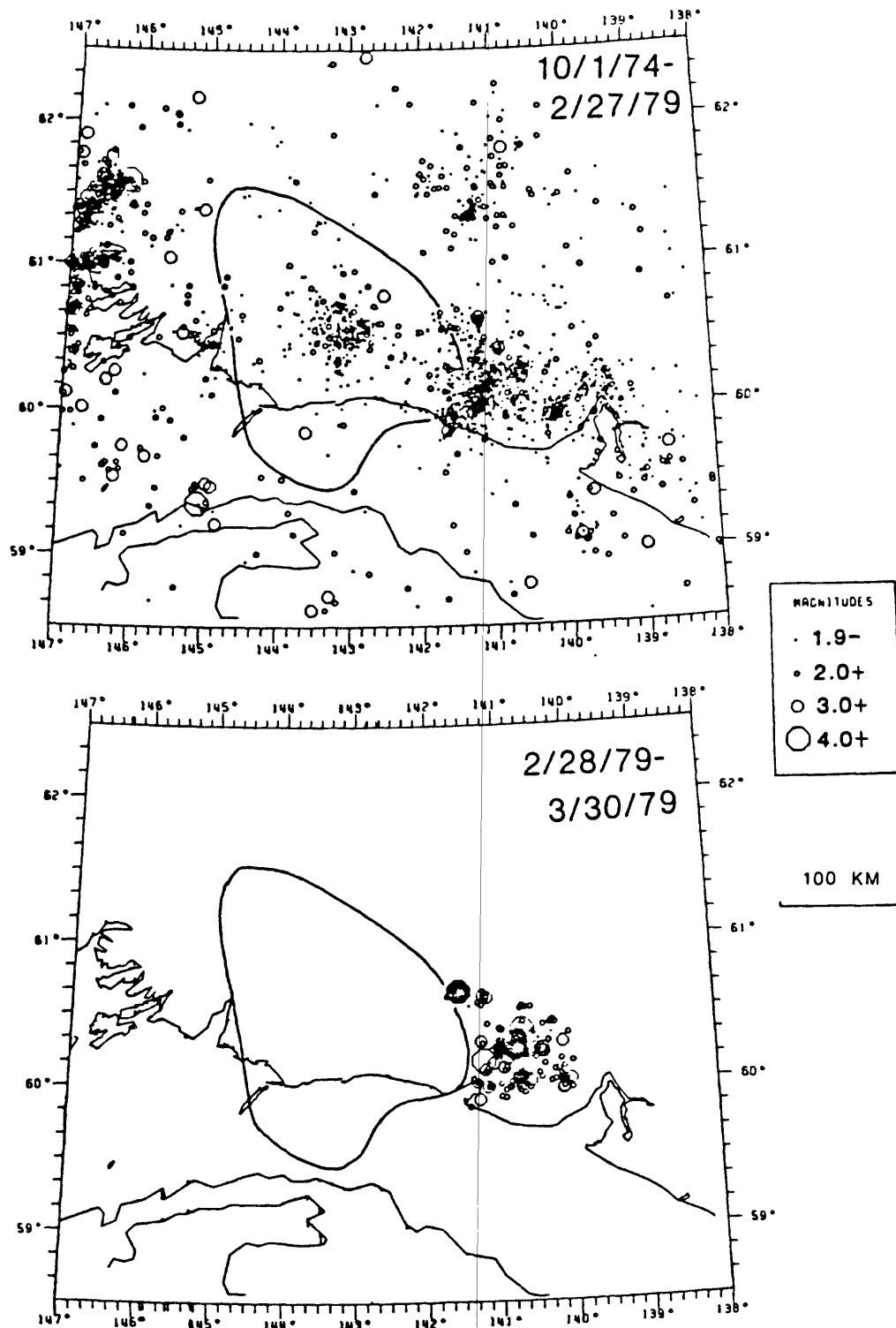
Fig. 6. Epicenters of earthquakes located with data from the regional
seismograph network. Symbol size indicates magnitude. Magnitudes
are based on coda duration. Coda magnitudes of 2.0, 3.0 and 4.0
approximately correspond to m_b magnituides 2.3, 3.7 and 5.1,
respectively. Yakataga seismic gap lies in center of maps. (Top)
Approximately 4 1/2-year interval before the 1979 St. Elias
earthquake. Shocks for October 1976 through September 1977 have not
been located and are not included. (Bottom) One-month interval after
the St. Elias earthquake (large solid symbol at northwest corner of
distribution). Only larger events within the rupture zone have been
located and are shown.
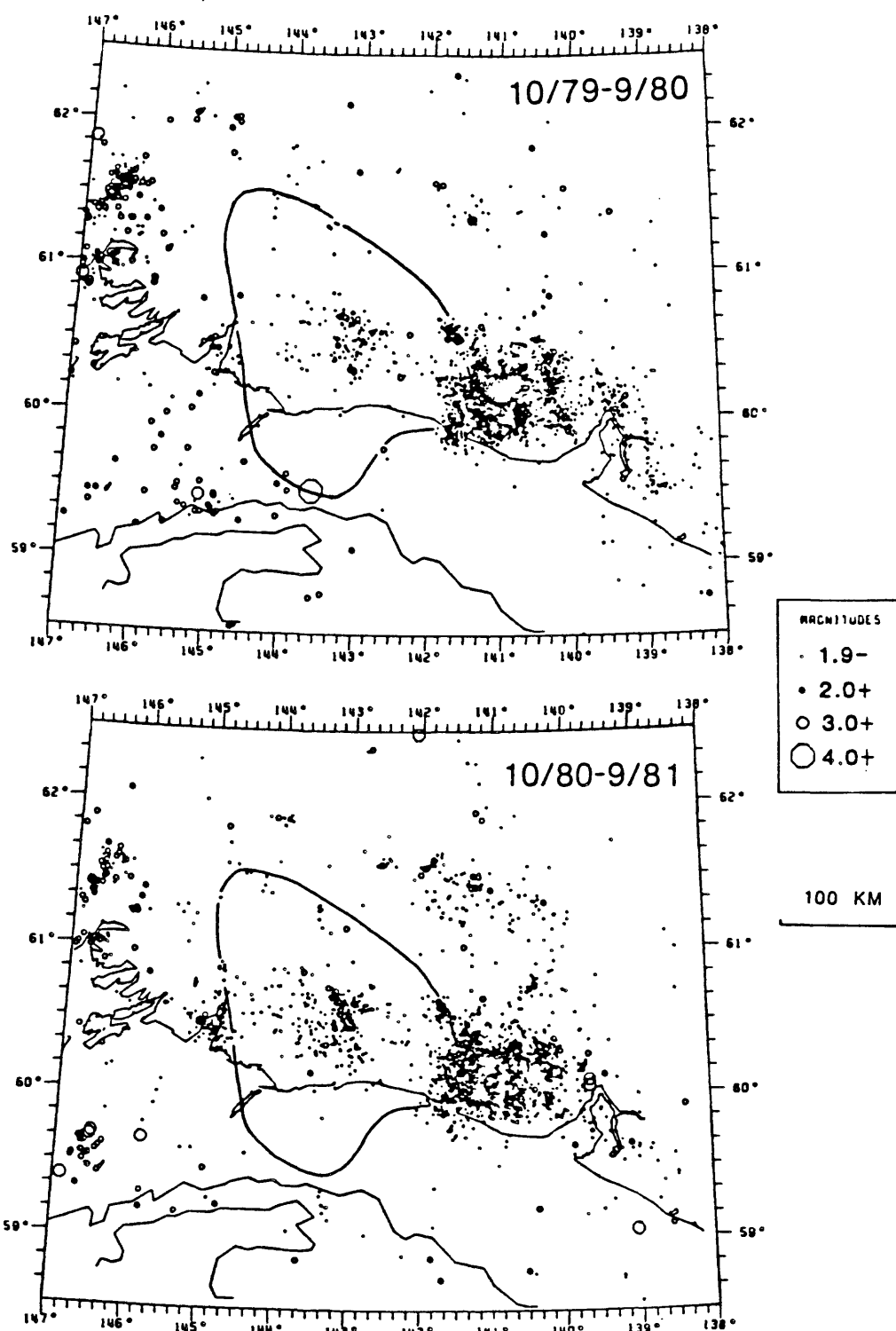
Fig. 7. Epicenters of earthquakes located with data from the regional seismograph network for 1979-80 and 1980-81. Symbols as in Fig. 6. (Top) Interval begins 7 months after the St. Elias earthquake. Note the abundant aftershock activity. Apart from the intense aftershock activity, there is a remarkable similarity in the gross features of seismicity with the 4 1/2-year interval before the St. Elias shock (Fig. 6, top). (Bottom) Succeeding interval beginning 1 1/2 years after the St. Elias earthquake.
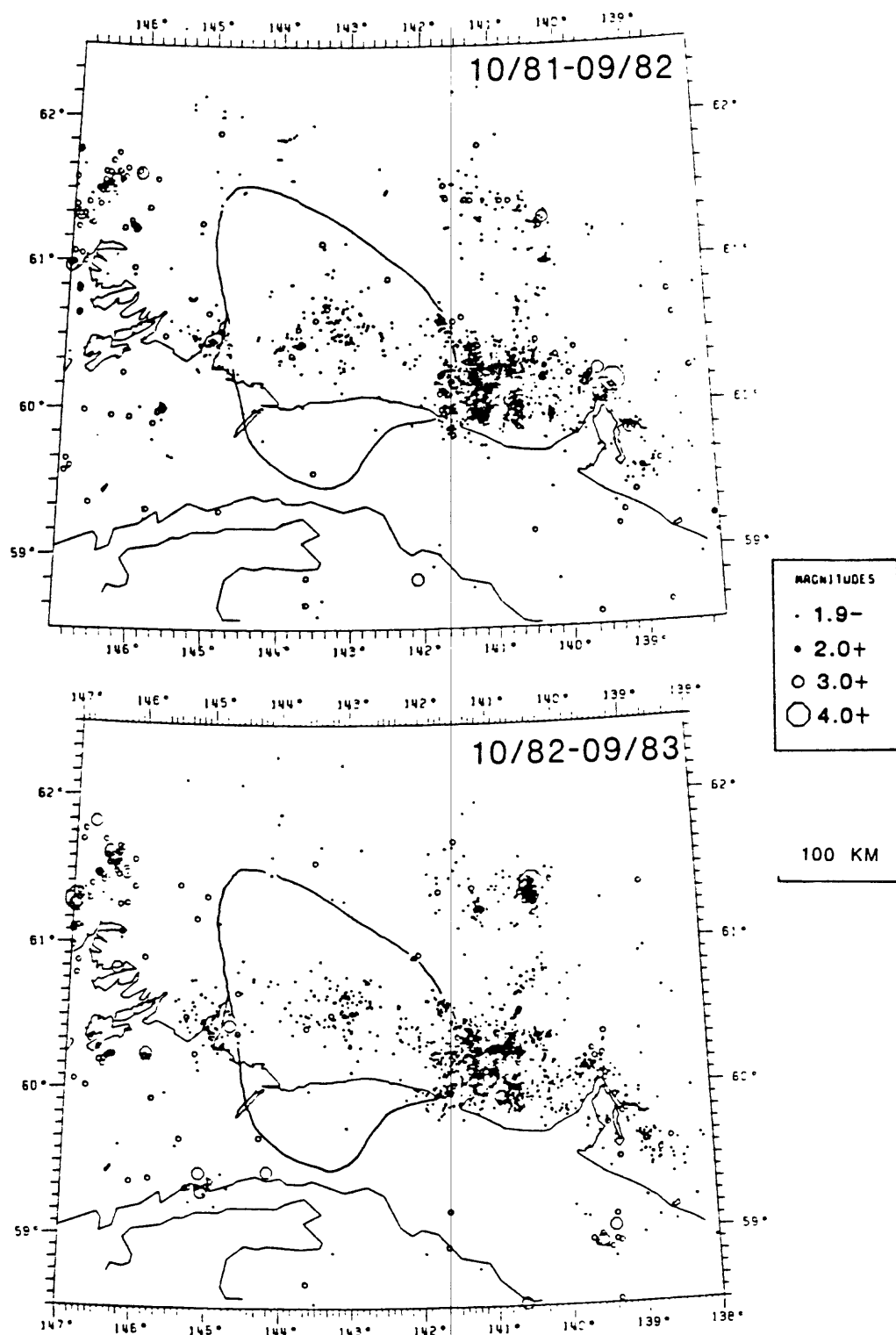
Fig. 8. Epicenters of earthquakes located with data from the regional
seismograph network for 1981-82 and 1982-83. Symbols as in Fig. 6.
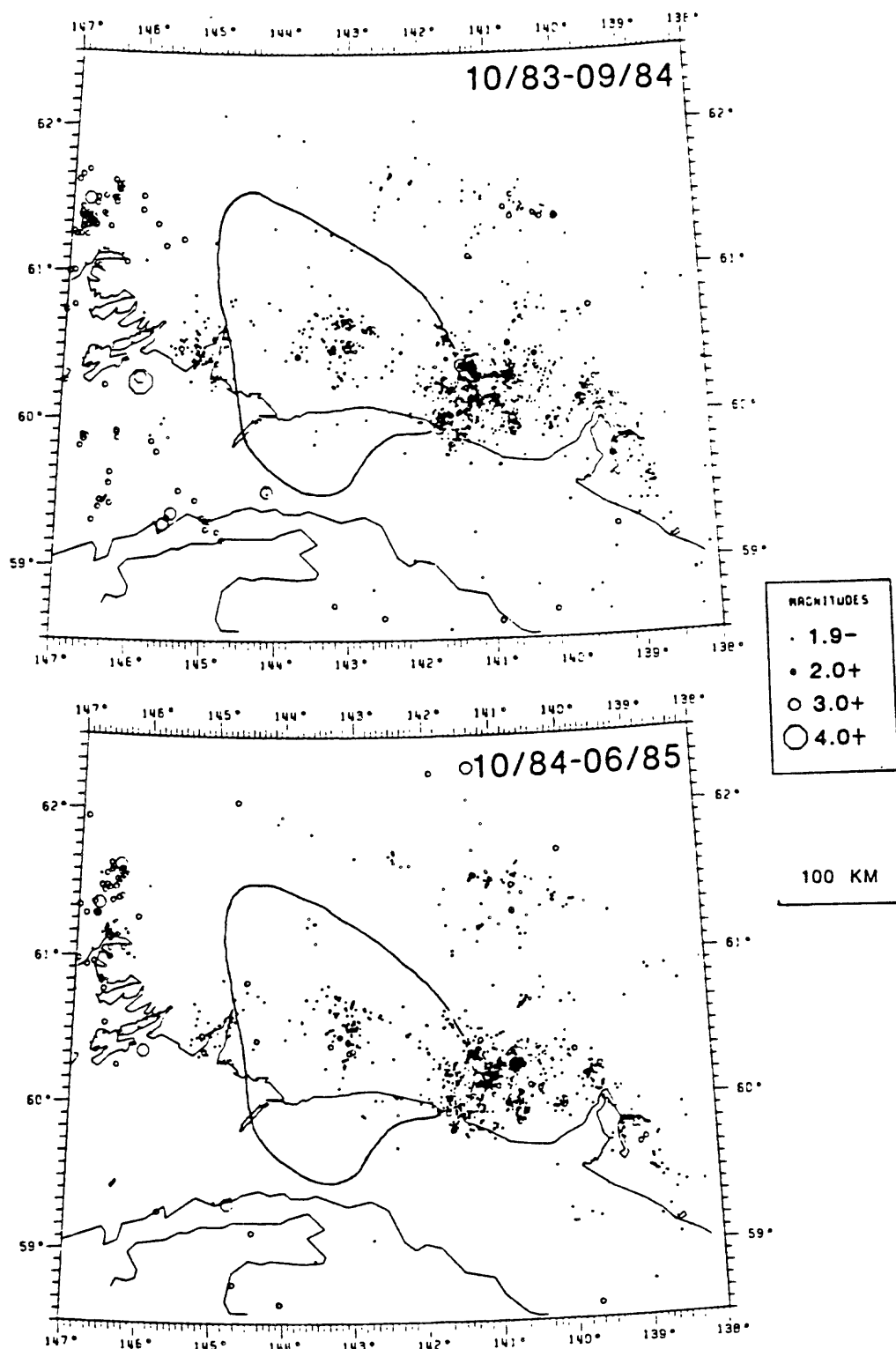
Fig. 9. Epicenters of earthquakes located with data from the regional seismograph network for 1983-84 and 1984-85. Symbols as in Fig. 6. Note last interval includes only 9 months.
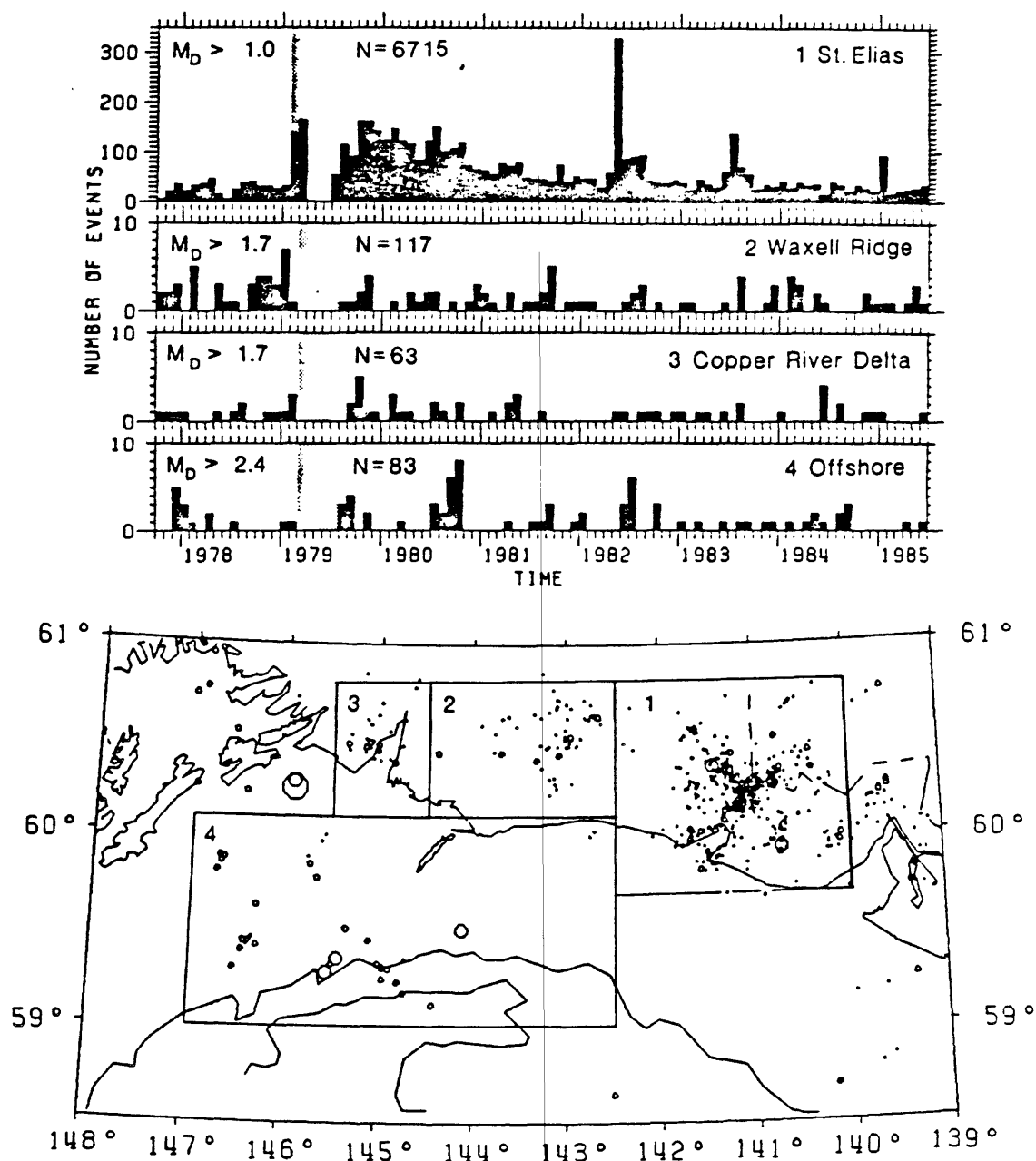
Fig. 10. Histograms of the monthly (30.4-day intervals) number of earthquakes (top) for selected areas in and around the Yakataga seismic gap (bottom). For each area, the magnitude threshold for completeness was inferred from cumulative distributions of coda magnitude; only events larger than the threshold magnitudes (M_D) are included. N, total number of events plotted. Shaded area indicates time for which the data have not been completely processed. Map (bottom) shows epicenters of earthquakes of coda magnitude 1.1 and larger that occurred in 1984.

APPENDIX B. 1.

Magnitudes and Movements of Duration

W. H. Bakun

Reprinted from the bulletin of the Seismological Society of America,
Vol. 74, No. 6, with permission of the Seismological Society of America

MAGNITUDES AND MOMENTS OF DURATION

By William H. Bakun

Abstract

Coda-duration τ at 42 of the stations in the U.S. Geological Survey's central California seismic network (CALNET) for earthquakes in five source regions of central California—the Parkfield and San Juan Bautista sections of the San Andreas fault, the Sargent fault, the Coyote Lake section of the Calaveras fault, and the Livermore area—are used to obtain empirical formulas relating local magnitude M_L and seismic moment M_0 to τ and epicentral distance Δ. Models with $\log^2 \tau$ fit the data better than those assuming a $\log \tau$ dependence. For 55 earthquakes with $1.1 \leq M_L \leq 5.3$, $M_L = 0.92 + 0.607(\pm 0.005)\log^2 \tau + 0.00268(\pm 0.00012)\Delta$. These M_L assume a Wood-Anderson seismograph magnification of 2800; 0.15 should be subtracted from these M_L for continuity with magnitudes obtained from or calibrated against typical (magnification ~ 2000) Wood-Anderson seismographs. For 53 earthquakes with $18.4 \leq \log M_0 \leq 22.3$, $\log M_0 = 17.97 + 0.719(\pm 0.0007)\log^2 \tau + 0.00319(\pm 0.00013)\Delta$. These relations provide unbiased estimates of M_L for $1.5 \leq M_L \leq 5.3$ and $19 \leq \log M_0 \leq 22.3$. Station corrections can significantly improve the accuracy and precision of M_L and $\log M_0$ estimates, particularly if τ from a small number of stations are used. Regional variations in station corrections reflect an increase in coda duration toward the south within the CALNET.

Introduction

Many seismic networks now use the coda duration as an estimate of earthquake size (Lee and Stewart, 1981). Magnitude or seismic moment are estimated from durations using empirical formulas derived for the particular region and network instrumentation. While the dependence of duration on tectonic environment and crustal structure is not established, it is clear that the duration formulas change with seismograph response (Bakun and Lindh, 1977). Given the widespread deployment of the instrumentation developed for the U.S. Geological Survey's (USGS) central California seismic network (CALNET), the coda-duration magnitude M_D formula of Lee et al. (1972) for the CALNET has been used extensively. Considering the availability of more numerous and better quality data, a reexamination of the duration magnitude formulation is in order.

Although magnitude is more common, the seismic moment M_0 is a more useful measure of earthquake size since M_0 is defined in terms of the parameters of the dislocation model (Aki, 1966). Empirical formulas (e.g., Thatcher and Hanks, 1973) relating $\log M_0$ and magnitude often are used to estimate M_0 from magnitude. Estimating M_0 directly from the duration measurements is a preferable approach. Consequently, formulas are developed to estimate M_L and $\log M_0$ from the duration measurements.

Lee et al. (1972) defined the coda-length duration τ to be the time from the P arrival to that time in the seismic coda when the largest amplitude as seen on develocorder film through a GEOTECH model 6585 film viewer (20X magnification) is less than 1 cm. They obtained the empirical relation $M_D = -0.87 + 2.00 \log \tau + 0.0035\Delta$, where M_D is an estimate of M_L and Δ the epicentral distance in kilometers. They used an average duration $\bar{\tau}$ calculated from the signal duration measured on all possible USGS central California seismic network (CALNET) stations and the

corresponding average epicentral distance $\bar{\Delta}$. Lee *et al.* (1972) is the point of departure for this paper. I adopt their definition of τ, but consider individual τ and Δ rather than averages of these parameters.

DATA

Fifty-five earthquakes (Table 1), seven from the Parkfield section of the San Andreas fault, thirteen from the San Juan Bautista section of the San Andreas fault, twelve from the Sargent fault, nine from the Coyote Lake section of the Calaveras fault, and fourteen from near Livermore, were selected from Bakun (1984). M_L are taken from Bakun and Joyner (1984) except for events 8, 32, 47, and 50; M_L for these four shocks were calculated using the $-\log A_0$ and the station corrections of Bakun and Joyner (1984). Log M_0 were estimated using long-period P- and S-wave spectra obtained from CALNET seismograms (Bakun, 1984); moments for events 8 and 50 which saturated the CALNET were not used in this study.

An attempt was made to read the duration for each earthquake at the same 42 arbitrarily selected CALNET stations (see Table 2 and Figure 1) using the prescription of Lee *et al.* (1972). Amplifier attenuation settings for these stations ranged from 6 dB, at the highest gain stations, to 36 dB at Parkhill, the lowest gain one-component (vertical) CALNET seismograph. The gain at several stations changed during the 1977–1981 time interval spanning the earthquakes used. A total of 1414 durations, 61 per cent of a possible 2310 readings, were obtained. For some of the smallest events, e.g., 4, 43, 53, and 54, only a few durations at the closest of the 42 stations could be measured. For several of these events, durations were measured for 90 per cent of the 42 stations. At least 15 duration measurements are available at each of the 42 stations.

ANALYSIS

Aki (1969) noted that the shape of the coda spectrum at a given time, measured from the origin time, is roughly independent of source size, a result expected for frequencies low enough so that the source can be regarded as a point. Although the amplitudes of body waves depend on radiation pattern, the seismic coda does not appear to be sensitive to source-to-receiver geometry, even for earthquakes characterized by unilateral rupture expansion (e.g., see Figure 2 of Bakun *et al.*, 1978). If an earthquake can be regarded as a point source and the source-to-receiver geometry ignored, then the earthquake source can be represented by a single scalar quantity in the analysis of the coda. That is, the coda is the response of the crust-seismograph system to a scalar input. The goal here is to quantify the scalar, M_L or log M_0, in terms of the duration of the coda. Following Lee *et al.* (1972), I used stepwise linear regression analysis (Draper and Smith, 1966) with independent variables $f(\tau)$ and Δ. Adding focal depth as a third independent variable does not result in significant improvements in the fits.

The M_D obtained by the USGS for central California earthquakes using $f(\tau) = \log \tau$ (Lee *et al.*, 1972) are smaller than M_L for $M \gtrsim 3\frac{1}{4}$ (Bakun, 1984). Nonlinear functions $f(\tau) = \log^2 \tau$ and $f(\tau) = \log^3 \tau$ as well as $f(\tau) = \log \tau$ were considered to correct this $M_D - M_L$ discrepancy. The $\log^3 \tau$ formulas overcorrected and hence will not be discussed further. The formulas obtained assuming a $\log^2 \tau$ dependence are preferred, consistent with the results of Real and Teng (1973) and Bakun and Lindh (1977).

TABLE 1

EARTHQUAKE SOURCE PARAMETERS*

Event No.	Date (yr mn-dy)	Origin Time (UTC)	Location† Latitude (°N)	Location† Longitude (°W)	Depth (km)	Local Magnitude (M_L)‡	Seismic Moment log M_0 (dyne cm)‡
1	79-10-04	1801-10.8	35°47.8′	120°20.8′	9.8	2.49 ± 0.04 (4)	19.786 ± 0.036 (11)
2	79-10-04	1805-13.5	35°48.0′	120°20.7′	9.8	2.52 ± 0.03 (4)	19.791 ± 0.044 (16)
3	79-12-03	2105-43.4	35°47.8′	120°20.2′	10.8	1.95 ± 0.06 (4)	19.072 ± 0.040 (13)
4	80-04-21	1935-55.3	35°57.7′	120°31.7′	11.8	1.12 ± 0.03 (5)	18.628 ± 0.040 (16)
5	80-05-19	0303-15.0	35°57.9′	120°32.0′	11.8	3.48 ± 0.05 (16)	21.122 ± 0.012 (14)
6	80-06-12	0927-58.0	35°57.8′	120°32.0′	12.0	2.71 ± 0.04 (4)	20.127 ± 0.118 (11)
7	81-01-17	0009-36.2	35°56.6′	120°29.5′	11.9	3.46 ± 0.08 (9)	21.254 ± 0.017 (6)
8	80-04-13	0615-56.3	36°46.8′	121°31.0′	6.5	4.89 ± 0.02 (4)	--
9	80-04-13	0620-40.1	36°47.7′	121°31.9′	5.7	3.25 ± 0.03 (23)	20.669 ± 0.038 (28)
10	80-04-13	1518-14.9	36°47.7′	121°32.0′	6.4	2.47 ± 0.04 (9)	20.013 ± 0.036 (18)
11	80-04-13	2151-25.1	36°47.7′	121°32.3′	6.4	2.81 ± 0.03 (17)	20.350 ± 0.023 (18)
12	80-04-13	2308-44.3	36°46.1′	121°30.2′	6.7	3.31 ± 0.04 (15)	20.928 ± 0.025 (14)
13	80-04-19	1245-50.8	36°48.2′	121°32.9′	6.5	3.05 ± 0.06 (18)	20.645 ± 0.039 (28)
14	80-04-28	1821-25.3	36°47.8′	121°32.9′	6.7	3.40 ± 0.03 (22)	20.882 ± 0.029 (27)
15	80-05-10	2230-38.4	36°50.1′	121°35.5′	5.9	2.78 ± 0.05 (15)	20.338 ± 0.033 (22)
16	80-06-18	0452-26.5	36°53.9′	121°38.2′	5.3	3.86 ± 0.11 (11)	21.768 ± 0.071 (8)
17	81-01-27	2210-53.8	36°50.7′	121°37.0′	3.9	3.91 ± 0.07 (13)	21.650 ± 0.082 (8)
18	81-05-23	0026-07.0	36°51.8′	121°38.0′	7.7	1.93 ± 0.04 (15)	19.314 ± 0.042 (12)
19	81-05-23	1622-35.3	36°52.1′	121°38.2′	8.4	1.55 ± 0.05 (11)	18.825 ± 0.038 (23)
20	81-06-12	0016-48.8	36°51.6′	121°37.1′	5.5	2.21 ± 0.03 (16)	19.742 ± 0.039 (30)
21	78-09-21	0318-56.9	36°59.4′	121°41.1′	4.5	3.11 ± 0.05 (12)	20.476 ± 0.050 (15)
22	79-01-11	1957-25.8	37°00.7′	121°44.1′	13.9	3.31 ± 0.03 (21)	20.762 ± 0.046 (28)
23	79-02-18	0138-28.6	36°57.0′	121°35.1′	5.7	2.85 ± 0.08 (11)	20.268 ± 0.050 (19)
24	79-09-14	0104-08.6	36°58.4′	121°38.9′	0.8	3.34 ± 0.06 (16)	20.388 ± 0.064 (32)
25	79-11-14	0613-13.7	36°57.2′	121°36.2′	1.7	2.59 ± 0.15 (4)	19.796 ± 0.039 (27)
26	80-06-13	0956-42.2	36°59.5′	121°43.7′	7.5	2.77 ± 0.05 (9)	20.072 ± 0.047 (27)
27	81-05-27	1526-17.4	36°56.8′	121°34.8′	8.5	2.18 ± 0.06 (16)	19.534 ± 0.050 (19)
28	81-06-03	1451-41.8	36°57.5′	121°39.6′	6.3	2.45 ± 0.03 (16)	19.882 ± 0.036 (25)
29	81-06-03	1504-03.4	36°57.5′	121°39.6′	6.0	2.17 ± 0.06 (19)	19.509 ± 0.042 (24)
30	81-06-06	0731-19.3	36°58.1′	121°39.1′	3.4	1.52 ± 0.06 (4)	18.992 ± 0.041 (23)
31	81-06-06	1540-05.3	36°57.8′	121°39.2′	3.9	1.26 ± 0.10 (2)	18.666 ± 0.052 (13)
32	81-11-20	0652-04.7	36°55.6′	121°32.5′	8.2	2.00 ± 0.03 (6)	19.330 ± 0.060 (13)
33	79-08-07	0155-12.8	37°02.3′	121°30.1′	9.4	2.37 ± 0.09 (6)	19.341 ± 0.058 (9)
34	79-08-07	0232-31.1	36°58.9′	121°28.7′	9.4	3.16 ± 0.04 (11)	20.433 ± 0.033 (11)
35	79-08-07	0525-56.7	37°01.1′	121°30.3′	5.4	1.74 ± 0.05 (2)	18.875 ± 0.056 (8)
36	79-08-07	0556-51.2	37°03.8′	121°30.3′	8.8	3.09 ± 0.04 (11)	20.358 ± 0.054 (11)
37	79-08-07	0731-09.6	36°58.9′	121°29.2′	8.3	2.71 ± 0.08 (8)	19.789 ± 0.042 (11)
38	79-08-09	1249-27.3	36°58.4′	121°28.9′	6.5	3.51 ± 0.04 (18)	20.887 ± 0.025 (14)
39	79-08-10	0025-20.5	37°01.6′	121°29.0′	9.3	3.69 ± 0.03 (16)	21.120 ± 0.042 (12)
40	79-08-19	0206-55.4	37°02.2′	121°30.0′	5.4	1.85 ± 0.11 (8)	19.122 ± 0.035 (24)
41	79-08-19	0442-02.8	37°00.5′	121°29.1′	7.1	1.45 ± 0.08 (8)	18.740 ± 0.032 (26)
42	77-06-21	0243-06.5	37°38.2′	121°40.0′	10.5	4.61 ± 0.02 (5)	22.289 ± 0.151 (3)
43	77-06-22	1614-22.7	37°37.7′	121°40.6′	8.4	2.01 ± 0.21 (3)	19.037 ± 0.080 (5)
44	77-06-23	1936-25.1	37°38.4′	121°40.4′	9.4	2.53 ± 0.08 (4)	19.634 ± 0.034 (8)
45	80-01-25	0314-00.9	37°50.2′	121°47.6′	3.2	2.72 ± 0.08 (8)	19.982 ± 0.084 (6)
46	80-01-25	0521-47.7	37°51.0′	121°47.0′	4.3	3.42 ± 0.05 (13)	20.953 ± 0.106 (9)
47	80-01-25	0524-36.6	37°51.1′	121°47.7′	5.0	4.24 ± 0.17 (9)	22.257 ± 0.122 (8)
48	80-01-25	0529-45.2	37°50.7′	121°48.0′	3.1	3.57 ± 0.08 (11)	20.896 ± 0.081 (10)
49	80-01-25	0629-15.4	37°50.7′	121°47.0′	5.8	3.14 ± 0.09 (7)	20.571 ± 0.073 (6)
50	80-01-27	0233-36.2	37°45.0′	121°42.8′	10.2	5.31 ± 0.20 (4)	—
51	81-03-25	1658-16.4	37°33.2′	121°41.4′	1.6	3.04 ± 0.10 (15)	20.360 ± 0.063 (20)
52	81-04-11	2347-10.4	37°46.9′	121°44.1′	12.6	3.58 ± 0.03 (15)	20.818 ± 0.096 (13)
53	81-05-28	0013-15.6	37°33.5′	121°40.5′	4.1	1.22 ± 0.12 (4)	18.380 ± 0.104 (7)
54	81-05-30	1422-19.9	37°50.4′	121°47.6′	15.0	1.56 ± 0.02 (2)	18.660 ± 0.094 (6)
55	81-05-30	1817-28.2	37°50.8′	121°47.6′	15.0	2.24 ± 0.29 (2)	19.554 ± 0.047 (13)

* Taken from Tables 1 to 5 of Bakun (1984).

† Events 1 to 7 from Parkfield, 8 to 20 from San Juan Bautista, 21 to 32 from Sargent fault, 33 to 41 from Coyote Lake, and 42 to 55 from Livermore source regions.

‡ Uncertainty in M_L and log M_0 = standard deviation of the mean. Number of records in parentheses. No M_0 estimates from CALNET data available for 8 and 50. M_L taken from Bakun and Joyner (1984) except for 8, 32, 47, and 50, where M_l was calculated using the results of Bakun and Joyner (1984).

TABLE 2

STATION CORRECTIONS $\delta(\dot{M}_L)_{STA}$ AND $\delta(\log \dot{M}_0)_{STA}$

Event No.	Code (Name)	Latitude (°N)	Longitude (°W)	Amplifier Attenuation (dB)	$\delta\dot{M}_{L,STA}$*	$\delta M_{L,STA}$†	$\delta\log\dot{M}_{0,STA}$†
1	BAV (Antelope Valley)	36°38.75'	121°01.79'	6	−0.17 ± 0.03 (44)	−0.16 ± 0.03 (44)	−0.21 ± 0.04 (41)
2	BBN (San Benito)	36°30.60'	121°04.53'	6	−0.32 ± 0.09 (26)	−0.29 ± 0.09 (26)	−0.38 ± 0.11 (26)
3	BMC (McPhails Peak)	36°39.40'	121°21.92'	6 and 18	−0.08 ± 0.03 (44)	−0.07 ± 0.04 (44)	−0.11 ± 0.03 (42)
4	BMH (Mt. Harlan)	36°41.18'	121°24.80'	6	−0.02 ± 0.04 (41)	−0.02 ± 0.04 (41)	−0.03 ± 0.03 (40)
5	BPI (Pinnacles)	36°29.40'	121°10.11'	6	−0.08 ± 0.04 (18)	−0.08 ± 0.05 (18)	−0.19 ± 0.04 (18)
6	BRV (Little Rabbit Valley)	36°25.49'	121°01.10'	6 and 18	−0.18 ± 0.08 (15)	−0.17 ± 0.08 (15)	−0.34 ± 0.10 (15)
7	BSG (Shirt Tail Gulch)	36°24.83'	121°15.22'	12 and 18	0.26 ± 0.04 (39)	0.27 ± 0.04 (39)	0.30 ± 0.05 (37)
8	BSR (Salinas Radio Site)	36°39.99'	121°31.12'	12	−0.04 ± 0.03 (46)	−0.02 ± 0.03 (46)	−0.03 ± 0.03 (45)
9	CAC (Antioch)	37°58.75'	121°45.62'	18 and 24	0.23 ± 0.04 (19)	0.22 ± 0.04 (19)	0.23 ± 0.04 (17)
10	CAL (Calaveras Reservoir)	37°27.07'	121°47.95'	6	−0.08 ± 0.02 (37)	−0.08 ± 0.02 (37)	−0.10 ± 0.03 (37)
11	CAO (Arnold Ranch)	37°20.96'	121°31.96'	6	−0.10 ± 0.03 (43)	−0.12 ± 0.02 (43)	−0.14 ± 0.03 (42)
12	CBW (Brookwood Reservoir)	37°55.45'	122°06.40'	18 and 24	0.13 ± 0.04 (29)	0.14 ± 0.04 (29)	0.13 ± 0.04 (27)
13	CDO (Doolan Road)	37°43.80'	121°50.12'	18 and 24	−0.05 ± 0.05 (35)	−0.03 ± 0.04 (35)	−0.09 ± 0.04 (33)
14	CMC (Mills College)	37°46.88'	122°10.55'	24	0.45 ± 0.04 (23)	0.47 ± 0.04 (23)	0.52 ± 0.04 (21)
15	CMO (Morgan Territory)	37°48.68'	121°48.15'	18	0.29 ± 0.04 (26)	0.28 ± 0.03 (26)	0.30 ± 0.05 (25)
16	CMR (Mines Road)	37°35.68'	121°38.22'	6 and 12	0.24 ± 0.06 (22)	0.27 ± 0.06 (22)	0.27 ± 0.04 (21)
17	CPL (Palomares Road)	37°37.88'	121°57.37'	18	0.34 ± 0.03 (38)	0.33 ± 0.03 (38)	0.37 ± 0.04 (36)
18	CSH (Cal State Hayward)	37°38.88'	121°02.75'	18	0.37 ± 0.04 (40)	0.35 ± 0.04 (40)	0.40 ± 0.05 (38)
19	HAZ (Anzar)	36°53.08'	121°35.45'	12	−0.04 ± 0.04 (40)	−0.04 ± 0.04 (40)	−0.05 ± 0.03 (39)
20	HCA (Canada Road)	37°01.52'	121°29.02'	12	−0.04 ± 0.02 (41)	−0.03 ± 0.02 (41)	−0.02 ± 0.03 (40)
21	HDL (Dillon Ranch)	36°50.12'	121°38.64'	12	−0.07 ± 0.04 (36)	−0.05 ± 0.04 (36)	−0.08 ± 0.03 (35)
22	HFH (Flint Hills)	36°53.29'	121°28.13'	18	−0.38 ± 0.07 (32)	−0.35 ± 0.07 (32)	−0.42 ± 0.08 (31)
23	HGW (Gilroy West)	37°01.02'	121°39.20'	12	0.24 ± 0.03 (44)	0.22 ± 0.03 (44)	0.26 ± 0.03 (42)

	Station				$\delta(M_L)_{STA}$ *	$\delta(M_l)_{STA}$ †	$\delta(\log M_0)_{STA}$ ‡
24	HJG (San Juan Grade)	36°47.88'	121°34.43'	12	0.12 ± 0.03 (42)	0.11 ± 0.03 (42)	0.12 ± 0.02 (40)
25	HJS (John Smith Road)	36°48.99'	121°17.92'	12	-0.12 ± 0.05 (36)	-0.09 ± 0.04 (36)	-0.14 ± 0.05 (35)
26	HOR (O'Connell Ranch)	36°55.03'	121°30.46'	18	-0.39 ± 0.04 (38)	-0.35 ± 0.04 (38)	-0.41 ± 0.04 (38)
27	HPH (Parkhill)	36°51.38'	121°24.37'	24, 30, and 36	0.01 ± 0.07 (27)	0.00 ± 0.07 (27)	0.02 ± 0.07 (25)
28	HPL (Pacheco Lake)	37°03.13'	121°17.40'	18	0.46 ± 0.06 (39)	0.41 ± 0.06 (39)	0.47 ± 0.07 (37)
29	HQR (Quien Sabe Road)	36°50.02'	121°12.76'	12	0.02 ± 0.03 (43)	0.02 ± 0.03 (43)	0.00 ± 0.04 (41)
30	JAL (Almaden)	37°09.50'	121°50.82'	18	0.31 ± 0.03 (44)	0.30 ± 0.04 (44)	0.35 ± 0.03 (42)
31	JBL (Camp Ben Lomond)	37°07.69'	121°10.08'	18	0.44 ± 0.04 (40)	0.43 ± 0.03 (40)	0.50 ± 0.04 (38)
32	JSF (Stanford Telescope)	37°24.31'	121°10.55'	24	0.25 ± 0.03 (34)	0.26 ± 0.03 (34)	0.30 ± 0.03 (32)
33	NHM (Hamilton Ranch)	38°09.28'	121°48.02'	18	-0.07 ± 0.06 (21)	-0.05 ± 0.05 (21)	-0.10 ± 0.06 (21)
34	PHC (Hearst Castle)	35°40.93'	121°09.15'	6 and 12	-0.28 ± 0.05 (27)	-0.27 ± 0.05 (27)	-0.37 ± 0.07 (25)
35	PIV (Indian Valley)	35°54.39'	121°40.94'	12, 18, and 24	-0.40 ± 0.06 (25)	-0.38 ± 0.06 (25)	-0.52 ± 0.08 (25)
36	PJL (Jolon Road)	36°05.39'	121°09.33'	6 and 12	-0.28 ± 0.03 (36)	-0.28 ± 0.03 (36)	-0.32 ± 0.03 (35)
37	PLO (Lone Oak Road)	36°14.79'	121°02.55'	18	-0.14 ± 0.05 (35)	-0.12 ± 0.04 (35)	-0.19 ± 0.05 (33)
38	PMG (Santa Margarita)	35°25.79'	120°31.22'	6 and 12	-0.10 ± 0.04 (26)	-0.08 ± 0.04 (26)	-0.12 ± 0.06 (25)
39	PPT (Peach Tree Valley)	36°06.50'	120°43.27'	12 and 18	-0.02 ± 0.05 (34)	-0.02 ± 0.05 (34)	-0.03 ± 0.06 (32)
40	PSM (Smith Mountain)	36°04.18'	120°35.68'	12	-0.15 ± 0.04 (31)	-0.15 ± 0.04 (31)	-0.18 ± 0.05 (29)
41	PTY (Taylor Ranch)	36°56.73'	120°28.45'	12	-0.11 ± 0.03 (32)	-0.10 ± 0.03 (32)	-0.15 ± 0.04 (30)
42	PWK (Work Ranch)	35°48.87'	120°30.67'	12 and 18	-0.36 ± 0.04 (26)	-0.32 ± 0.04 (26)	-0.42 ± 0.05 (26)

Uncertainty = standard deviation of the mean using the number of duration measurements in parentheses.

* $\delta(M_L)_{STA}$ using $M_L = -0.89 + 2.147 \log \tau + 0.00254 \Delta$.

† $\delta(M_l)_{STA}$ using $M_l = 0.92 + 0.607 \log^2 \tau + 0.00268 \Delta$.

‡ $\delta(\log M_0)_{STA}$ using $\log M_0 = 17.97 + 0.719 \log^2 \tau + 0.00319 \Delta$.

The regression analysis procedures were implemented in the following steps

1. Let $y = M_L$ or $\log M_0$ from Table 1.
2. Let $f(\tau) = [\log \tau]^n = \log^n \tau$, $n = 1$ or 2.
3. Apply regression analysis assuming $y = b_0 + b_1 f(\tau) + b_2 \Delta$.
4. Calculate station corrections $\delta(\hat{y})_{STA}$ = the average of $(y - \hat{y})$ for each of the 42 stations, using the b_0, b_1, and b_2 from step 3 to calculate the predicted value $\hat{y}$. [$\delta(\hat{y})_{STA}$ are listed in Table 2.]
5. Apply regression analysis assuming $y^* = y - \delta(\hat{y})_{STA} = a_0 + a_1 f(\tau) + a_2 \Delta$.
6. Calculate source region corrections $\delta(\hat{y})_{SOU}$ = the average $(y^* - \hat{y})$ for each of the five source regions, using the a_0, a_1, and a_2 from step 5 to calculate the predicted value $\hat{y}$. [$\delta(\hat{y})_{SOU}$ are listed in Table 3.]
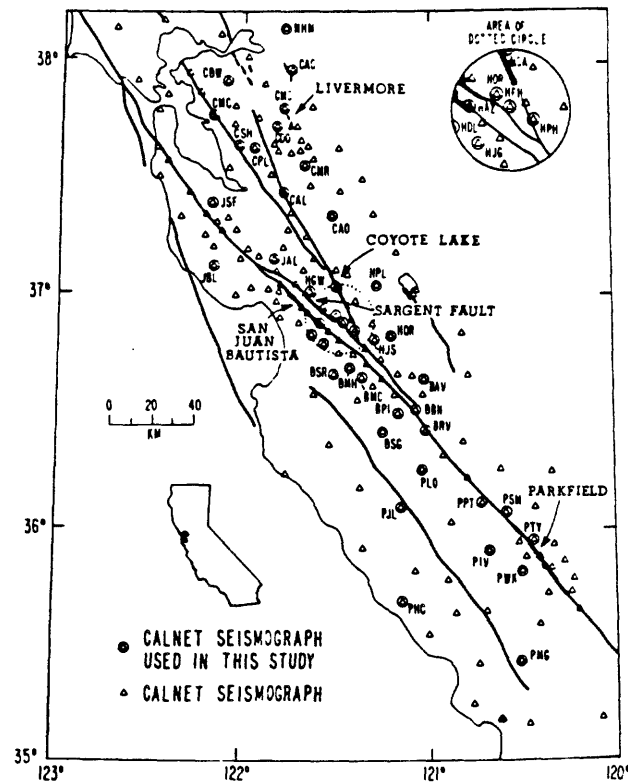
FIG. 1. Source areas (hatchured) and CALNET seismographs in central California.

The resulting regression relations are of the form, e.g.,

$$\hat{M}_L{}^{i,j} = a_0 + a_1 \log^2 \tau + a_2 \Delta + \delta(\hat{M}_L)_{STA_i} + \delta(\hat{M}_L)_{SOU_j},$$

where $\hat{M}_L{}^{i,j}$ is the estimate of local magnitude obtained using τ from station i for an earthquake in the source region j. The average of all available $\hat{M}_L{}^{i,j}$, is $\hat{M}_L$, the estimate of M_L for the earthquake. Ignoring the source region correction and the station correction result in progressively worse estimates, as discussed below. The superscripts i and j are omitted in the remainder of this paper wherever the meaning is clear.

MAGNITUDES AND MOMENTS OF DURATION

$M_L = f(\log \tau, \Delta)$. In order to illustrate the necessity of adopting $f(\tau) = \log^2 \tau$, I start by considering the $M_L = f(\log \tau, \Delta)$ form of Lee et al. (1972). With the appropriate station corrections given in Table 2,

$$M_L = -0.89 + 2.147(\pm 0.0019)\log \tau + 0.00254(\pm 0.00012)\Delta + \delta(\hat{M}_L)_{STA},$$

accounting for 91.1 per cent of the variance about the regression. $\hat{M}_L$ at $M_L \gtrsim 4$ are less than M_L (Table 4 and Figure 2). $\hat{M}_L$ is smaller than M_L for $\tau \gtrsim 175$ sec (see Figure 3), consistent with the systematic underestimates of M_L using the $M_D \sim \log \tau$ relation of Lee et al. (1972). As shown below, the discrepancy at $\tau \gtrsim 175$ sec disappears when $f(\tau) = \log^2 \tau$ is used.

$M_L = f(\log^2 \tau, \Delta)$. Using the appropriate station corrections in Table 2,

$$\hat{M}_L = 0.92 + 0.607(\pm 0.005)\log^2 \tau + 0.00268(\pm 0.00012)\Delta + \delta(\hat{M}_L)_{STA}, \qquad (1)$$

accounting for 91.5 per cent of the variance about the regression. For this relation, $\hat{M}_L$ are satisfactory for $1\frac{1}{2} \leq M_L \leq 5\frac{1}{4}$ (see Table 5 and Figures 4 and 5a). There is no apparent systematic error in the M_L estimates with τ (Figure 5b) or with Δ (Figure 5c). $\hat{M}_L$ has a positive bias for $M_L \leq 1\frac{1}{2}$ (Figures 4 and 5a).

$\log M_0 = f(\log^2 \tau, \Delta)$. Using the appropriate station corrections in Table 2,

$$\log \hat{M}_0 = 17.97 + 0.719(\pm 0.007)\log^2 \tau$$
$$+ 0.00319(\pm 0.00013)\Delta + \delta(\log \hat{M}_0)_{STA}, \qquad (2)$$

accounting for 90.8 per cent of the variance about the regression. In contrast to M_L, incorporating source region corrections significantly decreases the errors in the log M_0 estimates (see Figure 6 and Table 6). Although there are no obvious systematic trends in the residuals with τ or Δ (see Figure 7), the residuals tend to be positive for log $M_0 \leq 19$.

TABLE 3
SOURCE REGION CORRECTIONS*

Source Region	$\delta(\hat{M}_L)_{SOU}$[†]	$\delta(\hat{M}_L)_{SOU}$[‡]	$\delta(\log \hat{M}_0)_{SOU}$[§]
Parkfield	0.04 ± 0.02 (129)	0.05 ± 0.02 (129)	0.17 ± 0.02 (129)
San Juan Bautista	−0.04 ± 0.01 (379)	−0.02 ± 0.01 (379)	0.09 ± 0.02 (354)
Sargent Fault	−0.04 ± 0.02 (324)	−0.02 ± 0.02 (324)	−0.05 ± 0.01 (324)
Coyote Lake	−0.01 ± 0.01 (267)	−0.01 ± 0.01 (267)	−0.14 ± 0.01 (267)
Livermore	0.07 ± 0.01 (315)	0.04 ± 0.01 (315)	0.00 ± 0.01 (285)

* Uncertainties are standard deviations of the mean using the number of τ mesurements in parentheses.

[†] $\delta(\hat{M}_L)_{SOU}$ using $\hat{M}_L = -0.89 + 2.147\log \tau + 0.00254\Delta + \delta(\hat{M}_L)_{STA}$.

[‡] $\delta(\hat{M}_L)_{SOU}$ using $\hat{M}_L = 0.92 + 0.607\log^2 \tau + 0.00268\Delta + \delta(\hat{M}_L)_{STA}$.

[§] $\delta(\log \hat{M}_0)_{SOU}$ using $\log \hat{M}_0 = 17.97 + 0.719\log^2 \tau + 0.00319\Delta + \delta(\log \hat{M}_0)_{STA}$.

STATION CORRECTIONS

Station corrections can be viewed as systematic errors in the prediction of the duration of the seismic coda under the assumptions that propagation-path effects

WILLIAM H. BAKUN

can be represented by a single independent variable, Δ, and that the seismic source can be represented by another single variable, M_L or log M_0. Given the arguments already presented for representing the source by a single scalar, the station corrections represent additional propagation-path (and seismograph) effects. This as-
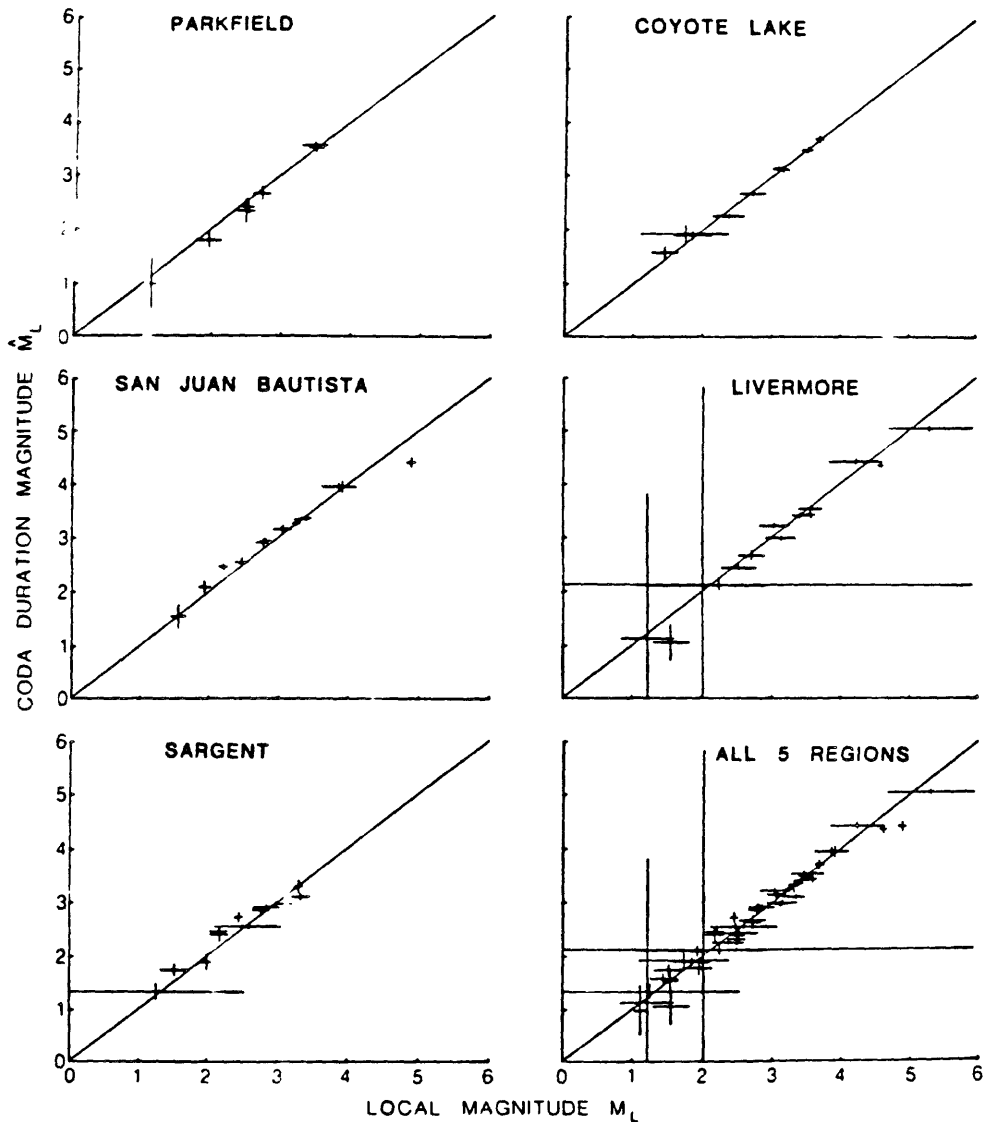
FIG. 2. coda-duration magnitude $\hat{M}_L$ using $\hat{M}_L = -0.89 + 2.147$ log $\tau + 0.00254\Delta + \delta(\hat{M}_L)_{STA}$ versus local magnitude M_L. Error bars are $\pm$ the 95 per cent confidence interval. Large error bars generally reflect a small number (2 or 3) of τ available to estimate M_L.

sumption—that the station corrections do not result from an inadequate representation of the seismic source—is implicit in the analysis that follows.

Stations corrections (see Table 2) are nearly identical for the three regression relationships discussed in the preceding section. Although in the following I refer

MAGNITUDES AND MOMENTS OF DURATION

TABLE 4

Coda-Duration Magnitude $\hat{M}_L$ Using $\hat{M}_L = -0.89 + 2.147 \log \tau + 0.00254\Delta$

Event No.	No. of τ	No Station or Source Corrections		Using Station Corrections		Using Station and Source Corrections	
		$\hat{M}_L$*	$M_L - \hat{M}_L$	$\hat{M}_L$*	$M_L - \hat{M}_L$	$\hat{M}_L$*	$M_L - \hat{M}_L$
1	13	2.44 ± 0.09	0.05	2.32 ± 0.10	0.17	2.36 ± 0.10	0.13
2	13	2.49 ± 0.05	0.03	2.39 ± 0.06	0.13	2.44 ± 0.06	0.08
3	11	1.95 ± 0.06	0.00	1.79 ± 0.06	0.16	1.83 ± 0.06	0.12
4	4	1.14 ± 0.19	−0.02	0.99 ± 0.15	0.13	1.03 ± 0.15	0.09
5	31	3.49 ± 0.04	−0.01	3.49 ± 0.04	−0.01	3.54 ± 0.04	−0.06
6	25	2.74 ± 0.08	−0.03	2.63 ± 0.06	0.08	2.68 ± 0.06	0.03
7	32	3.51 ± 0.05	−0.05	3.53 ± 0.03	−0.07	3.58 ± 0.03	−0.12
8	25	4.28 ± 0.04	0.61	4.40 ± 0.04	0.49	4.37 ± 0.04	0.52
9	38	3.24 ± 0.04	0.01	3.25 ± 0.02	0.00	3.21 ± 0.02	0.04
10	36	2.54 ± 0.05	−0.07	2.54 ± 0.04	−0.07	2.50 ± 0.04	−0.03
11	32	2.93 ± 0.05	−0.12	2.92 ± 0.02	−0.11	2.89 ± 0.02	−0.08
12	32	3.31 ± 0.04	0.00	3.33 ± 0.01	−0.02	3.29 ± 0.01	0.02
13	39	3.13 ± 0.05	−0.08	3.15 ± 0.03	−0.10	3.11 ± 0.03	−0.06
14	29	3.33 ± 0.05	0.07	3.36 ± 0.02	0.04	3.32 ± 0.02	0.08
15	35	2.89 ± 0.04	−0.11	2.90 ± 0.03	−0.12	2.87 ± 0.03	−0.09
16	38	3.91 ± 0.03	−0.05	3.94 ± 0.03	−0.08	3.90 ± 0.03	−0.04
17	12	3.65 ± 0.04	0.26	3.94 ± 0.05	−0.03	3.90 ± 0.05	0.01
18	24	2.05 ± 0.07	−0.12	2.09 ± 0.05	−0.16	2.05 ± 0.05	−0.12
19	11	1.53 ± 0.12	0.02	1.55 ± 0.10	0.00	1.51 ± 0.10	0.04
20	28	2.44 ± 0.06	−0.23	2.46 ± 0.03	−0.25	2.42 ± 0.03	−0.21
21	31	2.90 ± 0.04	0.21	2.97 ± 0.03	0.14	2.93 ± 0.03	0.18
22	28	3.29 ± 0.07	0.02	3.30 ± 0.06	0.01	3.26 ± 0.06	0.05
23	36	2.91 ± 0.06	−0.06	2.91 ± 0.03	−0.06	2.87 ± 0.03	−0.02
24	36	3.10 ± 0.05	0.24	3.10 ± 0.03	0.24	3.06 ± 0.03	0.28
25	33	2.57 ± 0.06	0.02	2.55 ± 0.02	0.04	2.51 ± 0.02	0.08
26	36	2.84 ± 0.06	−0.07	2.86 ± 0.03	−0.09	2.82 ± 0.03	−0.05
27	24	2.39 ± 0.07	−0.21	2.41 ± 0.07	−0.23	2.37 ± 0.07	−0.19
28	30	2.70 ± 0.06	−0.25	2.72 ± 0.05	−0.27	2.68 ± 0.05	−0.23
29	27	2.42 ± 0.07	−0.25	2.46 ± 0.04	−0.29	2.42 ± 0.04	−0.25
30	13	1.79 ± 0.07	−0.27	1.75 ± 0.05	−0.23	1.71 ± 0.05	−0.19
31	11	1.35 ± 0.08	−0.09	1.34 ± 0.06	−0.08	1.30 ± 0.06	−0.04
32	19	1.85 ± 0.10	0.15	1.89 ± 0.07	0.11	1.85 ± 0.07	0.15
33	27	2.23 ± 0.05	0.14	2.25 ± 0.02	0.12	2.25 ± 0.02	0.12
34	34	3.09 ± 0.06	0.07	3.12 ± 0.03	0.04	3.11 ± 0.03	0.05
35	18	1.98 ± 0.09	−0.24	1.93 ± 0.07	−0.19	1.92 ± 0.07	−0.18
36	39	3.15 ± 0.04	−0.06	3.14 ± 0.02	−0.05	3.13 ± 0.02	−0.04
37	37	2.66 ± 0.05	0.05	2.67 ± 0.03	0.04	2.66 ± 0.03	0.05
38	35	3.46 ± 0.04	0.05	3.49 ± 0.03	0.02	3.48 ± 0.03	0.03
39	33	3.73 ± 0.04	−0.04	3.70 ± 0.04	−0.01	3.69 ± 0.04	0.00
40	24	1.93 ± 0.07	−0.08	1.90 ± 0.04	−0.05	1.90 ± 0.04	−0.05
41	20	1.62 ± 0.09	−0.17	1.59 ± 0.05	−0.14	1.58 ± 0.05	−0.13
42	32	4.32 ± 0.05	0.29	4.35 ± 0.04	0.26	4.42 ± 0.04	0.19
43	2	2.14 ± 0.23	−0.13	2.11 ± 0.29	−0.10	2.18 ± 0.29	−0.17
44	24	2.37 ± 0.06	0.16	2.44 ± 0.03	0.09	2.51 ± 0.03	0.02
45	24	2.60 ± 0.07	0.12	2.67 ± 0.04	0.05	2.74 ± 0.04	−0.02
46	35	3.40 ± 0.06	0.02	3.41 ± 0.03	0.01	3.48 ± 0.03	−0.06
47	29	4.37 ± 0.04	0.13	4.41 ± 0.03	−0.17	4.49 ± 0.03	−0.25
48	34	3.53 ± 0.06	0.04	3.54 ± 0.02	0.03	3.61 ± 0.02	−0.04
49	29	2.96 ± 0.06	0.18	2.99 ± 0.03	0.15	3.06 ± 0.03	0.08
50	30	4.98 ± 0.04	0.33	5.04 ± 0.03	0.27	5.11 ± 0.03	0.20
51	35	3.21 ± 0.05	−0.17	3.22 ± 0.03	−0.18	3.29 ± 0.03	−0.25
52	27	3.46 ± 0.06	0.12	3.42 ± 0.03	0.16	3.49 ± 0.03	0.09
53	2	1.22 ± 0.22	0.00	1.14 ± 0.21	0.08	1.21 ± 0.21	0.01
54	3	1.00 ± 0.16	0.56	1.06 ± 0.08	0.50	1.13 ± 0.08	0.43
55	9	1.99 ± 0.09	0.25	2.13 ± 0.05	0.11	2.20 ± 0.05	0.04
Average (±)		0.070		0.050		0.050	
rms ($M_L - \hat{M}_L$)			0.18		0.16		0.15
rms $(M_L - \hat{M}_L)$†			0.34		0.24		0.24

* $\hat{M}_L$ is the mean of the estimates of M_l obtained using the number of durations (no. of τ) availabl Uncertainty is the standard deviation of the mean.

† rms error in $\hat{M}_L$ over the 1414 duration measurements (5 earthquakes).

exclusively to the station corrections corresponding to equation (1), analogous, if not identical, comments and results apply to the other two sets of station corrections. Scatter in the residuals at four representative stations is shown in Figure 8. (Note that the station corrections were used in these calculations so that the residuals shown in figure 8 have zero average.) The amount of scatter is not obviously correlated with either the station amplification, the size of the station correction, or time.

In using a 1-cm threshold irrespective of station amplification, Lee *et al.* (1972) assumed that τ does not depend critically on station amplification. Although there is no obvious change in the residuals when amplification changes at a station (e.g., see Figure 8), the station corrections are weakly correlated with station amplification
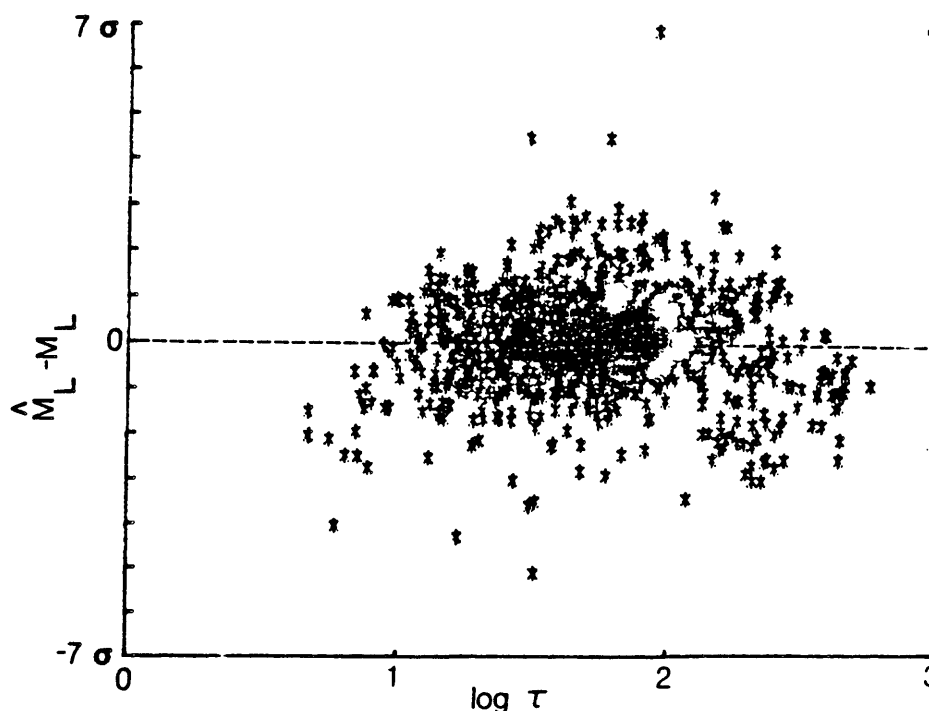
FIG. 3. Standardized residuals ($\sigma = 0.24$ M_L units) versus coda-duration τ for $\hat{M}_L = -0.89 + 2.117$ $\log \tau + 0.00254\Delta + \delta(M_L)_{STA}$.

(Figure 9). Figure 9 illustrates the not surprising result that lower gain stations tend to have shorter coda durations than high-gain stations.

The station corrections, with and without the seismograph amplification correlation removed, are plotted at the station locations in Figure 10. A negative (positive) station correction means consistently longer (shorter) than anticipated coda durations. There appears to be a regional trend, with station corrections increasing to the northwest. More specifically, the station corrections are negative in the Coast Ranges near Parkfield, mixed at sites on or near the sedimentary wedge (Hollister trough) between the San Andreas and Calaveras faults, and generally positive at the northern stations. The coda is composed of seismic waves backscattered by inhomogeneities within the crust and upper mantle (e.g., Aki, 1969). Thus, the regional differences in station corrections shown in Figure 10 imply a systematic

TABLE 5

Coda-Duration Magnitude $\hat{M}_L$ Using $\hat{M}_L = 0.92 + 0.607 \log^2 + 0.00268\Delta$

Event No	No. of r	No Station or Source Corrections		Using Station Corrections		Using Station and Source Corrections	
		$\hat{M}_L^*$	$M_L - \hat{M}_L$	$\hat{M}_L^*$	$M_L - \hat{M}_L$	$\hat{M}_L^*$	$M_L - \hat{M}_L$
1	13	2.44 ± 0.08	0.05	2.32 ± 0.09	0.17	2.37 ± 0.09	0.12
2	13	2.47 ± 0.05	0.05	2.38 ± 0.06	0.14	2.43 ± 0.06	0.09
3	11	2.04 ± 0.05	−0.09	1.89 ± 0.05	0.06	1.94 ± 0.05	0.01
4	4	1.51 ± 0.10	−0.39	1.37 ± 0.08	−0.25	1.42 ± 0.08	−0.30
5	31	3.44 ± 0.04	0.04	3.45 ± 0.04	0.03	3.50 ± 0.04	−0.02
6	25	2.71 ± 0.06	0.00	2.62 ± 0.05	0.09	2.67 ± 0.05	0.04
7	32	3.47 ± 0.05	−0.01	3.49 ± 0.03	−0.03	3.54 ± 0.03	−0.08
8	25	4.39 ± 0.05	0.50	4.51 ± 0.05	0.38	4.49 ± 0.05	0.40
9	38	3.17 ± 0.04	0.08	3.19 ± 0.02	0.06	3.17 ± 0.02	0.08
10	36	2.52 ± 0.04	−0.05	2.52 ± 0.03	−0.05	2.50 ± 0.03	−0.03
11	32	2.87 ± 0.04	−0.06	2.87 ± 0.02	−0.06	2.84 ± 0.02	−0.03
12	32	3.25 ± 0.05	0.06	3.27 ± 0.01	0.04	3.25 ± 0.01	0.06
13	39	3.07 ± 0.05	−0.02	3.09 ± 0.04	−0.04	3.07 ± 0.04	−0.02
14	29	3.27 ± 0.05	0.13	3.30 ± 0.02	0.10	3.28 ± 0.02	0.12
15	35	2.83 ± 0.04	−0.05	2.85 ± 0.03	−0.07	2.82 ± 0.03	−0.04
16	38	3.93 ± 0.04	−0.07	3.96 ± 0.03	−0.10	3.94 ± 0.03	−0.08
17	12	3.61 ± 0.05	0.30	3.90 ± 0.05	0.01	3.88 ± 0.05	0.03
18	24	2.11 ± 0.05	−0.18	2.15 ± 0.04	−0.22	2.12 ± 0.04	−0.19
19	11	1.75 ± 0.09	−0.20	1.77 ± 0.07	−0.22	1.75 ± 0.07	−0.20
20	28	2.43 ± 0.05	−0.22	2.45 ± 0.03	−0.24	2.42 ± 0.03	−0.21
21	31	2.84 ± 0.04	0.27	2.91 ± 0.02	0.20	2.89 ± 0.02	0.22
22	28	3.23 ± 0.07	0.08	3.25 ± 0.06	0.06	3.22 ± 0.06	0.09
23	36	2.84 ± 0.05	0.01	2.85 ± 0.03	0.00	2.83 ± 0.03	0.02
24	36	3.03 ± 0.05	0.31	3.04 ± 0.03	0.30	3.01 ± 0.03	0.33
25	33	2.54 ± 0.05	0.05	2.53 ± 0.02	0.06	2.51 ± 0.02	0.08
26	36	2.78 ± 0.05	−0.01	2.81 ± 0.03	−0.04	2.79 ± 0.03	−0.02
27	24	2.38 ± 0.06	−0.20	2.40 ± 0.06	−0.22	2.38 ± 0.06	−0.20
28	30	2.66 ± 0.06	−0.21	2.68 ± 0.04	−0.23	2.66 ± 0.04	−0.21
29	27	2.41 ± 0.06	−0.24	2.45 ± 0.03	−0.28	2.43 ± 0.03	−0.26
30	13	1.90 ± 0.05	−0.38	1.86 ± 0.04	−0.34	1.84 ± 0.04	−0.32
31	11	1.62 ± 0.05	−0.36	1.61 ± 0.05	−0.35	1.59 ± 0.05	−0.33
32	19	1.98 ± 0.07	0.02	2.01 ± 0.05	−0.01	1.99 ± 0.05	0.01
33	27	2.25 ± 0.04	0.12	2.27 ± 0.02	0.10	2.26 ± 0.02	0.11
34	34	3.03 ± 0.06	0.13	3.06 ± 0.03	0.10	3.05 ± 0.03	0.11
35	18	2.05 ± 0.07	−0.31	2.00 ± 0.05	−0.26	2.00 ± 0.05	−0.26
36	39	3.08 ± 0.04	0.01	3.08 ± 0.02	0.01	3.07 ± 0.02	0.02
37	37	2.62 ± 0.05	0.09	2.63 ± 0.02	0.08	2.63 ± 0.02	0.08
38	35	3.40 ± 0.05	0.11	3.44 ± 0.03	0.07	3.43 ± 0.03	0.08
39	33	3.71 ± 0.05	−0.02	3.69 ± 0.04	0.00	3.68 ± 0.04	0.01
40	24	2.02 ± 0.05	−0.17	1.99 ± 0.03	−0.14	1.99 ± 0.03	−0.14
41	20	1.80 ± 0.06	−0.35	1.77 ± 0.03	−0.32	1.77 ± 0.03	−0.32
42	32	4.43 ± 0.06	0.18	4.46 ± 0.04	0.15	4.50 ± 0.04	0.11
43	2	2.18 ± 0.20	−0.17	2.13 ± 0.27	−0.12	2.17 ± 0.27	−0.16
44	24	2.37 ± 0.05	0.16	2.43 ± 0.03	0.10	2.47 ± 0.03	0.06
45	24	2.58 ± 0.06	0.14	2.64 ± 0.03	0.08	2.68 ± 0.03	0.04
46	35	3.34 ± 0.06	0.08	3.35 ± 0.03	0.07	3.39 ± 0.03	0.03
47	29	4.48 ± 0.05	−0.24	4.53 ± 0.03	−0.29	4.57 ± 0.03	−0.33
48	34	3.49 ± 0.06	0.08	3.50 ± 0.03	0.07	3.53 ± 0.03	0.04
49	29	2.90 ± 0.06	0.24	2.94 ± 0.03	0.20	2.97 ± 0.03	0.17
50	30	5.34 ± 0.04	−0.03	5.40 ± 0.03	−0.09	5.43 ± 0.03	−0.12
51	35	3.15 ± 0.06	−0.11	3.16 ± 0.03	−0.12	3.20 ± 0.03	−0.16
52	27	3.41 ± 0.06	0.17	3.37 ± 0.04	0.21	3.41 ± 0.04	0.17
53	2	1.54 ± 0.13	−0.32	1.45 ± 0.11	−0.23	1.48 ± 0.11	−0.26
54	3	1.42 ± 0.09	0.14	1.48 ± 0.06	0.08	1.52 ± 0.06	0.04
55	9	2.05 ± 0.07	0.19	2.18 ± 0.03	0.06	2.22 ± 0.03	0.02
Average (±)		0.059		0.043		0.043	
rms ($M_L - \hat{M}_L$)			0.19		0.17		0.17
rms ($M_L - \hat{M}_L$)†			0.33		0.24		0.23

* $\hat{M}_L$ is the mean of the estimate of M_L obtained using the number of durations (no. of r) available. Uncertainty is the standard deviation of the mean.

† rms error in $\hat{M}_L$ over the 1414 duration measurements (55 earthquakes).

difference in the distribution of backscatterers in central California. The two stations HOR and HFH, with unusually long coda durations in relation to their amplificati)n (Figure 9), are located on the Hollister trough within 1 km of the San Andreas, Sargent, Calaveras, and Busch faults, intuitively the most likely place for extended c()das due to multiply reflected, trapped radiation. Fur her discussion here
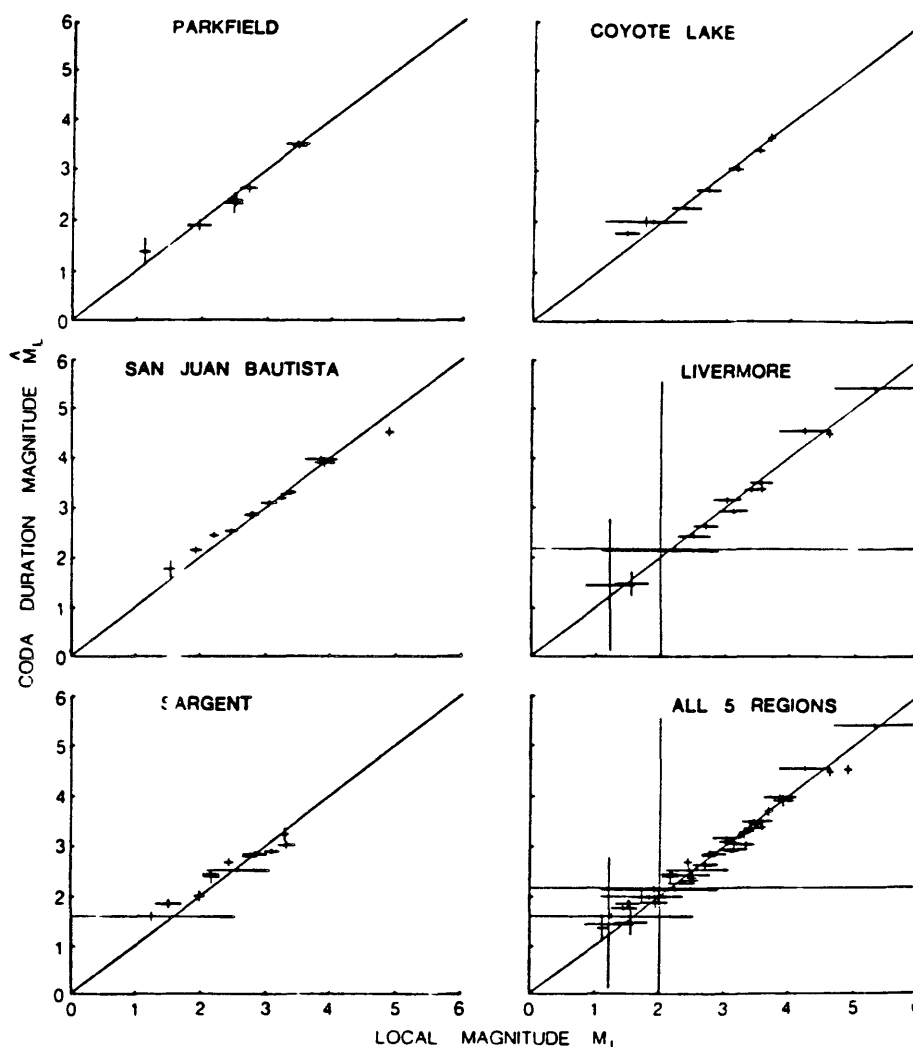
FIG. 4. Coda-duration magnitude $\tilde{M}_L$ using $\tilde{M}_L = 0.92 + 0.607 \log^2 \tau + 0.00268\Delta + \delta(\tilde{M}_L)_{STA}$ versus local magnitude M_L. See caption for Figure 2.

of the spatial pattern of station corrections is not justified; expansion of the station correction set to the entire CALNET should provide the data sufficient to support a detailed analysis.

SOURCE REGION CORRECTIONS

The source region corrections in Table 3 are the residuals *after* the station corrections in Table 2 have been applied. This analysis procedure— ising station
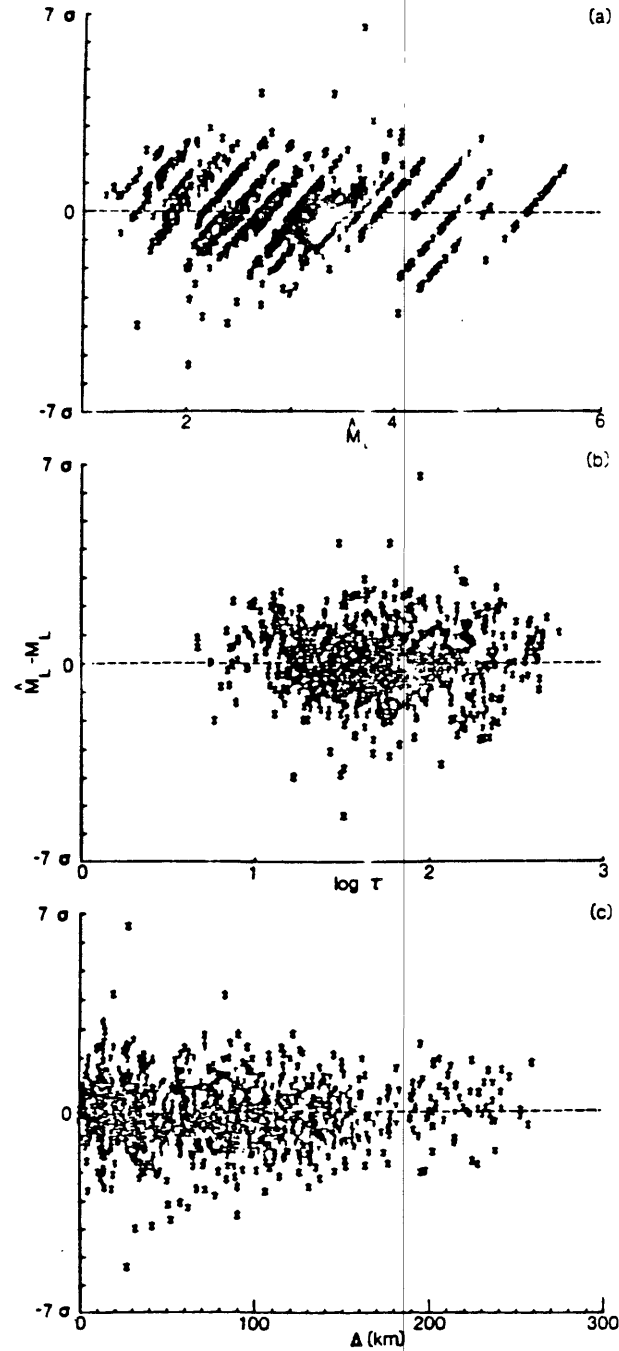
FIG. 5. Standardized residuals (σ = 0.24) versus (a) $\hat{M}_L$, (b) log τ, and (c) Δ for $\hat{M}_L$ = 0.92 + 0.607 log$^2 \tau$ + 0.00268Δ + $\delta(M_L)_{STA}$. 95.3 per cent of the residuals are $\leqq 2\sigma$.

corrections as the first-order adjustment and source region corrections as second-order, rather than determining joint station and source-region corrections—was selected for operational considerations. Station corrections are well defined and easy to use. In contrast, some epicenters will always be outside or between the

defined source regions so that which, if any, source region corrections are appropriate is often an arbitrary decision.

The source region corrections are not obviously consistent with the station corrections in the sense that negative station corrections were obtained for sites near Parkfield which has a positive source region correction. The "second-order" nature of the source region corrections complicates their interpretation. Although the station corrections were determined using sources from all of the five regions, it seems reasonable to expect that the nearby source regions, from which more numerous durations are generally available, are heavily weighted in the station
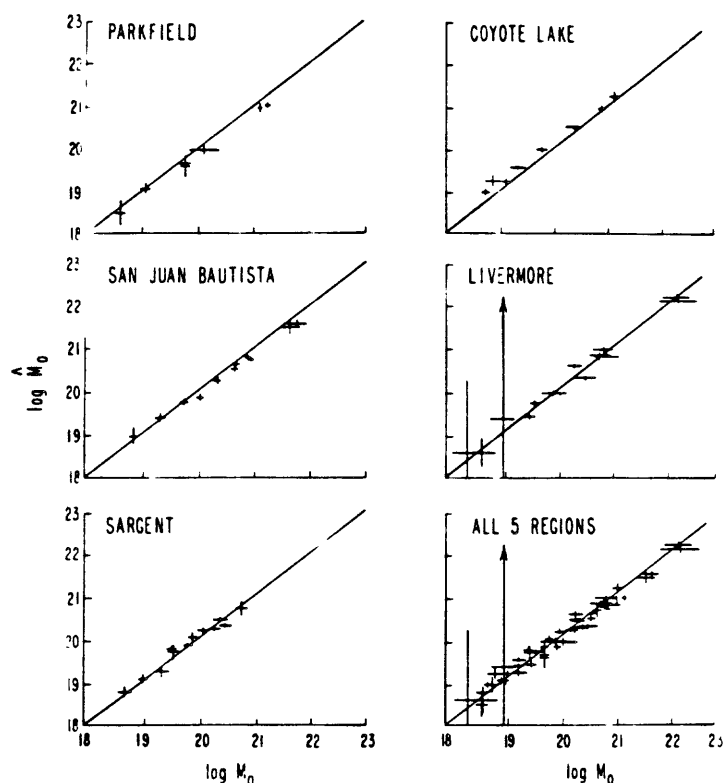
FIG. 6. Coda-duration seismic moment log $\hat{M}_0$ using log $\hat{M}_0 = 17.97 + 0.719 \log^2 \tau + 0.00319\Delta + \delta(\log M_0)_{STA}$ versus log M_0. See caption for Figure 2.

corrections. If this is the case, the residuals, i.e., the source region corrections, may not be a measure of backscattering local to the source regions but a complicated function of scattering over the entire network.

The size of the source region corrections generally is smaller than that of the station corrections, consistent with the use of the source region corrections as second-order adjustments. While the station corrections for the magnitude and moment relationships are consistent, the source region corrections are not. Also, the reduction in error in estimating log M_0 with source region corrections is considerably greater than that obtained in estimating M_L with source region corrections.

TABLE 6

CODA-DURATION MOMENTS LOG $\hat{M}_0$ USING LOG $\hat{M}_0$ = 17.97 + 0.719 LOG^2 τ + 0.00319Δ

Event No	No. of τ	No Station or Source Corrections		Using Station Corrections		Using Station and Source Corrections	
		log $\hat{M}_0$*	log M_0 −log $\hat{M}_0$	log $\hat{M}_0$*	log M_0 −log $\hat{M}_0$	log $\hat{M}_0$*	log M_0 −log $\hat{M}_0$
1	13	19.77 ± 0.09	0.02	19.60 ± 0.11	0.19	19.77 ± 0.11	0.02
2	13	19.80 ± 0.05	−0.01	19.66 ± 0.07	0.13	19.83 ± 0.07	−0.04
3	11	19.30 ± 0.06	−0.23	19.07 ± 0.06	0.00	19.24 ± 0.06	−0.17
4	4	18.67 ± 0.11	0.05	18.48 ± 0.10	0.14	18.65 ± 0.10	−0.03
5	31	20.96 ± 0.05	0.16	20.95 ± 0.05	0.16	21.12 ± 0.05	−0.01
6	25	20.10 ± 0.07	0.03	19.97 ± 0.06	0.16	20.14 ± 0.06	−0.01
7	32	20.99 ± 0.06	0.26	21.00 ± 0.03	0.25	21.17 ± 0.03	0.08
9	38	20.64 ± 0.05	0.03	20.64 ± 0.03	0.03	20.73 ± 0.03	−0.06
10	36	19.86 ± 0.05	0.15	19.85 ± 0.04	0.17	19.94 ± 0.04	0.08
11	32	20.28 ± 0.05	0.07	20.26 ± 0.02	0.09	20.35 ± 0.02	0.00
12	32	20.73 ± 0.05	0.20	20.74 ± 0.02	0.19	20.83 ± 0.02	0.10
13	39	20.51 ± 0.06	0.13	20.52 ± 0.04	0.13	20.61 ± 0.04	0.04
14	29	20.75 ± 0.06	0.13	20.78 ± 0.02	0.11	20.87 ± 0.02	0.02
15	35	20.23 ± 0.05	0.11	20.24 ± 0.04	0.10	20.33 ± 0.04	0.01
16	38	21.54 ± 0.05	0.23	21.56 ± 0.04	0.21	21.65 ± 0.04	0.12
17	12	21.16 ± 0.06	0.49	21.48 ± 0.06	0.17	21.57 ± 0.06	0.08
18	24	19.38 ± 0.06	−0.07	19.41 ± 0.04	−0.10	19.50 ± 0.04	−0.19
19	11	18.96 ± 0.11	−0.13	18.97 ± 0.09	−0.15	19.06 ± 0.09	−0.24
20	28	19.76 ± 0.06	−0.01	19.76 ± 0.03	−0.02	19.85 ± 0.03	−0.11
21	31	20.24 ± 0.05	0.24	20.31 ± 0.03	0.17	20.26 ± 0.03	0.22
22	28	20.70 ± 0.09	0.06	20.70 ± 0.07	0.06	20.65 ± 0.07	0.11
23	36	20.25 ± 0.06	0.02	20.24 ± 0.03	0.03	20.19 ± 0.03	0.08
24	36	20.47 ± 0.06	−0.08	20.45 ± 0.04	−0.06	20.40 ± 0.04	−0.01
25	33	19.90 ± 0.06	−0.10	19.85 ± 0.02	−0.06	19.80 ± 0.02	−0.01
26	36	20.18 ± 0.07	−0.11	20.19 ± 0.03	−0.12	20.14 ± 0.03	−0.07
27	24	19.70 ± 0.08	−0.16	19.71 ± 0.07	−0.18	19.66 ± 0.07	−0.13
28	30	20.03 ± 0.07	−0.14	20.04 ± 0.05	−0.16	19.99 ± 0.05	−0.11
29	27	19.73 ± 0.07	−0.22	19.77 ± 0.04	−0.26	19.72 ± 0.04	−0.21
30	13	19.13 ± 0.06	−0.14	19.08 ± 0.05	−0.09	19.03 ± 0.05	−0.04
31	11	18.80 ± 0.06	−0.13	18.78 ± 0.05	−0.12	18.73 ± 0.05	−0.07
32	19	19.22 ± 0.08	0.11	19.25 ± 0.06	0.08	19.20 ± 0.06	0.13
33	27	19.54 ± 0.05	−0.20	19.54 ± 0.02	−0.20	19.40 ± 0.02	−0.06
34	34	20.47 ± 0.07	−0.03	20.47 ± 0.03	−0.04	20.33 ± 0.03	0.10
35	18	19.31 ± 0.08	−0.43	19.23 ± 0.07	−0.36	19.09 ± 0.07	−0.22
36	39	20.53 ± 0.05	−0.17	20.50 ± 0.02	−0.14	20.36 ± 0.02	0.00
37	37	19.99 ± 0.05	−0.20	19.98 ± 0.03	−0.19	19.84 ± 0.03	−0.05
38	35	20.91 ± 0.06	−0.03	20.93 ± 0.04	−0.04	20.79 ± 0.04	0.10
39	33	21.28 ± 0.06	−0.16	21.22 ± 0.05	−0.10	21.08 ± 0.05	0.04
40	24	19.27 ± 0.06	−0.15	19.22 ± 0.03	−0.10	19.08 ± 0.03	0.04
41	20	19.02 ± 0.07	−0.28	18.97 ± 0.03	−0.23	18.83 ± 0.03	−0.09
42	32	22.13 ± 0.07	0.16	22.14 ± 0.05	0.15	22.14 ± 0.05	0.15
43	2	19.46 ± 0.24	−0.43	19.40 ± 0.31	−0.36	19.40 ± 0.31	−0.36
44	24	19.69 ± 0.06	−0.05	19.75 ± 0.03	−0.11	19.75 ± 0.03	−0.11
45	24	19.93 ± 0.07	0.05	19.99 ± 0.04	−0.01	19.99 ± 0.04	−0.01
46	35	20.84 ± 0.07	0.11	20.84 ± 0.04	0.12	20.84 ± 0.04	0.12
47	29	22.19 ± 0.06	0.07	22.23 ± 0.04	0.02	22.23 ± 0.04	0.02
48	34	21.01 ± 0.07	−0.12	21.00 ± 0.03	−0.11	21.00 ± 0.03	−0.11
49	29	20.32 ± 0.07	0.25	20.34 ± 0.03	0.23	20.34 ± 0.03	0.23
51	35	20.61 ± 0.07	−0.25	20.61 ± 0.03	−0.25	20.61 ± 0.03	−0.25
52	27	20.92 ± 0.07	−0.10	20.86 ± 0.04	−0.04	20.86 ± 0.04	−0.04
53	2	18.71 ± 0.15	−0.33	18.59 ± 0.13	−0.21	18.59 ± 0.13	−0.21
54	3	18.57 ± 0.11	0.09	18.60 ± 0.08	0.06	18.60 ± 0.08	0.06
55	9	19.31 ± 0.08	0.25	19.44 ± 0.03	0.11	19.44 ± 0.03	0.11
Average (±)		0.071		0.050		0.050	
rms (log M_0 − log $\hat{M}_0$)			0.18		0.16		0.12
rms (log M_0 − log $\hat{M}_0{}^\omega$)†			0.37		0.26		0.24

* log $\hat{M}_0$ is the mean of the estimates of log M_0 obtained using the number of durations (no. of τ) available. Uncertainty is the standard deviation of the mean.

† rms error in log $\hat{M}_0$ over the 1359 duration measurements (53 earthquakes).
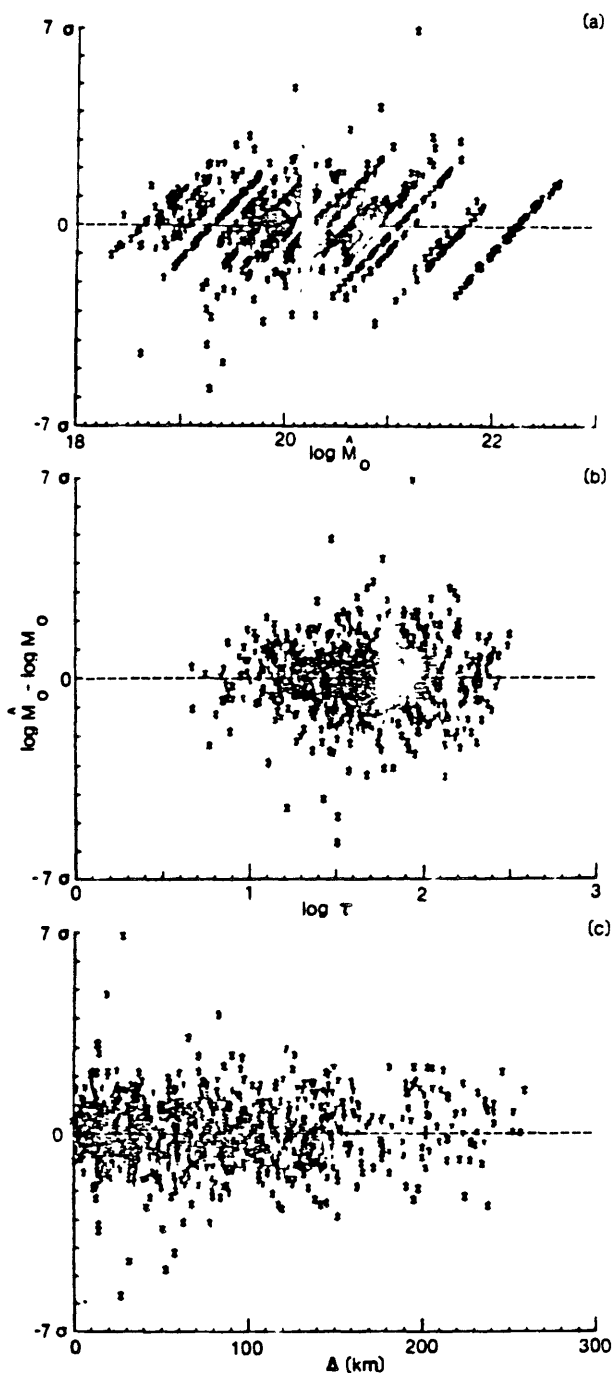
FIG. 7. Standardized residuals ($\sigma = 0.26$) versus (a) log $\hat{M}_0$, (b) log τ, and (c) Δ for log $\hat{M}_0 = 17.97 +$ 0.719 log$^2 \tau + 0.00319\Delta + \delta(\log M_0)_{STA}$. 95.4 per cent of the residuals are $\leq 2\sigma$.

DISCUSSION

This paper presents a strictly empirical study. Although equations (1) and (2) satisfy the available data, they are not based on any physics of the seismic coda. Intuitively important parameters, such as focal depth, are not accounted for. Also,

MAGNITUDES AND MOMENTS OF DURATION
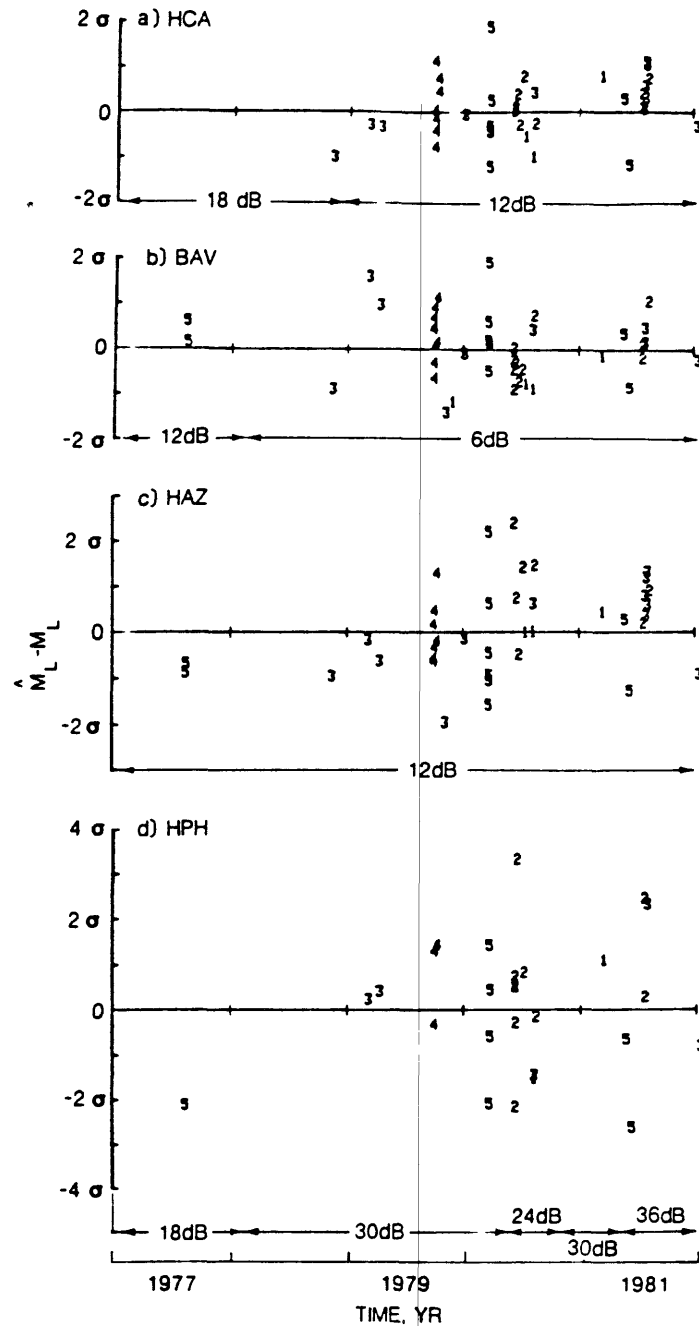
FIG. 6. Standardized residuals ($\sigma = 0.24$) for stations (a) HCA, (b) BAV, (c) HAZ, and (d) HPH using $M_l = 0.92 + 0.607 \log^2 \tau + 0.00268\Delta + \delta(M_L)_{STA}$ versus origin time. Symbols refer to the source region of the earthquake: 1, Parkfield; 2, San Juan Bautista; 3 Sargent fault; 4, Coyote Lake; and 5, Livermore. Decibel (dB) numbers are the amplifier attenuator settings.

convenient assumptions, such as additive station and source region corrections independent of earthquake size, distance, etc., may not be justified. Clearly more and better data and a comprehensive theory of the generation of the seismic coda might dictate coda-duration relationships different from those presented here.
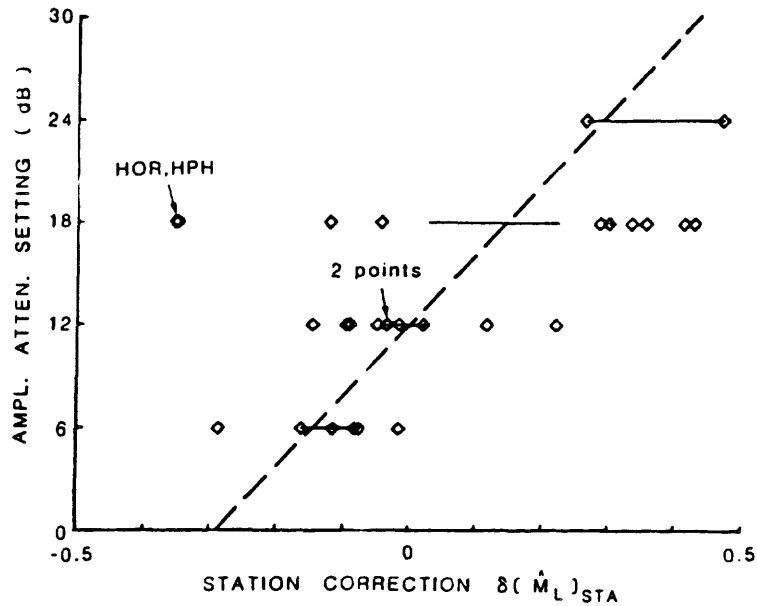
FIG. 9. Amplifier attenuator setting for the 26 stations with constant gain versus station corrections corresponding to $M_L = 0.92 + 0.607 \log^2 \tau + 0.00268\Delta$. Horizontal lines are the mean ($\pm$S.D.) of station corrections at each attenuator setting. The dashed line, $\delta(M_L)_{STA} = -0.29 + 0.024$ (dB setting) is the linear regression of $\delta(M_L)_{STA}$ on attenuator setting.
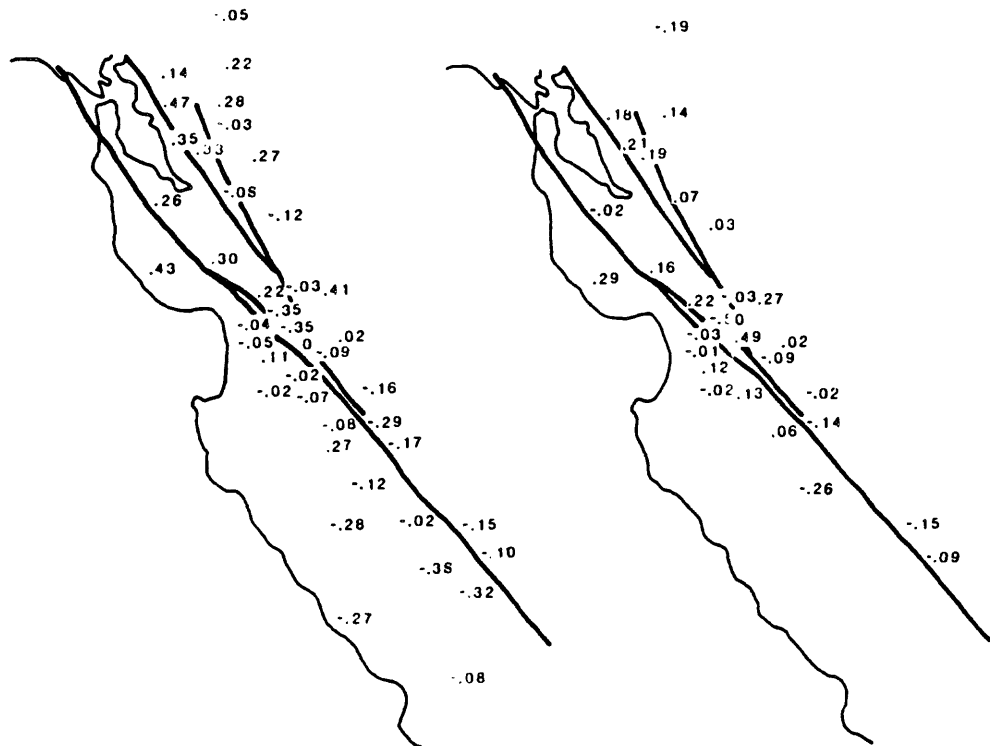
FIG. 10 (Left) Station corrections corresponding to $M_L = 0.92 + 0.607 \log^2 \tau + 0.00268\Delta$ (Right) Same for stations with constant gain with the effect of gain removed using the regression relationship given in Figure 9. Positive (negative) station correction implies that τ at the station tends to be smaller (larger) than expected.
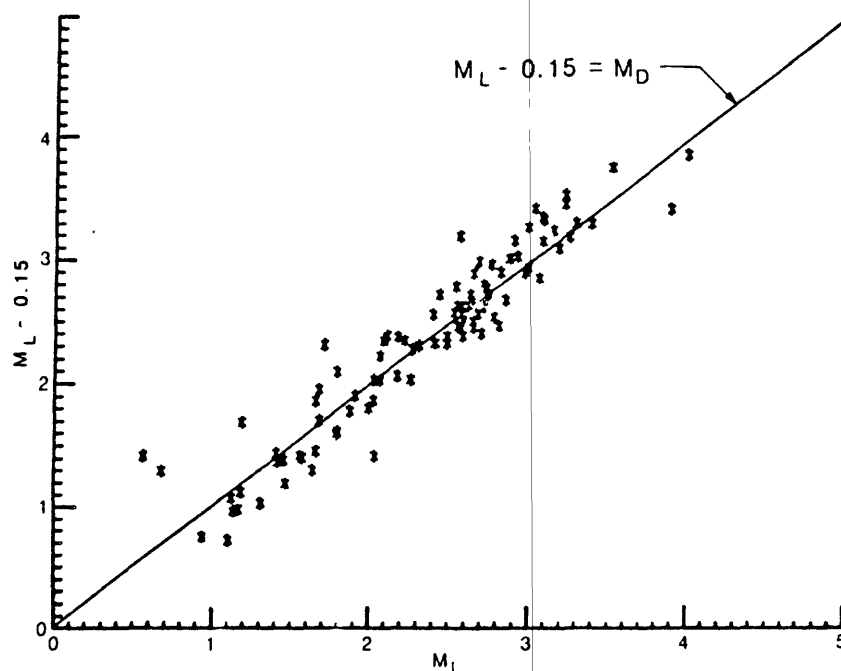
FIG. 11. $M_L - 0.15$ versus the coda-duration magnitude M_D obtained using the formulation of Lee et al. (1972) for the 98 of the 106 earthquakes used by Bakun and Joyner (1984) for which M_0 are available. $M_L - 0.15 \simeq M_D$, so that CALNET magnitude continuity is achieved by M_L using equation (3) rather than equation (1).

Equations (1) and (2) are based on data for $1.1 \lesssim M_L \lesssim 5.3$ and $18.4 \leq \log M_0 \leq 22.3$ shallow foc is strike-slip earthquakes in central California. Caution must be used in extrapolating these relations to other areas. Although data are presented for $M_L \gtrsim 5$ earthquakes, most events of this size are immediately followed by a sequence of aftershocks that preclude any meaningful measurements of τ for the main shock. Fortunately, earthquakes with $M_L \gtrsim 5$ are infrequent so that the traditional amplitude-based estimates of M_L and M_0 will continue to be used for these larger events.

The relationships do not provide unbiased estimates of M_L and $\log M_0$ for smaller ($M_L \lesssim 1.5$, $\log M_0 \lesssim 19$) earthquakes. Coda durations for these small shocks are less than about 15 sec; for these short durations, the durations measured are appar·ntly t·o large and may reflect the $S - P$ time as well as backscattered energy.

The M_L used to obtain equation (1) were calculated using the $-\log A_0$ and station corrections of Bakun and Joyner (1984). Bakun and Joyner (1984) note that v·hile their M_L implicitly assume a static gain of 2800 for Wood-Anderson (W-A) seismographs, W-A seismographs in general (and those in California in particular) have static gains of about 2000. M_L calculated assuming a W-A gain of 2800 shou d be $\log (2800/2000) = 0.15$ greater than M_L calculated using a W-A gain of 2000. Note that Bakun and Joyner's (1984) station corrections for the W-A seismograpns at Berkeley, Mt. Hamilton, and Mineral are 0.24, 0.05 and 0.03 greater than the station corrections used by the University of California, Berkeley, Seismographic Station (UCB) in their analysis of the amplitudes recorded at these stations.] Lee et al. (1972) calibrated their coda-duration relationship against the M_L obtained by UCB. Consequently, the 0.15 average difference between the M_L of Bakun and Joyner

(1984) and the M_D obtained for these events by CALNET using Lee et al.'s (1972) formulation (see Figure 11) is not surprising. For continuity with magnitude scales such as the M_D of Lee et al. (1972) that are calibrated against W-A seismographs with gains of 2000, equation (1) should be modified by subtracting 0.15, i.e.,

$$\hat{M}_L = 0.77 + 0.607 \log^2 \tau + 0.00268\Delta. \tag{3}$$

The adoption here of Lee et al.'s (1972) definition of τ has important practical consequences. Measurement procedures in network operations such as CALNET
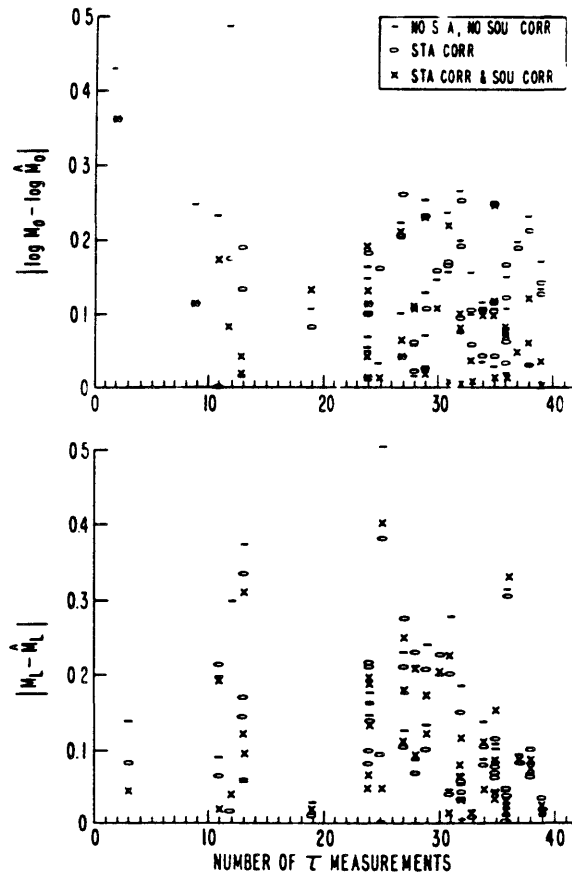
FIG. 12. Magnitude of errors in estimates in log M_0 (top) for log $M_0 \gtreqqless 19$ using equation (1) and in M_L (bottom) for $M_L \gtreqqless 1.5$ using equation (2). Only events with uncertainties (95 per cent confidence intervals), in log M_0 (top) or M_L (bottom) < 0.3 are shown.

that use Lee et al.'s (1972) coda-duration formulation for estimating M_L need not be changed. Estimates of M_L and M_0 using these new relations on the τ already measured for earthquakes over the past several years are easily obtained.

The M_L and log M_0 estimates are better if station corrections or station and source region corrections are used. For M_L and log M_0 determined from a single τ, rms errors decrease from about 0.35 to 0.25 M_L or log M_0 units if stations corrections are used (see entries at bottom of Tables 5 and 6). Although the corresponding rms errors in the M_L and log M_0 estimated from all available τ are smaller (~0.2 M_L or

log M_0 units for no corrections), the error is further reduced when corrections are applied. If the number of observations ≤ 15, the reduction in error is often dramatic (see Figure 12). For more than about 30τ, the use of both station and source region corrections significantly reduces the errors in the estimates, particularly for log M_0. It is clear from the average uncertainties, average ($\pm$) at the bottom of Tables 5 and 6, that the M_L and log M_0 estimates are more precise if corrections are used.

M_L and log M_0 calculated from the same set of coda-duration measurements clearly are not independent. Nevertheless, both belong in earthquake catalogs. M_L maintains continuity with earlier catalogs and facilitates communication with the nontechnical population. Since M_0 is defined in terms of the parameters of the dislocation source model, it is the most useful measure of earthquake size for many technical questions.

CONCLUSIONS

Regression analysis of M_L and log M_0 on coda-duration measurements and epicentral distance at 42 stations in the CALNET for 55 earthquakes from five distinct source regions in central California yielded empirical formulas [equations (1) and (2)] for estimating local magnitude M_L and seismic moment M_0. The formulas provide unbiased estimates of M_L for $1\frac{1}{2} \leq M_L \leq 5\frac{1}{4}$ and of M_0 for $19 \leq$ log $M_0 \leq 22.3$. For the earthquakes studied, durations available from the 42 stations yield average and rms differences in the estimated and measured M_L and log M_0 values of -0.01 and 0.19 for M_L and -0.02 and 0.18 for log M_0. If constant additive M_L and log M_0 station corrections are used, the corresponding average and rms differences are -0.02 and 0.17 for M_L and -0.01 and 0.16 for log M_0. If these station corrections and also constant additive M_L and log M_0 source region corrections are used, the corresponding average and rms differences are -0.03 and 0.17 for M_L and -0.02 and 0.12 for log M_0. For continuity with magnitude scales that use amplitudes from or are calibrated against W-A seismographs with static magnifications of 2000 rather than 2800, 0.15 should be subtracted from the $\hat{M}_l$ obtained using equation (1).

The station corrections are weakly correlated with seismograph amplification. Lower gain stations tend to have shorter coda duration than do the higher gain stations. The station corrections vary on a regional scale, consistent with shorter durations in the San Francisco Bay region, and longer durations in the Coast Ranges near Parkfield.

ACKNOWLEDGMENTS

REFERENCES

Aki, K. (1966). Generation and propagation of G waves from the Niigata earthquake of June 16, 1974. Part 2. Estimation of earthquake movement, released energy, and stress-strain drop from G wave spectrum, Bull. Earthquake Res. Inst. Tokyo Univ. 44, 73-88.

Aki, K. (1969). Analysis of the seismic coda of local earthquakes as scattered waves, J. Geophys. Res. 74, 615-634.

Bakun, W. H. (1984). Seismic moments, local magnitudes, and coda-duration magnitudes for earthquakes in central California, Bull. Seism. Soc. Am 74, 439-458.

Bakun, W. H. and A. G. Lindh (1977). Local magnitudes, seismic moments, and coda durations for earthquakes near Oroville, California, Bull. Seism. Soc. Am. 67, 615 629.

Bakun, W. H. and W. B. Joyner (1984). The M_L scale in central California, *Bull. Seism. Soc. Am.* **74**, 1827–1843.

Bakun, W. H., R. M. Stewart, and C. G. Bufe (1978). Directivity in the high-frequency radiation of small earthquakes, *Bull. Seism. Soc. Am.* **68**, 1253–1263.

Draper, N. R. and H. Smith (1966). *Applied Regression Analysis*, John Wiley and Sons, New York, 417 pp.

Lee, W. H. K. and S. W. Stewart (1981). Principles and applications of microearthquake networks, in *Advances in Geophysics 2*, Academic Press, New York, 293 pp.

Lee, W. H. K., R. E. Bennett, and K. L. Meagher (1972). A method of estimating magnitude of local earthquakes from signal duration, *U.S. Geol. Surv. Open-File Rept.*, 28 pp.

Real, C. R. and T. L. Teng (1973). Local Richter magnitude and total signal duration in southern California, *Bull. Seism. Soc. Am.* **63**, 1809–1827.

Thatcher, W. and T. C. Hanks (1973). Source parameters of southern California earthquakes, *J. Geophys. Res.* **78**, 8547–8576.

U.S. GEOLOGICAL SURVEY
345 MIDDLEFIELD ROAD
MENLO PARK, CALIFORNIA 94025

APPENDIX B. 2.

Work Plan to Update Magnitudes in USGS Catalogs

Work Plan to Update Magnitudes in USGS Catalogs

INTRODUCTION

Recently it has become apparent that the USGS CALNET earthquake catalogs for central California are used for purposes not explicitly anticipated in the CALNET design. In particular, much reliance is placed on the magnitudes of small earthquakes through the counting of shocks with magnitude at or nominally greater than the completeness level of the catalogs. Temporal variations in completeness threshold and/or in the magnitude scale used by CALNET are particularly troublesome for these studies.

In order to address possible temporal variations in the magnitude scale used by CALNET, we will undertake a systematic evaluation of the coda-duration magnitude scale M_D used by CALNET. Our goal is a summary catalog for 1969-1985, with magnitude and log seismic moment estimates for each shock. Each of these estimates will have attached an error estimate and the number of data used. In addition to the precision, we will test that the magnitude scales are consistent over the time period through frequent checks with amplitude magnitudes. We will rely on the coda duration readings τ already compiled by CALNET and build a station correction set for all CALNET seismographs. Our strategy will be to expand the magnitude and seismic moment $\log 2\tau$ reformulation of Bakun (1984) by establishing time dependent magnitude correction factors for all CALNET stations.

SPECIFIC TASKS

A. 1977-1981 We start with the 1977-1981 time period considered in Bakun (1984) where:

(1) Local magnitude M_L and log seismic moment, log M_0, are available for more than 100 earthquakes in central California; 55 of these shocks were used to reformulate the coda duration relationship of Lee et al. (1971). (The remaining shocks can be used as a test set).

(2) Additive M_D station corrections are available for 42 CALNET stations.

    I. Calculate an average M_D residual for each CALNET station.
        a) Supplement existing τ readings for the 55 shocks in the training set so that each station has a minimum of 25 readings. Try to get readings for each station from each of the 5 source regions represented in the calibration set.

        b) Check some of the τ readings by looking at develocorder films. Check the τ readings that were used in the calibration study.

        c) Identify stations with larger std. errors in the average residuals. Tag these as "bad" stations in the sense that they should be avoided in subsequent magnitude calculations.

        d) Calculate M_D and log M_0 for the test set (i.e., the shocks with independent M_L and log M_0 determinations that were not used in the coda-duration reformulation).

e) Check that there are no systematic dependence of M_D vs. τ , distance, focal depth, azimuth, etc.

II. Calculate Preliminary M_D and log Mo
   a) Use the station corrections obtained in (I) to calculate M_D and log M_O for all shocks in 1977-1981.

   b) Spot check the magnitudes with Berkeley W-A amplitude (i.e., M_L).

   c) Spot check the magnitudes with CALNET horiz comp. amplitudes (i.e., Eaton's mags.). Are areas not covered in the calib. data set (i.e., Mammoth, N. Calif., Sierras) served well by the new M_D and log M_O?

III. Calculate a M_D and log M_O residual history for each CALNET station.
   a) Check for patterns. (Changes in average residual or Std. dev. with time, magnitude, distance, duration, etc).

      1. Correlate with known changes in instrumentation or analysis procedures.

      2. Correlate with stations on the same phone line.

      3. Correlate with stations on the same network.

      4. Make necessary adjustments to station corrections (i.e., construct a time history of station corrections).

IV. Recalculate M_D and log Mo for all shocks in 1977-1981.
   a) Look for patterns a la Habermann. Have we missed anything symptomatic of a magnitude change?

B. 1969-1977. The following procedure, starting with 1976 (the year with the most stations), is performed iteratively, back to 1969. The analysis focuses on M_D, since we can calibrate against UCB W-A amplitudes. We assume that the coda reformulation is valid and that changes (instrumentation, etc.) will be reflected in the station correction set.

1. Select logical boundaries (dates) for the iteration process. Ie., known major instrumental changes such as network expansions and develocorder lineup changes.

II. Select a calibration set of earthquakes. Sample all major source regions and range of M_L.

   a) Calculate M_L from UCB WA seismograms.

   b) Spot check develocorder films to confirm τ on USGS phase cards. Add τ readings so that all CALNET stations have at least 15 readings and that a range of source regions are included.

c) Select a test set of shocks. Sample all major source regions.

III. Calculate an M_D station correction set for all CALNET stations.
  a) Calculate M_D from Υ using the results (station corrections of the previous iteration. (Use 1977-1981 for 1976 study).

  b) Calculate residual M_D for each Υ reading . Calculate average residual ▪ - increment to old station corrections. Calculate new station correction set.

  c) Test station correction coda formulation against M_L in test set of shocks.

IV. Calculate Preliminary M_D and log Mo for all shocks in iteration.

V. Calculate an M_D residual history for each CALNET station. Apply pattern tests outlined in A-III above.

VI. Recalculate M_D and log Mo if necessary.
  a) Look for patterns a la Habermann.

C. 1981-Dec 1983.
This period includes a number of fundamental changes in the way in which film-derived coda lengths were obtained, including changes in the develecorder speed and a decrease in the fraction of stations on develecorder, but is still a time period for which develecorder film codas are the only observed parameter from which magnitudes can be derived.

Thus for this time period it will suffice simply to check the regression parameters and station corrections (obtained in A) for 77-81) for bias and/or increase in variance.

D. Starting in Jan 1984, the fundamental data set is almost entirely based on machine derived (CUSP & RTP) coda lengths, amplitudes, etc. Thus all calibrations will have to be done from scratch. This problem divides into several parts, some of which are already underway.

I. Determine how the CUSP and RTP codas compare to film codas. A preliminary check has already been made at Parkfield; there the CUSP codas agree on the average to within 2% ($\pm$ 4%), while the RTP codas average 17% long ($\pm$ 3%). (Thus, it does not appear that systematic changes in coda lengths can account for any apparent quiescence at Parkfield since Jan 1984.)

II. Calibrate CUSP & RTP codas as in A). Presumably the systematics of the station corrections will remain approximately the same, so it will suffice to redo the regressions for M_D vs M_L. Data for this task has been assembled and is being entered into the CUSP system.

III. Calibrate M_c (Carl Johnson's CUSP derived magnitude) vs. measurements of coda amplitude & decay as has been done at Caltech since the late 1970's. Data for this task is being assembled and entered into CUSP, and Sam Stewart is working on getting Carl's calibration programs running in Menlo Park.

APPENDIX C.

Draft - Parkfield Earthquake Prediction Decision M trix

W. H. Bakun, A. G. Lindh, and P. Segall

DRAFT

UNITED STATES DEPARTMENT OF THE INTERIOR

GEOLOGICAL SURVEY

Parkfield Earthquake Prediction Scenarios and Response Plans

W. H. Bakun, J. Bredehoeft, R.O. Burford, W. L. Ellsworth, M.J.S. Johnston,
A. G. Lindh, C. Mortensen, S. Schulz, P. Segall, and
W. Thatcher

Open-File Report 85-

Table of Contents

SUMMARY

The purpose of this report is to define conditions that change the assessment of the earthquake hazard along the San Andreas fault near Parkfield, California. The most alarming conditions warrant an immediate communication from the United States Geological Survey (USGS) to the California Office of Emergency Services (OES). Emphasis is placed on extreme situations, such as large foreshocks or rapidly accelerating aseismic creep, that require decisions within a few hours or less. More gradually developing circumstances will allow time for additional data collection and interpretation. We define the following set of alarm levels in order of increasing concern and the corresponding USGS response:

Alarm Level	Anticipated Alarm Frequency (time between alarms)	Probability of earthquake in next 24 hours	Response
e	---	$\sim10^{-4}$ to 10^{-3} (=long term prob.)	Continue Normal Operation
d-	---	-------------	Project Maintenance
d	3 mo. - 6 mo.	$\sim10^{-3}$ to $\sim10^{-2}$	Alert Parkfield Working Group Alert Data Collection Operations.
c	6 mo. - 12 mo.	$\sim10^{-2}$ to $\sim10^{-1}$	Alert Office Chief, and response to Alarm Level d.

b   12 mo.- 24mo. $\sim 10\%$ to $\sim 40\%$ Alert Director, USGS and California Division of Mines and Geology (CDMG) and response to Alarm Level c.

a   >24mo. $\geq 40\%$ Issue Geologic Hazards Warning and response to Alarm Level b.

a*   >24mo. $\geq 40\%$(next hour)   Immediate call to OES and responses to Alarm Level a.

Observational networks at Parkfield are divided into four groups: seismic, creep, continuous strain, and geodetic survey. Preliminary alarm level criteria have been established for each network group where possible; seismic alarm criteria are based on probability estimates while the criteria for the other 3 network groups are based on how alarming and how infrequently certain signals are expected to occur. The earthquake probability is greatest immediately after the occurrence of an alarming signal and generally is expected to decrease with time to the long-term probability of 10^{-4} - 10^{-3}/day appropriate to alarm level e. Consequently, heightened alarm levels (a, b, c, or d) defined in this report have a finite lifetime of 72 hours after the end of the last alarming signal. Associated with each alarm level is an anticipated alarm frequency (e.g., once each 3 to 6 months for alarm level d) that can be used as an estimate of the rate of false alarms.

Alarm threshold·, on more than one observational network increase the earthquake probability; simu taneous alarms on two or more network groups are combined according to the following ·et of alarm-level combination rules:

Status of Network Alarm Levels

Rule	Network 1		Network 2		Network 3		Network 4	Combined Alarm Level
1)	e	+	e	+	e	+	e	⩾ e
2)	d	+	e	+	e	+	e	⩾ d
3)	d	+	d	+	(d or e)	+	(d or e)	⩾ c
4)	c	+	(d or e)	+	(d or e)	+	(d or e)	⩾ c
5)	c	+	c	+	(c,d, or e)	+	(c,d, or e)	⩾ b
6)	b	+	(c,d, or e)	+	(c,d, or e)	+	(c,d, or e)	⩾ b
7)	b	+	b	+	(b,c,d, or e)	+	(b,c,d, or e)	⩾ a
8)	a	+	(c,d, or e)	+	(d or e)	+	(d or e)	⩾ a
9)	a	+	c	+	c	+	(c,d, or e)	⩾ a*
10)	a	+	(a or b)	+	(a,b,c,d, or e)	+	(a,b,c,d, or e)	⩾ a*

The combination rules are applied by ranking the four network groups in decreasing order of current alarm-level status. For example, if the seismic, creep, continuous strain, and geodetic survey alarm levels were c, b, c, and d respectively, then the ranking of alarm levels would be b (creep), c (seismic), c (continuous strain), and d (geodetic survey), corresponding to rule 6. Rule 6 states that one b level alarm, two c level alarms, and one d level alarm combine to yield a b level alarm.

INTRODUCTION

The 25-km-long Parkfield section of the San Andreas fault, midway between San Francisco and Los Angeles, has experienced moderate-size (magnitude 6) earthquakes in 1881, 1901, 1922, 1934, and 1966. The mean interevent time of 21.8 ± 5.2 years, together with the 19+ years since 1966, suggest that the next shock is now due; estimates of the probability of its occurrence before 1993 range up to 95 percent.

The evidence supporting the long-term prediction of a magnitude 6 shock a Parkfield was independently reviewed and accepted by the National Earthquake Prediction Evaluation Council and the California Earthquake Prediction Evaluation Council. In a letter (dated April 4, 1985) to William Medegovich, the Director of the California Office of Emergency Service (OES), the Director of the U.S. Geological Survey reviewed the earthquake hazard situation at Parkfield and promised to notify OES immediately of any changes in the USGS assessment of the situation at Parkfield.

There is a need to develop specific plans to cope with public hazards. Testimony before the Atomic Safety and Licensing Board on the U.S. Nuclear Regulatory Commission makes clear that all decisionmakers responsible for protecting the public welfare need a plan that "provides for the removal of the effects of individuals' personalities, fears, biases, beliefs, notions, and so on, both from the decisions and from the process that links discovering the threat to seeing information about the threat conveyed to other responsible officials and to the public". The testimony further notes that lacking such a plan, the decisionmakers are in theory vulnerable to charges of "conflict of interest," such as delays in issuing public warnings or otherwise sharing threat

information and downplaying the threat in the information that is shared. Plans in which key decisions and transmittal instructions are formalized can minimize the possibility of "conflict of interest" hindering an emergency response.

The purpose of this report is to define those conditions that would so change our assessment of the earthquake hazard at Parkfield that a communication from the USGS to the California Office of Emergency Services would be warranted. The decision and response processes are also described. Emphasis is placed on extreme situations that require decisions within a few hours or less; more gradually developing circumstances will allow time for additional data collection and interpretation.

II. HI;TORICAL PRECURSORS AT PARKFIELD

All tne available evidence is consistent with the hypothesis that the 5

preceding Parkfield main shocks were similar, suggesting that the Parkfield

section is characterized by recurring earthquakes with predictable features.

The hypothesis of a characteristic earthquake means that the design of a

prediction experiment can be tailored to the specific features of the recurring

characteristic earthquake. We rely primarily on evidence of changes in

seismicity before the 1934 and 1966 Parkfield earthquakes and possible creep

anomalies before the 1966 shock as a guide to potential precursors to the

upcoming quake.

A. Seismicity The 1934 and 1966 main shocks were each preceded by prominent

foreshock activity located in the "preparation zone", a 2-km-long section of the

fault immediately northwest of the common epicenter of the main shocks. The

foreshock activity in 1934 and in 1966 included in each case a magnitude 5.1

shock 17 minutes before the main shock. (There were no foreshocks larger than

magnitude 4 1/2 in 1922 and no felt foreshocks reported in 1881 or in 1901). In

1934 fifteen magnitude 3 and larger foreshocks, including two with magnitude=

5.0-5.1, occurred in the 67 hours before the main shock. In 1966 three

magnitude 3 and larger foreshocks occurred, all in the 3 hours before the 1966

mainshock.

B. Fault Creep Although there were no instruments operating near Parkfield

capable of resolving short-term precursory deformation before the historic

Parkfield shocks, there were anecodotal accounts of changes in 1966 consistent

with significant ase smic slip on the Parkfield section of the San Andreas

fault. First, an irrigation pipeline that crosses the fault trace 5 km south of

Parkfield broke about 9 hours before the 1966 main shock. The magnitude of the

slip immediately preceding the main shock is unknown. Second, very fresh appearing en echelon cracks were observed along the fault trace near Parkfield twelve days before the 1966 shock. If tectonic in origin, these cracks imply 1-to-2 cm of aseismic slip within the three months preceding the mainshock. (It has been suggested, however, that the cracks were related to desiccation and are not tectonic in origin.)

III. POTENTIAL FOR PRECURSORY DEFORMATION

Theoretical and laboratory models of faulting predict accelerating deformation before the dynamic slip instability that constitutes an earthquake. The magnitude and character of the precursory deformation, the time scale of the process, and the dimensions of the fault zone involved in the deformation are, of course, major unknowns. While there are an infinite variety of possible precursory scenarios, it is possible to delineate end member cases consistent with what is known about previous Parkfield earthquakes.

An optimistic scenario might involve significant amounts of accelerating fault slip extending over the entire coseismic rupture surface for weeks to days before the earthquake. This would be revealed by foreshocks in the hypocentral region, accelerating fault creep, and changes in the local strain field. The large magnitude, extent, and time scale of such a precursory process make it rather straightforward to detect given current instrumentation.

A much more pessimistic scenario might involve a limited amount of preseismic deformation localized to a small section of the fault at depth near the expected main shock hypocenter. Such a process might be manifest solely by small foreshocks and low level strain changes that would be difficult to measure and interpret with existing instrumentation. These examples emphasize the uncertainties involved in formulating precursory scenarios without a widely accepted physical model of the failure process.

IV. SUMMARY OF CURRENT INSTRUMENTATION

The current instrumentation program at Parkfield are divided into four networks: (1) seismic, (2) creep, (3) continuous strain, and (4) geodetic survey. We restrict our attention in this report to establish~ed~ instrumentation for which there is a history of reliable observations; we do not consider here suggested precursors (e.g., U.S. radon and animal behavior) that are too poorly understood to be of use in predicting the next Parkfield earthquake.

A. <u>Seismic</u> The seismic instrumentation consists of the USGS CALNET stations, the borehole stations operated by P. Malin of UCSB, and the strong-motion accelerograph array operated by the Calif. Div. of Mines and Geology (CDMG).

<u>CALNET</u>. There are currently 18 high-gain, short period, vertical seismometers located within 25km of the town of Parkfield.

	Component(s)	Location relative to Parkfield
Antelope Grade (PAG)	Z	25km SE
Castle Mountain (PCA)	Z	10km E
Curry Mountain (PCR)	Z	22km N
Gold Hill (PGH)	Z	12km SE
Harlan Ranch (PHA)	Z	9km SE
Hog Canyon (PHO)	Z + 3 low-gain	5km SW
Hope Ranch (PHP)	Z + 2 horiz.	17km NW
McMillan Canyon (PMC)	Z + 3 low-gain	20km SW
Middle Mountain (PMM)	Z + 2 horiz.	8km NW
Maxie Ranch (PMR)	Z	23km SE
Portuguese Canyon (PPC)	Z + 2 horiz.	15km NW
Parkfield (PPF)	Z	4km SE
Smith Mountain (PSM)	Z	23km NW

Scobie Ranch (PSR)	Z	15km SE
Stockdale Mountain (PST)	Z	8km NW
Turkey Flat (PTF)	Z + 2 horiz.	3km SE
Vineyard Canyon (PVC)	Z + 2 horiz.	9km NW
Work Ranch (PWK)	Z	11km SW

This array permits routine location of M > 0.8 events along the Parkfield section of the San Andreas. The Menlo Park real-time processor (RTP) provides estimates of earthquake locations and magnitudes within 3-5 minutes of their occurrence. The seismic network is well suited to the detection of potential M $\geq$ 1 foreshocks at Parkfield.

Borehole Seismograph Network. Three 3-component borehole seismometers have been installed by Peter Malin of the Univ. of Calif. at Santa Barbara (UCSB) with support provided by the USGS external grants program. The borehole seismographs are currently in the test/evaluation phase; they should provide high-gain high frequency seismic information on M $\geq$ 0-1 shocks in the Parkfield area not obtainable from the CALNET systems.

Strong-motion Accelerographs Network. Nearly 50 SMA-1 strong motion accelerographs are operated by CDMG in the Parkfield area. This network is designed to record the details of ground motion during the Parkfield main shock and during any M3.5 or larger foreshocks or aftershocks. The accelerographs are recorded onsite so that data from the strong-motion network will probably not be useful for earthquake prediction.

B. Creep

There are 8 Parkfield area creepmeters that are on the beeper-paging alarm system. Locations on the fault from the northwest to the southeast: Slack Canyon (XSC1), Middle Mountain (XMM1), Parkfield (XPK1), Taylor Ranch (XTA1), Durham Ranch (XDR2), Work Ranch (WKR1), Carr Ranch (CRR1), and Gold Hill (XGH1). The Middle Mt. creepmeter is located in the epicentral region of past Parkfield main shocks and foreshocks. Six creepmeters (XSC1, XMM1, XPK1, XTA1, XDR2, XGH1) are invar-wire instruments with 0.05 mm resolution, and 2 (CRR1, WKR1) are invar-rod instruments with 0.5 mm resolution. Creep data is telemetered to Menlo Park every 10 minutes via GOES satellite and telephone telemetry.

C. Continuous Strain

Strainmeters - There are two types of strain measuring devces currently in use near Parkfield. Sacks-Evertson borehole dilational strainmeters (dilatometer) are located at three sites (Gold Hill 1, Gold Hill 2, and Eades) along the southern end of the expected rupture zone. The dilatometers are operated by the USGS in a cocperative effort with the Carnegie Institution of Washington. A single-component, linear strainmeter (extensometer) is sited on the Claussen Ranch (CLS 1) near Middle Mt. at the northern end of the rupture zone. The resolutior of the dilatometers range from 10^{-2} μstrain at periods of several weeks to 10^{-3} μstrain at much shorter periods. Resolution of the extensometer is 0.5 μstrain at short periods, unless severe meteorlogical conditions cause an increase in the noise level.

The data are both recorded on site and transmitted once every 10 minutes with digital telemetry via the GOES satellite or telephone telemetry to the low frequency data computer in Menlo Park.

Tiltmeters - A network of 4 closely-spaced shallow-borehole tiltmeters is operated at Gold Hill. These data are also recorded on site and are transmitted every 10 minutes with digital telemetry to the low-frequency data computer in Menlo Park. Although the tilts due to earth tides are coherent between sites, the long term tilts are not, indicating long-term instability in the near surface materials. The tilt resolution is of the order of 0.1-1 microradians at periods of days and 0.01-0.1 microradians at periods of hours.

Water Wells - Water level fluctuations in a network of 5 wells (3 or 4 more are planned) near Parkfield are now monitored by the USGS Water Resources Division (WRD). These wells all record clear earthtides, and have sensitivities comparable to the dilatometers. At periods as long as at least 2 weeks, water levels respond to the local volume strain, so that water level changes can be directly compared to dilatometer data. Water levels in wells at Gold Hill, Turkey Flat, and Flinge Flat sampled every 15 minutes are transmitted every 3 hours by GOES satelite to the low frequency data computer in Menlo Park and also to WRD in Phoenix and then by the WRD data network to a WRD computer in Menlo Park; water levels in wells at Joaquin Canyon and Vineyard Canyon are currently recorded only at the well head.

Differential Magnetometers - Local magnetic fields are monitored with absolute total field magnetometers at 7 sites [Varian Ranch (VRRM), Long Canyon (LGCM), Turkey Flat (TFLM), Hog Canyon (HGCM), Gold Hill (GDHM), Antelope Grade (AGDM), and Grant Ranch (GRAM)] in the Parkfield region. The data are synchronized to within 0.1 sec and are transmitted with 16- bit digital telemetry to Menlo Park. The measurement precision in the period range 10 min to tens of days is about 0.2 nT. Changes of 0.5 nT corresponding to stress changes of several bars according to current models, can be detected with the present instrumentation.

D. Geodetic Survey

There are several dense geodetic networks, both trilateration and leveling, in the Parkfield region.

Two-color Laser Geodimeter Network - A trilateration network employing an observatory-based two-color laser electronic distance measuring system was deployed in 1984 by the Co-operative Institution for Research in the Environmental Sciences (CIRES) at the University of Colorado and is operated through a cooperative USGS/CIRES program. The network currently consists of 17 reflector sites distributed radially around the central instrument site, which is located just south of Parkfield. Under optimal conditions the network can be reobserved nightly. Typical standard errors of individual line length measurements are 0.5-0.7 mm for 4-6 km long lines.

Geodolite Network - A network of 80 geodolite lines spans the Parkfield region. Standard errors of individual line-length measurements range from 3 mm to 7 mm for lines 4 km to 33 km in length. It is anticipated that at least part of the network will be reobserved annually. Four "monitor" lines near the southern end of the rupture zone will be surveyed quarter y.

Small Aperature Networks - Three small aperture trilateration networks span the Parkfield section of the San Andreas fault. Standard errors for individual measurements are 4 mm. Thirty one near-fault lines are scheduled to be surveyed quarterly.

Leveling Network - A 51-km long network of leveling lines in the Parkfield region have been periodically resurveyed since 1979. The network consists of four lines; a 10-km long line perpendicular to the fault at Parkfield, a 32-km long line in the vicinity of Middle Mtn., a 17-km long line

perpendicular to the fault at the southern end of the rupture zone, and a 24-km long fault-parallel line. Short (~1 km) sections of these long lines are surveyed 3-4 times/yr in a joint effort with the University of California at Santa Barbara (UCSB).

V. ALARM THRESHOLDS.

Based on analyses of the historic seismicity at Parkfield, the long-term probability of a characteristic Parkfield earthquake is about 10^{-4}/day. Anomalous signals that are sufficient to activate the automatic beeper alarm systems raise the our estimate of the daily probability by at least a factor of 10. Such anomalies are significant in that they initiate a series of alarms: e.g., notification of the Parkfield Working Group (see Appendix A) and other personnel responsible for the operation and maintenance of the USGS data collection systems. In addition to the automatic beeper alarm systems, data from all of the monitoring networks described in this report are reviewed each day so that anomalous signals that were not anticipated in the design of the beeper alarm algorithms are detected and evaluated.

Based on past experience, including historical precursors to prior Parkfield shocks, it is possible to identify the kinds of signals that would contribute to a reassessment of the short term earthquake hazard in the Parkfield region. Whereas the observations of foreshocks before the 1934 and 1966 shocks permit estimates of the probability of an imminent earthquake, the other, more-recently established observation networks can only be analyzed in terms of the expected frequency of a range of anomalous signals. While probabilities can be subjectively associated with these expected frequencies, there is no sound statistical basis for assigning earthquake probabilities that these anomalous signals would incur. We attempt to define alarm levels that correspond in our best judgement to the following probabilities and/or anticipated alarm frequency:

Anticipated

Alarm Level	Alarm Frequency (time between alarm)	Probability of shock in next 24 hours
d	3mo. to 6mo.	$\sim 10^{-3}$ to $\sim 10^{-2}$
c	6mo. to 12mo.	$\sim 10^{-2}$ to $\sim 10_{-1}$
b	12mo. to 24mo.	$\sim 10\%$ to $\sim 40\%$
a	>24mo.	$\geq 40\%$
a*	>24mo.	$\geq 40\%$ (next hour)

The occurrence of anomalous signals intuitively increases the earthquake probability for some time immediately thereafter. It is clear that unless the anomaly continues or unless other anomalous signals occur, the heightened earthquake probability decreases monotonically with time back to the pre-anomaly state. That is, the level of concern implicit in the alarm has a natural lifetime. Although there is not sufficient data to define these lifetimes empirically, the 67-hour-long duration of foreshock activity before the 1934 shock suggests that a 3 day (72 hour) lifetime is appropriate.

There is a subset of alarm level combinations that are so alarming that our estimate of the probability of the anticipated earthquake in the next several minutes is significantly enanced. For example, the magnitude 5 foreshocks that preceded b th the 1934 and the 196 earthquakes by 17 minutes suggests that there is a significant chance that any magnitude 5 shocks located near the preparation zone will be followed within minutes by the anticipated magnitude 6 shock. Consequenctly, we include a speci l alarm level, a*, which, if reached, would warrant not only the response to alarm level a, but also an immediate warning of the imminent hazard to OES.

The anticipated alarm frequency in the above table emphasizes that use of any set of formal alarm criteria implies the occurrence of some false alarms. Whereas the rate of alarms for level d implies 2 to 4 "inhouse" alarms per year, the more stringent criteria for level a imply an anticipated alert to OES less frequent than once every two years. Given the Parkfield seismic window of 1988 $\pm$ 5.2 years, we expect that the use of the criteria in this report could result in up to 3 or 4 false alarms to OES.

A. Seismic

Seismic signals from the CALNET stations are telemetered to Menlo Park and processed by computer in real time to provide estimates of earthquake locations and magnitudes within 3-5 minutes of their occurrence. Alarm thresholds that signal unusual Parkfield seismicity activate paging systems that alert the seismologists responsible for surveillance at Parkfield. Two alarm thresholds are used: (1) a magnitude 2.5 or larger shock in the general Parkfield area alarm zone, and (2) either a magnitude 1.5 shock, or 2 magnitude 1.0 shocks within a 72-hour period, in a restricted middle mountain zone that includes the Parkfield preparation zone. (There is also a general central California seismic alarm threshold of magnitude 3.5). Since at least 2 of the past 4 Parkfield shocks had foreshock sequences including magnitude 3-5 events, our judgement is that the probability that the next Parkfield shock will have foreshocks of magnitude 1 or larger is at least 50 percent.

Based on recent seismicity rates, we expect the automated seismicity detector to be triggered 3-5 times per year, for a total of 25 alarms by 1993. According to a rather simple statistical model, each of those alarms raises the probability of a Parkfield main shock occurring in the next 72 hours by a factor of 100 over the long term probability. Alarms triggered by M 3-5 earthquakes would seem to imply a substantially greater hazard; we can attempt an estimate for M5 events. Excluding main shocks and aftershocks, there have been six M5 $\pm$ 1/4 events in the Middle Mt. alarm zone since 1934. Three of these were foreshocks (2 in 1934 and 1 in 1966). The probability that

any magnitude 4 3/4 - 5 1/4 shock in the Middle Mountain alarm zone will be followed by the Parkfield main shock within the next 24-72 hours is thus estimated to be 30-50 percent.

Probability estimates, conditioned by the reasonable assumption that there is a 50% probability that the next Parkfield earthquake will be preceeded by a foreshock, have been used to identify seismicity criteria corresponding to the different alarm levels:

Seismic Alarm Level	Seismicity	Estimated Prob. of earthquake in next 24 hrs.	Anticipated Alarm Frequency (time between alarms)
d	One M 3.5 shock in the general Parkfield area, one M 2.5 shock in the general Parkfield alarm zone or one M 1.5 shock in the Middle Mt. alarm zone, or two or more M1.0 shocks in a 72-hour period in the Middle Mt. alarm zone.	.004	3mo. to 6mo.
c	One 3.5 shock in the general Parkfield alarm zone, one M2.5 shock, or two or more M 1.5 shocks, in a 72 hour period in the Middle Mt. alarm zone.		6mo. to 9mo.
b	One M3.5 shock, or two or more M2.5 shocks in a 72-hour period, in the Middle Mt alarm zone.	5 - 10	18mo. to 24mo.

| a (a*) | One M5, or two or more M4 | 30% - 50% | >24mo. |

shocks in a 72-hour period,

in the Middle Mt. alarm zone.

B. Creep

Parkfield-area creepmeters exhibit long-term annual creep rates ranging from 22 mm/yr at Middle Mt. to 4 mm/yr at Gold Hill. Data from the eight Parkfield creepmeters are sampled every 10 minutes. The alarm detector compares the average creep at the 8 sites in the past hour with the average level in the preceding 23 hours. A change of 0.25 mm or greater activates the paging device. In the past year, 16 beeper-paging alarms were triggered by creep events.

Creep Alarm Level	Creep Observations (in the absence of M 3.5 or larger shocks)	Anticipated Alarm Frequency (time between alarm)
d- (Creep Beeper Alarm)	(1) At one site, a step >0.25 mm within one 10-minute telemetry sample period (in the past 2 years, there have been at least 6 of these alarms, all due to battery, telemetry, and/or telephone transmission failures.)	< 4 mo.
	(2) At one site, a small creep event; i.e. creep exceeding 0.25 mm within 30 minutes with slip velocity decreasing exponentially within 45-90 minutes after onset.	< 2 mo.

d   (1) At any one site other than XSC1,   6 mo.

a nearly continuous increase

in creep that exceeds 0.25mm within

7 days and continues at a comparable

or greater rate over a period greater

than 10 days. XSC1 normally moves

0.25 - 0.5mm/week. (This alarm

has been reached 4 times in the

period 198?-1985).

(2) At one site, an unusually large creep   ⁻ 6 mo.

event (see definition above) at that

site. For creepmeters northwest of

XDR2 (XSC1, XMM1, XPK1, XTA1, and XDR2)

events with creep >0.5mm in the first

30 min. would be unusually large. For

creepmeters southeast of XDR2 (WKR1,

CRR1, and XGH1), events with creep >0.33mm

in the first 30 minutes would be unusually

large.

c   Nearly simultaneous onset of creep at 2 or   6 mo.- 12mo.

more creepmeters that exceeds 0.5mm in the

first hour, or more than 1mm of creep on the

Middle Mt. creepmeter in the first hour.

(Alarm level c has been reached 10 times

over the past 6 years. Alarm level c for

the Middle Mt. creepmeter has not been

reached in the past 12 months; 0.5mm at

Middle Mt has been reached once during

this period.)

b   More than 5mm of slip in 72 hours at Middle >24mo.

       Mountain, or on 2 or more creepmeters located

       elsewhere on the Parkfield segment.

a   Creep rates on multiple instruments (or at >24mo.

       Middle Mountain alone) in excess of 0.5mm

       /hour sustained for 6-10 hours or cumulative

       slip in excess of 5 mm in a shorter period.

C. <u>Continuous Strain</u> (strainmeters, tiltmeters, water wells, and differential magnetometers.)

It is possible, with a few simple assumptions, to calculate the signals expected at the current monitoring sites for postulated fault slip. For example, if slip of 1cm occurs on the fault between 2 and 10 km depth and along a length of 5km near Gold Hill, the strain change at the Gold Hill dilatometers and tiltmeters would be about 0.2 microstrain and microradians, respectively.

Data from the Parkfield strainmeters, tiltmeters and magnetometers are sampled automatically every 10 minutes and the data are transmitted to Menlo Park. For the dilational strain data, average strain for the last 60 minutes is computed. Earth tides and atmospheric pressure loading, determined from a theoretical earth tide model and an onsite pressure transducer, respectively, are removed from the data. Provided the instruments and telemetry are operating correctly, changes in strain of 0.2 microstrain over several days (<u>longer term</u>) or 0.4 microstrain at periods less than a day, (<u>short term</u>), can be clearly detected. Short term strain changes are detected by an algorithm that identifies strain changes of more than 0.4 microstrain in a 24 hour period. Longer term strain changes are detected by an algorithm that identifies changes in strain rate normalized by estimates of noise in the data.

Although only three borehole strainmeters now operate in the Parkfield region, during the past two years (Nov. 83-Nov. 85) four longer-term alarms have been triggered for strain rate increases of about 0.03 microstrain/day for periods of about a week. One of these strain perturbations occurred on a dilatometer at the same time as minor seismicity and a creep event at Middle Mountain. All four longer-term strain perturbations were independently recorded and identified in water level data in a well at Gold Hill. Simultaneous strain changes greater than 0.4 microstrain on several separated dilatometers, corroborated by water well data, combined with changes in local magnetic field greater than 1 nT of east-side magnetometers with respect to westside magnetometers, would constitute an unmistakable anomaly. This has happened three times during the past year in the Parkfield region and has not been seen clearly elsewhere. No changes in strain of 0.4 microstrain within a 24 hour period have been observed during the past two years.

There is, at present, one small cluster of 4 tiltmeters in the Parkfield area at Gold Hill. Tiltmeters have not yet been installed at sufficient depth to avoid long term near-surface noise. Although coherent tilts of 0.1 microradians at periods less than one day would be clearly detected, and would be considered unusual, formal alarm criteria for tilt observations await future installations of more stable tiltmeters.

Differential magnetic field data is perused daily and routinely plotted weekly. Changes of 1 nT within a day or at longer periods, are considered anomalous. This has happened only once, during the few months following the May 1983 Coalinga earthquake.

Continuous Strain   Changes in strain

  Alarm Level

---

d-   Changes of 0.2 microstrain or greater on only one instrument. This may occur frequently or infrequently depending on phone line outages, telemetry malfunctions, instrument malfunctions, etc, and generally triggers maintenence, trouble shooting, or repairs at the project level.

d   Changes of 0.2 microstrain per week on two independent instruments or changes of 0.4 microstrain within a 24 hour period on one instrument with indications of a simultaneous signal on a second independent instrument. Although this has occurred several times during the past year in the Parkfield region, it is highly unusual in other areas.

c   Changes of 0.4 microstrain per week on two or ore independent instruments, or changes of 0.8 microstrain within a 24 hour period on one instrument with indications of a simultaneous signal on a second independent instrument. As noted above this has occurred three times during the past year but is generally very unusual.

b   Changes exceeding 1 microstrain per week on two or more instruments, or changes of more than two microstrain within a 24 hour period on one instrument with indications of a simultaneous signal on a second independent instrument.

a   Given the lack of experience at Parkfield, there are no c ear
           thresholds that lacking other data would warrant a warning to
           OES.

Continuous Magnetic

Field Alarm Level   Changes in Magnetic Field

d-   Changes of 1 nT or greater between one pair on instruments
           This may occur infrequently if clock syncronization fails nd
           generally triggers routine maintenance at the project leve .

d   Changes of 1 nT or more in a day or longer between tv o
           instruments. This has occurred only once during the past five
           years in the Parkfield region.

c   Changes of 1 nT or greater in a day or longer on two independent
           instrument pairs. This has iot occurred during the past five
           years in the Parkfield region.

b   Given the lack of experience at Parkfield, there are no clear
           thresholds that lacking other data would warrant warnings to the
           Directors of USGS and CDMG.

a   Given the lack of experience at Parkfield, these are no clear
           thresholds that lacking other data would warrant a warni ig to
           OES.

D. Geodetic Survey

Currently, observations from the two-color laser EDM system are collected every other night so that the two-color observations are more appropriate for a more slowly developing situation than has been considered in this report. Nevertheless, it is possible to identify circumstances under which these relatively infrequent discrete measurements would contribute to a rapid reassessment of the Parkfield earthquake hazard. Sufficient data now exist to define specific criteria for alarm level d; specific criteria for alarm levels a, b, and c must be developed as history of line length changes is obtained.

Two-Color Alarm Level	Line-Length Changes Between Successive Measurements	Anticipated Alarm Frequency (time between alarms)
d	(1) Three lines with coherent (at least 4 length determinations confirming the change on each line) length changes $\geq$ 3.5mm in a 20-day period, with at least one of the line changes $\geq$4.5mm. The change must be twice the uncertainty of the change calculated using analysis of variance techniques. (There have been two such occurrences between Oct. 84 - Oct. 85).	6mo.
	(2) Three lines with coherent (at least 9 length determinations on each line, 6 before and 3 during or after the change) departures $\geq$ 0.175mm/day from the linear length change trend of the previous 30 days.	

c   Not yet defined.

b   Not yet defined.

a   Given the lack of expertise at Parkfield, there are no clear

            threshold that lacking other data would warrant a warning to OES.

E. Alarm Thresholds on Multiple Instrument Networks

Clearly anomalous signals on several networks would increase our concern that a Parkfield earthquake is imminent. Simultaneous alarms can combine to establish a level of concern appropriate to a higher alarm threshold. We propose that a set of simple alarm level combination rules be applied to the alarm levels for the individual network group:

Status of Network Alarm Levels

Rule	Network 1		Network 2		Network 3		Network 4	Combined Alarm Level
1)	e	+	e	+	e	+	e	➤ e
2)	d	+	e	+	e	+	e	➤ d
3)	d	+	d	+	(d or e)	+	(d or e)	➤ c
4)	c	+	(d or e)	+	(d or e)	+	(d or e)	➤ c
5)	c	+	c	+	(c,d, or e)	+	(c,d, or e)	➤ b
6)	b	+	(c,d, or e)	+	(c,d, or e)	+	(c,d, or e)	➤ b
7)	b	+	b	+	(b,c,d, or e)	+	(b,c,d, or e)	➤ a
8)	a	+	(c,d, or e)	+	(d or e)	+	(d or e)	➤ a
9)	a	+	c	+	c	+	(c,d, or e)	➤ a*
10)	a	+	(a or b)	+	(a,b,c,d, or e)	+	(a,b,c,d, or e)	➤ a*

To apply these rules, rank the four network groups in decreasing order of current alarm level status. For example, if the seismic, creep, continuous strain, and geodetic survey alarm levels were c, b, c, and d respectively, then creep, seismic, continuous strain, and geodetic survey would be labelled networks 1, 2, 3, and 4. That is, the networks alarm level status would be b, c, c, d, corresponding to combination rule 6. Rule 6 states that one level b, two level c, and one level d alarm are <u>not</u> sufficient to warrant an alarm level a response - i.e., a warning to OES. It is important to note that the combination rules are non-linear and non-commutative-although rule 5 indicates that two level c alarms combined to yield a level b alarm and rule 7 indicates that two level b alarms combine to yield a level a alarm, rule 6 states that b+c+c+d>b rather than b+(c+c)+d>a.

VI. RESPONSE

The responsibility for initiating the earthquake prediction alarm levels described in this report reside with the project chiefs of the individual Parkfield earthquake prediction networks. Each project chief has the following specific responsibilities:

1) Maintain a real-time monitor system for the data collected by the project.

2) Maintain an effective real-time alarm system capable of detecting signals that exceed the thresholds established for the different alarm levels.

3) Immediately alert the chief scientist and the chief of the Seismology Branch or Tectonophysics Branch of all a, b, c, or d level alarms.

4) Train and maintain an alternate capable of assuming the above responsibilities.

5) Delegate these responsiblities to the alternate whenever the project chief cannot adequately perform these responsibilities. The chief scientist and the appropriate branch chief (Seismology or Tectonophysics) must be notified of this delegation of responsibility.

The earthquake-prediction decision process is summarized in the following flow chart:

Alarm Level d, c, b, or a

Alert Chief Scientist and Branch Chiefs

Alert all Parkfield Project Chiefs

Evaluate Status of all Parkfield Networks. Apply combination rules to determine combined alarm level

Alarm level a, b, or c? — NO

YES

Alert Office Chief

Alarm level a or b? — NO

YES

Alert Director USGS and Alert Calif. State Geologist CDMG

Activate Intensive Reconnaisence Surveys and Intensive Monitoring Efforts

Alarm Level a? — NO

YES

Issue Geologic Hazards Warning to OES
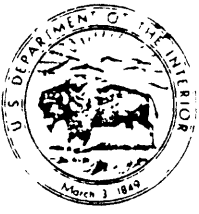
Detail on next page

Detail of decision process
flow chart or preceding
page.

APPENDIX D. 1.

1979 letter to Dr. Ross Schaff, Alaska State Geologist, from Directo·,
USGS, regarding earthquake potential of the Yakaga region of Alaska

United States Department of the Interior

GEOLOGICAL SURVEY
RESTON, VA. 22092

In Reply Refer To:
Mail Stop 905

MAY 3 1 1979

Dr. Ross Schaff
State Geologist
Division of Geology and
  Geophysical Surveys
3001 Porcupine Drive
Anchorage, Alaska 99501

Dear Dr. Schaff:

As Governor Hammond's representative for receiving U.S. Geological
Survey (USGS) information on geologic-related hazards, we are bringing
to your attention some recent conclusions by scientists at the Lamont-
Doherty Geological Observatory, USGS, and others regarding the
earthquake potential of the Yakataga region of Alaska.

Because south-central Alaska is a region in which potentially damaging
earthquakes must be anticipated, the identification of that part most
likely to be the source for the next major earthquake is subject of much
interest. A number of investigators over the past several years have
suggested that the area between Icy Bay and Kayak Island might be a
"seismic gap," that is, a region of unrelieved strain accumulation
between the rupture zones of the 1964 and 1958 earthquakes. The
occurrence of the 1979 St. Elias earthquake (magnitude 7.7) on the
eastern margin of this quiescent zone between the 1958 and 1964
aftershock zones, together with a recent study of seismicity patterns in
this region by Lamont seismologists, raises our concern that one or more
major earthquakes with magnitude near 8 are likely in the Yakataga
seismic gap between Icy Bay and Kayak Island.

The identification of this region as the possible site for a major
earthquake was first suggested a decade ago by Lamont scientists based
on the absence of large earthquakes during the last several decades
along the part of the active plate boundary. Prior to this year, no
large earthquakes had occurred along this segment since 1900. However,
recent investigations of the geologic setting and current earthquake
activity in the region by USGS and Lamont scientists have provided an
understanding of the geologic features and processes that are likely to
cause future major earthquakes in the region.

One Hundred Years of Earth Science in the Public Service

Lamont-Doherty and USGS scientists feel that the recent magnitude 7.7 earthquake of February 28, 1979, near Mt. St. Elias at the eastern end of the Yakataga seismic gap, is an indication of a high level of strain accumulation in the region that may lead to one or more larger earthquakes rupturing the entire gap. At this time, however, there is no way of telling when such an earthquake or earthquakes might occur.

The enclosed manuscript (Enclosure 1), "Yakataga Seismic Gap: Seismic History and Earthquake Potential," by W. R. McCann, O. J. Perez, and L. R. Sykes, which has been submitted to Science for publication, presents the case for heightened concern. As you know, there have been substantial uncertainties about the nature and location of the boundary between the Pacific and North American plates in this region (and hence the source locations for future large earthquakes), and about the nature and amount of slip accompanying the large earthquakes in 1899 and 1900. With the encouragement of the Lamont group, we convened an ad hoc panel of experts from within and outside the USGS on May 21, 1979, to review the current situation. While members of the panel disagreed with some details of the Lamont interpretation, they agreed with the overall concept.

The principal unresolved question remaining from this interpretation is when such an earthquake or earthquakes might be expected to occur. Current observations and understanding do not permit a confident estimate of the time of occurrence of such a future large earthquake. However, arguments based on plate tectonics and known earthquake recurrence rates for similar geologic environments offer some feeling for the imminence of such earthquakes. These and alternative interpretations are discussed in Enclosure 2.

Experts judge that such an earthquake could occur today, but they would not be surprised if it did not occur for several decades. It is possible, though judged significantly less likely, that the region could go for an additional 100 years without a large earthquake.

During the last several years, the USGS has carried out studies in southern Alaska as part of our Earthquake Hazards Reduction Program. In response to the emerging information about the seismic potential of the Yakataga region, and in agreement with the ad hoc panel's recommendation, we intend to intensify our monitoring activities. The two goals are to: 1) obtain any possible precursory information, and 2) develop a clearer understanding of the processes leading to large earthquakes. Activities planned for intensification include:

1. Installation of strainmeters, tiltmeters, strong-motion instruments, and sea-level monitors;

2. Geodetic leveling and trilateration networks;

3. Geologic mapping of faults and coastal terraces; and

4. If possible, precision bathymetric and subbottom acoustic
    profiling.

We will, or course, keep you fully, informed of the results of these
studies as they emerge, especially as they may effect our estimate of
the likelihood or magnitude of an expected earthquake.

We appreciate that the interpretation of this information involves
significant uncertainties which may require additional explanation. We
would be glad to meet with you or other members of Governor Hammond's
staff to answer any questions and to offer any technical assistance we
can in developing plans in response to the potential for a large
earthquake. Because of the possible impact such an earthquake may have,
we are sending copies of this letter to the persons listed on
Enclosure 3.

Sincerely yours,

BILL MENARD

Director

Copy to: Governor Jay S. Hammond

cc: Dir Chron 114
     General 114
     Division 911
     OES File 905
     OES Chron 905
     Wesson 905
     Everyone on Enclosure 3 (External Distribution)
     Everyone on Attached List (Internal Distribution)

GD:RLWesson:jac-5-30-79:860-6471

APPENDIX D. 2.

November 28, 1985, letter from the Council to Director, USGS,
regarding short-term predictions at Parkfield, California;
central California seismicity; and Alaskan seismicity

28 November 1985

Dr. Dallas Peck
Director
U.S. Geological Survey
MS 106 National Center
12201 Sunrise Valley Drive
Reston, Virginia 22092

Dear Dallas,

I am reporting to you several of the important results a d di scussions that came out of the recent meeting of the National Earthquake P ediction Evaluation Council (NEPEC) in Anchorage in September 1985.   At that meeting we reached several conclusions about 1) Parkfield, 2) that section of the San Andreas fault extending from the mid-San Francisco Peninsula to San Juan Bautista and 3) the Calaveras fault of central California.   Those areas were reviewed at our July meeting and were discussed further in executive sessions in September.   At that executive session, the Council also reviewed a proposed decision matrix for Parkfield that was presented by U.S.G.S. personnel.   The decision matrix outlines recommended actions to be taken by U.S.G.S. in response to various observed changes in one or several of the phenomena that are being monitored at Parkfield.   The aim of the decision matrix is to allow such changes to be utilized on a timeframe of a few hours to a few weeks such that a short-term prediction could be made of a forthcoming earthquake at

Parkfield. In addition, much of the meeting in September was devoted t)
a major review of earthquake prediction and earthquake risk for several
parts of Alaska.

In summary, the Council recomme ids:

- The prompt development and adoption of a decision matrix relating
  the observation of potential precursory phenomena to the anticipated
  Parkfield earthquake, and administrative actions, including the
  delegation of authority for the issuance of predictions and rapid
  communication with State and local officials.

- Communication to the Director of the California Office of Emergency
  Services of the levels of concern and ongoing discussions about the
  earthquake potential of the section of the San Andreas fault from
  Black Mountain to San Juan Bautista and of the Calaveras fault north
  of the zone of the 1984 Morgan Hill earthquake.

- Communication with appropriate officials of the State of Alaska
  regarding
  - the high probability for a great earthquake off the Alaska Penin-
    sula to the southwest of Kodiak Island during the next one to two
    decades, and
  - continuing concern about the potential for large earthquakes in
    the "Yakataga seismic gap".

- Periodic communication with appropriate Federal and State of Alaska
  officials about the current level of understanding and concern about

earthquake potential throughout Alaska, the most seismically active region in the Nation.

DECISION MATRIX FOR SHORT-TERM PREDICTIONS AT PARKFIELD, CALIFORNIA

The National Earthquake Prediction Evaluation Council recognizes that as part of the Parkfield earthquake prediction experiment, an opportunity may arise to make a successful and useful short-term earthquake prediction (that is, a prediction in a time frame of a few hours to a few weeks). Furthermore, NEPEC believes that the attempt to make such a prediction should be an important element of the experiment.

In order to translate quickly the occurrence of premonitory signals into a formal prediction and related administrative actions, NEPEC recommends that a decision matrix (e.g., like the draft presented at the September 1985 meeting of NEPEC) be developed that states what physical signals, and what thresholds of signals, are expected to demand what administrative actions. A decision matrix should be formally adopted by the Director, U.S.G.S., after review and advice from NEPEC and other concerned groups. NEPEC further recomends that, for the shortest-term, highest-urgency categories in the matrix, the Director, U.S.G.S., develop a plan to delegate to offices near the data-gathering effort the issuance of predictons and rapid communication of the earthquake alert to selected federal and state officials and other offices. The NEPEC suggests that only by such pre-approval and delegation of action can the shortest-term prediction (i.e., "imminent alerts" as defined by Wallace, Davis, and McNally) be issued rapidly enough for useful reaction, given lead times of only a few hours to a few days. A draft of a decision matrix prepared

by the U.S.G.S. staff wa reviewed at the September meeting of NEPE , and the following comments and suggestions are made:

- NEPEC applauds the September 1985 draft as an excellent step in the right direction.

- A termination date, or a time for a review and upda e, should be prescribed in any earthquake prediction, short- or long-term.

- The possibility that a prediction may be a false alarm should be specifically acknowledged as part of the predictive statement.

- In more general statements about prediction research, the philosophy o willingness to accept some false alarms as a necessary part of the learning process should be more fully acknowledged by the scientific community. Decisionmakers and the public should be made more aware of this possibility and should develop means to minimize the adverse effects of false alarms.

- NEPEC will review a revised draft of the decision matrix as soon as a more-nearly final draft is available. Considering the possible imminence of the Parkfield earthquake, action on the decision matrix should be completed very promptly.

SAN ANDREAS FAULT BETWEEN BLACK MOUNTAIN AND SAN JUAN BAUTISTA AND THE CALAVERAS FAULT

At the July 26-28, 1985 meeting of NEPEC presentations were given that focused on the portion of the San Andreas fault in California extending from San Juan Bautista 75 km north to Black Mountain just west of Cupertino on the San Francisco Peninsula and a portion of the Calaveras fault directly northwest of the rupture zone of the Morgan Hill earthquake of 1984.

The section of the San Andreas fault corresponds to the southernmost portion of the 1906 earthquake fault break. The creeping portion of the San Andreas fault of central California extends south from San Juan Bautista to Parkfield. The Calaveras fault zone runs through Hollister and just east of Gilroy, Morgan Hill, and San Jose. The Council considers the southern portion of the 1906 break currently to have higher risk than adjacent sections of the San Andreas fault for generating a large earthquake because: 1) the 1906 fault offsets in this area were significantly less than the offsets to the north and may now be fully recovered and 2) earthquakes in 1838 and 1865 were possible demonstrations of the capability of this section of the San Andreas fault to generate earthquakes independent of great 1906-type events. The Council also considers the section of the Calaveras fault just northwest of Morgan Hill to possess the potential for a moderate earthquake in the next decade because of low seismic slip in this 20 km region and because of the lack of any clearly identifiable recent moderate earthquakes in the zone.

Several independent investigations of the Black Mountain-San Juan Bautista zone of the San Andreas fault have concluded that there exists a high potential for rupture of at least part of this section of the fault sometime in the coming 20 years. Because of uncertainties intrinsic to the historic data and uncertainties as to the details of the fault slip budget in this area, there is a divergence of scientific opinion about the probability of a large earthquake that would rupture the entire 75 km section of the fault. However, one interpretation admissible by the data is that 1906 slip on the entire 75 km section has now been recovered as

strain build-up and consequently this area may now be capable of generating a large earthquake. Should this entire section rupture, the resulting earthquake would have a magnitude of about 7.0. Because of the proximity of the area to the large populaton centers of the south San Francisco Bay region, such an earthquake would have significant public impact.

The segments of the Calaveras fault that broke in the 1979 Gilroy (Coyote Lake) and 1984 Morgan Hill earthquakes experienced slip deficits in the decades before those events. This appears to be the case now for the section of the Calaveras fault directly northwest of Morgan Hill. Historical seismicity suggests the earthquake recurrence rate for segments of the Calaveras fault to be approximately 80 years. Some uncertainty concerning the association of certain nineteenth century and early twentieth century earthquakes with the Calaveras fault preclude statistical treatment and quantitative statements regarding the imminence of future events northwest of Morgan Hill along the Calaveras fault. However, available evidence does indicate that consideration should be given to the occurrence of an intermediate-sized event of approximately magnitude 6 on the Calaveras fault northwest of Morgan Hill during the next decade.

The Council will examine these areas at future meetings with the aim of clarifying present ambiguities in the interpretations. The Council regrets that the available data do not permit more quantitative and unequivocal statements to be made concerning these fault zones; however, it recommends that the Director of the California Office of Emergency Services be appraised of our current understanding of the potential for a large and moderate earthquake in these areas.

ALASKA AND ALEUTIAN ISLANDS

NEPEC has been meeting about four times per year to review the most recent data and to update our understanding of the seismic potential of some of the regions of the United States where seismic risk is significant and where there may be important public policy issues related to earthquake prediction. In the fourth and most recent of these meetings, NEPEC met in Anchorage, Alaska, September 8-9, 1985 to consider the seismic potential of three areas along the Alaska-Aleutian plate boundary. These areas are the Adak Island vicinity in the central Aleutian Islands, the Shumagin Islands vicinity along the Alaska Peninsula, and the Yakataga vicinity just to the east of Prince William Sound in the northern Gulf of Alaska. Below we summarize the findings of our review of the seismic potential of each area and we give our recommended actions with respect to each area. In addition, we make some general observations about the state of earthquake prediction and earthquake studies in Alaska, including those areas away from the main plate boundary.

Yakataga Seismic Gap

On May 31, 1979, the Director of the U.S. Geological Survey wrote to the State Geologist of Alaska expressing concern about the earthquake potential of the Yakataga region of Alaska, the so called "Yakataga seismic gap". In that letter, the Director indicated that the U.S.G.S. would support additional sutdies in the Yakataga region with the aim of clarifying the earthquake potential, and if possible, to gain insight into when a large earthquake would occur in the region. Since that time a number of geologic and geophysical investigations have been carried out.

On September 8 and 9, 1985, NEPEC met in Anchorage and reviewed the results of investigations to date in the Yakataga region. Observations made since 1979 have not significantly altered the assessment of lon - term seismic risk in the Yakataga seismic gap that were made followi g the 1979 M=7.7 St. Elias earthquake. Trilateration surveys made in the region since 1980 indicate continuing deformation consistent with accum- ulating elastic strains that will even ually be released by the expected gap-filling earthquake. Although the anticipated event is about magn - tude 8, now studies of uplifted coastal terraces between Cape Yakataga and Icy Bay suggest larger events (≈12 m uplift) with longer recurrence intervals (≈1500 years) might also be expected. Indeed, the geolog c record indicates it has been more than 1500 years since the last event f this type. At the same time, investigations to date have not produced any information that might be interpreted as a short- or intermediate- term precursor, which might -- or might not -- precede the expected earthquake. Therefore, the Council concurs with the previous assessment that the earthquake could occur today, or sometime in the next several decades, but that it is significantly less likely that the region could go for an additional 100 years without a large earthquake.

Alaska Peninsula

The question of the seismic potential of the Shumagin seismic gap along the Alaska Peninsula has been under investigation by scientists for a decade and a half. Investigations have included examinations of spatial and temporal patterns of earthquakes along the Alaska-Aleutian plate boundary using data collected by the World-Wide Seismic Network, the

collection and analysis of data from a local seismic network centered in the Shumagin Islands, the examination of historical information on great earthquakes contained in the Russian-language documents of the period from 1738-1867 and the collection and analysis of sea-level, short base-line tilt and intermediate baseline strain data.

It is clear from the spatial and temporal patterns of past seismic activity that there exists a seismic gap of long temporal extent that extends for some 200-250 km along the Aleutian arc in the vicinity of the Shumagin Islands. The answer to the central question of "what is the seismic potential of the Shumagin gap itself" rests on two conflicting sets of data. The tilt and strain data collected over the past 5 to 10 years, and to a lesser extent over the period 1913 to 1984, indicates negligible strain accumulation raising the possibility of aseismic subduction in the Shumagin gap. However, the descriptions of two large earthquakes in 1788 contain reports of local tsunamis with run ups of the order of 10 m at sites ranging from Kodiak Island to Unga and Sanak Island, a distance of about 600 km (400 miles); of strong ground shaking lasting for several minutes; of strong aftershocks lasting for months; and of permanent subsidence on Kodiak Island of several feet. These observations suggest strongly that a great earthquake of about magnitude $M_w=8$ 1/2 ruptured the plate boundary from Kodiak to Sanak Island. There are several significant, unresolved questions having to do with the repeat times for events in the Shumagin gap; however, several lines of evidence suggest that it might be in the range of 50-90 years.

Further, there is evidence that sufficient strain may have accumulated in the adjacent areas that ruptured in the 1938 and 1946 earthquakes and

that the entire region from the southwest tip of Kodiak Island to Unimak Island could rupture in a single event of the size of the 1788 quake. NEPEC is concerned about various evidence that suggests generally high probabilities for rupture of an extensive region offshore of the Alaska Peninsula in the next one to two decades, moreso than it was about the Shumagin region by itself. NEPEC membrs observed with some concern that there is presently no seismic or geodetic monitoring in the area of the 1938 aftershock zone.

NEPEC recommends that the Director of the U.S. Geological Survey issue an advisory to the State of Alaska outlining the above findings and data, indicating that s th consensus of NEPEC that there exists a significantly high probabili y for a great earthquake off the Alaska Peninsula to the southwest of Kodiak Island during the next one to two decades. That broad region and the Yakataga area appear to have significantly higher probabilities of rupturing on that time scale that do other portions of the Alaska-A eutian plate boundary in the United States. NEPEC suggests that it woulc be prudent to consider the consequences of strong shaking and tsunami ii nundation on coastal communities of southern Alaska that are likely to be affected by the occurrence of large earthqu..kes near the Alaska Peninsula and in the Yakataga gap.

Adak Region of Central Aleutians

Dr. Carl Kisslinger presented data indicating a period of seismic quiescence in the Adak Canyon region in the central Aleutians. On the basis of this quiescence as well as the historical seismicity data in the region, he concludes that an earthquake with surface-wave magnitude   or

greater will occur there. On the assumption that the observed case of a three-year premonitory quiescence is characteristic, he suggests that the most likely time is before the end of October 1985. Kisslinger stated hat, because of the remoteness of the area, the social impact of an M of about 7 earthquake in this area is considered relatively minor.

The area in question is near Adak Canyon, which is located in the rupture zone of the great Fox Island earhtquake (M=9±) in 1957. Prior to the 1957 event, earthquakes of about magnitude 7 or greater occurred in the Adak Canyon region at approximately 10 year intervals. Since the 1957 event, the area has been quiet, except an M=7.2 earthquake, which occurred in 1971.

Kisslinger presented evidence that a similar seismic quiescence was observed before an M=7.2 earthquake that occurred in the Adak Island region in 1971. However, the pattern of quiescence preceding the 1971 event is more obvious in the teleseismic data than is the present pattern.

In general, the Council thinks that prediction methodology based on seismic quiescence is not established yet, and requires further investigation as to its general applicability, false alarm rate, etc.

Kisslinger's data provide a means for testing this methodology. Nevertheless, the Council is of the opinion that in view of the ambiguity of the data and the methodology of this prediction, as well as the relatively low hazard potential of the predicted event, no public action is waranteed at this time with respect to this prediction.

The Council thinks, however, that the probability of an earthq ake with M greater than 7 o curring in the area in the near future is h gh, solely on the basis of he historical seismicity data, so that the area needs to be carefully wat hed regardless of this prediction.

State of Earthquake Prediction in Alaska

The quantitative assessment of the probability of a future, great earthquake, that is one of magnitude $M_w \geq 7.8$, that would rupture a specific segment of the Alaska-Aleutian plate boundary rests critically on knowing when that segment last rup ured and on a determination of the average recurrence interval (and the associated variance) for great ear hquakes along that segment. Most of the Alaska-Aleutian plate boundary as ruptured relatively recen ly (since 1938) so the date of the last event is generally well known. However, only the date of at most one revious event that ruptured a given segment is known, so that calculati n of an average recurrence interval and its variance depends on indirect method that use averages determined for the entire plate boundary, or that use the rate of relative plate motion as a basis for calculation of the expected interval. Fu ther, there exists some controversy about how to reconcile the relatively long recurrence intervals (500 to 2,000 years) determined for uplift of marine terraces at Middleton Island and along the mainland coast between Yakataga and Icy Bay with the shorter intervals (50-150 years) between great earthquakes observed and calculat d from seismological data.

Our knowledge of the seismic potential of specific fault segments for crustal faults away from the plate boundary is even more limited. Sinc

1900 in south central and interior Alaska there have been at least a dozen potentially damaging earthquakes ($M_s \geq 6.5$) that occurred at shallow depths in the crust to the north of Anchorage. None of these events has been unequivocally associated with any mapped fault; on the basis of proximity alone (without benefit of supportive focal mechanisms or observed ground breakage) a few of these events may be presumed to have been associated with a specific fault.

In summary, it is evident that much basic work remains to be done before the data will be available on the basis of which sound earthquake predictions could be made for specific fault segments. In this light, it is clear that renewed emphasis needs to be placed on those studies that will yield fundamental information about recurrence intervals and characteristic earthquakes for faults in Alaska. Such studies would include seismic and geodetic monitoring, historical seismology, basic geological mapping, and focussed geological studies such as trenching which have come under the heading of paleoseismology.

In the meantime, these limitations on our ability to make specific earthquake predictions should not prevent us from communicating what we do know. Alaska includes some of the most seismically active regions in the world. It is the most active state in the United States. Federal, State, local and private investment continues to develop an increasingly interrelated infrastructure in Alaska that is vulnerable to this severe seismic hazard. In planning and designing for this development it is important for federal and state agencies in Alaska to take the lead in the incorporation of measures to reduce losses from future earthquakes.

To this end, it would be he pful for the Director of the U.S. Geological Survey to periodically communicate to appropriate Federal and State officials in Alaska the current level of understanding and concern that exists among professionals working on earthquake problems in Alaska. Some points which could be emphasized in a letter from the Director are summarized below:

- Alaska contains some of the most seismically active regions in the world. In this century three of the ten largest earthquakes in the world occurred along the Alaska-Aleutian subduction zone.

- The U.S. portion of the Alaska-Aleutian subduction zone, which extends from Attu to Cordova and includes the Anchorage area, experiences a potentially damaging earthquke ($M_s > 6.5$) every 8 months on the average. Since the turn of the century there have been 7 great (magnitude $M_s > 7.8$) earthquakes in the region; about one every 12 years. The last such event occurred in 1965. Three of these events had magnitudes greater than 8.7 and are among the 10 largest earthquakes to occur in the world during this century: 1957 Andreanof-Fox Island, $M_w = 8.7$; 1964 Prince William Sound, $M_w = 9.2$; 1965 Rat Island, $M_w = 8.7$.

- The southeast Alaska transform-fault zone, which extends from Cordova to Ketchikan, experiences a potentially damaging earthquake ($M_s \geq 6.5$) every 3 years on the average. Since the turn of the century there have been 3 great ($M_s \geq 7.8$) earthquakes in this region; about one every 28 years. The last such event occurred in 1958. Horizontal displacement on the Fairweather fault during the 1958

event reached 21 feet near Crillon Lake, and the stron; sha ing that
resulted caused a hugh rockslide in Lituya Bay which in tur created
a water wave that washed all the soil and trees from the opposite
shore to an elevation of 500 m (1700 feet) above sea level.

- The central Alaska seismic zone is included in the broad are encom-
  passed by Anchorage, Tok, Kotzebue and Nome. Most of the ear hquakes
  in this zone occur in the vicinity of the transportation corridor
  between Fairbanks and Anchorage, with a few of the larger events
  occurring to the west of Fairbanks in a broad area extending through
  the Seward Peninsula.   Potentially damaging earthquakes ($M_s > 6\,5$)
  occur in the central Alaska seismic zone every five years on the
  average.   Since the turn of the century 6 major ($M_s = 7.25$) earth-
  quakes have occurred in this zone; about one every 14 years.   The
  last such event was in 1958 near Huslia.

- In addition to the strong shaking associated with every large earth-
  quake, the coastal regions of southern Alaska also have experienced
  the destructive power of tsunamis (sea waves generated by the
  large-scale motion of the sea floor during a major earthquake).
  Since the turn of the century 14 tsunamigenic earthquakes have
  occurred along the south coast of Alaska from Amchitka to Sitka.
  Five of these events cause local run-up (maximum height above sea
  level of the wave as it crests on shore) in excess of 6 m (20
  feet).   During the 1964 Prince William Sound earthquake more than
  100 of the 130 total lives lost were a direct result of the
  tsunami.   In southeast Alaska landslides without earthquakes have
  also been a significant source of water waves with large local

run-up: two such events have caused run-up in excess of ɔ m (20 feet).

- There are two areas of southern Alaska that are of special concern because their specific earthquake history suggests that the probability of a great earthquake in these regions during the next one or two decades, is significantly higher than other areas of southern Alaska. One is the Alaska Peninsula area from the southeast end of Kodiak Island to Unimak Island and the other is the Yakataga area from Cordova to Icy Bay. (See the detailed discussion above about these two areas.)

Copies of the summaries of various papers presented at the September meeting in Ancorage will be sent to you separately and will be included in an Open File report along with a revised copy of the decision matrix for Parkfield. The letter of May 31, 1979 from the Director of the U.S.G.S. to the State Geologist of Alaska will be included as an appendix along with a paper describing planned updating of magnitudes in the U.S.G.S. catalogs for California, which was presented to the executive session of NEPEC on September 9.

Sincerely yours,

Lynn R. Sykes
Chairman, National Earthquake
Prediction Evaluation Council

LRS/llm

In summary, the Council recommends:

The prompt development and adoption of a decision matrix relating the observation of potential precursory phenomena to the anticipated Parkfield earthquake, and administrative actions, including the delegation of authority for the issuance of predictions and rapid communication with State and local officials.

- Communication to the Director of the California Office of Emergency Services of the levels of concern and ongoing discussions about the earthquake potential of the section of the San Andreas fault from Black Mountain to San Juan Bautista and of the Calaveras fault north of the zone of the 1984 Morgan Hill earthquake.

- Communication with appropriate officials of the State of Alaska regarding
    - the high probability for a great earthquake off the Alaska Peninsula to the southwest of Kodiak Island during the next one to two decades, and
    - continuing concern about the potential for large earthquakes in the "Yakataga seismic gap".

- Periodic communication with appropriate Federal and State of Alaska officials about the current level of understanding and concern about earthquake potential throughout Alaska, the most seismically active region in the Nation.

APPENDIX D. 3. a.

K. Jacob and J. Taber - seismicity in the Shumagin Islands

Lamont-Doherty Geological Observatory | *Palisades, N.Y. 10964*
of Columbia University

December 2, 1985

Dr. Lynn Sykes
Chairman, National Earthquake Prediction
  Evaluation Council
Lamont-Doherty Geological Observatory
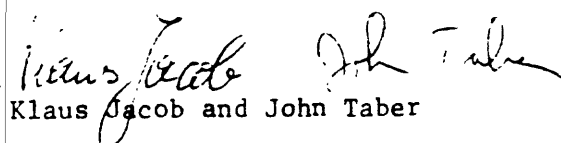 of Columbia University
Palisades, NY 10964

Dear Lynn:

We strongly feel that recent seismicity in the Shumagin Islands warrants an update to our presentation at the NEPEC meeting held in September in Anchorage. At that time we did not have the now available data to identify any intermediate- to short-term precursors. The recent seismicity in the Shumagins may represent such a precursor.

In our judgment the new information contained in the attached report is not sufficient grounds for a more precise temporal prediction of any impending large or great earthquakes in the Eastern Aleutians, because we do not know the false alarm rate or precursor duration (if any) that might be associated with such seismicity changes. However, we feel strongly that an increased state of awareness for the possibility of large or great future events is necessary. Our recommendations are both short- and long-term. We have sent a short note to John Davies, the Alaska state seismologist, which he is circulating within the state to increase awareness of state agencies. We are in the process of devising a plan of action so that we can respond quickly if a major event occurs.

By early 1986 we will be able to monitor the seismicity in nearly real time. The hardware for our new automatic processing system is close to operational and we are working hard on completing and implementing the necessary software. Once installed, it will be a great improvement over our current 2-3 week lag between the collection of the data and their arrival at Lamont. John Beavan is currently in China so he is not available for suggestions, but we feel that more intensive and more frequent, perhaps continual crustal deformation measurements are needed in the region. Additional tilt meters or more frequent geodetic leveling surveys and laser trilateration could be a valuable addition to the current telemetered precision sea level gauges, yearly leveling and bi-annual geodimeter surveys. If the NEPEC panel is available at the Fall AGU meeting, we could present an update of the situation at that time. Of course we cannot exclude the possibility that a significant event may occur even prior to that time. We will keep you informed of any new developments.

Sincerely,

Klaus Jacob and John Taber

KJ:JT/ajd
Enc.

Recent Seismicity Data from the Eastern Aleutians

John Taber and Klaus Jacob
Lamont-Doherty Geological Observatory of Columbia University
Palisades, NY 10964

Estimates of long term probabilities for the occurrence of great earthquakes (Mw ≥ 7.8) in the Alaska-Aleutian seismic zone have revealed a broad region in the Eastern Aleutians with moderate to high probabilities for great earthquakes during the next two decades (Jacob, 1984; Nishenko and Jacob, 1985). The probabilities range from 30% to more than 90% for the 20 year period from 1985 to 2005. Temporal variations of seismicity and crustal deformation in the Shumagin Islands have been noticed during the last ten years, but none of the variations were considered intermediate- to short-term precursors for a great earthquake (Hauksson et al, 1984; Beavan et al, 1983, 1984). Unusual seismicity patterns and rates extending over the entire high-probability region during the period 10/01/85 to 11/15/85 may represent such a pre-cursor.

Five years of relative quiescence at the Mb ≥ 5.5 level in the Shumagins (Hauksson et al, 1984) has now been followed by a high rate of seismicity. In the 5-week interval between October 9 and November 14, 1985 a sequence of 5 moderate events with Mb = 6.4, 5.0, 5.2, 5.0, and 5.6, occurred in the Shumagin Islands region of the Eastern Aleutians. This level of activity is considerably higher than the average rate over the past 22 years, during which time there have been only 30 events with Mb > 4.9. Without eliminating possibly dependent events, the nominal long-term average rate prior to the recent sequence was thus one event about every 9 months. Figure 1 (top) shows eastern Aleutian events shallower than 70 km with Mb > 4.9 that have occurred between 1964 and September, 1985. The space-time plot (Figure 1, bottom) plots the same data as the top figure except that events near the trench have been removed and the recent sequence has been included. Several temporal clusters of events can be seen in the Shumagin seismic gap over the 22-year period but none have had as many

events as the recent sequence.

This situation may be analogous to both the 1957 and 1964 great earthquakes, where there was an increase of seismicity prior to the mainshock (Kanamori, 1981). In the case of the 1957 earthquake (Mw ~ 9) there was a clustering of events before the mainshock at both ends of the subsequent rupture zone (House et al, 1981). The cluster at the western end developed over a three year period while the eastern cluster occurred two months before the mainshock. Figure 2 compares the seismicity in the eastern Aleutians for the 9-month time period 85/01/01 - 85/09/30 to the six-week period 85/10/01 - 85/11/15 using events > 4.9 from the Preliminary Determination of Epicenters (PDE) catalogue. Clustering is evident in the shorter, more recent plot both in the Shumagin Islands and the Unalaska area. The entire area between the two clusters is part of Nishenko and Jacob's (1985) high-probability zone. Thus we may be witnessing a precursory sequence for not just the Shumagin gap, but for the Unalaska gap (House et al, 1981; Boyd and Jacob, 1986) and intervening area as well.

The significance of the apparent clustering depends on two questions: 1. Can the Shumagin earthquakes be considered a mainshock-aftershock sequence? And 2. How often has similar clustering not been followed by an earthquake? We have not finished the analysis of the sequence, but while several of the 5.0 events would be expected in the aftershock sequence, it seems uncertain whether the Mb 5.6 event 5 weeks after the mainshock should be considered an aftershock. The question of clustering is perhaps best addressed by the cumulative seismicity plot in Figure 3. The lower two lines are the cumulative number of events in the regions 157-162 and 166.5-171.5 degrees W longitude, while the upper line is the sum of the two regions. The recent increase in seismicity shows up clearly in the eastern region and the sum of the regions, but the short-term increase is not unusual for the western region. There is perhaps only one other time (early 1974) in the last 22 years when there was an increase in both regions simultaneously. We infer from this observation that the recent clustering is somewhat unusual. However, there may not have been a great earthquake

in the Shumagin gap since 1847 (Davies et al, 1981) so we are only examining 22 years out of a 138 year cycle.

In addition to the "clustering" for moderate-sized earthquakes, the microseismicity rate in the Shumagin region has increased by 35 to 80% during the past six months (Figure 4). The rate increases were calculated by comparing the rate during the 6-month period (April, 1985 through September, 1985) to rates during previous periods since 1979. Note that the rate calculations do not include the October 9, Mb=6.4 mainshock and its aftershocks. The rate increase preceding the clusters of moderate sized events extends to the deepest events (~250 km) and covers the entire network and areas to the west. The value of the rate of change depends on the magnitude cutoff and the size of the region used. For events with magnitudes ≥ 2.5 that lie between 158.5 and 166 degrees W longitude the rate increase for the 6 months since April, 1985 is 37% and is significant at the 98% confidence level (z-test of Habermann (1981)). The catalog should be complete at this level (Hauksson et al, 1984). The highest rate of increase is observed when smaller magnitude events are included but we can't guarantee that this is not due in part to a change in the detection threshold.

The regional extent of the rate increase is in contrast to a proposed, mostly aseismic slip event in 1978-80 (Beavan et al, 1983,1984). In that case a similar or larger rate increase occurred, but it was confined to only a ~100 km wide portion of the 350 km wide Shumagin gap. One might imply that now the entire gap is in the early stages of an aseismic slip event that could represent slip-weakening precursory to a significant strain releasing event. We are awaiting processing of the Shumagin tide gauge data to see whether there is any tilt signal resolvable above the noise.

Another possible parallel to the earlier aseismic slip event concerns Pavlof volcano. There has not been an eruption at Pavlof volcano up to November 30 of this year nor at any time last year. Pavlof has erupted almost yearly and usually in November or December since monitoring began in 1973, except during the years 1977-1979, which

included the aseismic slip event (McNutt and Beavan, 1986). Both the increase in microseismicity and the temporary cessation of Pavlof eruptions started perhaps as much as a year before a change in ground tilt was measured in the previous aseismic slip event. Whether the new increase in seismicity and the recent inactivity of Pavlof is followed by another slip event (either seismic or aseismic) remains to be seen.

In our judgement this new information is not sufficient grounds for a more precise temporal prediction of any impending large or great earthquakes in the Eastern Aleutians because we do not know the false alarm rates or precursor durations (if any) that might be associated with the above observations. None of the patterns taken individually are unique but the combined data suggest that some widespread change in the tectonic activity may have occurred in the last few weeks or months in the eastern Aleutian region. Thus we strongly feel that an increased state of awareness for the possibility of large or great future events is necessary, and we have conveyed this concern to the proper agencies of the state of Alaska.

References

Beavan, J., E. Hauksson, S.R. McNutt, R. Bilham, and K.H. Jacob, Tilt and seismicity changes in the Shumagin seismic gap. *Science, 222*, 322-325, 1983.

Beavan, R.J., R. Bilham, and K. Hurst, Coherent tilt signals observed in the Shumagin seismic gap: Detection of time-dependent subduction at depth?, *J. Geophys. Res., 89*, 4478-4492, 1984.

Boyd, T.M., and K. Jacob, Seismicity of the Unalaska region, *Bul. Seimol. Soc. Am.*, in press, 1985.

Davies, J.,L. Sykes, L. House, and K. Jacob, Shumagin seismic gap, Alaska Peninsula: History of great earthquakes, tectonic setting and evidence for high seismic potential, *J. Geophys. Res., 86*, 3821-3856, 1981.

Habermann, R.E., Precursory seismicity patterns: Stalking the mature seismic gap, in *Earthquake Prediction, An International Review, Marice Ewing Series, 4*, edited by D.W. Simpson and P.G. Richards, pp. 29-42, AGU, Washington, D.C., 1981.

Hauksson, E., J. Armbruster, and S. Dobbs, Seismicity patterns (1963-1982) as stress indicators in the Shumagin seismic gap, *Bul. Seimol. Soc. Am.,74* 2541-2558, 1984.

House, L.S., L.R. Sykes, J.N. Davies, and K.H. Jacob, Identification of a possible seismic gap near Unalaska Island, Eastern Aleutians, Alaska, *Earthquake Prediction, An International Review, Marice Ewing Series, 4*, edited by D.W. Simpson and P.G. Richards, pp. 81-92, AGU, Washington, D.C., 1981.

Jacob, K.H., Estimates of long-term probabilities for future great earthquakes in the Aleutians, *Geophys. Res. Lett., 11*, 295-298, 1984.

Kanamori, H., The nature of seismicity patterns before large earthquakes, *Earthquake Prediction, An International Review, Marice Ewing Series, 4*, edited by D.W. Simpson and P.G. Richards, pp. 1-19, AGU, Washington, D.C., 1981.

McNutt, S.R., and J. Beavan, Periodic Eruptions at Pavlof Volcano: The effects of sea level and an aseismic slip event, submitted to *J. Geophys. Res.*, 1985.

Nishenko, S.P. and K.H. Jacob, Hazards evaluation for large and great earthquakes along the Queen Charlotte - Alaska - Aleutian seismic zone: 1985-2005, presented at NEPEC meeting, September, 1985, Anchorage, Alaska.

Figure Captions

Figure 1. Top: Shallow seismicity (< 70 km, Mb > 4.9) in the eastern Aleutians from 1964 through September, 1985 from the Preliminary Determination of Epicenters catalog. Events south of the dashed line are not included in the space-time cross section along line A-A' plotted below. The recent Shumagin sequence is not shown but the area is circled.

Bottom: Space-time cross section along line A-A' above. Same data as above except the recent sequence is included and trench events are excluded.

Figure 2. Comparison of 9 months of recent seismicity (top) to the last 6 weeks using the same selection criteria as Figure 1. Note the high rate during the recent 6-week period and the clustering of the events in the areas marked east and west.

Figure 3. Cumulative number of events from the PDE catalog for the eastern and western regions marked in Figure 2. The top line is the sum of the two regions. Possibly dependent events are not removed.

Figure 4. Cumulative number of events located by the network between 158.5 and 166 degrees W longitude. The top line (lefthand scale) includes all magnitudes while the lower curve (righthand scale) includes magnitudes $\geq$ 2.5. Possibly dependent events are not removed. The lower curve starts at a later date because of incomplete magnitude determinations in the earlier data. The 37% change in rate in April 1985 is significant at the 98% confidence level. Its approximate onset is marked by an arrow.
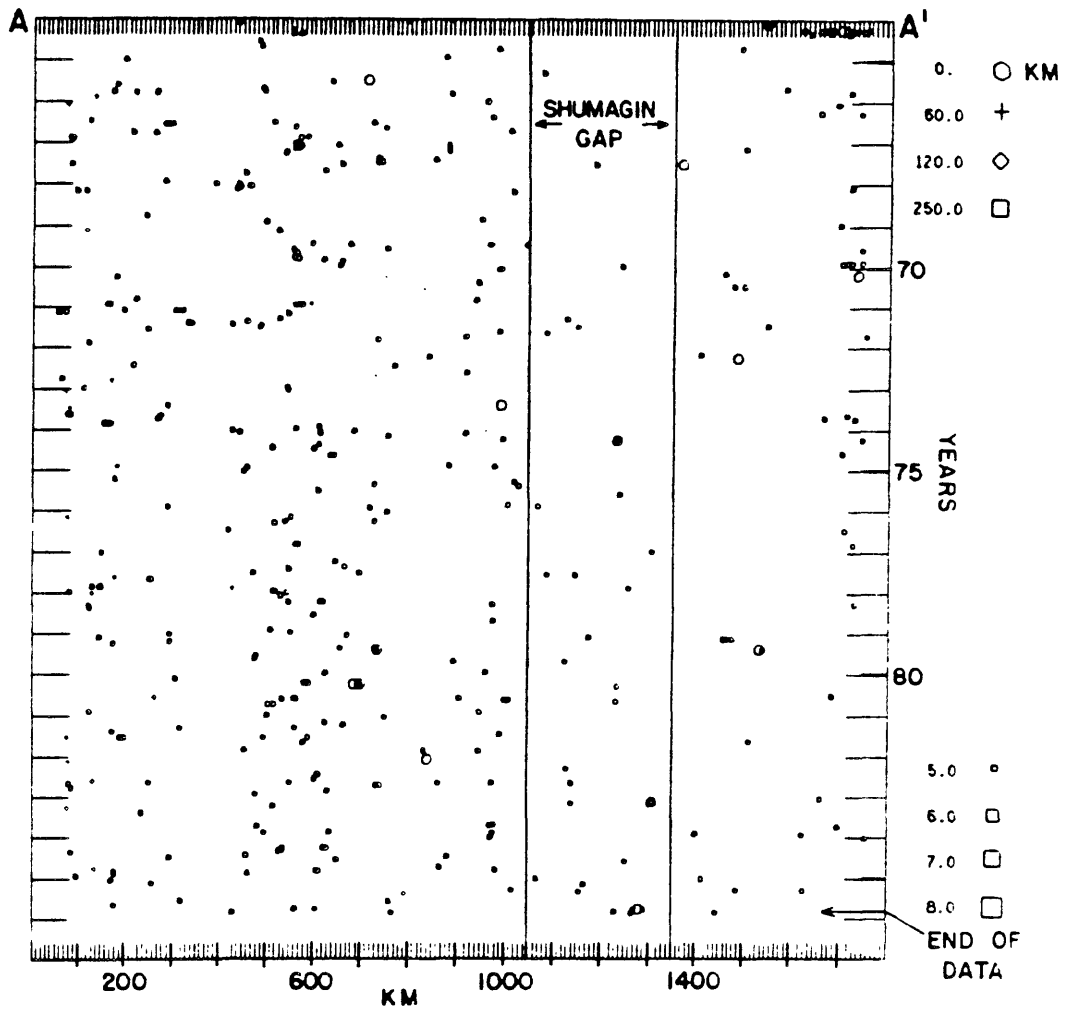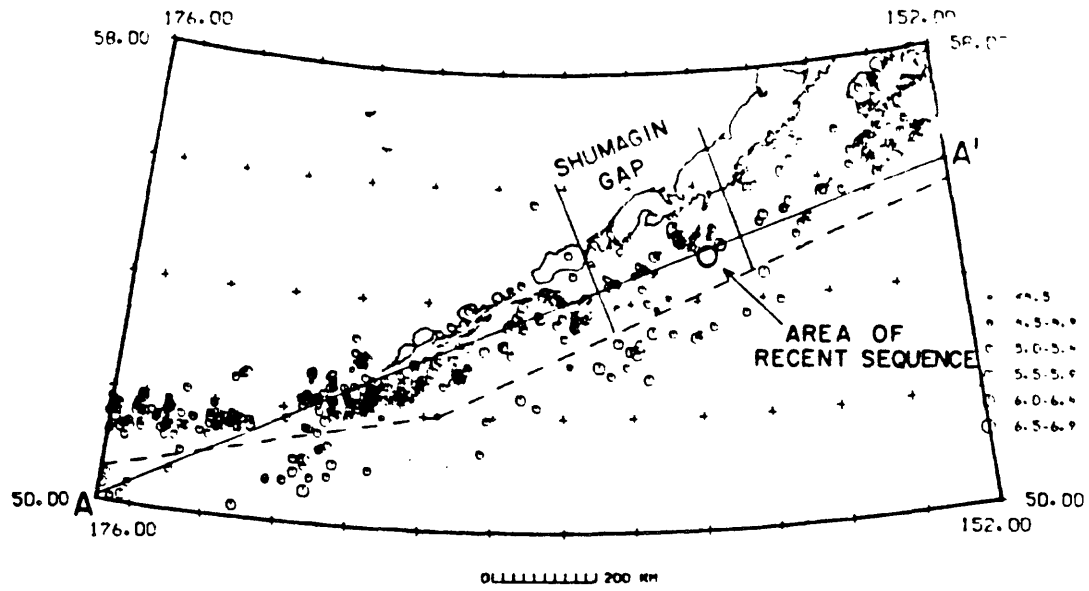
SHUMAGIN
GAP

AREA OF
RECENT SEQUENCE

A'

A

SHUMAGIN
GAP

0.   ○ KM
60.0   +
120.0   ◇
250.0   □

70

YEARS

75

80

5.0   ○
6.0   □
7.0   □
8.0   □
END OF
DATA

200   600   1000   1400
KM

85/01/01 - 85/09/30   9 MONTHS
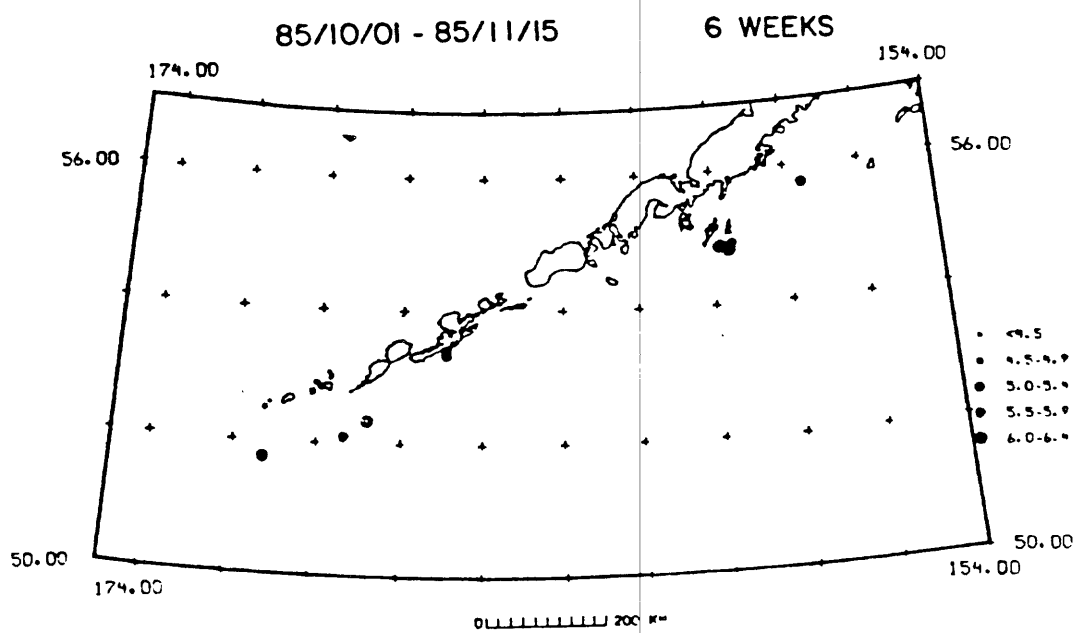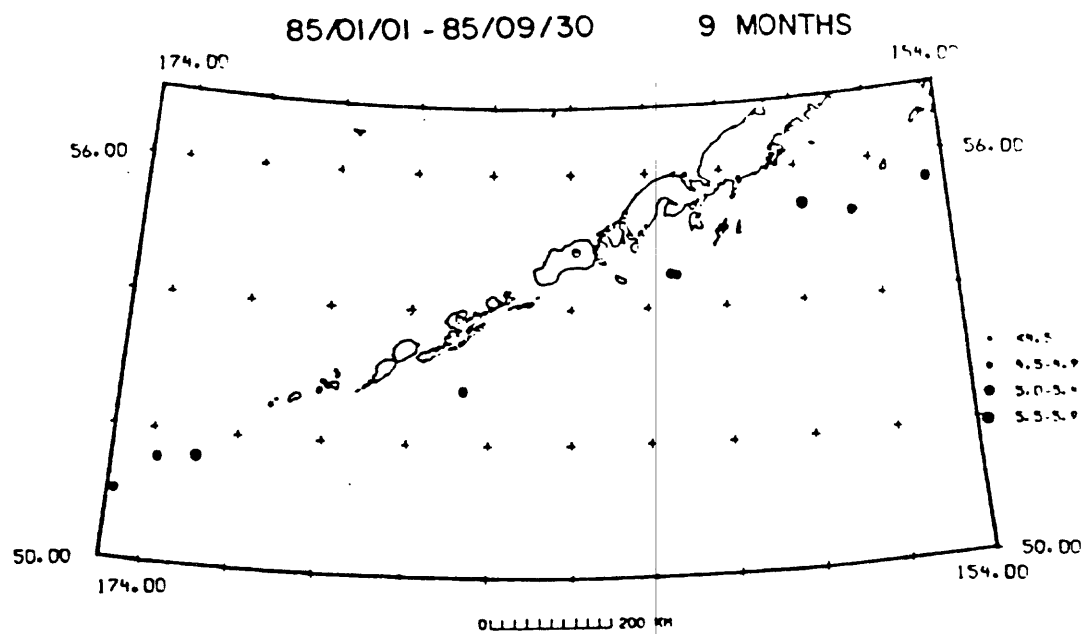

85/10/01 - 85/11/15   6 WEEKS

Figure 2.

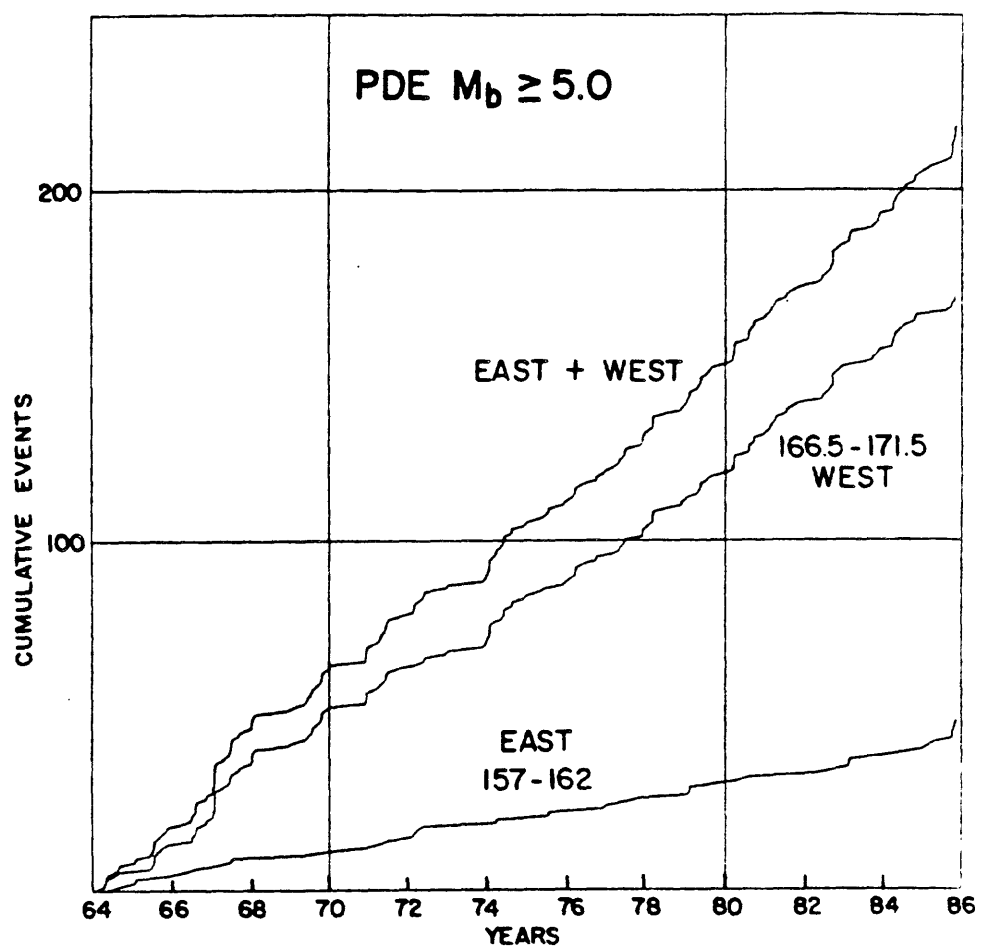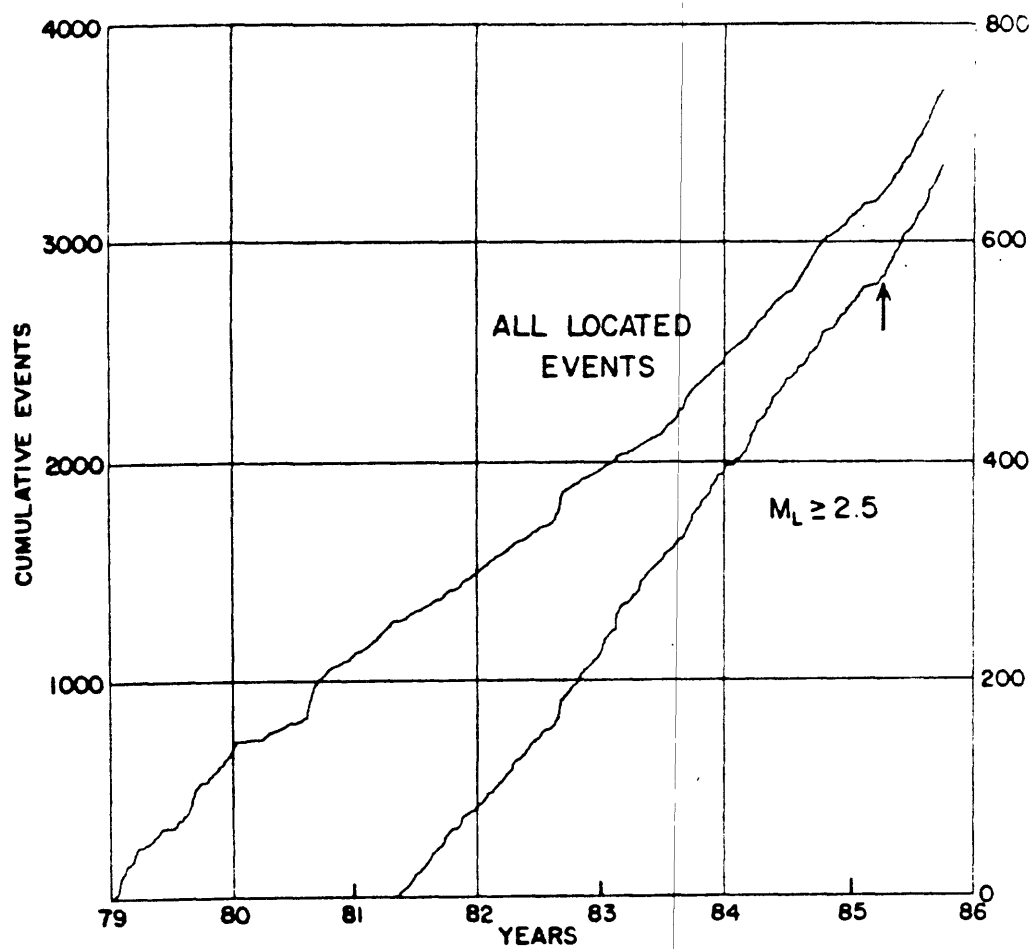Figure.

APPENDIX D. 3. b.

C. H. Scholz - seismic hazard on the San Andreas fault from
mid-San Francisco peninusla to San Juan Bautista

Lamont-Doherty Geological Observatory | *Palisades, N.Y. 10964*
of Columbia University

November 15, 1985

Prof. Lynn R. Sykes
National Earthquake Prediction Evaluation Council
Lamont-Doherty Geol. Obs.
Palisades, NY 10964

Dear Lynn:

At the NEPEC meeting of July 27, 1985, I presented a case for relatively high seismic hazard for the southern section of the 1906 rupture on the San Andreas fault, from Black Mountain to San Juan Bautista. At the meeting, Wayne Thatcher, of the USGS, presented a contrary view: based on his (Thatcher, 1975) inversion of geodetic data, he concluded that there was no slip deficit for the southern part of the 1906 rupture and hence that the record of surface slip, critical to my argument, was not representative of slip at depth.

Thatcher pointed out that his inversion of triangulation data included both the era of the 1868 earthquake and the 1906 earthquake, but that he doubted that the 1868 earthquake contributed significantly to the geodetically measured earth movements. A review of the data does not confirm this opinion. Hayford and Baldwin (1908) analyzed the same data but divided it into the two eras of the 1868 and 1906 earthquakes. Their results are shown in Map 24 of the Lawson (1908) report.

From that figure and the accompanying report we can see that the only triangulation point which is diagnostic of slip on the San Andreas fault between Black Mountain and San Juan Bautista is Loma Prieta, and that movement of this point would thus dominate any inversion scheme for this part of the fault. Hayford and Baldwin's result is that the movement of Loma Prieta was 3.3 M SSE in 1868 and only 0.97 M SSE in 1906. Thus Thatcher's inversion of this data for this section of the fault primarily reflects movements in the 1868 earthquake and not of the 1906 earthquake. Hayford and Baldwin's results for the movement of Loma Prieta in 1906 is, within the estimated error, consistent with the measured surface slip (1-1.4 M) for that section of the fault, and hence is consistent with the case made by me concerning seismic hazard for that fault segment.

Since this point is a serious one, and from my reading of the NEPEC meeting minutes, entered seriously into the deliberation of the Council on this matter, I wish this reply to be circulated to the Council members and appended to the open-file report on the meeting.

Prof. Lynn R. Sykes
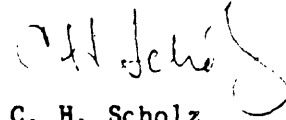Nat'l Earthquake Pred. Eval'n Council   November 15, 1985

References:

Thatcher, W. Strain accumulation and release mechanism of the 1906 San Francisco Earthquake, J. Geophys. Res., 80, 4862-4872, 1975.

Hayford, J.F. and A.L. Baldwin, Geodetic Measurements of Earth Movements in, The California Earthquake of April 18, 1906, ed. Lawson, A.C. et al., Carnegie Inst., Washington, pp. 114-140, 1908.

Sincerely,

C. H. Scholz

CHS/ajd

APPENDIX D. 3. c.

G. Plafker - marine terraces of Middleton Island

United States Department of the Interior

GEOLOGICAL SURVEY
Branch of Alaskan Geology
345 Middlefield Road, MS 904
Menlo Park, California 94025

September 11, 1985

Memorandum

To   : Jim Dietrich, Tectonophysics Branch, U.S.G.S., Menlo Park, CA

From   : George Plafker, Br. of Alaskan Geology, U.S.G.S., Menlo Park, CA

Subject: Question you posed at NEPEC meeting regarding removal of evidence
          for the 1964 marine terrace at Middleton Island

I regret that I could not think quickly enough on my feet to understand what
you were driving at when you asked about the possibility that post-1964
marine erosion could remove all evidence for the 1964 co-seismic terrace at
Middleton Island. My reply that it could happen, although correct, did not
get at the heart of what I suspect you really wanted to know. A more
complete answer to your question is that the terrace certainly <u>can</u> be
removed, but only <u>after</u> erosion of the bedrock platform seaward of the
terrace has progressed to the point where it intersects the terrace. In
fact, all but the higher two terraces were cut into and removed in exactly
this way along the southern windward side of the island as was indicated on
the profiles and map I showed during my presentation (they are also in my
paper on the Middleton Island terraces in OF 78-943).

The most effective surf erosion occurs in the lower part of the intertidal
zone which is 200-700 m offshore. Thus, a slope break will develop at about
the low tide position and it will gradually cut back across the platform
towards the shoreline. The slope break will also progressively increase in
height reaching about 2.5 m (the average tide range) at the present
shoreline. <u>Only then</u> could erosion of the 1964 terrace begin. Note that if
a co-seismic uplift occurs at some time after the notch in the intertidal
zone develops and before it cuts away the 1964 terrace, it would be recorded
as a new sea cliff and corresponding terrace providing that the uplift is
large enough to raise those features above the extreme high tide level. The
attached cartoon illustrates the process.

Judging from the profiles of the dated marine terraces and the submarine
platform, this process would require centuries at the south end of the
island where the platform is narrowest and erosion rates are highest; it
could easily be a millennium or more at the north end of the island where
the platform is 700 m wide. Your question has got me thinking about the
possibility of reexamining the profiles of dated terraces and the
bathymetric data in order to quantify the rate of terrace cutting at
Middleton Island as good data on this subject are virtually non-existent
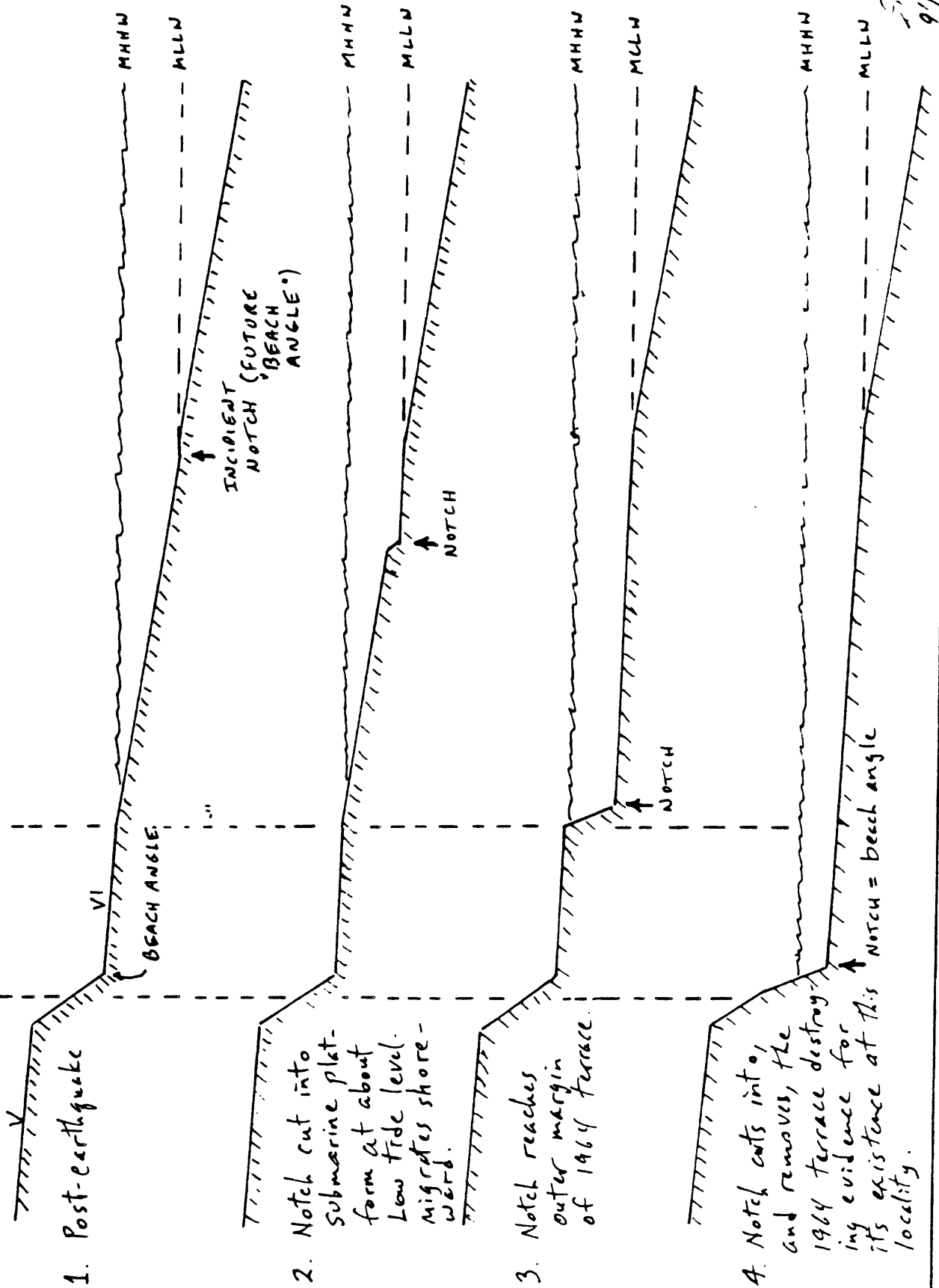elsewhere.

I hope this clears up the matter, but please let me know if problems remain. Copies of this memo are being sent to the other committee members for their information.

George Plafker

cc: NEPEC members

261

1964 TERRACE

1. Post-earthquake

V1

BEACH ANGLE

MHHW

MLLW

INCIDENT NOTCH (FUTURE "BEACH ANGLE")

2. Notch cut into submarine platform at about low tide level. Migrates shoreward.

MHHW

MLLW

NOTCH

3. Notch reaches outer margin of 1964 terrace.

MHHW

MLLW

NOTCH

4. Notch cuts into, and removes, the 1964 terrace destroying evidence for its existence at this locality.

MHHW

MLLW

NOTCH = beach angle

SP
9/10/85

Schematic evolution of shoreline and offshore intertidal zone following the 1964 uplift at Middleton Island.

APPENDIX D. 3. d.

J. Beavan - sea-level measurements in the Shumagins

RECENT SEA-LEVEL DATA FROM THE SHUMAGIN SEISMIC GAP
- DETECTION OF REVERSE TILT ??

John Beavan

Lamont-Doherty Geological Observatory of Columbia University
Palisades NY 10964

It is the purpose of this note to bring to NEPEC's attention data acquired since the October 1985 meeting that possibly signals the onset of a reverse slip event in the Shumagin Islands, similar to that observed in 1978-80.

Since July 1985 three sea-level gauges using Paros pressure sensors have operated in the Shumagins. These sensors have much improved long-term stability than the previous ones, and we are now confident of detecting long-term relative sea-level changes at the 10mm level. Low-pass filtered differences between the gauges are shown in Fig. 1, with a sea-level scale on the left and a ground-tilt scale on the right. A change from essentially no long-term tilt to ~ 2.5μrad/yr down away from the trench occurred in September or October, just before the recent sequence of M5 and M6 earthquakes. This tilt is in the same direction and at approximately the same rate as the 1978-80 tilt reversal detected by level lines. The tilt change is observed on both difference signals (SQH-PRS and PRS-SIM) and is therefore unlikely to represent instrument malfunction. The relative sea-level change between SQH and SIM is ~ 60mm between October 1985 and December 1985; we believe this is substantially greater than could be accounted for by instrument drift, temperature or salinity effects. It is therefore possible that the October - December 1985 apparent tilt may represent the onset of a tilt reversal similar to that in 1978-80, whose implications for a major earthquake were discussed at the October NEPEC meeting.

However, there is an alternative, non-tectonic, explanation of the observed signals. This alternative is oceanographic in origin, but it will be possible to use the data to distinguish the tectonic from the oceanographic source. An ~ 300 mm annual cycle exists in sea-level from the Gulf of Alaska to the Aleutians. This is due to seasonal fluctuations in the North Pacific gyre. Sea-level typically begins to rise in September/October, then to fall in February/March. It is possible that the amplitude of this cycle decreases with distance from the coast, so that it is substantially smaller at SIM than at SQH; our previous years' data (using less stable sensors) are equivocal on this point. However, such a scenario could explain our present observations.

By the end of March 1986, assuming the gauges survive the worst of the winter storms, it will be clear which explanation holds: if the observed signal has changed direction by then, it is probable that the oceanographic "annual cycle" mechanism is responsible; if not, then the tectonic mechanism becomes more likely. This information will be passed on to NEPEC as soon as it is available.
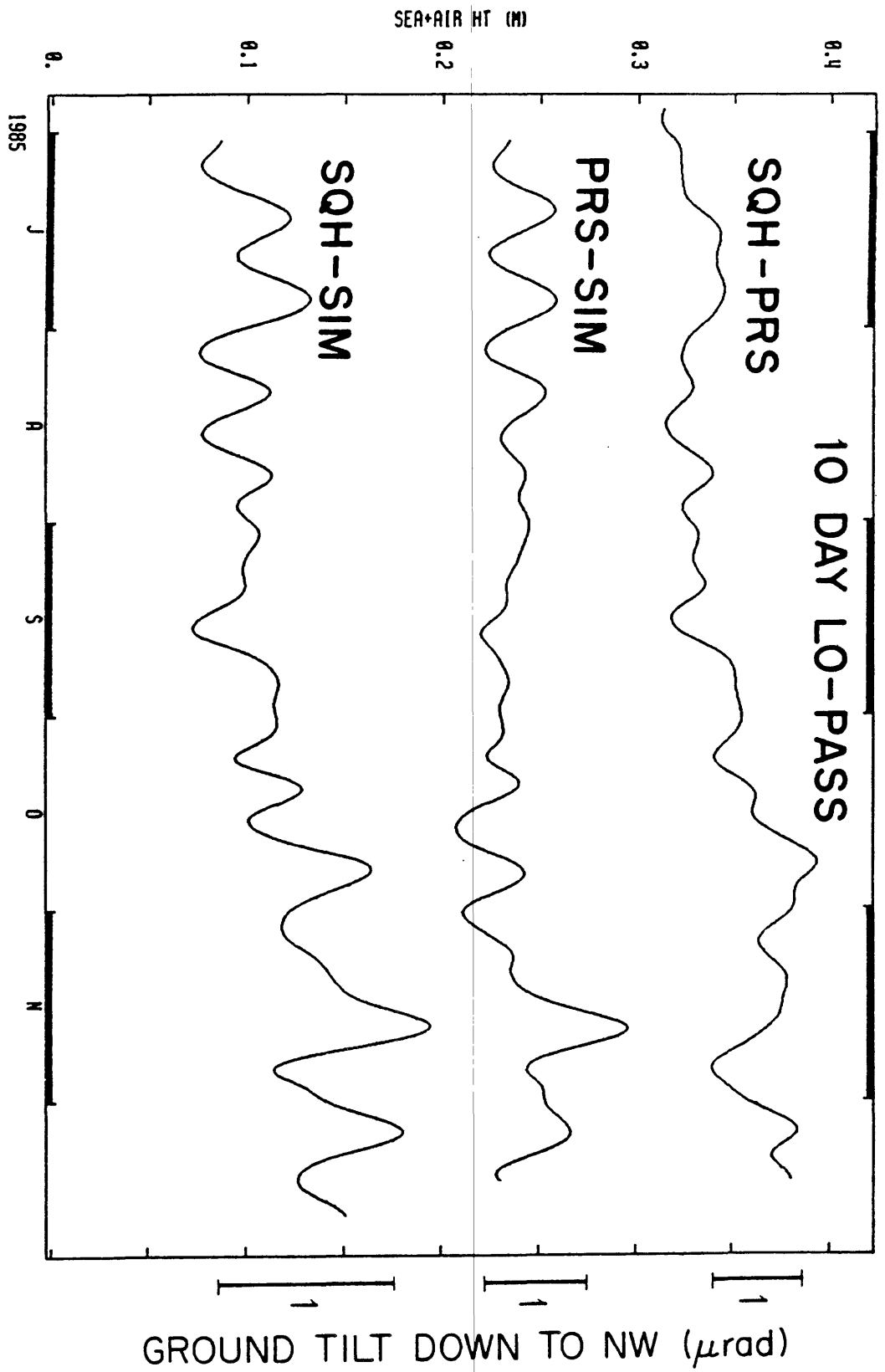
December 24, 1985.

Fig. 1. Low-passed sea-level differences from the Shumagins between late June and mid December 1985. A sea-level scale is shown at left, and a ground-tilt scale at right. The lowest plot is the sum of the upper two. Superimposed on short-term fluctuations of up to 50mm amplitude is a clear change in long-term trend that begins in September or October.

APPENDIX E.

November 21, 1985, Press Release from the Alaska Division
of Geological Surveys regarding possibility of a great earthquake in the
Alaska peninsula area

FROM: JOHN DAVIES (GEOPH. INST. FBK)
BT

ALASKA DGGS PRESS RELEASE
FOR RELEASE NOVEMBER 1985

RECENT EARTHQUAKE ACTIVITY IN THE SHUMAGIN ISLANDS HAS CAUSED
SCIENTISTS AT THE ALASKA DIVISION OF GEOLOGICAL SURVEYS TO COMMUNICATE
THEIR CONCERN ABOUT THE POSSIBILITY OF A GREAT EARTHQUAKE IN THE ALASKA
PENINSULA AREA TO THE GOVERNOR AND OTHER STATE OFFICIALS (SEE ATTACHED
MEMO). ALTHOUGH THE RECENT SEQUENCE OF FOUR MODERATE EARTHQUAKES IN THE
SHUMAGIN ISLANDS AND OTHER CHANGES IN THE PATTERN OF EARTHQUAKE ACTIVITY
IN THE AREA HAVE NOT LED SCIENTISTS TO MAKE ANY DEFINITE PREDICTIONS
ABOUT WHEN THE EXPECTED GREAT (RICHTER MAGNITUDE > OR EQUAL TO 7.8)
EARTHQUAKE MIGHT OCCUR, THEY ARE MORE CONCERNED ABOUT IT NOW THAN THEY
WERE A MONTH AGO.

THE SCIENTISTS' DILEMMA IS THAT THERE ARE SEVERAL INTERPRETATIONS OF THE
DATA. ONE INTERPRETATION IS THAT THE LOCALE OF THE RECENT EARTHQUAKE
SEQUENCE IS AN AREA OF LOW STRENGTH WHERE MODERATE EARTHQUAKES ARE
EXPECTED TO OCCUR; THEIR OCCURRENCE HAS NO PREDICTIVE VALUE FOR A
POSSIBLE GREAT EARTHQUAKE IN THE REGION. ANOTHER INTERPRETATION IS THAT
THIS SEQUENCE IS PART OF A PROCESS CALLED SLIP WEAKENING, IN WHICH EACH
SEQUENCE OF MODERATE EARTHQUAKES BRINGS THE AREA CLOSER TO THE TIME WHEN
A MUCH LARGER PORTION OF THE PLATE BOUNDARY FAILS IN A SINGLE GREAT
EARTHQUAKE. BECAUSE THERE IS NO WAY TO CHOOSE BETWEEN THESE
ALTERNATIVES AT PRESENT, SCIENTISTS AT THE STATE SURVEY SUGGEST THAT
STATE AND LOCAL PREPAREDNESS OFFICIALS REVIEW THEIR LONG-TERM PLANS TO
COPE WITH A GREAT EARTHQUAKE.

EVEN IF THE PRESENT ACTIVITY IS NOT A SIGNAL THAT A GREAT EARTHQUAKE IS
IMMINENT, THE AREA HAS A RELATIVELY HIGH, LONG-TERM POTENTIAL FOR SUCH
AN EVENT. ALONG THE ALASKA-ALEUTIAN SUBDUCTION ZONE (FROM CORDOVAL
TO SHEMYA), SEVEN GREAT EARTHQUAKES HAVE OCCURRED IN THE PAST 89 YEARS,
AN AVERAGE OF ABOUT ONE EVERY 10 YEARS. THE LONGEST PREVIOUS INTERVAL
BETWEEN GREAT EARTHQUAKES IN THIS SUBDUCTION ZONE IS 18 YEARS, AND IT
HAS BEEN 20 YEARS SINCE THE LAST GREAT EARTHQUAKE SHOOK THE RAT ISLANDS
IN 1965. SEISMOLOGISTS HAVE IDENTIFIED THE SHUMAGIN AND YAKATAGA
SEISMIC GAPS AS HIGHLY LIKELY SITES OF THE NEXT GREAT EARTHQUAKE ALONG
THE SUBDUCTION ZONE. ESTIMATES OF THE PROBABILITY FOR A GREAT
EARTHQUAKE IN THE NEXT 20 YEARS RANGE FROM ABOUT 30 TO 90 PERCENT FOR
BOTH GAPS.

IF A GREAT EARTHQUAKE OCCURS NEAR THE SHUMAGIN ISLAND, IT COULD BE
CENTERED ANYWHERE FROM DUTCH HARBOR TO THE SEMIDI ISLANDS (SOUTHWEST OF
KODIAK ISLAND), AND WOULD CAUSE VERY STRONG SHAKING THAT LASTS FOR
SEVERAL MINUTES. OTHER POSSIBLE RESULTS MAY INCLUDE PERMANENT CHANGES
OF SEVERAL METERS IN RELATIVE SEA LEVEL, LAND SLIDING, SNOW AND ROCK
AVALANCHES, AND SUBMARINE SLUMPS: OF MOST CONCERN, WATER-WAVE RUN-UP OF
UP TO 30 METERS (OR MORE IN VERY EXTREME CASES) MAY RESULT FROM A
TSUNAMI GENERATED BY THE MOTION OF THE SEA FLOOR OR BY RESONANCE EFFECTS
CAUSED BY SUBMARINE SLUMPS OR LARGE AVALANCHES INTO LOCAL BAYS.

FOR FURTHER INFORMATION, CONTACT
JOHN N. DAVIS, 907-474-7190

THRU: ESTHER C. WUNNICKE, COMMISSIONER, DEPARTMENT OF NATURAL RESOURCES

FROM: ROSS G. SCHAFF, DIRECTOR
        JOHN N. DAVIES, STATE SEISMOLOGIST

SUBJECT: BASIS FOR AN INCREASED LEVEL OF CONCERN
        FOR THE POSSIBILITY OF A GREAT EARTHQUAKE IN
        OR NEAR THE SHUMAGIN ISLANDS AREA OF THE
        ALASKA PENINSULA

BACKGROUND

IN THE PAST 89 YEARS, SEVEN GREAT (RICHTER MAGNITUDE > OR EQUAL TO 7.8)
EARTHQUAKES HAVE OCCURRED IN THE ALASKA-ALEUTIAN SUBDUCTION ZONE
(SHEMYA-CORDOVA). THE MEAN INTEREVENT TIME FOR THESE EARTHQUAKES IS 9.7
YEARS WITH A RANGE OF 1.0 to 18.3 YEARS. THE LAST GREAT EARTHQUAKE IN
THE REGION WAS THE RAT ISLANDS EVENT IN 1965, A LITTLE OVER 20 YEARS
AGO. BECAUSE THE PRESENT INTERVAL IS LONGER THAN ANY PREVIOUS
INTEREVENT TIME, ANOTHER GREAT EARTHQUAKE IN THE SUBDUCTION ZONE IS
OVERDUE.

TWO REGIONS OF THE SUBDUCTION ZONE HAS BEEN IDENTIFIED BY SEISMOLOGISTS
AS SEISMIC GAPS WITH A HIGH POTENTIAL FOR A GREAT EARTHQUAKE WITHIN THE
NEXT 20 YEARS. THE SHUMAGIN ISLANDS AREA OF THE ALASKA PENINSULA AND
THE YAKATAGA REGION (ROUGHLY CENTERED AROUND CORDOVA). FOR BOTH GAPS,
ESTIMATES OF THE PROBABILITY FOR A GREAT EARTHQUAKE IN THE NEXT 20 YEARS
RANGE FROM ABOUT 30 TO 90 PERCENT. THEREFORE, IT IS REASONABLE TO
EXPECT THAT THE NEXT GREAT EARTHQUAKE IN THE SUBDUCTION ZONE WILL OCCUR
IN ONE OF THESE TWO GAPS.

RECENT EVENTS

DURING THE 3-WEEK INTERVAL FROM OCTOBER 9 TO NOVEMBER 14, 1985, A
SEQUENCE OF FOUR MODERATE EARTHQUAKES WITH RICHTER MAGNITUDES OF 6.4,
5.2, 5.0, AND 5.7 OCCURRED IN THE SHUMAGIN ISLANDS REGION OF THE EASTERN
ALEUTIAN ISLAND ARC. THE EVENTS IN THIS SEQUENCE OCCURRED NEAR THE
EASTERN EDGE OF THE SHUMAGIN SEISMIC GAP, CLOSE TO THE EPICENTERS OF TWO
EVENTS OF RICHTER MAGNITUDE 6.0 THAT OCCURRED IN FEBRUARY 1983. AN
EVENT OF RICHTER MAGNITUDE 5.8 ALSO RECENTLY OCCURRED IN THE UNALASKA
REGION NEAR THE WESTERN EDGE OF THE GAP. IN ADDITION, SEISMOLOGISTS AT
LAMONT-DOHERTY GEOLOGICAL OBSERVATORY REPORT THAT THE MICROSEISMICITY
RATE IN THE SHUMAGIN REGION HAS NEARLY DOUBLED DURING THE PAST 6
MONTHS. INCLUDED ARE EVENTS ALONG THE SUBDUCTING PACIFIC PLATE TO
DEPTHS AS GREAT AS 250 KM. BECAUSE WE DO NOT KNOW THE FALSE-ALARM RATES
ASSOCIATED WITH SUCH SEISMICITY CHANGES, THIS INFORMATION IS NOT
SUFFICIENT FOR MORE PRECISE TEMPORAL PREDICTION OF ANY IMPENDING LARGE
OR GREAT EARTHQUAKES IN THE EASTERN ALEUTIAN ISLANDS. HOWEVER, WE FEEL
THAT AN INCREASED STATE OF AWARENESS OF THE POSSIBILITY FOR SUCH EVENTS
IS WARRANTED.

IT IS POSSIBLE THAT DURING THE NEXT YEAR NO EARTHQUAKES LARGER THAN
RICHTER MAGNITUDE 5.0 WILL OCCUR NEAR THE SHUMAGIN GAP, AND THE
SEISMICITY RATE DETECTED BY THE LOCAL NETWORK MAY RETURN TO NORMAL. IN
THIS CASE, OUR LEVEL OF CONCERN WILL RETURN TO THAT EXPRESSED IN THE
BACKGROUND INFORMATION ABOVE.

RECOMMENDED ACTION

WE SUGGEST THAT OUR INCREASED LEVEL OF CONCERN BE COMMUNICATED TO
COGNIZANT STATE AND LOCAL OFFICIALS WHO ARE RESPONSIBLE FOR LONG-TERM
PREPAREDNESS PLANS TO RESPOND TO EFFECTS OF GREAT EARTHQUAKES. SUCH AN
EVENT MIGHT BE CENTERED ANYWHERE FROM DUTCH HARBOR TO THE SEMIDI ISLANDS
(JUST SOUTHWEST OF KODIAK ISLAND) AND WOULD RESULT IN VERY STRONG
SHAKING THAT LASTS FOR SEVERAL MINUTES. OTHER POSSIBLE RESULTS MAY
INCLUDE PERMANENT CHANGES OF SEVERAL METERS IN RELATIVE SEA LEVEL, LAND
SLIDING, SNOW AND ROCK AVALANCHES, AND SUBMARINE SLUMPS: OF MOST
CONCERN, WATER-WAVE RUN-UP OF AS MUCH AS 30 METERS (OR MORE IN EXTREME
CASES) MAY RESULT FROM A TSUNAMI GENERATED BY THE MOTION OF THE SEA
FLOOR OR BY RESONANCE EFFECTS CAUSED BY SUBMARINE SLUMPS OR LARGE
AVALANCHES INTO LOCAL BAYS.